https://doi.org/10.15388/vu.thesis.736
https://orcid.org/0000-0002-8707-6598

VILNIUS UNIVERSITY

Kristina Žukauskaitė

Impact of Gastrointestinal Cancer Therapies on the Gut Microbiome: Findings from Clinical Studies and an *In Vitro* Modelling

DOCTORAL DISSERTATION

Natural Sciences,
Biology (N 010)

VILNIUS 2025

The dissertation was prepared between 2021 and 2025 at the Institute of Biosciences, Life Sciences Centre, Vilnius University, Vilnius, Lithuania, and the Division for Gastroenterology and Hepatology, Department of Internal Medicine, Medical University of Graz, Graz, Austria. The research was supported by Vilnius University, which also provided a scholarship.

Academic supervisor – Prof. Dr. Sonata Jarmalaitė (Vilnius University, Natural Sciences, Biology – N 010).

Academic consultant –
Dr. Angela Horvath (Medical University of Graz, Medicine and Health Sciences, Medicine – M 001).

This doctoral dissertation will be defended in a public meeting of the Dissertation Defence Panel:

Chairman – Prof. Dr. Eglė Lastauskienė (Vilnius University, Natural Sciences, Biology – N 010).
Members:
Dr. Aurelijus Burokas (Vilnius University, Natural Sciences, Biology – N 010),
Dr. Daiva Dabkevičienė (Vilnius University, Natural Sciences, Biology – N 010),
Prof. Dr. Barbara Obermayer-Pietsch (Medical University of Graz, Medicine and Health Sciences, Medicine – M 001),
Prof. Dr. Tomas Poškus (Vilnius University, Medicine and Health Sciences, Medicine – M 001).

The dissertation shall be defended at a public meeting of the Dissertation Defence Panel at 13:00 on the 7th of March 2025 in Room R401 of the Vilnius University Life Sciences Center.
Address: Saulėtekio ave. 7, LT-10257, Vilnius, Lithuania
e-mail: *kristina.zukauskaite@medunigraz.at*

The text of this dissertation can be accessed at the libraries of Vilnius University, as well as on the website of Vilnius University: *www.vu.lt/lt/naujienos/ivykiu-kalendorius*

https://doi.org/10.15388/vu.thesis.736
https://orcid.org/0000-0002-8707-6598

VILNIAUS UNIVERSITETAS

Kristina Žukauskaitė

Gastroenterologinio vėžio gydymo poveikis žarnyno mikrobiomui: įžvalgos iš klinikinių tyrimų ir *in vitro* modeliavimo

DAKTARO DISERTACIJA

Gamtos mokslai,
Biologija (N 010)

VILNIUS 2025

Disertacija rengta 2021–2025 metais Biomokslų institute, Gyvybės mokslų centre, Vilniuje, Lietuvoje ir Vidaus ligų klinikos Gastroenterologijos ir hepatologijos skyriuje, Graco medicinos univeristete, Grace, Austrijoje.
Mokslinius tyrimus rėmė ir stipendiją suteikė Vilniaus universitetas.

Mokslinė vadovė – prof. dr. Sonata Jarmalaitė (Vilniaus universitetas, gamtos mokslai, biologija – N 010).

Mokslinė konsultantė – dr. Angela Horvath (Graco medicinos universitetas, medicinos ir sveikatos mokslai, medicina – M 001).

Gynimo taryba:

Pirmininkė – prof. dr. Eglė Lastauskienė (Vilniaus universitetas, gamtos mokslai, biologija – N 010).
Nariai:
dr. Aurelijus Burokas (Vilniaus universitetas, gamtos mokslai, biologija – N 010),
dr.. Daiva Dabkevičienė (Vilniaus universitetas, gamtos mokslai, biologija – N 010),
prof. dr. Barbara Obermayer-Pietsch (Graco medicinos universitetas, medicinos ir sveikatos mokslai, medicina – M 001),
prof. dr. Tomas Poškus (Vilniaus universitetas, medicinos ir sveikatos mokslai, medicina – M 001),

Disertacija ginama viešame Gynimo tarybos posėdyje 2025 m. kovo mėn. 7 d. 13 val. Vilniaus universiteto Gyvybės mokslų centro R401 auditorijoje. Adresas: Saulėtekio alėja 7, LT-10257, Vilnius, Lietuva
el. paštas *kristina.zukauskaite@medunigraz.at*

Disertaciją galima peržiūrėti Vilniaus universiteto bibliotekoje ir Vilniaus universiteto interneto svetainėje adresu: *https://www.vu.lt/naujienos/ivykiu-kalendorius*

ABBREVIATIONS

5-FU – 5-fluorouracil

BL – Baseline

CIMP – Cytosine and guanine island methylator phenotype

CIN – Chromosome instability pathway

CRC – Colorectal cancer

dMMR – Mismatch-repair-deficient

FDA – U.S. Food and Drug Administration

GC – Gastric cancer

GI – Gastrointestinal

LDA – Linear Discriminant Analysis

LEfSe – Linear discriminant analysis Effect Size

LOH – Loss of heterozygosity

M cells – Microfold cells

MBP – Mechanical bowel preparation

MMR – Mismatch repair

MSCs – Mesenchymal stem cells

MSI – Microsatellite instability

MSI-H – High levels of microsatellite instability

MSI-L – Low levels of microsatellite instability

MSS – Microsatellite-stable

NAC – Neoadjuvant chemotherapy

NCBI – National Center for Biotechnology Information

OP – Oral preparation

PCoA – Principal Coordinate Analysis

pMMR – Mismatch-repair-proficient

POD – Postoperative day

Post-SX – Post-surgery

PPI – Proton pump inhibitor

qPCR – Quantitative polymerase chain reaction

RDA – Redundancy analysis

RE – Rectal enema

SCFAs – Short-chain fatty acids

TME – Tumour microenvironment

TABLE OF CONTENTS

INTRODUCTION 10
1. LITERATURE OVERVIEW 13
1.1. Structure of the Gastrointestinal Tract 13
1.1.1. Structure of Upper Gastrointestinal Tract 14
1.1.2. Structure of Lower Gastrointestinal Tract 16
1.2. Physicochemical Parameters of the Human Gastrointestinal Tract 17
1.2.1. pH 17
1.2.2. Gastrointestinal Gases 18
1.2.3. Gastrointestinal Volume and Transit Time 19
1.3. Gastrointestinal Tract Microbiome 20
1.3.1. Small Intestinal Microbiome 23
1.3.2. Large Intestinal Microbiome 24
1.4. Gastric Cancer 25
1.5. Colorectal Cancer 25
1.6. Molecular Pathways of Sporadic Gastrointestinal Cancer 26
1.6.1. Chromosome Instability Pathway 26
1.6.2. Microsatellite Instability 28
1.6.3. CpG Island Methylator Phenotype 28
1.7. Gut Microbiome and Gastrointestinal Cancer 29
1.7.1. Adhesin-Receptor Interaction 30
1.7.2. Genotoxin-Mediated Promotion of Cancer 31
1.7.3. Microbiome-Diet Interplay 32
1.7.4. Interactions with Host (Epi)Genetics 33
1.7.5. Biofilm Formation 34
1.8. Gut Microbiome and Gastrointestinal Cancer Treatment 35
1.8.1. Surgical Treatment 35
1.8.2. Chemotherapy 37

1.8.3. Radiotherapy 38
1.9. *In Vitro* Models to Study Gastrointestinal Cancer 40
1.9.1. Cell Culture-Based Models 40
1.9.2. Bioreactor-Based Models 43
1.10. Bioreactor-Based Approaches to Study Gastrointestinal Cancer 44
1.11. Bioreactor-Based Models to Study Cancer Treatment Side Effects 46
1.11.1. Chemotherapy and Antibiotics-Induced Dysbiosis 46
1.11.2. Radiotherapy-Induced Toxicity 47
1.11.3. Oralization 48
2. STUDY COHORTS AND METHODS 49
2.1. Study Design and Ethics 49
2.2. Study Participants 49
2.2.1. Exclusion Criteria 49
2.2.2. Inclusion and Interventions 50
2.3. Fresh Stool Sample Collection 51
2.4. *16S rRNA* Gene Sequencing 51
2.5. Processing of the Sequencing Data 52
2.6. Sequencing Data Analysis 53
2.7. *In Vitro* Model Development 53
2.7.1. Setup of the *In Vitro* Model 53
2.7.2. Anaerobic Inoculum Preparation 54
2.7.3. Supplementation of Fresh Nutrients 56
2.7.4. Spiking 57
2.7.5. Supplementation with Probiotic Products 58
2.7.6. Quality Control of Supplementation Products 58
2.7.7. DNA Extraction 59
2.7.8. Quantitative Polymerase Chain Reaction 59
2.8. Statistical Analysis 61

3. RESULTS 62
3.1. Effect of Preoperative Treatment and Surgery 62
3.2. Effect of Neoadjuvant Chemotherapy and Gastrectomy 68
3.3. Development of *In Vitro* Model of Cancer Treatment Side Effects 76
3.3.1. Optimization of Anaerobic Microbiome Collection Procedure . 76
3.3.2. Impact of Bioreactor Operation Modes 81
3.3.3. *In Vitro* Modulation of Oralization Process 87
3.3.4. Testing of Probiotic Products to Prevent Oralization of the Gut 87
4. DISCUSSION 90
CONCLUSIONS 97
RECOMMENDATIONS 98
ACKNOWLEDGMENTS 99
REFERENCES 100
SUPPLEMENTARY MATERIALS 131
LIST OF PUBLICATIONS 137
LIST OF INTERNATIONAL CONGRESSES 139
FINANCIAL SUPPORT 142
TRAINEESHIPS 142
SANTRAUKA 143

INTRODUCTION

Gastrointestinal cancers, including colorectal and gastric cancers, are significant contributors to global mortality and pose a major challenge to public health [1]. A critical yet underexplored aspect of these cancers is their association with the gut microbiome. Research indicates that the gut microbiome changes not only during the development of gastrointestinal cancer but also throughout its treatment [2]. However, the complex interactions between cancer progression, treatment, side effects of the cancer treatment, and the gut microbiome remain largely understudied.

Animal models are frequently used in cancer research but often fall short due to ethical considerations and biological differences from humans [3]. Traditional *in vitro* systems – alternatives to *in vivo* models – lack the complexity to replicate the dynamic interactions between host cells and the gut microbiome [4]. Bioreactor-based *in vitro* models have been developed to address this gap, offering a more comprehensive platform to study these interactions. Despite their potential, models, which include stool microbiome, are not widely utilized, especially in examining the side effects of cancer treatment.

A prevalent side effect of cancer treatment is the oralization of the gut microbiome, characterized by the invasion and colonization of oral bacteria within the gastrointestinal tract. This condition can result from long-term usage of medications like proton pump inhibitors or surgical interventions [5,6].

In this doctoral dissertation, we aim to reduce the reliance on animal models by developing an easy-to-use *in vitro* model that includes the human stool microbiome. We chose this approach to replicate the human gut environment better, providing a more accurate platform for studying the interactions between gastrointestinal cancers, their treatments, and the gut microbiome. Research often centers on creating new cancer drugs, but in our study, we emphasize reducing current treatment side effects to improve the well-being of cancer patients. We adapted a newly developed *in vitro* model to evaluate various probiotic and prebiotic combinations that could potentially reduce post-therapy side effects of oralization.

Aim and Tasks

In this doctoral dissertation, we first aimed to investigate the impact of various gastrointestinal cancer treatment methods on gut microbiome composition, and second, to develop a novel bioreactor-based *in vitro* model

that could be adapted to simulate the human gut microbiome. The final goal of this work was to use this newly developed *in vitro* system to test a new combination of probiotic products that could potentially alleviate the side effects of cancer treatment, thereby reducing the reliance on animal testing.

To achieve this aim, the following tasks have been carried out:

1. To identify the effect of preoperative mechanical bowel preparation with oral agents and rectal enema impact on the gut microbiome composition and postoperative complications in colorectal cancer patients;
2. To identify the effect of neoadjuvant chemotherapy and radical surgery on the gut microbiome in gastric cancer patients;
3. To establish a novel bioreactor-based *in vitro* model of the human gut that could be used to model the side effects of gastrointestinal cancer treatment;
4. To adopt a newly developed *in vitro* model in testing various probiotic products that could alleviate the side effects of gastrointestinal cancer treatment, such as the oralization of the gut microbiome.

Scientific Novelty and Practical Value of the Study

This doctoral dissertation is unique in several aspects. First, it includes two prospective clinical studies involving gastrointestinal cancer patients with two distinct types—gastric and colorectal cancer. Patients in these cohorts underwent different preoperative procedures, and their stool samples were used for an in-depth analysis of gut microbiome composition.

The colorectal cancer patient cohort analysis provided valuable insights into preoperative mechanical bowel preparation techniques. For the first time, we showed that the effect of rectal enema on the gut microbiome composition (dysbiosis) is comparable to that of oral agents. This finding suggests that both methods can be effectively used for mechanical bowel preparation before left-sided colorectal cancer surgery.

The gastric cancer patient cohort analysis revealed that neoadjuvant chemotherapy before radical gastrectomy did not significantly impact the gut microbiome composition. In contrast, neoadjuvant chemotherapy, followed by radical gastrectomy, resulted in significant changes to the gut microbiome, including the oralization of the gut.

The next phase of this doctoral dissertation work aimed to develop a novel bioreactor-based *in vitro* model to study the side effects of gastrointestinal

cancer treatments, including oralization, on the gut microbiome. This area remains underexplored, as few studies incorporated the stool microbiome to study the side effects of cancer treatment.

Oralization, a known side effect of the long-term usage of proton pump inhibitors, and identified side effect of the radical gastrectomy treatment in the gastric cancer cohort, was modeled using the newly developed bioreactor-based *in vitro* model that utilized stool samples. We proved this model to be effective for studying gut microbiome oralization, and was further adapted to evaluate probiotic-containing products for their potential to reduce this side effect. The *in vitro* model demonstrated that the tested composition of probiotics can reduce the growth of oral bacteria in the context of gut microbiome, suggesting their potential to be used as supplements for cancer patients to mitigate this side effect.

Defending Statements

1. The impact of mechanical bowel preparation with oral agents and rectal enema on the gut microbiome in colorectal cancer patients is comparable regarding dysbiosis.
2. The radical treatment of advanced gastric cancer, involving neoadjuvant chemotherapy followed by radical surgery, is associated with long-term effects on the gut microbiome. These enduring changes are primarily due to radical gastrectomy rather than neoadjuvant chemotherapy.
3. The experimental conditions for an *in vitro* model of the human gut microbiome were carefully optimized using the DASbox® mini bioreactor system and human stool samples. This innovative *in vitro* model is adapted to study the side effects of gastrointestinal cancer treatments, with a particular emphasis on oralization.
4. The tested probiotic composition significantly reduces the growth of oral bacteria in a bioreactor-based *in vitro* model. This result indicates that probiotics may be beneficial in clinical settings to improve patient outcomes during and/or after cancer treatment.

1. LITERATURE OVERVIEW

1.1. Structure of the Gastrointestinal Tract

The human gastrointestinal (GI) tract comprises a tubular structure lined with smooth muscle. It consists of the mucosa, encompassing the epithelium, lamina propria, and muscularis mucosae, followed by the submucosa, muscularis propria, and a typically variable outer layer of serosa and adventitia [7–9].

The GI tract has three main functions: digesting, absorbing, and protecting [10]. Digestion breaks down large food molecules into smaller ones that enterocytes can absorb. Absorption occurs when the intestine's contents enter the mucosa's epithelial cells, are transported to the basement membrane, and eventually reach the portal vein or lymphatic system. In its protective role, the gut acts as a barrier against pathogens and toxins in the body. The GI tract uses a significant amount of energy to carry out these critical functions, making up about 25% of the body's total energy expenditure [10]. The GI tract can be divided into upper and lower GI tracts.

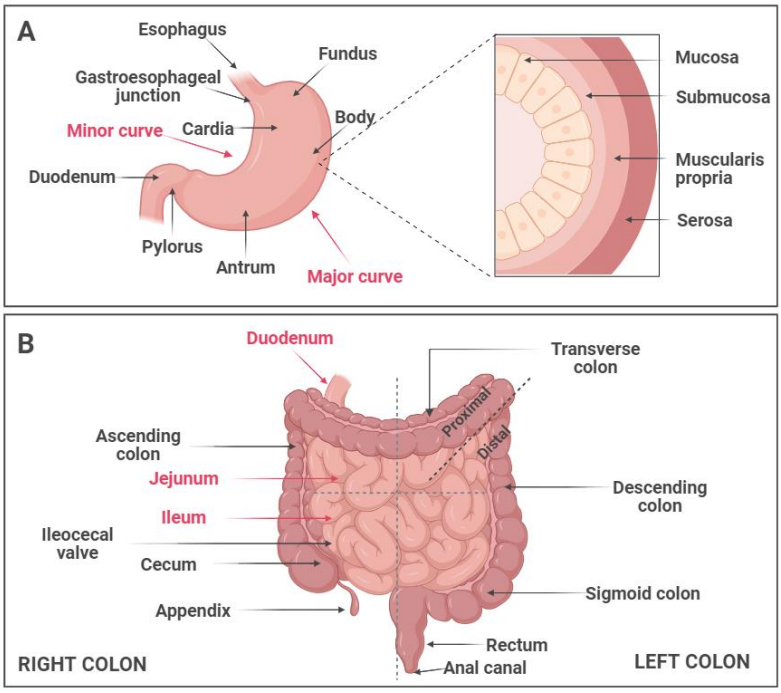

Fig. 1.1. The structure of the (**A**) stomach and (**B**) small and large intestine (segments of the small intestine are marked in pink). The illustration is created with *BioRender.com* based on the [10,11].

1.1.1. Structure of Upper Gastrointestinal Tract

The oral cavity, esophagus, stomach, and small intestine, including the duodenum, jejunum, and ileum, make up the upper GI tract [9,10].

Food is physically broken down by chewing in the oral cavity. Salivary alpha-amylases also break down starch during chewing and swallowing. The esophagus carries ingested food from the oral cavity to the stomach. While in transit, lipase released from the pharyngeal mucosa breaks down certain triglycerides and fatty acids [9,10].

The stomach is divided into four main parts: the gastroesophageal junction, fundus, antrum, and pylorus, which connect to the small intestine. The layers of the stomach wall consist of the gastric mucosa, submucosa, muscularis, and serosa (**Fig. 1.1A**). Its functions include storing food, breaking it down to create an emulsion, and transporting it to the small intestine via the duodenum [9,10].

The stomach's mucous lining can be divided into different anatomical sections: cardia, fundus, antrum, corpus, and pylorus. The section identified as the cardia starts 1-3 cm below the junction between the esophagus and the stomach. The top part of the stomach, located above this junction, is called the fundus. The middle section, which comprises most of the stomach, is called the corpus. The lower part of the stomach, situated near the pyloric sphincter and duodenum, is composed of the antrum and pylorus [9]. To ensure various functions, stomach tissues have a specialized composition of cells. Crypt cells within the gastric mucosa mature into surface epithelial cells as they move along deep glands. Different types of cells, such as pepsinogen-secreting zymogen cells, hydrochloric acid-secreting parietal cells, and mucous cells, are interspersed among the maturing epithelial cells. Hydrochloric acid is a barrier to bacterial overgrowth in the proximal small intestine by destroying most bacteria ingested with a meal. Pepsinogen is transformed into the active form of pepsin, initiating proteolysis. Mucus cells produce mucin and bicarbonate, which combine to form a protective layer over the gastric mucosa, shielding it from acid and pepsin digestion [10].

The small intestine begins at the pylorus and is approximately 700 cm long (with an average length of 690.1 ± 93.7 cm) [12,13]. It consists of three distinct parts: the duodenum, jejunum, and ileum (**Fig. 1.1B**). It also includes folds known as *plicae circularis*, arranged circularly around the lumen. These folds, along with villi and microvilli, cover the apical surface of the small intestine, thereby increasing the surface area available for nutrient absorption – the key function of the small intestine [12,14].

The intestinal epithelium ensures the protective barrier function [15]. It is the most rapidly renewing epithelium in the body, with a complete renewal occurring every 4–5 days [9,16]. The outer layer of intestinal epithelial is supported by the underlying stroma, encompassing mesenchymal cells, neurons, and vasculature [17]. The lining of the villi consists of different types of cells: enterocytes, enteroendocrine cells, goblet cells, Paneth cells, stem cells, tuft cells [9], and microfold (M) cells [18] (**Fig. 1.2**). Goblet, enteroendocrine, and tuft cells are mainly situated on the villi, whereas Paneth cells are found at the base of the crypt, and M cells line the Peyer's patches. Enterocytes comprise the largest proportion of cells in the intestinal epithelium (80%). They are responsible for the final breakdown of polysaccharides and peptides and the absorption of nutrients within the intestinal lumen [19]. The cells lining the intestinal tract create biochemical defenses to block the passage of pathogens, toxins, and allergens from the lumen to the mucosa [20]. Stem cells located at the bottom of the crypts in the small intestine guarantee the fast regeneration of the epithelial lining. They go through the process of differentiation as they move from the base of the crypt up along the crypt-villus axis [21,22]. The specialized secretory cells known as Paneth cells are found in the crypts and contain eosinophilic granules in the cytoplasm. These granules contain antimicrobial peptides and immunomodulating proteins that protect against pathogens [23]. The GI tract contains scattered enteroendocrine cells dispersed throughout the epithelium, constituting about 1% of all epithelial cells [24]. They release hormones in response to food stimuli and are characterized by secretory vesicles [25]. Goblet cells are responsible for the mucus production [14]. The number of goblet cells increases from the proximal to the distal direction, with the lowest number in the duodenum and the highest in the rectum [26]. Goblet cells, like enterocytes, have a short lifespan and move along the crypt-villus and crypt-surface axis. They can be found at the end of the villus and the colonic surface, where they are shed [22]. Tuft cells play a significant role as guardians in the GI tract by monitoring intestinal content through succinate and sweet and bitter taste receptors. Additionally, they are recognized as the initial responders to parasitic infections in the intestine [27]. Tuft cells are characterized by a layer of tuft- or brush-like microvilli on the top of the cell that extend into the lumen. Some tuft cells also have thin lateral microvilli called cytospinules, which protrude from the tuft cell and enter neighboring cells. These cytospinules come into physical contact with the cell nucleus, and their tips are enveloped by the nuclear membrane of the neighboring cell. This type of intercellular contact is uncommon and is thought to be involved in transferring cargo or genetic material [28]. M cells are special epithelial cells

found in the follicle-associated epithelium. Their role is to sample antigens and transport luminal antigens and microorganisms across the epithelium to start immune responses [18].

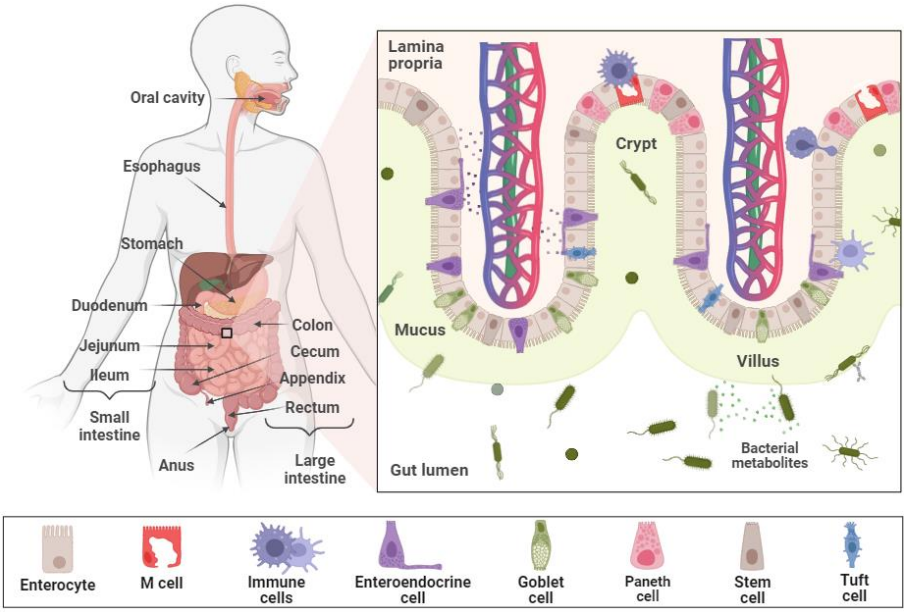

Fig. 1.2. The graphical representation of the structure of the intestine epithelium. Created with *BioRender.com*. The illustration is partially based on [18,29].

1.1.2. Structure of Lower Gastrointestinal Tract

The lower segment of the GI tract, also known as the large intestine, consists of the cecum, appendix, colon, rectum, and anal canal. The right side of the colon includes the appendix, cecum, ascending colon, and transverse colon. Meanwhile, the left side of the colon originates approximately at the midpoint of the transverse colon, encompassing the descending colon, sigmoid colon, and rectum (**Fig. 1.1B**) [30]. The colon serves multiple functions, including the breakdown of carbohydrates and amino acids through fermentation, absorption of minerals and bile acids, synthesis of vitamins, metabolism, and elimination of various substances, and the reabsorption of water [31,32].

The cecum is located following the ileocecal valve and forms an uninterrupted section of the upper colon [30]. In this section of the colon, intestinal bacteria carry out the fermentation of dietary fiber and saccharides, resulting in the production of short-chain fatty acids (SCFAs) [33–35]. The

appendix in humans comes from the cecum, situated beneath the ileocecal junction. It is a short, closed-ended tube, typically measuring around 9 cm (with a range of 2-20 cm). Its role involves supporting the immune system by promoting the growth of beneficial bacteria. This enables the appendix to provide a „*refuge*“ for beneficial bacteria to recolonize the colon in the disease [30].

The large intestine distally connects to the rectum, the final 20 cm of the GI tract. The rectum is then connected to the anal canal, which measures 3.8-5 cm in length, and finally ends at the anus [36].

1.2. Physicochemical Parameters of the Human Gastrointestinal Tract

1.2.1. pH

The pH changes significantly throughout the GI tract. The stomach requires a strong bactericidal effect because it is exposed to the external environment. Therefore, in healthy individuals, gastric juice is highly acidic with a pH of 1.0-3.5 in a fasted state [37,38]. The stomach controls this pH level by using gastrin to stimulate the secretion of hydrochloric acid [38]. After eating, gastric pH levels usually stay between 3 and 7. Depending on the meal size, the gastric pH returns to its lower fasted-state values within 2-3 hours [37].

The pH levels in the intestines are elevated compared to those in the stomach due to the pancreas secreting bicarbonate ions into the small intestine, which neutralizes the gastric acid [37]. The pH level of the proximal small bowel in the small intestine ranges from 6.1 to 6.5 on average, while it increases to around 7.5 near the ileum in the distal small bowel [38,39]. Shortly after that, it decreases to around 6.0 close to the cecum. This rapid decrease happens because of the production of SCFAs and other metabolites, which result from the fermentation of dietary fibers and carbohydrates [40]. Due to the progress of amino acid fermentation, the concentration of alkaline metabolites increases at the entrance of the large intestine [40]. Subsequently, the concentration increases as it progresses toward the rectum, peaking at approximately 7.0 near the end of the large intestine [38]. Several important physiological effects are associated with colonic pH, such as impacting bile acid solubility and the availability of different cations [41].

1.2.2. Gastrointestinal Gases

The total gaseous intestinal volume is approximately 100-500 cm^3 [42]. The production of intestinal gases can stem from either exogenous factors, such as air ingestion, or endogenous factors, such as gas production by commensal microorganisms, or transmembrane diffusion from the bloodstream into the intestinal lumen [42].

The composition of human intestinal gas varies along the GI tract (**Table 1.1**). Swallowed air is the primary source of nitrogen (N_2) and oxygen (O_2), while carbon dioxide (CO_2) comes from both – swallowed air and intestinal production [43]. A large amount of intestinal gases is produced in the colon by microorganismal fermentation. These gases include CO_2, hydrogen (H_2), and methane (CH_4). These gasses make more than 99% of the expelled intestinal gas [44]. The remaining 1% consists of odorous compounds such as hydrogen sulfide, sulfur dioxide, sulfur-containing mercaptans, ammonia, indole, skatole, volatile amines, acetic acid, propionic acid, butanoic acid, isobutyric acid, pentanoic acid, and others [42].

Table 1.1. Approximate percentage of different gasses in various gastrointestinal compartments. The values can vary depending on the food that was eaten and may be present in widely different proportions in each bowel region. The table was adapted from [42].

	Atmosphere	**Stomach**	**Colon**
Nitrogen (N_2)	78	~78 ± 1.0	~65 ± 2.1
Oxygen (O_2)	21	~15 ± 0.7	~2.3 ± 1.0
Carbon dioxide (CO_2)	0.04	~7 ± 2.1	~9.9 ± 1.6
Hydrogen (H_2)	Traces	Traces	3 ± 0.7
Methane (CH_4)	Traces	0	14.4 ± 3.7
Hydrogen sulphate (H_2S)	Traces	0	Traces
Sulfur dioxide (SO_2)	Traces	Traces	Traces

Compared to other intestinal gases, N_2 moves more slowly by gradient diffusion between the lumen and blood. This means that most of the N_2 is not taken in, but instead pushed toward the lower intestinal tract by the gradient established by CO_2, CH_4, and H_2 [43]. Therefore, gastric N_2 comes only from swallowed air, while a certain amount of N_2 in the colon comes from blood diffusion [42]. Unlike inert atmospheric, the N_2 present in the intestines plays a crucial role in the metabolism of nitrogenous compounds. Within the lumen of the small intestine, the microbiome deaminates, hydrolyzes, incorporates, or degrades amino acids and endogenous proteins. The ammonia (NH_3)

derived from N_2, which is produced by bacterial urease in the colon, serves as an N_2 source for amino acid synthesis for surrounding bacteria. Additionally, enterocytes utilize NH_3 through glutamate, glutamine, citrulline, and urea synthesis [42,45].

The O_2 levels decrease gradually along the digestive tract. The air is composed of around 21% O_2, but the stomach contains about 15-16% due to absorption of some swallowed O_2 through intestinal vessels. The majority of O_2 is extracted in the colon, reducing to about 2% of the gaseous volume [46]. A small quantity of O_2 inside the colon promotes the growth of commensal anaerobic microorganisms [43].

CO_2 is generated in various intestinal segments. The CO_2 content in the stomach is much higher than in swallowed air since it is produced during periods of high gastric acid secretion via HCl neutralization [42]. The partial diffusion of CO_2 from the proximal intestinal lumen into the blood is insufficient to prevent the accumulation of CO_2 in the duodenum and proximal jejunum. CO_2 from the intestines enters red blood cells and is transformed into carbonic acid, which then dissociates into hydrogen ions and bicarbonate. In the lungs, two-thirds of the bicarbonate is converted back into CO_2 and exhaled [43]. Additional quantities of CO_2 are produced in the jejunum through the breakdown of dietary triglycerides into fatty acids [47]. SCFAs acetate, propionate, and butyrate are the dominant fermentation acids that accumulate to high concentrations in the colon and produce large amounts of CO_2 [48].

H_2 accounts for approximately 3% of the colonic gasses and is almost entirely produced by the dietary fiber‘s intraluminal fermentation performed by anaerobic commensals in the colon [46]. The movement of luminal colonic H_2 between the lumen and blood occurs through free diffusion. Approximately 15% of H_2 diffuses back into the bloodstream and is eliminated by the lungs during breathing [42].

1.2.3. Gastrointestinal Volume and Transit Time

Information regarding the distribution of fluids in the human GI tract varies throughout the studies. One of the best examples is a study by Schiller *et al*. that was specifically designed to determine the GI volume. This study analyzed the volume and the distribution of intestinal fluid within the lumen of the GI tract using magnetic resonance imaging techniques on twelve healthy volunteers [49]. Before the meal, participants underwent testing in the fasted state, and testing was conducted after eating. Fluid volumes in the stomach during the fasted state ranged from 13 to 72 mL, while in the fed

state, they ranged from 534 to 859 mL. The fluid volumes in the small intestine of the fasted subjects varied widely, measuring between 44 and 319 mL (**Table 1.2**). Following the meal, there was a significant decrease in small intestinal volumes, which ranged from 20 to 156 mL [49].

The length of time it takes for food to pass through the small intestine ranges from 196 to 287 minutes due to peristalsis, segmentation, and mixing, and this time varies depending on the group being studied and the method of measurement [50–56]. Throughout this period, the food encounters various pancreatic and intestinal enzymes and physicochemical conditions. Nutrient absorption is made possible by specific receptors present in the intestinal epithelium. Additionally, the metabolic functions of the intestinal microbiome aid the host by breaking down nutrients that the host's digestive enzymes cannot digest [12].

The movement of the small intestine is more intricate than just being dependent on intestinal motility and flow. It was found that the flow in the small and large intestines is not constant [57]. The time it takes for food to pass through the stomach, small intestine, and large intestine can vary from a few hours to several days, with the most variation occurring in the colon [58]. It was shown that total transit times in healthy volunteers can range from 5.1 to 58.3 h (median 27.4 h) [59].

Table 1.2. Gastrointestinal fluid volumes were determined by magnetic resonance imaging under fasting conditions and 1 h after a meal (n = 12). Table is from [49].

	Stomach [volumes (mL)]	**Small intestine [volumes (mL)]**	**Large intestine [volumes (mL)]**
		Fasting	
Minimum	13	45	1
Maximum	72	319	44
Median	47	83	8
Mean (s.d.)	45 (18)	105 (72)	13 (12)
		Fed	
Minimum	534	20	2
Maximum	859	156	97
Median	701	39	18
Mean (s.d.)	686 (93)	54 (41)	11 (26)

1.3. Gastrointestinal Tract Microbiome

The human gut microbiome consists of a wide variety of microorganisms, including bacteria, viruses, fungi, and protozoa [60]. In adults, the gut

microbiome encompasses over 1000 distinct species of microorganisms and more than 7000 unique bacterial strains [61]. The gut microbiome has three main functions: structural, protective, and metabolic [60]. It plays an essential role in nutrient and mineral absorption, the synthesis of different enzymes, vitamins (such as riboflavin, vitamin B1, biotin, vitamin K, and cobalamin [62] and amino acids, and the production of SCFAs from non-digestible carbohydrates [63]. The byproducts of gut microbiome fermentation play a crucial role in maintaining gut health by supplying energy to epithelial cells, strengthening the integrity of the epithelial barrier, offering immunomodulation, and protecting against pathogens [64]. The shift in the microbial community is known as dysbiosis. This leads to changes in the intestine's metabolism, which disrupts not only the microbiome but also the functions of other body systems [60].

Although the GI tract was more discussed as separate compartments in previous chapters, it is essential to emphasize that the digestive tract is continuous. In this case, several taxa are found along the whole length of the digestive tract, showing a transmission from the oral cavity to the colon (**Table 1.3**) [65–67].

Table 1.3. Human microbiome composition varies by location in the gastrointestinal tract. This summary table shows predominant bacterial genera in healthy individuals. It is based on [68–75].

GI Tract	Bacterial Count (cells/mL)	pH	Bacterial Composition
Oral cavity	10^{11}–10^{12}	6.2-7.5	*Actinomyces* *Corynebacterium* *Fusobacterium* *Gemella* *Granulicatella* *Haemophilus* *Neisseria* *Prevotella* *Pseudomonas* *Rothia* *Streptococcus* *Veillonella*
Esophagus	10^{8}–10^{10}	< 4.0	*Bulleidia* *Citrobacter* *Escherichia* *Eubacterium* *Gemella* *Granulicatella*

GI Tract	Bacterial Count (cells/mL)	pH	Bacterial Composition
			Haemophilus *Helicobacter* *Klebsiella* *Prevotella* *Proteobacteria* *Rothia* *Streptococcus* *Veillonella*
Stomach	10^1–10^4	1-2	*Bacillus* *Enterobacter* *Helicobacter* *Pseudomonas* *Rothia* *Staphylococcus* *Enterococcus* *Lactobacillus* *Streptococcus* *Veillonella*
Duodenum/Jejunum	10^3–10^4	5.7-6.4	*Actinomyces* *Bifidobacterium* *Clostridium* *Corynebacterium* *Enterococcus* *Fusobacterium* *Gemella* *Granulicatella* *Haemophilus* *Lactobacillus* *Prevotella* *Streptococcus* *Veillonella* *Neisseria* *Rothia*
Ileum	10^8	7.3-7.7	*Bacteroides* *Eubacterium* *Bifidobacterium* *Clostridium* *Enterococcus* *Escherichia coli* *Escherichia-Shigella* *Fusobacterium* *Haemophilus*

GI Tract	Bacterial Count (cells/mL)	pH	Bacterial Composition
			Klebsiella *Enterobacter* *Lactobacillus* *Peptostreptococcus* *Prevotella* *Ruminococcus* *Streptococcus* *Veillonella*
Colon	*Ascending:* 10^{11}-10^{12} *Transverse:* 10^{11}-10^{12} *Descending:* $>10^{12}$	5.5-6.8	*Akkermansia* *Bacteroides* *Bifidobacterium* *Clostridium* *Enterobacter* *Enterococcus* *Lachnospiraceae* *Lactobacillus* *Peptostreptococcus* *Prevotella* *Ruminococcus* *Streptococcus*

1.3.1.Small Intestinal Microbiome

The relatively fast transit time and a wide range of pH in the small intestine lead to a dynamic environment that is less diverse and less densely populated by microorganisms in comparison to the colonic microbiome [74,76]. From the duodenum to the large intestine, the typical concentration of bacteria increases from 10^3 to 10^{12} cells/ mL, with the highest density found in the colon [72,76]. Furthermore, the small intestine has relatively high O_2 levels, which decrease from the duodenum to the ileum until the anaerobic conditions prevail in the colon [77]. Additionally, the vascular system underneath the epithelium provides oxygenation of the intestinal tissue, creating the O_2 gradient between the mucosa and lumen [78]. Facultative anaerobes regulate O_2 availability by gradually depleting it in the lumen [79,80]. These changing conditions, combined with dietary nutrients, create specialized niches for microbial communities throughout the different sections of the small intestinal tract.

At the phylum level, the small intestine microbiome is generally composed of *Firmicutes*, *Bacteroidetes*, *Proteobacteria*, *Fusobacteria*, and *Actinobacteria* in varying abundances [74]. While *Firmicutes* dominate in the duodenum, *Proteobacteria* abundance increases from the proximal to the

distal part of the small intestinal tract. *Bacteroides* are more abundant in the ileum where the environmental conditions more closely resemble the colon and the feces [74].

At the genus level, *Streptococcus*, *Veillonella*, *Prevotella*, *Fusobacterium*, and *Haemophilus* are identified as the core members of the microbiome as these genera are consistently found in the small intestine, independently of the sampled section. The duodenum and jejunum‘s microbiome is similar and distinct from the ileum [74]. In addition to this core microbiome, other segment-specific members commonly found include *Neisseria*, *Granulicatella*, *Gemella*, *Rothia*, and *Actinomyces* in the duodenum and the jejunum, and *Bacteroides*, *Escherichia-Shigella*, *Ruminococcus*, *Bifidobacterium*, *Clostridium*, and *Lactobacillus* in the ileum [74].

Several studies aimed to compare both the mucosal and luminal compartments of the small intestine. Overall, the most differences were observed in the relative abundance of *Streptococcus* and *Prevotella*, while the presence/absence of specific microbial taxa seems to be fairly similar between these two sites [81,82]. The constant regeneration of the mucus layer, which leads to the shedding of its associated bacteria into the lumen, may account for these observations. Additionally, the challenge of obtaining samples in this area of the GI tract could also contribute to these findings [74].

1.3.2.Large Intestinal Microbiome

The colon exhibits the highest density and variety of microbes among all body parts. Due to its elevated pH, an abundance of nutrients, and low levels of bile salts and pancreatic secretions, the colon is a highly favorable environment for bacterial growth [83]. At the phylum level, *Bacteroidetes*, *Firmicutes*, *Verrucomicrobia*, *Proteobacteria*, and *Actinobacteria* dominate in the colon [84]. Microorganisms that prioritize dietary starches and nutrients are located in the colonic lumen. The outer intestinal mucus layer is inhabited by organisms able to utilize mucin, including *Akkermansia*, *Ruminococcus*, and certain *Bacteroides* species [73]. These oxygen gradients have an impact on the types of microbes present in the colon. For instance, the phyla Proteobacteria and Actinobacteria are more commonly found near the rectum than in feces as a consequence [85]. The small and large intestine both contain *Streptococcaceae* and *Veillonellaceae*, but these bacteria are present in the feces in smaller proportions [74]. SCFAs such as acetate, propionate, and butyrate are produced by *Bacteroides*, *Bifidobacterium*, *Clostridium*, *Lactobacillus*, *Prevotella*, and *Propionibacterium* [86]. *Bacteroidetes* are

mainly involved in the production of propionate, whereas *Firmicutes* are mainly involved in the production of butyrate [87].

1.4. Gastric Cancer

Gastric cancer (GC) is the fifth most frequently occurring form of cancer and the fourth highest contributor to cancer-related deaths globally. There are over 1 million new cases of GC and approximately 769,000 deaths each year [88]. About 95% of GCs are adenocarcinomas, which have been categorized based on location as cardia/proximal cancer. Cancers in the lower part of the stomach are associated with *Helicobacter pylori* infection [89]. The most commonly used classifications are those of Lauren [90] and the World Health Organisation [91].

The current standard curative approach for locally advanced GC involves neoadjuvant chemotherapy (NAC) followed by radical surgery. Despite advancements in treatment strategies over recent decades, managing GC remains challenging due to poor survival rates [92], high incidence of treatment-related complications [93], and impaired quality of life in long-term survivors [94,95].

Three phenotypes of instability have been identified in GC: (1) microsatellite instability (MSI) due to a defect in the DNA mismatch repair pathway; (2) chromosomal instability (CIN), which is characterized by an increased rate of loss or gain of whole chromosomes or parts of chromosomes during cell division due to mutations in genes controlling the segregation of genetic material during mitosis, and (3) the cytosine and guanine island methylator phenotype (CIMP) [89]. Chapter 1.6 will describe these molecular phenotypes in more detail. However, the majority of illustrative mechanisms will be drawn from studies on colorectal cancer (CRC).

1.5. Colorectal Cancer

CRC is the most commonly diagnosed malignancy and the second leading cause of cancer-related death, with approximately 1.8 million new cases worldwide [96]. More than 90 percent of the cases occur sporadically. Hereditary CRC cases account for <5% of all CRC cases [97]. Most sporadic CRC originates from polypoid adenomas and is preceded by intramucosal carcinomas. These carcinomas can develop into malignant forms through the adenoma-carcinoma sequence [98].

The increasing worldwide incidence of CRC may be linked to environmental factors that increase risks, including poor diet, being

overweight, obesity, type 2 diabetes, lack of physical activity, smoking, and alcohol intake [99]. The increase of early-onset CRC, known as CRC in individuals under 50 years old, has become a growing concern in recent years globally [60].

Despite being located in the large intestine, CRC displays significant heterogeneity in its subtypes, causes, and clinical outcomes. CRC subtypes are categorized into three segments based on their anatomical location: the proximal colon, distal colon, and rectum [100].

1.6. Molecular Pathways of Sporadic Gastrointestinal Cancer

1.6.1. Chromosome Instability Pathway

Malignant tumours may be characterized by high levels of abnormal genomic alterations referred to as genomic instability [101]. The gain or loss of chromosomes or chromosomal regions defines CIN, leading to a rearrangement of chromosomes from cell to cell [101]. CIN can have different results from defects in chromosome segregation with subsequent aneuploidy, telomere dysfunction, or defects in the DNA damage response mechanisms [102]. The consequence is an imbalance in chromosome number, chromosomal genomic amplifications, and a high frequency of loss of heterozygosity (LOH) [102]. CIN also plays a role in the development of tumors by accumulating mutations in certain oncogenes [102,103].

The most common characteristic of sporadic GC is CIN, which has been identified in as many as 84% of GI tumors [104,105]. CIN is the most common cause of genomic instability in CRC, it appears in 70% of sporadic CRC cases [106]. Allelic loss of chromosome 5q has been reported in 20-50% of sporadic CRCs [98]. Two important genes are located on this part of chromosome 5: *Adenomatous polyposis coli* (*APC*) and *Mutated in Colorectal Cancer* (*MCC*). Somatic *APC* mutations are seen in 60-80% of CRCs and are known to occur early in colon carcinogenesis [107].

The mutation in *APC* disrupts the binding between APC and β-catenin, leading to an accumulation of β-catenin in the cytoplasm and excessive activation of the Wnt signaling pathway [108]. The mutation of *APC*, transforming normal colorectal epithelium to an adenoma, is followed by oncogenic *KRAS* mutation (**Fig. 1.3**). This protooncogene is mutated in 30-60% of CRC and large adenomas [106]. The mutated KRAS protein is locked in the active form due to the impaired GTPase activity [109]. KRAS activates the mitogen-activated protein kinase (MAPK) pathway, eliciting the nuclear expression of early response genes. It is proposed that activated KRAS may

play an important role in transition from adenoma to carcinoma through the activation of downstream targets including *BCL-2*, *H2AFZ*, *RAP1B*, *TBX19*, *E2F4*, and *MMP1* [110].

The *mutated in colorectal cancer* (*MCC*) gene is located on the 5q21. It is commonly silenced in CRCs through hypermethylation [111,112]. MCC has been identified as one of the „*driver genes*“, as it codes a cell cycle regulatory protein that induces cell cycle arrest in response to DNA damage [113]. Also, it is known that MCC can also inhibit Wnt/β-catenin signal transduction independently from APC [111].

The *deleted in colon cancer* (*DCC*) gene is localized in the chromosome band 18q21.2 and is deleted in approximately 70% of cases [114]. *DCC* encodes a protein that belongs to the immunoglobulin superfamily; it plays a role in the regulation of cell adhesion and migration [115]. The SMAD proteins are involved in TGF-β signalling and in the regulation of genes involved in cell cycle programming [116]. Since *SMAD2* and *SMAD4* are located on chromosome 18q, the loss of it leads to the deregulation of the TGF-β signaling pathway, which contributes to colorectal carcinogenesis [117].

Loss of 17p is reported in 75% of CRC but not in adenomas, suggesting that loss of this segment, which contains the tumor suppressor gene *p53*, is a late event in the process of colorectal tumorigenesis [106,118]. The majority of *p53* mutations detected in CRC are missense mutations with AT for GC substitution [119]. Protein p53 is known to be „*the guardian of the genome*“ due to its ability to respond to mutagenic stress, such as DNA damage and repair, cell cycle arrest, and apoptosis [120]. It also inhibits the development of new blood vessels [121].

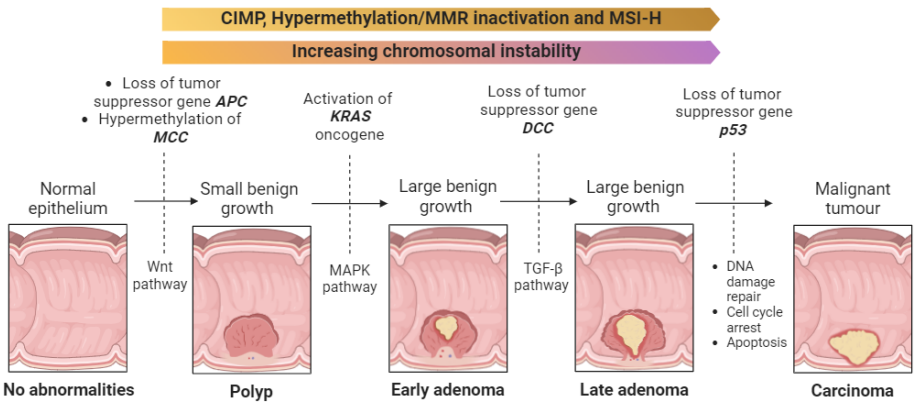

Fig. 1.3. Schematic representation of CRC development on a molecular level by Fearon and Vogelstein's proposed model. This model describes various

genetic events occurring at the different stages of tumor development. This figure is created by *BioRender.com* and is partially based on the [98,118].

1.6.2. Microsatellite Instability

Microsatellites are short repeat nucleotide sequences that are spread out over the whole genome and are prone to errors during replication due to their repetitive manner [106]. MSI is the second most common genomic instability [122]. The cause of MSI is usually linked to faulty mismatch repair (MMR) and the slipping of DNA polymerase, which results in a temporary insertion-deletion loop [122]. The MMR system identifies and fixes errors in base-pair matching that occur during DNA replication. The instability of microsatellites reflects the MMR system's inability to correct these mistakes and is evident through frameshift mutations in the microsatellite repeats. [106]. The DNA MMR system has several proteins such as MSH2, MHL1, MSH6, PMS2, MLH3, MSH3, PMS1, and Exo1 [122]. Patients who lack the ability to deactivate one of these proteins cannot naturally fix errors that occur during DNA replication. These errors result from the DNA polymerase slipping during DNA synthesis, causing the appearance of new alleles not found in normal DNA. This is known as the „*MSI phenotype*“ or „*replication error phenotype*“. MSI can lead to subsequent genetic alterations, typically frameshift mutations, in hundreds to thousands of genes [123].

The reported frequency of MSI in GC varies between 15 and 38% [124,125]. Overall, the frequency of MSI is higher in intestinal-type GC, older age females, and distal GC [126,127]. In most GC, MSI was due to hypermethylation of the *MLH1* promoter [128]. Around 15-20% of CRC tumors display MSI phenotype. MSI tumors have a favorable prognosis and decreased chance of spreading compared to microsatellite stable tumors, underscoring the importance of MSI as a prognostic indicator in CRC. While 5-fluorouracil-based chemotherapy is the standard treatment for CRC, it provides minimal benefit in early MSI CRC. Irinotecan-based regimens and other medications may show potential and are under investigation for use in MSI CRC [129,130].

1.6.3. CpG Island Methylator Phenotype

Changes in gene expression or function that do not involve altering the DNA sequence are known as epigenetic alterations [106]. The abnormal methylation of CpG-rich regions leads to the suppression of genes and is frequently observed in cancer. This can lead to unregulated cell growth,

invasion of blood vessels, and the spread of cancer to other parts of the body. Methylation of the promoter region of a gene causes the gene to be silenced, offering an alternative way for tumor suppressor genes to lose their function [131,132].

The methylation of CpG islands is elevated in the healthy mucous membrane of individuals with persistent inflammatory conditions like *H. pylori* and Epstein-Barr virus infections. It has been regarded as a preliminary abnormality preceding the onset of GC [133] and has been described in up to 50% of GC [134,135]. Approximately 30-35% of colorectal adenoma cases are contributed to by the CpG island methylator phenotype, and this occurs at an early stage [118]. Genes implicated in the development of CRC are known to be suppressed through DNA hypermethylation. These genes include *APC*, *MCC*, *MLH1*, *MGMT*, and several others [106].

1.7. Gut Microbiome and Gastrointestinal Cancer

The gut microbiome has been discussed widely over the past decades and plays an important role in all of the different steps of cancer progression, from oncogenesis to metastasis, from treatment to prognosis prediction [64,136]. Mechanistic insights into a microbiome‘s contributions to carcinogenesis support that gut microbiome alterations induce genotoxin production, inflammation, metabolic regulation, and local and systemic immune response, thus influencing the development of cancer [137].

In recent studies it has been mentioned that individuals suffering from CRC show reduced bacterial diversity and richness in fecal samples and intestinal mucosa in comparison to healthy individuals [138,139]. In addition, CRC patients show a significant increase in *Bacteroides fragilis*, *Fusobacterium nucleatum*, *Enterococcaceae* or *Campylobacter*, *Peptostreptococus*, *Enterococcus faecalis*, *Escherichia coli*, *Shigella* and *Streptococcus gallolyticus*, and a decrease in *Faecalibacterium*, *Blautia*, *Clostridium*, *Bifidobacterium* and *Roseburia* [140]. These changes could lead to an overgrowth of potentially harmful pro-inflammatory microorganisms and a reduction in beneficial bacteria that produce butyrate. This imbalance in the gut microbiome could potentially contribute to the development of tumors [141–143]. Additionally, research has indicated that individuals with early-stage colorectal tumors display a distinct microbiome makeup compared to those with advanced-stage tumors. This suggests that the gut microbiome may play a significant role not only in the onset of the disease but also in its progression [2,140,144]. Besides changes in the microbiome composition, pathogenic bacteria might contribute to the onset of cancer. Carcinogenic

bacteria can promote tumor formation through various mechanisms. They can stimulate the growth of epithelial cells, compromise the integrity of the epithelial barrier, and trigger inflammation [2].

1.7.1. Adhesin-Receptor Interaction

Patients with CRC often have activated oncogenic signaling pathways, including WNT-β-catenin, MAPK, and PI3K-AKT cascade, and these signaling cascades can be intensified by bacteria [106]. Several microorganisms transduce their signals by directly interacting with receptors expressed on the surface of colonic epithelial cells. In 2012, *Fusobacterium nucleatum*, a Gram-negative, anaerobic periodontal pathogen, was reported to be associated with non-colitis-associated CRC among cases of sporadic CRC [145,146]. Bacteria produce a surface protein called FadA, which connects with E-cadherin on cells lining the colon and triggers a signaling pathway involving β-catenin (**Fig. 1.4**). This leads to an increase in the expression of cyclin D1, annexin A1, and Chk2, contributing to the development of tumors. The significance of this process in colon tumorigenesis was demonstrated by removing FadA, which resulted in a decreased ability of *F. nucleatum* to bind to mammalian cells [147]. The expression of FadA is consistently elevated in colon tissue samples from CRC patients, and this elevation is associated with the activation of Wnt signaling, leading to the production of an inflammatory response [148,149]. Another study suggests that Fad results in the displacement of vascular endothelial cadherin from intracellular junctions, which increases the permeability of endothelial cells. This allows bacteria to move through the junctions [150]. Fap2 is an additional *F. nucleatum* adhesin that binds to Gal-GalNAc on the colonic epithelium cell surface, enabling the bacterium to approach these cells [151]. Fap2 has the capability to attach to the inhibitory immune receptor TIGIT (T cell immune receptor with Ig and ITIM domains) found on natural killer and T cells and modify their function [152]. The results indicate that *F. nucleatum* may not only be linked to CRC but could also promote the development of CRC, potentially during the early stages of cancer formation [97]. Additionally, Mima *et al.* detected the *F. nucleatum* DNA in the tissue of 1069 CRC cases and they confirmed that the presence of *F. nucleatum* DNA was linked to reduced survival in patients with CRC [153].

Another bacterium that is often enriched in CRC patients is *Peptostreptococcus anaerobius*. It uses its putative cell binding repeat 2 (PCWBR2) protein to interact with integrin α2β1 on CRC cells, which in turn activates the PI3K-AKT signaling pathway through the FAK kinase [154].

Porphyromonas gingivalis can selectively enter CRC cells and trigger MAPK-ERK signaling by utilizing the gingipain protease located on the cell surface [155].

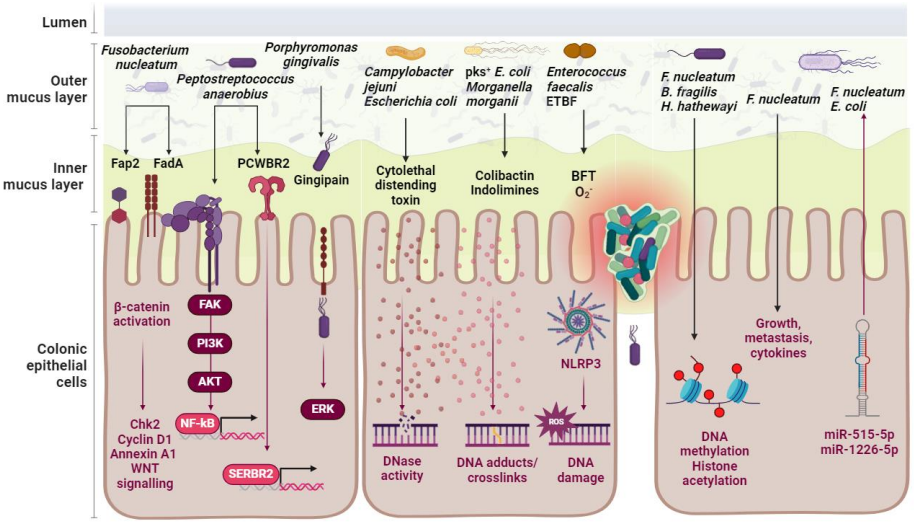

Fig.1.4. Schematic representation of CRC promotion by the gut microbiome. Created in *BioRender.com* partially based on the [147,156,157].

1.7.2. Genotoxin-Mediated Promotion of Cancer

Alterations in the genetic makeup that result in the activation of oncogenes and/or the suppression of tumor suppressor genes are a crucial part of tumor formation [158]. Pathogenic microorganisms can promote the emergence of genetic alterations by producing genotoxins. *Escherichia coli* is a Gram-negative and facultatively anaerobic bacterium that can be divided into five phylogenetic groups (A, B1, B2, D, and E) [159]. Buc *et al.* discovered that the *E. coli* strains belonging to the B2 phylogroup had a preference for colon cancer colonization [160]. It contains the polyketide synthetase (pks) island, whose product is a genotoxin called colibactin [161]. Colibactin forms DNA adducts [162] and crosslinks [163], leading to double-strand breaks and causing gene instability by hindering DNA mismatch repair, which leads to the occurrence of CRC. Pathogenic *E. coli* can also synthesize toxins cyclomodulins, such as cytolethal distending toxin, a potent DNase that induces double-strand breaks [164], it can also be produced by *Campylobacter jejuni* [165].

Similarly to colibactin, indolimines are a class of microbial metabolites containing a functional imine group that are secreted by the commensal

Morganella morganii, which is enriched in fecal samples obtained from patients with inflammatory bowel disease and those with CRC. These indolimines can also cause DNA damage and contribute to the development of CRC [166].

The anaerobe *Bacteroides fragilis* is a commensal bacterium in the gut, which can be classified into two subtypes: nontoxigenic and enterotoxigenic *B. fragilis* [159]. Toxin from enterotoxigenic *B. fragilis* causes DNA damage in colon cells [167]. It has been proposed that *B. fragilis* toxin can directly induce the production of ROS, which can further activate NLRP3 inflammasome [167]. NLRP3 inflammasome is a crucial immune response initiator and critical for genotoxicity. It can cause DNA damage and subsequently initiate inflammation [156]. Additionally, the *B. fragilis* toxin molecule induces the breakdown of the intercellular adhesion molecule E-cadherin in colonic epithelial cells. This action leads to an increase in colonic permeability and consequently impacts the function of the intestinal barrier [168].

Enterococcus faecalis also promotes genomic instability in the colon cells through a similar mechanism. It also produces extracellular superoxide that, when converted to hydrogen peroxide, may cause DNA damage in intestinal epithelial cells [169]. Then, DNA damage can induce NF-κB and lead to inflammatory responses [156,170]. Also, it is known that superoxide can promote CIN in mammalian cells [169]. The formation of extracellular superoxide from *E. faecalis* can enhance the expression of cyclooxygenase-2 in macrophages, thereby promoting CIN and ultimately inducing the occurrence of CRC [157].

1.7.3. Microbiome-Diet Interplay

The World Cancer Research Fund has identified sixteen dietary factors as potential risk factors for early-onset CRC [171]. These include a Westernized dietary pattern, a higher intake of sugar-sweetened beverages or added sugars, red or processed meats, dairy products, and a high-fat diet. A lower dietary fiber intake, fish, vegetables, legumes, fruits, and key nutrients like beta-carotene, calcium, folate, vitamin C, vitamin D, and vitamin E is also associated with an increased CRC risk [172]. Notably, high-fat diets significantly promote the occurrence and progression of GI tumors, primarily through metabolic reprogramming and changes in various carcinogenic molecules [173]. Dietary habits also influence the development of GC. Studies suggest that the gut microbiome is significantly involved in gastric carcinogenesis through its metabolic activity. Microbial metabolites such as

SCFAs, polyamines, N-nitroso compounds, and lactate have been shown to contribute to the inflammatory environment in the stomach, promoting GC development [174]. Also, high-salt diets, typical in Western and traditional diets, are strongly associated with an increased risk of GC [175]. This dietary factor promotes microbial imbalances, favoring the overgrowth of pathogens such as *H. pylori*, a bacterium directly linked to chronic inflammation and GC [176].

Among lifestyle factors, diet is one of the most significant contributors to the intestinal microbiome [177,178]. Evidence suggests that consuming whole grains, dairy products, dietary fibers, and calcium supplements is likely associated with a reduced risk of CRC. Additionally, limited evidence points to a potential link between the consumption of fish, vitamin D, multivitamin supplements, and foods rich in vitamin C with a decreased CRC risk [172]. Animal studies have further elucidated the mechanisms behind these dietary influences, revealing that diet can reshape the community structure of the gut microbiota and affect its function by modulating metabolite production. Butyrate is an important energy source for colonocytes and helps protect colonic epithelial cells from tumourigenesis. This protection occurs through butyrate's anti-inflammatory and antineoplastic properties, influencing cell metabolism, microbiota homeostasis, cell proliferation, immune responses, and genetic/epigenetic regulation [179]. Conversely, protein fermentation and bile acid deconjugation can damage colonic cells, promoting inflammation and increasing cancer risk through proinflammatory mechanisms [179]. In addition to the protective role of SCFAs, other microbial metabolites, such as polyamines, N-nitroso compounds, and lactate, may significantly contribute to the inflammatory environment in the gastric mucosa, promoting the development of gastric cancer [174]. Salt intake has been shown to promote *H. pylori* colonization by altering the gastric pH and weakening the mucosal barrier, thereby facilitating chronic inflammation [175].

1.7.4. Interactions with Host (Epi)Genetics

Correlations between *KRAS* and MSI status have been investigated in multiple studies. In one study, *Peptostreptococcus* and *Parvimonas* were found to be strongly enriched in patients with KRAS-mutant CRC, while *Gallionella* and *Dechloromonas* are enriched in patients with MSI-high CRC [180]. p53, a transcription factor that suppresses tumors, undergoes mutations that lead to a loss of normal function. These mutations may result in acquiring specific cancer-causing properties or even developing new tumor-suppressive functions in about 50% of all CRCs [147]. The level of certain pathogenic

bacteria, such as *F. nucleatum* and *Hungatella hathewayi*, showed strong correlations with CpG methylation in clinical specimens. Monocolonization by single strains of pathogenic bacteria such as *B. fragilis*, *F. nucleatum*, and *H. hathewayi* is associated with promoter hypermethylation of CpG islands of tumour supressor genes, such as *MLH1* and *CDX2*. Inoculation with *F. nucleatum* or *H. hathewayi* has been found to upregulate the expression of DNA methyltransferase 1 (DNMT1) and DNMT3A, indicating a direct role in *de novo* DNA methylation [147,181].

The gut microbiome have also been linked with non-coding RNAs in CRC samples [182]. 76 microRNAs showed differential expression in CRC tumours and normal tissue; among them were the established oncogenic microRNAs miR-182, miR-503, and the mir-17-92 cluster. The relative abundances of various bacterial taxa, such as Firmicutes, Bacteroidetes, and Proteobacteria, were found to be correlated with the expression levels of these differentially expressed microRNAs [182]. On the other hand, host-cell secreted miR-515-5p and miR-1226-5p can enter gut bacteria like *F. nucleatum* and *E. coli*, causing an increase in bacterial gene transcripts and facilitating bacterial growth [183], highlighting a role for microRNAs in enabling host-bacteria crosstalk, including in CRC [184].

1.7.5. Biofilm Formation

In typical physiological conditions, there is a dynamic balance in the communication and interaction between the inner and outer layers of the intestinal mucosa [185]. Nevertheless, if there is inflammation, it disrupts homeostasis and leads to a breakdown in barrier integrity. Then intestinal microorganisms can find a niche to invade, grow, and reproduce, which initiates the formation of biofilms [157]. Organisms create biofilms to survive within the human body and advance the development of disease [186].

The normal mucus barrier has been shown to be damaged by the emergence of tumors [187]. Interestingly, the proliferation of tissue is simultaneously increased by biofilms [188]. The connection between the formation of biofilms and sporadic human CRC has been documented. Researchers observed that colorectal mucosa of patients with CRC or adenoma had more frequent polymicrobial biofilm formation than control subjects with negative results from screening colonoscopy. A study from 2014 revealed that biofilms are nearly always present on proximal CRC tumors but are much less commonly found on distal tumors [188–190].

The composition of microorganisms in biofilms undergoes dynamic changes during the progression of CRC. Therefore, distinct bacterial

communities will be evident at different stages and will exert varying effects as the tumor advances [157]. Evidence also indicates that the cancer-causing impacts of biofilm are associated with metabolites. Specifically, SCFAs such as butyrate, propionate, and acetate produced by biofilm seem to be significant carbohydrate-derived metabolites in CRC carcinogenesis. These metabolites can be readily absorbed and supply energy to colon cells [191,192]. Recently, harmful effects on CRC have been attributed to *Fusobacterium* biofilms precisely due to their ability to suppress the release of butyrate. It is believed that the reduction of butyrate release by *Fusobacterium* biofilms leads to a decrease in the number of apoptotic CRC cells, thereby contributing to the progression of CRC [157,191].

1.8. Gut Microbiome and Gastrointestinal Cancer Treatment

1.8.1. Surgical Treatment

Options for removing GC surgically include total gastrectomy, proximal gastrectomy, distal gastrectomy, and pylorus-preserving distal gastrectomy. The decision on which surgical approach to use for gastric adenocarcinoma depends on factors such as the location of the tumor's center, how much of the stomach is involved, the specific type of cancer cells, and the genetic etiology [193]. Complete histopathological clearance is the goal of gastrectomy as a curative resection for GC, which includes the radical removal of the primary site, as well as the resection of affected lymph nodes and neighboring organs if needed. Subtotal gastrectomy is another option that could be suggested for distal tumours. The rate of wound infection, anastomotic fistula, and mortality is greater in total gastrectomy compared to subtotal gastrectomy. There is no disparity in postoperative mortality or 5-year survival rates between these groups. Additionally, patients who received radical subtotal gastrectomy experienced enhanced quality of life compared to the total gastrectomy cohort [194].

Growing evidence suggests a potential connection between the gut microbiome and postoperative results following gastrectomy. For instance, individuals with GC may face a higher likelihood of developing metachronous cancers, such as CRC, after undergoing gastrectomy [195,196]. Based on the previous study, it was proved that the relative abundance of aerobes and facultative anaerobes was higher in postgastrectomy patients compared with the control group [197]. Another possibility might be the migration of oral bacteria into the gut – oralization process. Several bacteria frequently detected in the oral cavity were significantly abundant in postgastrectomy patients.

They included several species of the genera *Streptococcus, Veillonella,* and *Prevotella*. *Veillonella* seemed to play a crucial role in altering the microbial community in the gastrectomy group by acting as a network hub [197]. Subtotal gastrectomy with Billroth II reconstruction results in increased gastric pH and diminished gastric barrier [5]. Horvath and colleagues demonstrated that undergoing subtotal gastrectomy with Billroth II reconstruction leads to changes in the gut microbiome, which is associated with an increased risk of oralization. Furthermore, they found that intestinal inflammation and microbiome alterations were linked to gastrointestinal symptoms. The research supported the idea that targeting the gut microbiome could be a novel approach to enhancing long-term survivors' quality of life and overall health following subtotal gastrectomy with Billroth II reconstruction [5].

Surgery is the first curative treatment for CRC but may alter the anatomical structure and function of the colorectum, and it is preferred for stage I-III CRC patients without distant metastasis. Although surgical treatment is the most effective treatment for resectable CRC, the cancer's biological characteristics of recurrence and metastasis have determined that surgery cannot completely cure CRC [198]. Especially for the patients with stage II and more advanced stages, there is still a risk of short-term local recurrence and distant metastasis even with surgical treatment [199,200].

Surgical stress is determined by treatments before and after surgery, including mechanical bowel preparation (MBP), antibiotic exposure, proton pump inhibitors, and fasting. Also, the surgery seems to reduce the biodiversity of the gut microbiome [201,202]. It was found that colon resection could change the normal gut microbiome composition and increase the number of commensal microbiome and opportunistic pathogens [203]. Deng *et al*. reported a reduction of Bacteroidetes and Firmicutes and an increase of Proteobacteria in patients surgically treated for CRC compared to healthy volunteers [204]. Similar studies on patients after surgery for CRC confirmed a reduction of obligate anaerobes, including several species of *Clostridium, Bacteroides,* and *Prevotella,* together with a reduction of Bifidobacterium. On the contrary, *Enterococcus*, *Staphylococcus*, and *Pseudomonas* resulted enriched after surgical treatment [203].

Unfortunately, a proportion of patients undergoing CRC surgery develop major postoperative complications, including anastomotic leakage, wound infection, ileus, and bleeding, leading to an increased risk of morbidity and mortality, length of hospital stay, and re-admission [205]. Interestingly, the gut microbiome could be a crucial predictive factor in these complications [206].

1.8.2. Chemotherapy

Chemotherapeutic drugs are a significant staple of cancer therapy, and they can act on different parts of the growth and proliferation of tumour cells. Commonly used chemotherapeutic drugs include alkylating agents, antimetabolites, antitumour antibiotics, and platinum [207]. In GC, two chemotherapy strategies may be adopted in appropriate cases: neoadjuvant treatment before gastrectomy or primary surgical resection followed by chemotherapy [208]. GC is relatively sensitive to chemotherapy drugs, and it is equally important as a surgery for the treatment. There is no standard for selecting the agents used for adjuvant chemotherapy; the decision is based mainly on the results of computer tomography, barium meal, the accurate application of a gastroscope, and even laparoscopic staging. The focal application of neoadjuvant chemotherapy in GC can significantly reduce tumour staging, increase the surgical success rate, and prolong patient survival time. In cases of laporatomy for unresectable GC, neoadjuvant chemotherapy can make reoperation for complete tumour resection possible [209].

The gut microbiome regulates the response to cancer chemotherapy through various mechanisms, such as immune regulation, translocation, and enzymatic degradation. Chemotherapeutic drugs alter the tumour microenvironment (TME) and evoke tumour-destructive immune responses through commensal bacteria [207,210,211]. For instance, the platinum compounds oxaliplatin and cisplatin cause tumour cytotoxicity by forming platinum DNA adducts and intrastrand cross-links [212]. However, their antitumour effect is attenuated significantly by antibiotic treatment. Antibiotic treatment reduces the expression of proinflammatory genes induced by oxaliplatin and the genes related to monocyte differentiation, activation, and function, suggesting that the microbes play an important role in the antitumour effect of chemotherapeutic drugs. Antibiotic treatment not only attenuates the production of ROS, which is required for oxaliplatin to exhibit genotoxicity in tumour cells, but also hinders ROS production by tumour-infiltrating immune cells [212,213].

The intestinal barrier in cancer patients is greatly damaged. The symbiotic microbiome and pathogenic bacteria can therefore translocate to the pancreatic lymph nodes or distant organs through the impaired barrier, regulating the efficacy of chemotherapeutic drugs via inducing immune effects [213]. For example, cyclophosphamide is a widely used anti-neoplastic agent. However, cyclophosphamide-induced toxicity is not limited to tumour tissue but also hematopoietic and intestinal epithelial cells, leading to alteration in the gut microbiome. Administration of cyclophosphamide

increases the abundance of potentially pathogenic bacteria (*E. coli*, *Enterobacteriaceae*, *Pseudomonas*, and *Enterococci*) and disrupts the intestinal mucosal barrier, thus facilitating bacterial translocation from the gut to circulation [213]. Cyclophosphamide also promotes the translocation of distinct Gram-positive bacteria, such as *Lactobacillus johnsonii* or *Enterococcus hirae*, into secondary lymphoid organs [214].

The cytotoxic effects of chemotherapy give rise to a wide range of toxicities. Chemotherapy-induced diarrhea is a common side effect in patients receiving chemotherapy for cancer. The study by Fei *et al.* aimed to study the association between gut microorganisms and chemotherapy-induced diarrhea from the CapeOX regimen in resected stage III CRC patients. The gut microbial community richness and community diversity were lower in chemotherapy-induced diarrhea. *Klebsiella pneumoniae* was the most predominant species among the gut microbiome in CRC patients with chemotherapy-induced diarrhea [215]. *F. nucleatum* has also been associated with resistance to the CRC chemotherapy agent oxaliplatin by inducing autophagy via Toll-like receptor 4 [152].

1.8.3. Radiotherapy

Radiotherapy is a standard treatment and is often combined with chemotherapy to treat cancer, prevent the recurrence of the disease, and improve quality of life [216]. Approximately 50 percent of all cancer patients receive radiotherapy during their cancer treatment [217]. In recent years, radiation therapy in GC has received increased attention. It is being developed as a palliative treatment and adjuvant to neoadjuvant therapy for GC [218]. Although the continuous development of radiotherapy technology has reduced the volume and dose administered to the irradiated stomach, radiation-induced gastric injury is still inevitable [219]. Radiotherapy may also damage the small intestine. Because the tolerance of small intestinal epithelial cells to radiation is low, acute intestinal mucosal congestion, edema, and even stripping can result in dehydration, electrolyte disorders, infection, bleeding, and even death [209].

Radiation damage can also affect a patient‘s quality of life. Patients who have received pelvic radiation often show symptoms such as diarrhea, rectal bleeding, tenesmus, and fecal incontinence [220]. These side effects can greatly impair the quality of life of the patients as well as add to the cost of medical treatment, including additional use of analgesics and pain medication and prolonged hospital stays [217,221]. Ionizing radiation activates the coagulation system, leading to ulceration, which exposes the underlying

tissues to enteric bacteria and increases the inflammation response because the immune system struggles to contain bacterial translocation, and the ulcer may then progress to fibrosis [222]. Current studies on the mechanism of diarrhea following radiotherapy suggest that it is associated with increased intestinal peristalsis, decreased intestinal immune function [223], intestinal crypt stem cell destruction [224], bile salt malabsorption [225], and disruption of the intestinal microbiome [226].

Radiation may lead to alterations in the gut microbiome, but relatively little is known about how the gut microbiome regulates the host response [227]. The interaction of the gut microbiome and cancer therapies, including radiation, is a bidirectional function in that anticancer treatments can disrupt the microbiome, and those disruptions can influence the effectiveness of the anticancer treatments [228]. One clinical study showed that pelvic radiotherapy of gynecological cancer patients resulted in remodelling of the overall gut microbiome composition, with a 10% decrease in *Firmicutes* and a 3% increase in *Fusobacterium* phyla [220]. A systematic review by Touchefeu *et al.* showed that patients receiving cytotoxic and radiation therapy exhibit marked changes in the intestinal microbiome, with most frequently, a decrease in *Bifidobacterium*, *Clostridium cluster XIVa*, *Faecalibacterium prausnitzii*, and increase in *Enterobacteriaceae* and *Bacteroides*. These changes may contribute to the development of mucositis, particularly diarrhea, and bacteremia [229]. However, some patients develop severe diarrhea after radiotherapy, and some do not [230], suggesting that personalized treatment planning and identification of biomarkers with which to predict which patients are likely to respond to treatment or are at risk of developing severe toxicities would help to improve treatment outcomes [228].

Autophagy is related to the radiosensitivity/radioresistance of the tumor. Inhibition of autophagy induces radioresistance, whereas induction of autophagy induces radiosensitivity [231]. *Fusobacterium nucleatum* has been shown to activate autophagy, leading to chemoresistance [232]. Additionally, there are additional studies on the gut microbiome as a booster for radiation therapy, these studies are reviewed in [233].

Studying the intricate interactions of the human gut microbiome, cancer, and cancer treatment, as well as their side effects, necessitates using complex modeling systems. In cancer research, *in vivo* models are frequently utilized, but they present certain challenges due to their biological and genetic differences from humans, as well as bioethical considerations. Therefore, various *in vitro* models can be employed in GI cancer studies, which will be discussed in the following chapter.

1.9. *In Vitro* Models to Study Gastrointestinal Cancer

Several groups of *in vitro* models can be used to modulate the complex structure of the human GI tract. Simple models are based on cell culture, encompassing various 2D and 3D cell-culture models, collectively called cell culture-based *in vitro* models. Alternatively, more advanced bioreactor-based models can be utilized, incorporating host cells or solely the gut microbiome for GI tract modulation. The following section will discuss the benefits, drawbacks, and existing as well as future uses of these models.

1.9.1. Cell Culture-Based Models

Cell cultures are commonly used to study cellular behaviour observed *in vivo*. The biochemical and biomechanical microenvironment intricately influences various processes, including cell differentiation, migration, and growth [234]. Understanding the mechanisms driving these behaviours is paramount in the context of cancer development.

Epithelial cells in GI tract models come from cell lines or primary intestinal cells [235,236]. Despite new and more advanced *in vitro* models, the usage of intestinal epithelial cells in monolayer cultures remains common due to their ability to resemble the parent tissue phenotype [237]. Short-term monolayer cultures of intestinal epithelial cells have proven useful for assessing the impact of growth factors and morphogens on the behaviour of these cells [237]. Additionally, the techniques and instruments commonly used in standard laboratories are more readily available as most imaging and manipulation methodologies were developed for 2D cultures [15]. Their availability in large quantities and their relatively stable phenotypes, transcriptomes, and functional characteristics represent obvious advantages [238]. This simplified *in vitro* modelling system can be highly valuable for studying distinct aspects of disease mechanisms or the impact of various substances (e.g., anti-cancer drugs and bacterial metabolites) on the host cells.

Primary cells are derived from patient tissues and processed for cell culture [239]. In 2014, researchers developed an enhanced human GI epithelial culture system. They isolated crypts from obtained biopsies during routine endoscopy procedures to create 65 epithelial cell lines cultured in conditional media to form spheroids. Cell lines were generated from 47 individuals, including 25 patients with inflammatory bowel disease. These cells formed spheroids, which were grown on Transwell® membranes to establish functional, polarized monolayers covered by a secreted mucus layer. The study also identified various adherence patterns with different strains of

pathogenic *Escherichia coli* [240]. The advantages of this system involve using endoscopic biopsy tissue as the initial material and quickly expanding the spheroids. This allows for establishing a line from an individual patient within a timeframe that aligns with patient care, approximately 2 to 3 weeks. Another advantage of this spheroid culture system is that the protocol is relatively simple. The same protocol can be used to establish and maintain spheroid lines from any accessible GI site, and there is no requirement for a cell sorting.

However, despite these benefits, in monolayer cultures, cells lose their ability to self-renew and eventually undergo terminal differentiation. Thus immortalized cells are used more for epithelium studies [241]. Immortal cell lines are widely used due to their easy handling, repeatability, availability, and cost-effectiveness [236].

Mesenchymal stem cells (MSCs) are another source of cells for GI bioengineering and can be derived from bone marrow [242,243]. These cells can differentiate into epithelial [244] and smooth muscle cells, and act as a cell source for the tissue-engineering source of the small intestine [245]. Another type of stem cell that can be used for disease modelling is cancer stem cells (CSCs). These are the cells within tumour that can initiate tumor growth [246].

However, 2D cell culture models come with significant limitations. For instance, they typically involve single layers of cells and lack the diversity of cell types present in actual tissues, leading to the absence of crucial interactions between different types of cells. Moreover, the conditions in which they are cultivated may not faithfully replicate the natural environment, as serum in the culture medium introduces unknown variables [247]. Thus, there is a growing interest in employing interdisciplinary approaches, combining tissue engineering and microfabrication techniques, to create more relevant and accurate tissue models [235].

To address the limitations of 2D cultures, the previously mentioned Transwell® system was developed. It involves seeding epithelial cells onto a membrane within an insert. This insert divides the system into apical and basal compartments, representing the intestinal lumen and blood vessels, respectively. Thus it offers a mimicry of the *in vivo* gut barrier [248]. However, while these Transwell®-based models are more improved than 2D cultures, they still lack the complexity of *in vivo* systems. These limitations have prompted the development of 3D models to mimic better the heterogeneous 3D environments regulating cell behaviour *in vivo* [249].

An organoid is a self-organizing 3D structure cultivated *in vitro*, comprising organ-specific cells with restricted lineage commitment and

demonstrating organ-like functions [15]. Primary intestinal epithelial cells can be cultured as self-organizing epithelial organoid units [250] or as mixed cultures of epithelial and mesenchymal cells [251]. Generated from single stem cells, embryonic stem cells, or induced pluripotent stem cells, these organoids have the capability for long-term culture, forming spherical or budding structures. These models provide near-physiological systems for diverse applications [15]. Tissue-specific adaptation techniques have facilitated the generation of organoids from nearly all parts of the GI tract, spanning from the small intestine and colon to the stomach, gallbladder, oesophagus, liver, pancreas, salivary glands, and even taste buds [252]. Most importantly, organoids can also be co-cultured with microorganisms, offering insights into pathogenesis and host-microbe interactions [253]. Before 2014, the culture of normal human gastric primary epithelial cells for extended experimental investigations was not feasible. However, a study by Schlaermann *et al.* introduced gastric organoids derived from normal human corpus mucosa. These organoids served as an advanced cell culture model, enabling *in vitro* studies on *H. pylori* infection [254]. Another study demonstrated that organoids develop a sealed lumen containing concentrations of α-defensins, effectively inhibiting the growth of various strains of *Salmonella enterica* for at least 20 hours post-infection [255]. Likewise, experiments involving injecting bacteria like *H. pylori* into the lumens of gastric organoids have triggered robust inflammatory reactions in gastric gland cells. It was shown that this system can be used to study *H. pylori* infection and other gastric pathologies [253]. These advancements underscore how organoid cultures serve as excellent models for studying various diseases. Furthermore, numerous studies have focused on establishing "*Living Organoid Biobanks*" by collecting organoids derived from diverse GI tract tissues and diseases, facilitating a range of applications including personalized and regenerative medicine, drug discovery and testing, biomarker development, and disease modelling [256,257].

Advanced 3D intestinal models feature multi-layered organization with cells embedded in ECM-like substrates like Matrigel® or hydrogels. An example includes a 3D co-culture model of human intestinal epithelial cells with immunocompetent macrophages and dendritic cells, successfully replicating an elevated inflammatory cytokine response [258]. However, it is crucial to note that despite their 3D structure, these models do not feature the characteristic crypt and villi architecture. To overcome this drawback, biofabricated scaffolds were created to imitate the gut's villi and crypt architecture or even tubular structure [249]. These models have an enhanced understanding of cell-to-cell interactions and the pathophysiology of GI

diseases and hold the promise of providing targeted and personalized treatments for individuals with GI dysfunction [259]. The development of dynamic 4D systems was one of the achievements made possible by 3D cell cultures. Han and colleagues created a hydrogel that responded to various stimuli such as temperature, small molecules, and enzymes by forming macropores [260]. This method showed potential applications in studying how changes in surface features affect cells and as a means for delivering cells. The future of 4D systems will depend on the further progress in material systems that have adjustable structures, and responsive signalling [261].

Additionally, mammalian cells can be incorporated into complex systems – bioreactors – that provide precisely controlled environments. Considering the significance of the gut microbiome on GI cancer development and progression [262,263], it would be advantageous to additionally incorporate it as a crucial variable in bioreactor-based disease development. The next section of this chapter will examine the potential for GI tract modulation using bioreactor systems.

1.9.2. Bioreactor-Based Models

Technological advancements play a vital role in understanding the diversity and functions of the gut microbiome. Bioreactor-based *in vitro* gut fermentation models offer valuable insights into the composition and functionality of the microbiome derived from the stool samples while reducing animal testing and overcoming the lack of complexity of cell culture-based models.

The standard bioreactor design is a glass, carbonate, or stainless-steel cylinder with a flat bottom, which maximizes the vessel area or dished/hemispherical bottom as that shape can handle a higher pressure [264]. The vessel contains an impeller driven by an overhead motor, which is essential for mixing the components. The impeller is usually located at a distance equal to the stirrer diameter above the bottom of the vessel. The number of impellers depends on the aspect ratio, spaced from 1 to 2 times the stirrer diameter distance. Typically, only 75-80% of the volume of stirred bioreactors is filled with liquid to allow for the disengagement of droplets from the exhaust gas and to accommodate any foam [265].

Microbiome cultivation success is highly dependent on the stool sampling procedure. The simplest method is when donor collects their stool in a special container, which helps to prevent sample contamination and ensure the right conditions for transportation. The main advantages of this method for donors are simplicity, affordability, and non-invasiveness. For the

researchers, it is advantageous as there are guidelines and protocols for stool collection, transportation, and following procedures [266]. Another method to collect microbiome samples is aspiration of intestinal fluid. It could be achieved through capsules, tubes, or endoscopic aspiration. This method prevents contamination, as the sample is isolated from the external environment after collection. However, it is technically challenging and time-consuming. Also, it is invasive, and the donor cannot perform the sampling procedure by himself [267]. In addition, samples can be collected during the capsule endoscopy procedure. The donor swallows the capsule, which moves through the GI tract by peristalsis. The main advantages are low invasiveness, accurate location of sampling points, and high technological content (e.g., locomotion mechanisms, wireless connection, temperature, pH, pressure, oxygenation, oxidation/reduction conductivity sensors, multi-axial accelerometers and gyroscopes for inertial navigation and positioning). However, there are drawbacks, such as high cost, risk of capsule aspiration or retention [267], and possible sample contamination by intestinal fluid from non-collected sites [268].

The *in vitro* models aim to mimic the GI environment's biological conditions to support the microorganisms' optimal growth. Stability in the culture is achieved by controlling process parameters and maintaining constant environmental conditions throughout the culture period [267]. *In vitro* models typically are categorized into two groups: (**i**) batch fermentation and (**ii**) continuous fermentation models, both designed to simulate the human GI tract [269]. In the recent review it was chosen to depart from this categorization and instead organize the models based on the number of vessels and the level of throughput [270].

1.10. Bioreactor-Based Approaches to Study Gastrointestinal Cancer

The lack of progress in finding effective cancer treatments may be due, in part, to the lack of accurate models that mimic pathological processes. Conventional 2D cell cultures have provided great insight into the ability of tumour cells to grow, but they do not provide information about the complex interactions between the cancer cells and the physicochemical environment within living tumours. For this reason, many groups have explored the use of 3D *in vitro* models, and more recently, microfluidic devices have been applied for this purpose as well [271]. Most importantly, *in vitro* models can be customized to replicate specific aspects of GI diseases, focusing on one part or imitating different parts of the GI tract. This includes incorporating factors

like inflammation, dysbiosis, and altered host-microbe interactions to study disease mechanisms and test potential therapeutic interventions.

Several research groups utilized bioreactor-based *in vitro* systems to modulate CRC and tumour microenvironment. Manfredonia *et al.* used a perfused bioreactor to investigate if this system can maintain the main TME cellular components in primary CRC samples [272]. Fragments from freshly resected tumours were placed in the bioreactors and cultured for 3 days using static or continuous operation mode with perfusion. It was found that static culture resulted in complete tissue loss, while perfusion-based culture of primary CRC specimens resembled key features of TME [272]. A study by La Rocca *et al.* used spinner flask bioreactors to produce 3D *in vitro* CRC tumour microtissues to reproduce TME. This study included CRC cell line HCT-116 and primary normal human dermal fibroblasts [273]. Microtissues were cultured for 12 days using semi-continuous operation mode with the medium exchange every two days. The efficacy of developed microtissues as a drug-screening platform was evaluated by examining the impact of 5-fluorouracil (5-FU), curcumin-loaded nanoemulsions, and their combination. The newly developed microtissues have been observed to accurately replicate the TME by demonstrating extracellular matrix remodelling, cell proliferation, and the induction of normal fibroblasts into an active phenotype. Furthermore, the authors state that these microtissues have the potential to be integrated with tissue-on-a-chip technologies to further investigate studies related to cancer progression and drug discovery [273]. These studies offer valuable insights into the development of the TME, which is a contributing factor in the progression of the disease.

An additional crucial consideration is the development of reliable and reproducible cancer models to facilitate the evaluation of various substances, including new anti-cancer drugs. The methodology employed by Hirt *et al.* involved the cultivation of CRC cells in porous scaffolds under perfusion flow to engineer tissue-like structures [238]. In this study, perfused 3D cultures demonstrated more uniform cell seeding and higher cell counts than static cultures. Transcriptome analysis further indicated a stronger correlation between xenografts and perfused 3D cultures. Notably, treatment with 5-FU triggered apoptosis, down-regulated anti-apoptotic genes, and reduced cell numbers in 2D cultures, whereas it only induced "nucleolar stress" in perfused 3D cultures and xenografts [238]. In 2021, Gouws *et al.* demonstrated the significance of bioreactor-based models in drug testing. The study evaluated South American medicinal plants *Sutherlandia frutescens* and *Xysmalobium undulatum* for potential activity against CRC. The researchers employed clinostat-based rotating bioreactors operating in semi-continuous mode and

utilized a 3D sodium alginate-encapsulated LS180 CRC, spheroid model. This approach effectively assessed the anti-cancer potential of the plant extracts against CRC.

The Rotary Cell Culture Systems were employed to investigate the potential impact of altered gravity on cell viability, drug delivery efficacy, and the modulation of treatment-resistance-related gene expression in the context of gastric cancer [274,275]. In a study, both daunorubicin-sensitive and daunorubicin-resistant gastric cancer cell lines were cultured in bioreactors for 96 hours.

However, it is important to mention that none of the previously mentioned studies considered the gut microbiome, as they did not use the fecal microbiome as inoculum for the bioreactors.

1.11. Bioreactor-Based Models to Study Cancer Treatment Side Effects

Several research studies have addressed this limitation by integrating the microbiome in bioreactors and utilizing it as a fecal inoculum. These investigations encompassed the evaluation of adverse effects of cancer treatment, including radiation-induced toxicity, dysbiosis resulting from chemotherapy and antibiotic use, and oralization process induced by prolonged proton-pump inhibitor (PPI) use or surgical treatment.

1.11.1. Chemotherapy and Antibiotics-Induced Dysbiosis

A study by Ichim *et al.* (2018) implemented a Triple-SHIME system to study chemotherapy and antibiotic-induced dysbiosis [276]. This study aimed to evaluate the bioactivity of a supplement consisting of capsules with a blend of probiotics of the genera *Lactobacillus* and *Bifidobacterium* plus ten digestive enzymes in protecting the human GI tract from chemotherapy and an antibiotic. A fecal sample from a healthy adult donor was used to inoculate the system, microbiome was co-cultured with Caco-2 and THP-1 cells. Interestingly, the probiotic with digestive enzymes supplemented fermentation activity in the colon reactors and accelerated the recovery of microbial populations following 5-FU/vancomycin treatment. In the proximal colon, preventative administration of the supplement resulted in full recovery of the gut microbial community after cessation of 5-FU and vancomycin treatment [276]. Perturbation of the colonic ecosystem by antibiotic therapy was also modulated using the ARCOL model and fecal samples from three healthy donors [277]. A simpler bioreactor system, consisting of the gas impermeable bottles sealed with butyl rubber caps and inoculated with the

fecal microbiome from CRC patients, was used to study the association of colonic methane, formed by methanogenic archaea, and pH with gastrointestinal symptoms induced by adjuvant 5-FU chemotherapy. It was found that methane producers had less frequent diarrhea during chemotherapy than non-producers and more frequent constipation. Baseline fecal pH was also associated with symptoms during chemotherapy: the higher the pH, the lower the risk of diarrhea and the higher the risk of constipation. This study also underscores the importance of the intestinal microbiome in the development of intestinal toxicity during 5-FU therapy [278]. Another study by Blaustein *et al.* (2021) developed an *in vitro* model to characterize the key changes in bacterial community dynamics under chemotherapeutic treatment and the role of bacterial interactions in drug detoxification to promote microbiome resilience. For this goal batch fermentation was used, but no stool inoculum was used. Inoculation occurred with a special bacterial composition that had drug-sensitive strains with five different combinations of drug-resistant and drug-transforming bacterial strains. Bacteria with predicted resistance involving biotransformation significantly lowered concentrations of doxorubicin in culture media, permitting the growth of drug-sensitive strains in monoculture. Such protective effects were not produced by strains with drug resistance conferred solely by efflux. In the mixed communities, the resilience of drug-sensitive members depended on the presence and efficiency of transformers, as well as drug exposure concentration. The fitness of bacteria that were resistant to doxorubicin via efflux, though not transformation, also improved when the transformers were present [279].

1.11.2. Radiotherapy-Induced Toxicity

The intestine is a rapidly renewing tissue, that has led it to be the major target organ for radiation damage and it is one of the most common diseases following radiation exposure [280]. Radiotherapy is currently employed as a CRC treatment strategy, but due to the radiotoxicity, it has an impact on healthy tissues and can raise health concerns [281]. Acute radiation-induced intestinal damage refers to direct damage to the intestinal mucosa, generally causing diarrhea, within 2-12 weeks, that subsides naturally [280].

Many CRC survivors have undergone radiation therapy for tumours in the pelvis or abdomen, thus rendering the bowel at risk for injury. The current prevalence of patients with long-term radiation-induced intestinal side effects exceeds that of ulcerative colitis and Crohn's disease combined [282]. A recently published review by Bogues *et al.* [31] focused on translational research for pelvic radiotherapy-induced toxicity. It reviewed a humanized *in*

vitro models, focusing on the benefits of patient-derived tumour organoids that mimics radiotherapy treatment conditions and allows the assessment of radioprotective agents without animal testing. Also, the potential of microfluidic systems for gut microphysiological modelling and radiotherapy assessment was explored. However, the discussion raised the question of whether integrating a microphysiological system with a radiotherapy setup could provide representative treatment conditions.

1.11.3. Oralization

Another cancer treatment side effect could be an oralization process, which can be induced by the usage of PPIs [5,6]. Tsuda and colleagues used sequencing to examine the impact of gastric acid suppression and on the GI tract microbiome by comparing PPI users and controls not using PPI [283]. Studies of the gastric fluid showed that bacterial cell numbers identified by culture increased significantly in PPI users. They suggested that bacterial overgrowth in the stomach after PPI treatment may not be due to the proliferation of bacteria but rather a lack of bacterial killing in the acid-suppressed stomach [284]. The proof-of-concept study by Etienne-Mesmin (2023) proposed a new model (M-ARCOL) of oral-to-gut invasion by the combined use of an *in vitro* model simulating both the physicochemical and microbial parameters of the human colon [285]. This study used stool samples from two healthy donors to inoculate the bioreactor. Oral invasion of the intestinal microbiome was simulated by injection of enriched saliva in the *in vitro* colon model inoculated with a fecal sample from the same healthy adult donor. The mucosal compartment of M-ARCOL was able to retain the highest species richness levels over time, while species richness levels decreased in the luminal compartment. This new model of oral-to-gut invasion provided useful mechanistic insights into the role of oral microbiome in various disease processes.

In this doctoral dissertation we aimed to develop a bioreactor-based *in vitro* model of the gut microbiome oralization, which adapts the commercially available DASbox® mini bioreactor system and uses the stool samples from healthy donors for the inoculation. The benefit of this system, compared to the previously mentioned, is that it does not require saliva samples from donors, as it implements previously confirmed oralization biomarkers *Streptococcus salivarius* and *Veillonella parvula* [6], and allows a precise spiking strategy, which can be further used for microbiome-drug interaction studies. We chose oralization as an example of the diverse spectrum of side effects of GI cancer treatment and model it using a bioreactor-based *in vitro* system that utilizes stool samples, in order to try to revert it using the probiotic products.

2. STUDY COHORTS AND METHODS

This work involves two prospective clinical studies, including GC and CRC patients, as well as an *in vitro* study that models GI cancer treatment side effects using gut microbiomes taken from the stool of healthy volunteers.

2.1. Study Design and Ethics

Clinical studies were conducted at the National Cancer Institute, Vilnius, Lithuania, after the protocols were approved by the Vilnius Regional Biomedical Research Ethics Committee (No. 2019/6-1133-631 and 2020/1-1185-675) in Lithuania and registered in the *clinicaltrials.gov* (NCT04013841 and NCT04223401) registry. The principal investigator of both clinical studies was Augustinas Baušys, MD, PhD.

The *in vitro* modelling study was conducted at the Medical University of Graz, Graz, Austria, after the local Ethics Committee approved it (protocol No. 34-323 ex 21/22 1126/2022). The principal investigator of this part of the study was Prof. Vanessa Stadlbauer-Köllner, MD, PhD.

All parts of this study were conducted according to the ethical standards of the Helsinki Declaration of 2013. All study participants were at least 18 years old and provided written informed consent before participating.

2.2. Study Participants

Clinical studies included GI cancer patients aged 18 years or older with (**i**) histologically confirmed or clinically suspected left-sided CRC, and (**ii**) GC patients scheduled for radical surgery after NAC, as determined by multidisciplinary team meetings. (**iii**) *In vitro* modelling of GI cancer treatment side effects included only healthy volunteers.

2.2.1. Exclusion Criteria

The exclusion criteria in the CRC group were: (**a**) surgery with preventive ileostomy, (**b**) a history of allergy to OP agents, (**c**) required multi-visceral resection, (**d**) emergency surgery, (**e**) a history of inflammatory bowel disease, (**f**) previous GI surgery, (**g**) clinical signs of bowel obstruction, which would contraindicate OP and (**h**) pregnant patients.

The exclusion criteria for the GC group were: (**a**) surgery due to GC recurrence, (**b**) patient's conditions did not allow surgery to be postponed for at least 4 weeks, and (**c**) inability to participate in the prehabilitation program

due to the patient's physical or mental condition, (**d**) chemotherapy or radiotherapy within 12 months before inclusion, (**e**) use of antibiotics, pro-, pre-, or synbiotics within 1 month before inclusion, (**f**) history of any major gastrointestinal tract resections, and (**g**) current non-gastric malignancies.

The exclusion criteria for *in vitro* modelling of cancer treatment side effects study was the use of antibiotics, pro-, pre-, or synbiotics within 1 month before inclusion to the study.

2.2.2. Inclusion and Interventions

Between April 4, 2021, and November 30, 2021, 40 CRC patients were randomized to oral preparation (OP; n = 20) or rectal enema (RE; n = 20) groups. After allocation, 2 (10%) patients in the OP group were excluded due to their inability to provide stool samples on both postoperative day (POD) 06 and POD30. For preoperative MBP, patients in the OP group received 4 liters of the oral agent „Macrogol 4000 " (73.69 mg per 1 liter; Fortrans; Ipsen Pharma, Paris, France) starting the afternoon before surgery. RE was administered by 2 liters of 0.9% NaCl via an irrigator (Plasti-med, Istanbul, Turkey) the evening before surgery. All patients were given antibiotic prophylaxis before the surgery: a single dose of Cefazolin 2 g and Metronidazole 500 mg intravenously, administered 30-60 minutes before the incision. All patients received standardized surgery per the institutional protocol at the National Cancer Institute, Vilnius, Lithuania.

Between 13 April 2021 and 22 September 2022, 38 GC patients were included in the study. Patients diagnosed with distant metastases exhibited positive peritoneal cytology and no other distant metastases. After enrolment in the study, all patients underwent NAC followed by radical surgery. All patients were given antibiotic prophylaxis before the surgery: a single dose of Cefazolin 2 g and Gentamicin 240 mg intravenously. All patients received standardized surgery per the institutional protocol at the National Cancer Institute, Vilnius, Lithuania.

Between 20 April 2022 and 22 July 2024, 9 healthy donors were included in the *in vitro* modelling of cancer treatment side effects' study. Healthy donors had no history of GI cancer, other GI diseases or did not have infections, nor did they exhibit any gastrointestinal symptoms or complaints during the time of recruitment. They did not undergo any medical interventions and provided fresh stool samples for the study. In the anaerobic microbiome collection optimization and PPI model establishment parts, three (n = 3) healthy females aged 25-30 (avg. 27.7 ± 5 years) were included. In the optimization of the operation modes part of the study, two healthy females and

one healthy male (n = 3 in total) were included, aged 26-31 (avg. 28.7 ± 5 years). In the section of *in vitro* oralization modeling six healthy volunteers: three males (average age 28.0 years; range 26-29) and three females (average age 29.7 years; range 27-32) were included.

2.3. Fresh Stool Sample Collection

Fresh stool samples were collected from the CRC patients at baseline (BL) 1 day before the bowel preparation, on the POD06, and POD30. From GC patients fresh stool samples were collected at BL, before the surgery within a week after NAC (post-NAC), and 12 months after the start of the treatment, ensuring a minimum of 6 months post-surgery (post-SX). Stool samples were immediately stored at − 80 °C until the DNA extraction and other experiments were conducted. Fresh stool samples for *in vitro* modelling were collected from the study participants using anaerobic microbiome collection containers GutAlive® (MicroViable Therapeutics, Spain) according to the manufacturer's instructions and were kept in the room temperature for up to two days.

2.4. *16S rRNA* Gene Sequencing

After all samples from clinical studies were collected, fozen stool samples from the National Cancer Institute, Vilnius, Lithuania, were shipped using the dry ice to the Medical University of Graz, Graz, Austria. DNA from frozen stool samples (both clinical studies and *in vitro* modelling) and bacterial pellets (*in vitro* modelling) was extracted with the MagNA Pure LC DNA Isolation Kit III (Bacteria, Fungi) (Roche, Mannheim, Germany) or SphaeraMag® Genomic DNA Fecal Purification Kit (Procomcure Biotech, Austria) according to the manufacturer's recommendations. The samples were processed one by one in tubes to reduce the chance of cross-contamination. Library preparations and *16S rRNA* gene sequencing were conducted using the Illumina protocol. The hypervariable regions V1–V2 were selected for sequencing because they align with previous studies conducted by our group on similar samples, ensuring comparability. Furthermore, the V1-V2 primers are well-established and proven reliable for the sample type used. These regions were amplified using specifically designed primers: F-AGAGTTTGATCCTGGCTCAG; R-CTGCTGCCTYCCGTA (F-AGAGTTTGATCCTGGCTCAG, R-TGCTGCCTCCCGTAGGAGT for optimization of stool collection part of the study) and sequenced using an

Illumina MiSeq or Illumina NextSeq2000 instrument according to the application notes.

2.5. Processing of the Sequencing Data

Raw next-generation sequencing data was demultiplexed using BaseSpace Sequence Hub with the application BaseSpace DRAGEN Analysis (v1.3.0) or BCL Convert (v2.4.0). Raw sequencing data were processed using QIIME 2 tools on a local Galaxy instance [286], and quality was checked with FastQC and MultiQC. Based on the quality reports to ensure the integrity of the sequencing data and based on the quality report, forward and reverse read sequences were truncated. Truncating length, and the reads that remained after processing, filtering, and rarefying the sequencing data are presented in **Table 2.1**. Denoising was done with DADA2, made available through the QIIME2 tool [287,288]. Taxonomy was assigned based on the Silva 132 database release at 99% operational taxonomic unit level with a naïve Bayes classifier. A phylogenetic tree was built by creating a sequence alignment using MAFFT (when necessary). The resulting masked alignment was used to infer a phylogenetic tree and then root it as its midpoint using FastTree. If the phylogenetic tree was built, the resulting count table, classification, and rooted tree were imported into the R-based CBmed Microbiome Analysis Platform using the *qza_to_phyloseq()* function from the *qiime2R* package [289]. OTUs that were abundant in negative sequencing controls and Cyanobacteria were removed from further analysis as potential contaminants.

Table 2.1. Summary of the sequencing reads after filtering and rarefaction depth of the stool and bacterial pellet samples used in this study; bp – base pairs, F – forward, R – reverse, CRC – colorectal cancer, GC – gastric cancer.

Part of the study	Truncating length, bp	The number of sequencing reads				Chosen rarefaction depth
		Total	Average	Minimum	Maximum	
Clinical study including CRC patients	F-250 R-200	2,180,886	22,483	3,348	31,882	3,348
Clinical study including GC patients	F-280 R-250	13,476,299	132,120	58,842	277,248	58,842
In vitro study: Microbiome Preservation	F-250 R-200	1,588,387	33,091	13,302	74,263	13,302
In vitro study: Operation Modes	F-280 R-250	11,487,131	147,270	49,554	480,337	49,554

2.6. Sequencing Data Analysis

Alpha diversity analysis was quantified by the Richness, Shannon index, Inverse Simpson, and Evenness (and Phylogenetic Diversity) indices. Beta diversity was examined by principal coordinate analysis (PCoA) based on a on the unique fraction metric (*unifrac*), weighted unifrac (*wunifrac*), Bray-Curtis' and Jaccard's dissimilarity matrix and results were evaluated using Permutational Multivariate Analysis of Variance (PERMANOVA) using R (R Core Team, 2023, version 4.3.0) through RStudio interface. The PERMANOVA results were confirmed by the redundancy analysis (RDA), which was conducted using the vegan package. Subsequently, the Linear discriminant analysis Effect Size (LEfSe) analysis was performed to identify features that exhibit differential abundance between compared groups and to determine their effect sizes, using the *microbiomeMarker* package [290]. Subsequently, a linear model was employed to ascertain the statistical significance of the obtained results using the *lme4* package [291]. Figures were created using the *ggplotify* package [292].

2.7. *In Vitro* Model Development

2.7.1. Setup of the *In Vitro* Model

The developed *in vitro* model was based on the DASbox® mini bioreactor system (Eppendorf, Germany) consisting of four glass vessels equipped with optical and electrochemical sensors (**Fig. 2.1**). Sensors monitor key bioprocess parameters, including temperature (Eppendorf, Germany), optical cell density at 600 nm wavelength, pH, and dissolved O_2 (all Hamilton, United States) (**Table 2.2**). Process parameters of this system were automatically monitored and controlled in real-time using a specialized DASware® control 5 software (Eppendorf, Germany). Technical details and specifications of the system are presented in **Supplementary Material 1**. All materials, devices, and reagents used in this study are presented in **Supplementary Material 2-3**.

Table 2.2. Process parameters of the *in vitro* human gut microbiome model based on the DASbox® mini bioreactor system. Rpm – revolutions per minute; sL – standard liters.

Bioreactor Process Parameter	Setting/Setpoint
Temperature	37 ºC
Agitation rate	200 rpm

Bioreactor Process Parameter	Setting/Setpoint
Starting pH (medium)	5.9 ± 0.2 (at 25 ºC)
Working volume	120-200 mL
Dissolved oxygen	0%
Dissolved nitrogen	100%
N_2 destination	Submersed
Constant gas flow	1 sL/h

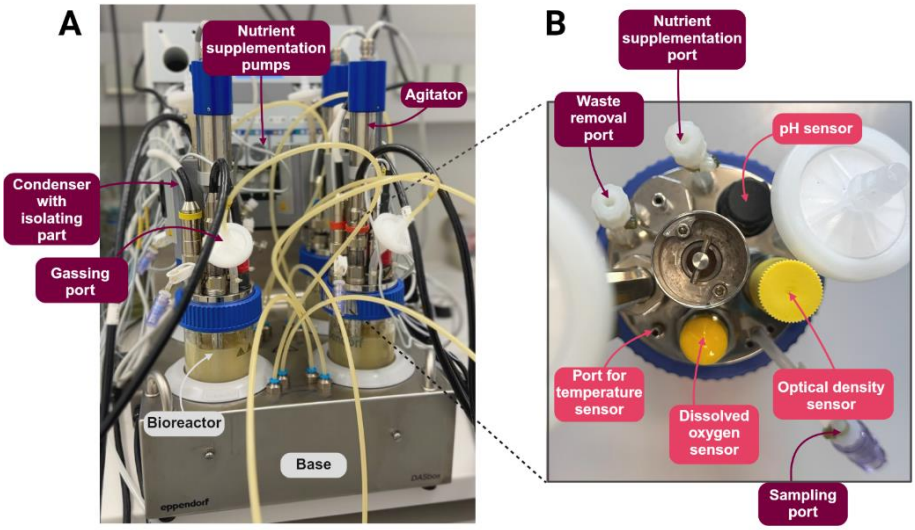

Figure 2.1. Experimental setup of the *in vitro* human gut microbiome model based on the DASbox® mini bioreactor system. (**A**) A frontal view of the base shows the bioreactor vessels connected to sensors and gassing tubing. (**B**) Top view of a bioreactor, illustrating the sensors used in this setup. Original pictures modified using *BioRender.com*.

2.7.2. Anaerobic Inoculum Preparation

Stool collection containers with the samples were opened in a Whitley A85 anaerobic workstation (Don Whitley Scientific, United Kingdom). Stool samples were mixed with Bryant and Burkey anaerobic culture medium (NutriSelect® Plus, Merck, Germany, or prepared from separate components according to **Supplementary Material 4**). The medium's anaerobic state was indicated by a visible colour change, as shown in **Fig. 2.2**.

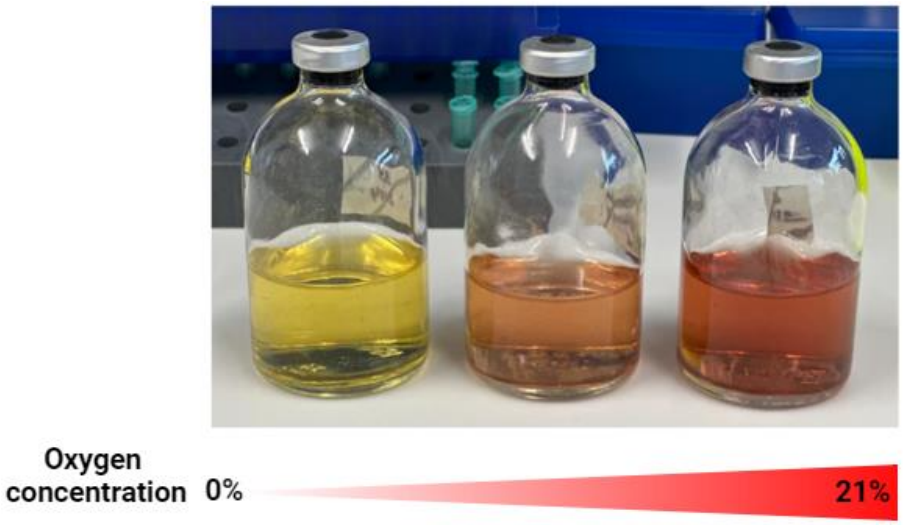

Fig. 2.2. Bryant and Burkey fermentation medium's anaerobic state was indicated visually through colour changes: yellow indicates an anaerobic medium, orange indicates oxygen contamination, and red indicates aerobic medium.

Based on the working volume of the bioreactors, 10% or 20% inoculum was prepared. Glass bottles or tubes (50 mL Polypropylene Centrifuge Tube with Flat Screw Cap, Corning, Mexico) were sealed and centrifuged at 180 x *g* for 10 min in 4ºC to sediment insoluble stool contents. Glass bottles containing the inoculum were opened in the anaerobic workstation, the supernatant was filtered from the debris using 10 µM strainer and transferred to the sterile glass inoculum tubes. Glass tubes containing inoculum were sealed, and outside the anaerobic workbench gassed for >15 s with N_2 using syringe filters (Nalgene® Syringe Filter with SFCA Cellulose Acetate Membrane or Nalgene® Syringe Filter, Sterile SFCA membrane, both Thermo Scientific, China) to increase the pressure in the tube (**Fig. 2.3**).

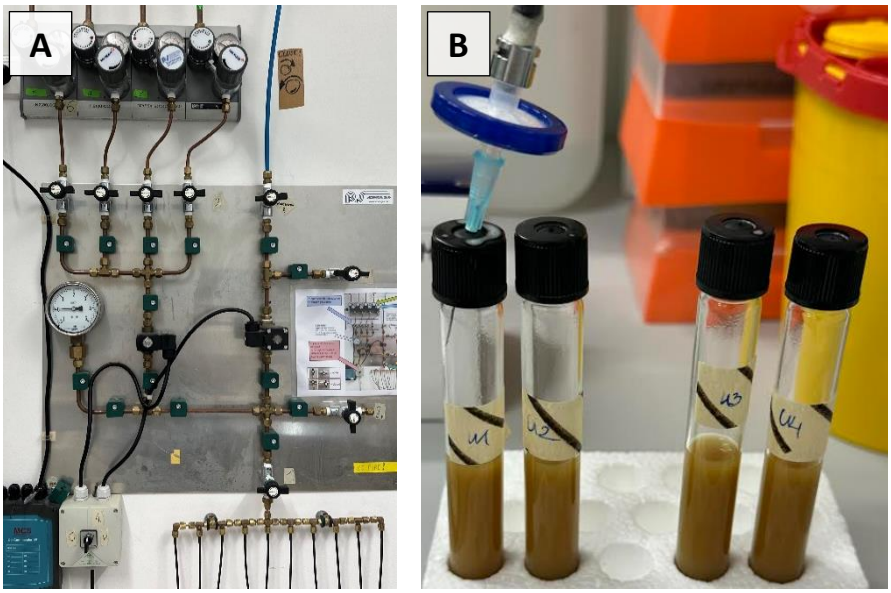

Fig. 2.3. Sterile gassing of inoculum with N_2 to create internal pressure needed for the anaerobic inoculation. (**A**) This process is carried out using a gassing station equipped with multiple valves, the capability to utilize various gases, and a vacuum function. At the end of the system, there are gassing tubes through which the gases flow. (**B**) Gassing tubes are attached to the anaerobic inoculum tube through sterile syringe filters and sterile needles.

The pressure differences between the bioreactor and the inoculum tube, caused by additional gassing step, enabled an anaerobic inoculation process. This was achieved by connecting the inoculum tube to the nutrient supplementation port of the bioreactor using a sterile needle (VACUETTE® Luer Adapter 20G sterile, Nipro Medical Industries Ltd., Japan).

2.7.3. Supplementation of Fresh Nutrients

Bryant and Burkey fermentation medium introduced fresh nutrients daily to enhance the cultivated gut microbiome beginning 24 hours after inoculation. Observations indicated that the microbiome reaches a stable composition at this timepoint. Thus, interventions (medium exchange, supplementation) were started at this timepoint. Four different nutrient supplementation strategies (*further* – operation modes) were tested: (**1**) batch operation mode, where no culture medium was added or removed throughout culture time; (**2**) continuous operation mode with the fresh nutrient flow (along with waste removal) of ~3 mL/hour rate; (**3**) semi-continuous operation

mode with 50% medium exchange daily; (**4**) semi-continuous operation mode with 25% medium exchange twice daily, with an 8-hour interval between exchanges. The semi-continuous medium exchange procedure is illustrated in **Fig. 2.4**.

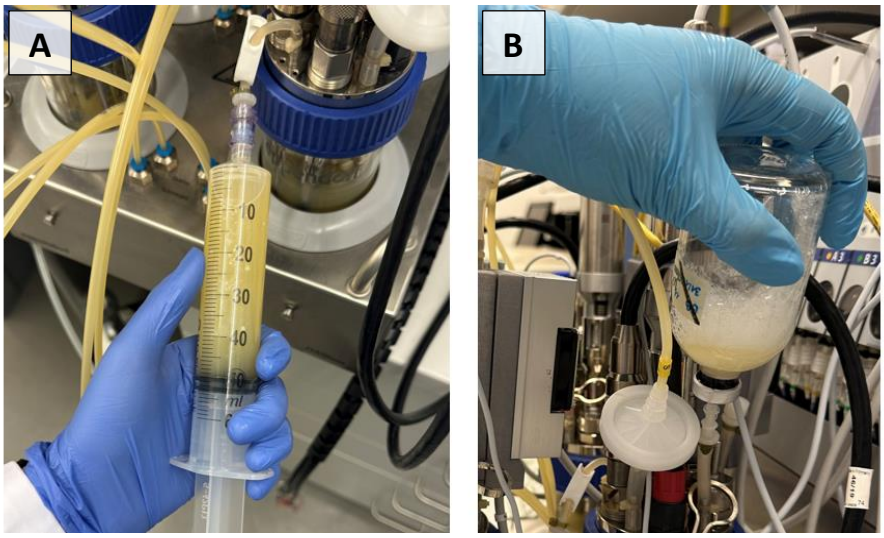

Fig. 2.4. The process of anaerobic semi-continuous medium exchange by (**A**) removal of the medium with bacteria and waste products from the bioreactors and (**B**) anaerobic supplementation with fresh medium through a needle that is attached to the nutrient supplementation port. The flow of medium from the glass flask into the bioreactors was accomplished due to pressure differences between the flask and the bioreactors. Consequently, there is no oxygenation throughout this process.

2.7.4. Spiking

The gut microbiome oralization model was established by introducing oral bacteria, specifically *Veillonella parvula* and *Streptococcus salivarius*, into the bioreactors. The oralization biomarkers were selected based on the previous study [6]. The oral bacteria used for spiking were pre-cultivated overnight for *S. salivarius* and 48 hours for *V. parvula*. The composition of the oral bacteria pre-culturing medium is provided in **Supplementary Material 5**. The concentration of oral bacteria cultures and total bacteria in the bioreactors was determined using QUANTOM™ Total Cell Staining Kit and QUANTOM Tx™ Microbial Cell Counter (Logos Biosystems, South Korea), according to the manufacturer's recommendations. The spiking

procedure was integrated with a semi-continuous medium exchange occurring once daily. Following clinical data, the spiking concentration for *V. parvula* was 0.2%, and for *S. salivarius*, it was 0.6% of the total calculated bacteria concentration in the bioreactors. To mimic various scenarios, four different spiking strategies were chosen: (**i**) spiking once after inoculation; (**ii**) spiking once 48 h after inoculation; (**iii**) spiking every day, starting after inoculation; (**iv**) spiking every day, starting 48 h after inoculation. Samples from the DASbox® mini bioreactor system were collected at 24-hour intervals throughout the 120-hour cultivation period.

2.7.5. Supplementation with Probiotic Products

Five different products were used for the supplementation of the microbiome. Tested products included (**i**) placebo control, (**ii**) corn starch control, (**iii**) probiotic, (**iv**) prebiotic, and (**v**) a combination of probiotic and prebiotic products. Two grams of each product were weighed, added to a glass flask of fresh anaerobic feeding medium, and mixed. This step was done in the anaerobic chamber to avoid contamination with the O_2. Prepared glass flasks were gassed with an anaerobic gas mixture to ensure anaerobic conditions. This step was done using the four-eye principle, where an independent staff member observed the preparation of the supplementation medium and feeding procedure.

Tested probiotics were obtained from Winclove Probiotics, Amsterdam, The Netherlands, and contained a mixture of the following bacteria (information about the strains is confidential at the time of doctoral dissertation preparation): *Lactobacillus plantarum*, *Bifidobacterium animalis*, *Lactobacillus acidophilus*, *Lactobacillus casei*, *Lactobacillus rhamnosus*, *Pediococcus acidilactici*; tested prebiotics were fructooligosaccharides.

2.7.6. Quality Control of Supplementation Products

To maintain quality control, in cooperation with an independent researcher, we employed a four-eye principle to verify the sterility of the placebo and the viability of the probiotic strains in the study product. The independent researcher plated the supplementation products with sterile cotton swabs on a sterile Bryant and Burkey agar medium. Additionally, an open Petri dish was left to confirm the sterility of the environment in which the products were tested, and a clean cotton swab was used to test the sterility of the swabs. All plates were then anaerobically incubated for 48 hours at 37°C. The suitability of the supplementation products was confirmed when placebo control, starch

control, prebiotic products showed no growth, and probiotic-containing products exhibited growth. Any samples in doubt were further analyzed using the Matrix-assisted laser desorption/ionization (MALDI-TOF) method by independent researchers.

2.7.7. DNA Extraction

DNA extraction for quantitative polymerase chain reaction (qPCR) was performed by mixing bacterial pellets with 180 µL TRIS-HCl lysis buffer (**Supplementary Material 6**) and transferring them into tubes (1.5 mL SC Micro Tube PCR-PT, SARSTEDT, Germany) containing glass pellets (Assistent, Germany), which were subjected to oscillation by MagNa Lyser (Roche Company, Penzberg, Germany) for 45 s 6500 x *g*. DNA from the bacterial pellets was further extracted using DNeasy Blood & Tissue Kit (QIAGEN, Valencia, CA, USA), according to the manufacturer's instructions. DNA purity and concentration were measured by NanoDrop™ 2000/2000c spectrophotometer (Fisher Scientific, USA). The final DNA concentration employed for qPCR was set at 2.5 ng/µL.

2.7.8. Quantitative Polymerase Chain Reaction

QPCR was employed to ascertain the abundance of oral bacteria in the DASbox® mini bioreactor system (Eppendorf, Germany). The qPCR analyses were conducted using the Bio-Rad CFX instrument and Bio-Rad CFX Maestro software (v1.1) from Bio-Rad, USA. Primer sequences used for oral bacteria detection, data normalization, composition of the PCR reaction mixtures, and temperature regimes are provided in **Table 2.3-2.5**. All samples underwent duplicate testing to ensure the results' reliability and consistency.

Table 2.3. Sequences of primers used for the testing of oral bacteria abundance in the bioreactors and data normalization; F – Forward primer, R – Reverse primer, bp – base pairs.

	PMID		**Primer sequence**	**Amplicon size, bp**
Veillonella parvula	27326455	F	GTAACAAAGGTGTC GTTTCTCG	311
		R	CGTAACATCTTCCG AAACTTTC	

	PMID	Primer sequence		Amplicon size, bp
Streptococcus salivarius	30022122	F	TGAACAAGCRGTWG TCGGTAAC	108
		R	ACTCCGTGTCCAAC CAAATC	
16S rRNA gene F1048/R1194		F	GTGSTGCAYGGYTG TCGTCA	146
		R	ACGTCRTCCMCACC TTCCTC	

Table 2.4. Components of the quantitative polymerase chain reaction for testing oral bacteria abundance in the bioreactors and data normalization; F – Forward primer, R – Reverse primer.

Reaction component	Final concentration per well		
	V. parvula	***S. salivarius***	***16S rRNA* gene**
GoTaq® qPCR Master Mix	0.75x	0.5x	0.7x
Primer Mix (F + R)	0.05 µM	0.05 µM	0.05 µM
Nuclease Free Water	-	-	-
DNA sample	0.25 ng/µL	0.5 ng/µL	0.25 ng/µL
Final volume per well (µL)	10	10	10

Table 2.5. Temperature regimes that were used for quantitative polymerase chain reaction to test the abundance of oral bacteria in the bioreactors and data normalization.

Process	Temperature (°C)	Time	Cycles
Streptococcus salivarius			
UDG Activation	50	2 min	35
DNA polymerase activation	95	10 min	
Denaturation	95	15 sec	
Annealing/Extension	60	1 min	
Melting Curve	55 to 95	Increment 1 °C	
Veillonella parvula			
DNA polymerase activation	95	3 min	

Process	Temperature (°C)	Time	Cycles
Denaturation	95	30 sec	36
Annealing	53	30 sec	
Extension	72	1 min 30 sec	
Melting Curve	55 to 95	Increment 0.5 °C	
	***16S rRNA* gene**		
DNA polymerase activation	95	10 min	39
Denaturation	95	15 sec	
Annealing/Extension	60	1 min	
Melting Curve	60 to 95	Increment 1 °C	

2.8. Statistical Analysis

Statistical analysis of clinical parameters was performed using IBM SPSS Statistics (IBM Corp., Chicago, IL, USA, version 29.0.1.0). The Shapiro-Wilk test was used to test normality. Categorical variables were compared using the Chi-squared or Fisher exact test, while continuous variables were assessed using the Mann-Whitney U test. Spearman's rank correlation coefficient was employed to investigate relationships between the variables. The Log-rank test evaluated the predicted infection probability between MBP groups in the CRC patient cohort. A linear model was employed to ascertain the statistical significance of the obtained qPCR results using the *lme4* package [291] in R. A level of $p < 0.05$ was used to determine statistical significance.

3. RESULTS

3.1. Effect of Preoperative Treatment and Surgery

At first, the effects of preoperative interventions in cancer treatment on the gut microbiome composition and postoperative outcomes were determined. In this case, CRC patients that were recruited for left-sided CRC surgery underwent two types of MBP – RE or OP, and after that received surgery. Stool samples were collected before treatment, POD06 and POD30, to determine if the bowel preparation effect on the gut microbiome is lasting.

The alpha diversity determined by Richness, Shannon, Inverse Simpson index, and Evenness was not significantly different between the OP and RE groups throughout the study. The alpha diversity slightly decreased in the OP group on POD06 and POD30 but not in the RE group. The most notable alterations were observed in the Evenness and Inverse Simpson index (**Fig. 3.1**, **Table 3.1**).

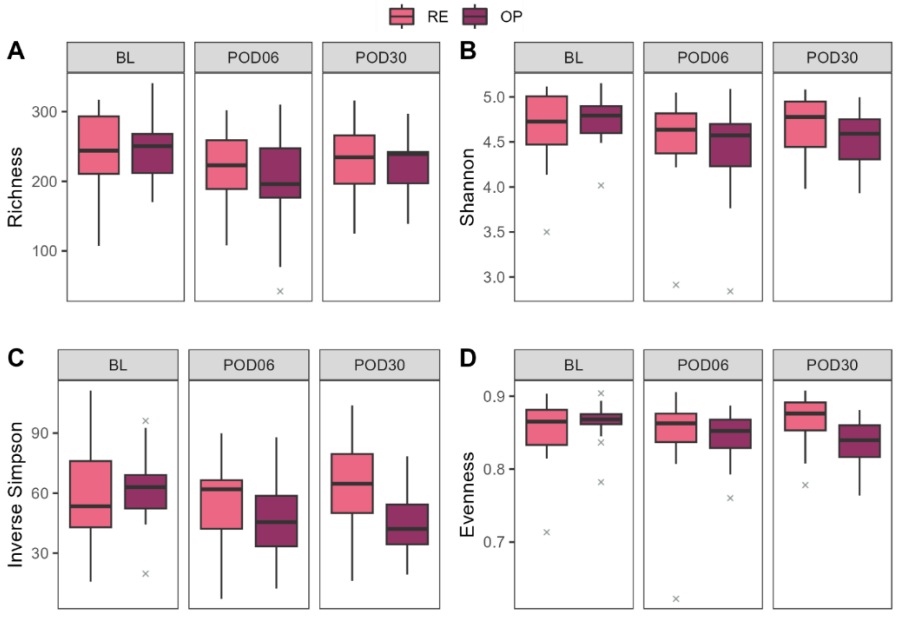

Fig. 3.1. Changes of alpha-diversity parameters in patients undergoing bowel preparation before left-side colorectal resection; outliers are marked in grey; RE – rectal enema, OP – oral preparation method. Alpha-diversity parameters: (**A**) Richness, (**B**) Shannon index, (**C**) Inverse Simpson index, (**D**) Evenness.

Table 3.1. Linear mixed-effects model results for alpha-diversity parameters. The table presents the estimates, standard errors (S.E.), t-values (t val.), degrees of freedom (d.f.), and *p*-values for four alpha diversity indices: Richness, Shannon, Inverse Simpson, and Evenness. MBP – mechanical bowel preparation. The linear mixed-effects model suggests that the factors MBP and Timepoint, as well as their interaction, do not have statistically significant effects on the assessed diversity indices, except for a marginal trend in the case of the Evenness.

Source of variation	**Est.**	**S.E.**	***t* val.**	**d.f.**	***p*-value**
Richness index					
MBP	-7.04	15.56	-0.45	69.15	0.65
Timepoint	-0.39	0.66	-0.58	69.57	0.56
MBP*Timepoint	0.13	0.91	0.15	65.83	0.88
Shannon index					
MBP	0.00	0.11	-0.04	76.20	0.97
Timepoint	0.00	0.00	0.16	73.57	0.87
MBP*Timepoint	-0.01	0.01	-0.80	69.63	0.43
Inverse Simpson index					
MBP	-1.36	5.99	-0.23	70.30	0.82
Timepoint	0.08	0.26	0.32	70.72	0.75
MBP*Timepoint	-0.52	0.35	-1.49	67.10	0.14
Evenness index					
MBP	0.01	0.01	0.70	75.99	0.49
Timepoint	0.00	0.00	0.81	73.29	0.42
MBP*Timepoint	0.00	0.00	-1.79	69.31	0.08

Baseline beta diversity was comparable between the study groups (p = 0.226). Primary outcome analysis showed no difference in beta diversity on POD06 between the study groups (p = 0.198). Similarly, no differences were observed on POD30 (p = 0.310) (**Fig. 3.2A**).

Despite the lack of differences between the study groups, both interventions for MBP (OP or RE) followed by colorectal resection resulted in significant alterations in gut microbiome composition at POD06 compared to baseline (p = 0.001). These differences remained significant 30 days after surgery compared to baseline (p = 0.001) (**Fig. 3.2B**). Comparison of POD06 and POD30 also showed significant differences (p = 0.002). Visual examination of the graphs alongside the accompanying statistical data reveals

that the MBP-induced changes in microbiome composition start to recover over time. However, this recovery process may necessitate a duration longer than 30 days.

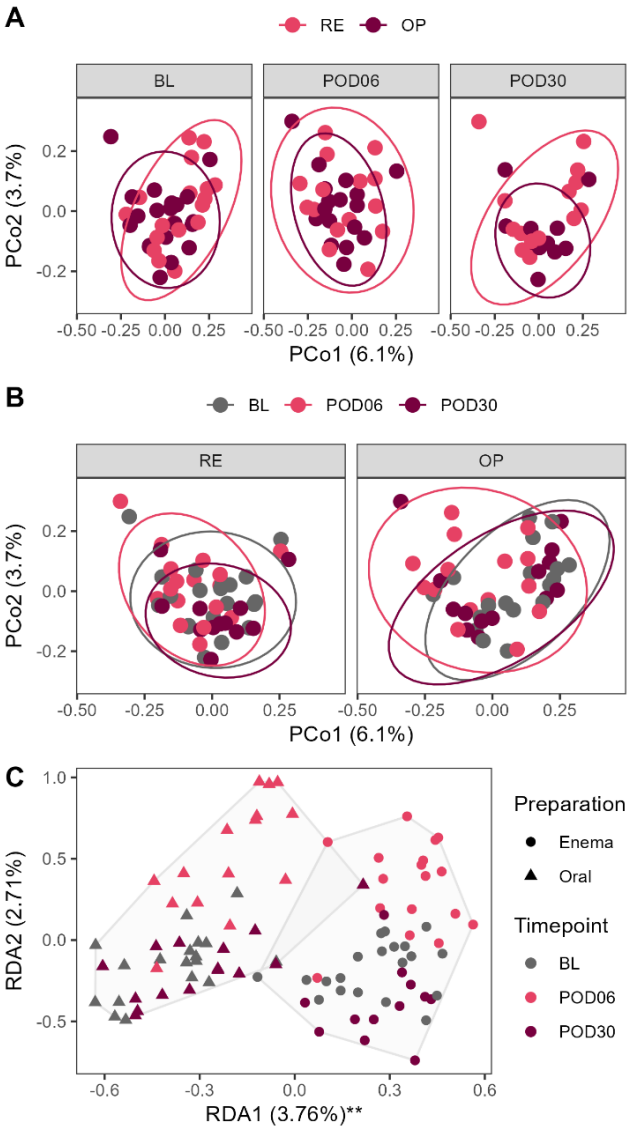

Fig. 3.2. Principal coordinate (PCo) analysis plot based on Bray–Curtis' dissimilarity (**A**, **B**). BL – baseline, POD – postoperative day, RE – rectal enema, OP – oral preparation method. PCo1 and PCo2 correspond to the first and second principal coordinates, derived from the Bray–Curtis dissimilarity matrix. These axes capture major variations in microbiome composition

between samples. (**C**) Redundancy analysis (RDA) of the microbiome composition shows a significant impact of MBP on the microbiome composition. RDA1 and RDA2 represent the first and second axes of redundancy analysis, summarizing the relationships between MBP groups and microbial community composition.

The LEfSe analysis, coupled with linear model analysis, unveiled significant shifts in the microbiome throughout the study in both groups. In the case of MBP with RE followed by resection, there was an increase in the abundance of *Actinomyces*, *Enterococcus*, *Parabacteroides*, and *Ruminococcus* 2 genera in the short-term (POD06 *vs.* BL) post-intervention. However, most of these changes reverted to BL by POD30, except for the *Ruminococcus* 2 genus, which exhibited further increased abundance on POD30 (**Fig. 3.3**).

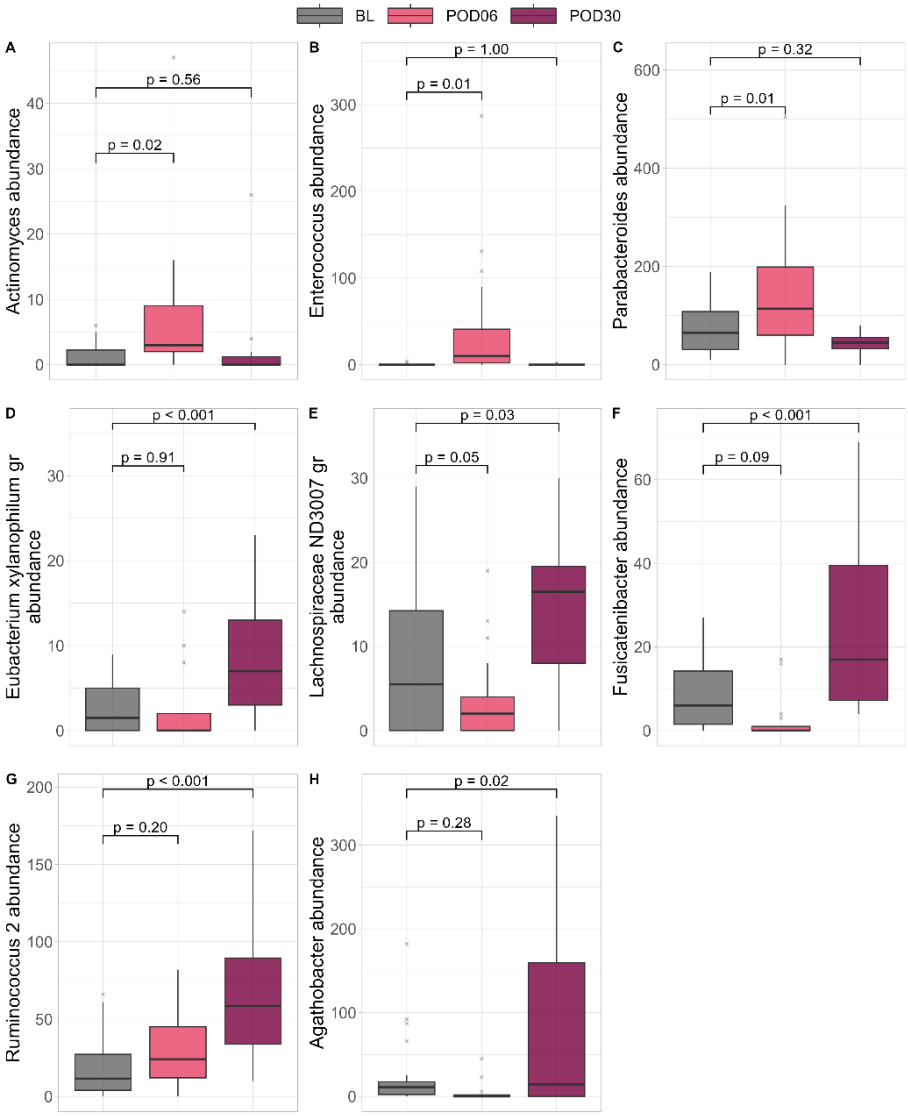

Fig. 3.3. Comparative assessment of genera abundance in the RE group between different time points (compared to the BL) using Linear discriminant Effect Size (LEfSe) analysis. A linear model was employed to ascertain the statistical significance of the obtained results ($p < 0.05$). **(A-H)** Distribution of selected genera throughout the 30-day follow-up period in the RE group. BL – baseline, POD – postoperative day.

In the OP group, interventions led to a temporary decrease in *Dialister* genus abundance, observed at POD06, which returned to BL levels by POD30. Persistent changes detected at both POD06 and POD30 included a decrease in

Porphyromonas and an increase in *Citrobacter* genera. Moreover, the prolonged impact of OP, measured at POD30, showed an increased abundance of *Eubacterium coprostanoligenes*, *Eubacterium hallii* group, and *Collinsella* genera (**Fig. 3.4**).

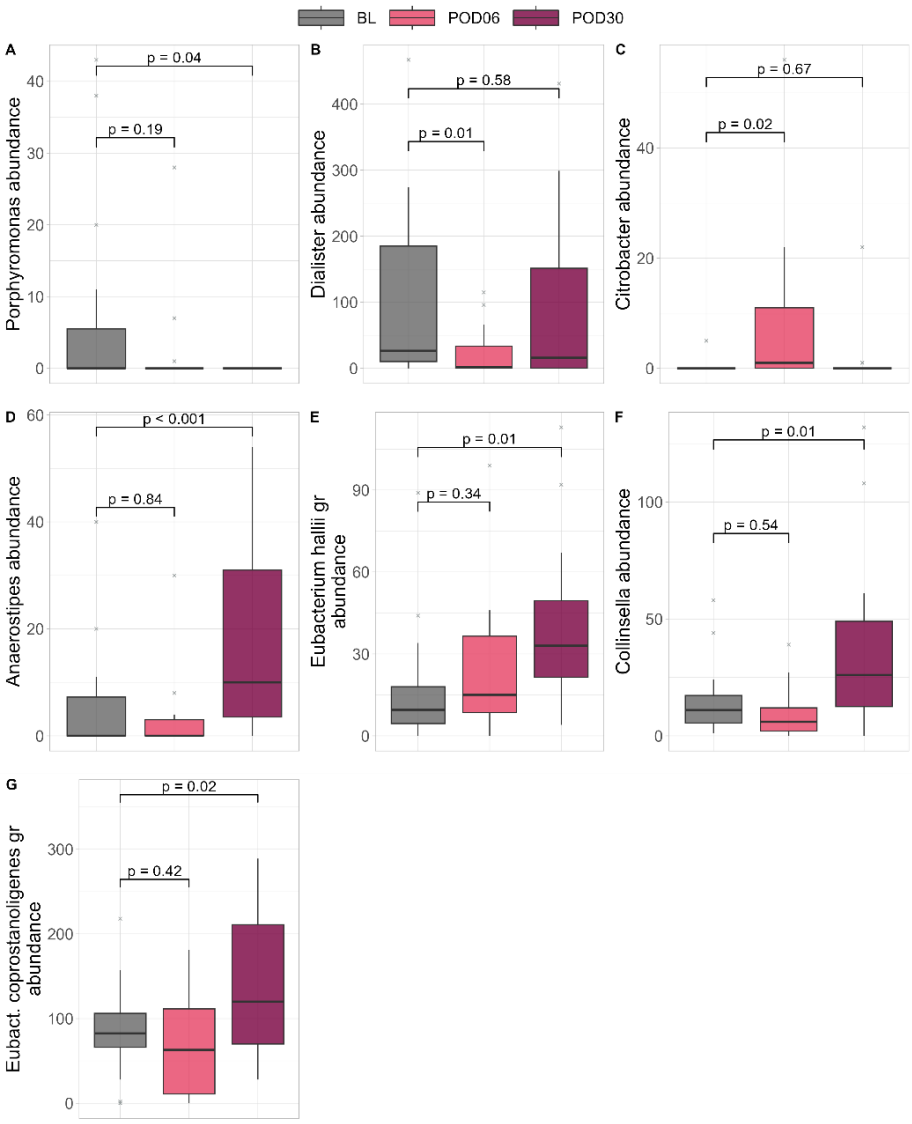

Fig. 3.4. Comparative assessment of genera abundance in the OP group between different time points (compared to the BL) using Linear discriminant analysis Effect Size (LEfSe) model analysis. A linear model was employed to ascertain the results' statistical significance ($p < 0.05$). (**A-G**) Distribution of

selected genera throughout the 30-day follow-up period in the OP group. BL – baseline, POD – postoperative day.

The analysis of the association between gut microbiome changes and postoperative infections was conducted as well. Patients suffering postoperative infections (irrespective of the MBP method) showed a higher abundance of Pseudomonadales and Actinomycetales orders, Actinobacteria class, Actinomycetaceae family, *Actinomyces* genus, uncultured *Sutterella*, and *Enterococcus faecalis* species on POD06 compared to patients that did not develop post-operative infection (**Fig. 3.5**).

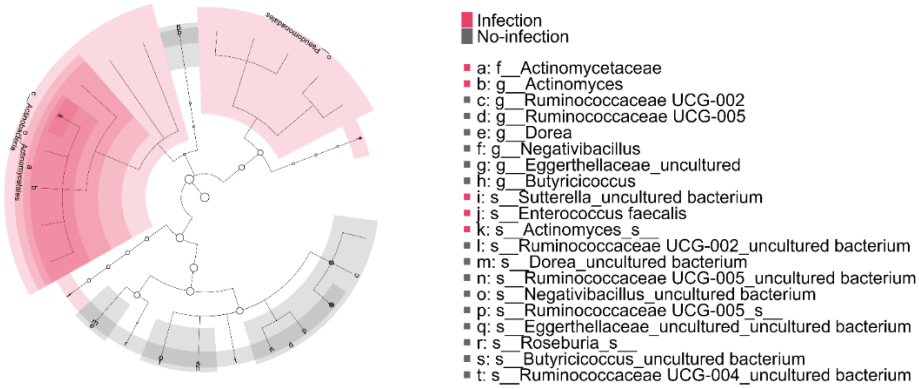

Fig. 3.5. Link between postoperative infection and gut microbiome changes: cladogram analysis of POD06 samples in CRC patients, according to the infection status.

3.2. Effect of Neoadjuvant Chemotherapy and Gastrectomy

Next, we aimed to determine how NAC, followed by surgical treatment, can impact the gut microbiome composition. This part of the study focused on elucidating the changes in the gut microbiome throughout GC treatment and delineating the specific effects of NAC and radical surgery. These insights suggest that targeting the gut microbiome could be a promising therapeutic approach to enhance the quality of life and overall health in cancer patients undergoing treatment and long-term survivors.

Alpha diversity was measured as Richness, Shannon, Inverse Simpson indices, Evenness, and Phylogenetic Diversity. Interestingly, this part of the study revealed that NAC did not affect alpha diversity parameters, whereas surgery significantly affected Richness, Shannon index, and Phylogenetic Diversity (all $p < 0.001$ **Fig. 3.6**, **Table 3.2**).

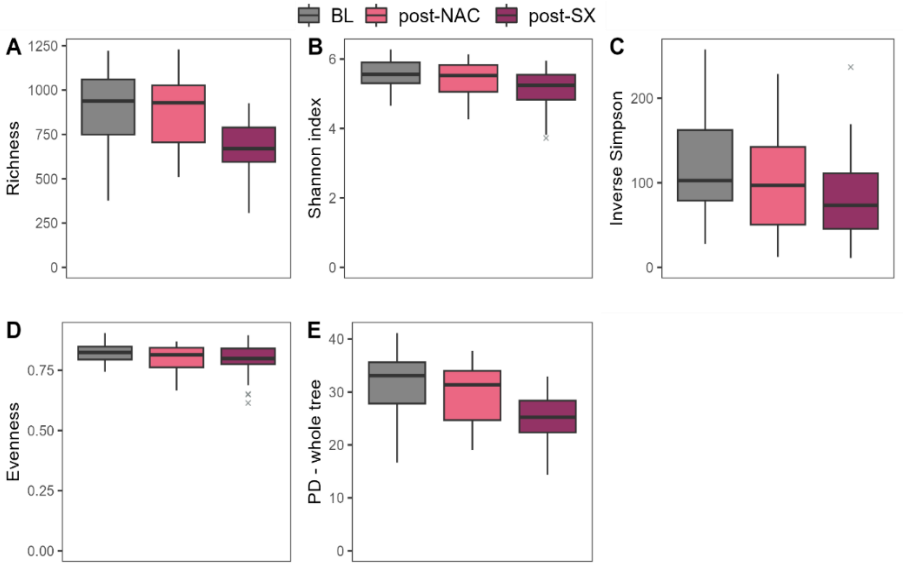

Fig. 3.6. Changes of alpha-diversity parameters in patients undergoing advanced gastric cancer treatment; outliers are marked in grey; Alpha-diversity parameters: (**A**) Richness, (**B**) Shannon index, (**C**) Inverse Simpson index, (**D**) Evenness, (**E**) Phylogenetic Diversity (PD). BL – baseline, NAC – neoadjuvant chemotherapy, SX – surgery.

Table 3.2. Linear mixed-effects model results for alpha-diversity parameters. The table presents the estimates, standard errors (S.E.), t-values (t val.), degrees of freedom (d.f.), and p-values for five alpha diversity indices: Richness, Shannon, Inverse Simpson, and Evenness, and PD—whole tree. It compares baseline (BL) and gastrectomy (SX – surgery) with neoadjuvant chemotherapy treatment.

Source of variation	**Est.**	**S.E.**	***t* val.**	**d.f.**	***p*-value**
		Richness index			
BL	21.408	41.229	0.519	64.068	0.605
post-SX	-206.852	43.085	4.801	65.468	**<0.0001**
		Shannon index			
BL	0.158	0.105	1.504	64.327	0.137
post-SX	-0.278	0.110	-2.524	65.535	**0.014**
		Inverse Simpson index			
BL	13.679	10.886	1.257	65.169	0.213
post-SX	-20.512	11.397	-1.800	65.881	0.076
		Evenness index			

Source of variation	Est.	S.E.	*t* val.	d.f.	*p*-value
BL	0.021	0.011	1.837	65.003	0.071
post-SX	-0.009	0.012	0.791	66.111	0.432
		PD – whole tree			
BL	1.828	1.076	1.699	64.891	0.094
post-SX	-4.786	1.126	-4.252	65.923	**<0.0001**

Beta diversity analysis, using principal coordinate analysis (PCoA) based on the unique fraction metric (*unifrac*), weighted unifrac (*wunifrac*), Bray-Curtis, and Jaccard's dissimilarity, showed a significant difference between post-surgery and post-NAC timepoints (all $p = 0.001$) (**Fig. 3.7**, **Table 3.3**). Redundancy analysis confirmed the profound impact of radical surgery on the gut microbiome changes ($p = 0.014$).

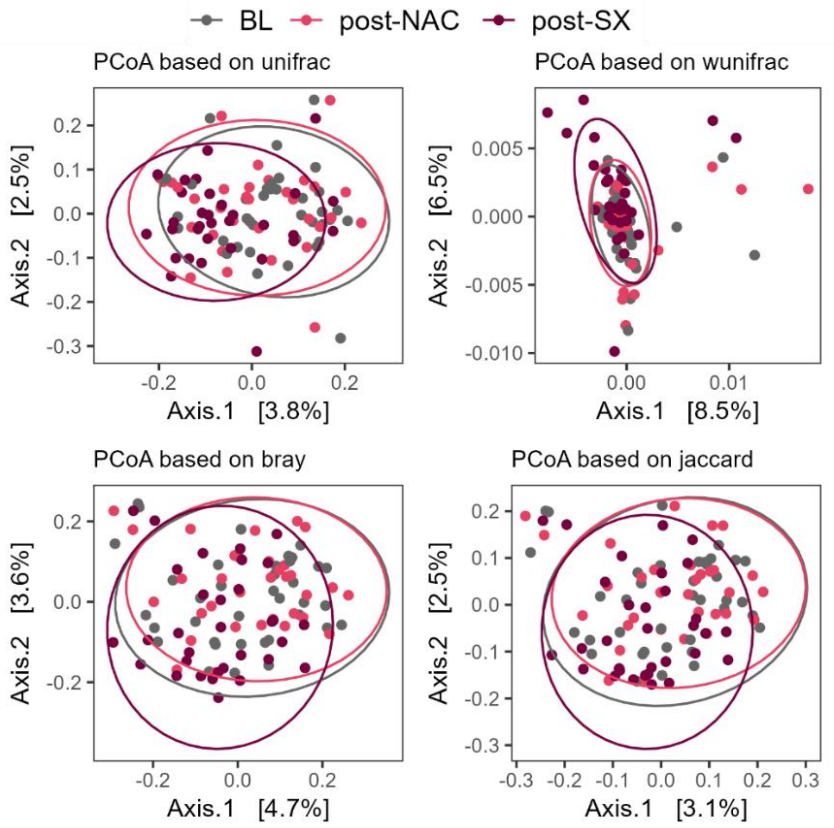

Fig. 3.7. Changes of beta-diversity parameters in patients undergoing chemotherapy and surgery combined with chemotherapy; BL – baseline, NAC – neoadjuvant chemotherapy, SX – surgery.

Table 3.3. PERMANOVA analysis results of microbiome composition changes throughout the treatment of gastric cancer.

Source of variation	d.f.	Sum of sq.	R^2	F	*p*-value
BASELINE *vs.* NAC					
PCoA analysis based on unifrac					
Treatment Timepoint	1	0.2671	0.01045	0.7182	0.055
PCoA analysis based on wunifrac					
Treatment Timepoint	1	0.000073	0.00786	0.5388	0.537
PCoA analysis based on bray					
Treatment Timepoint	1	0.2226	0.00832	0.5708	0.420
PCoA analysis based on jaccard					
Treatment Timepoint	1	0.3031	0.01005	0.6901	0.375
NAC *vs.* GASTRECTOMY					
PCoA analysis based on unifrac					
Treatment Timepoint	1	0.4726	0.02017	1.2761	**0.001**
PCoA analysis based on wunifrac					
Treatment Timepoint	1	0.0002823	0.03065	1.9607	**0.001**
PCoA analysis based on bray					
Treatment Timepoint	1	0.5858	0.02313	1.4678	**0.001**
PCoA analysis based on jaccard					
Treatment Timepoint	1	0.548	0.0195	1.233	**0.001**

The study showed the gut microbiome composition changed throughout the treatment of GC (**Fig. 3.8**). At the phylum level, NAC treatment did not alter the microbiome composition. In contrast, radical surgery led to an increased abundance of Bacteroidetes ($p = 0.004$) and Proteobacteria ($p < 0.0001$) and a decreased abundance of Firmicutes ($p < 0.0001$) and Actinobacteria ($p = 0.001$) compared to NAC (**Table 3.4**).

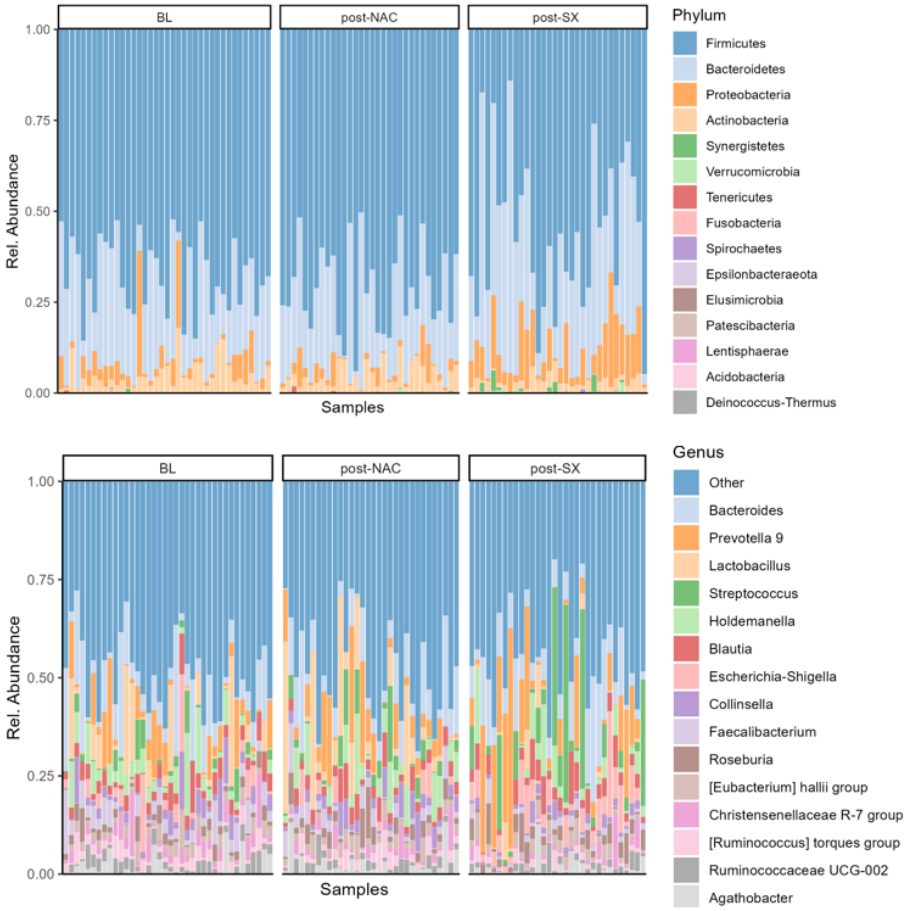

Fig. 3.8. Bacterial composition of the gut microbiome at the phylum and genus levels at different treatment timepoints; BL – baseline, NAC – neoadjuvant chemotherapy, SX – surgery.

Table 3.4. Linear mixed-effects model results for the relative abundance of the most common phylum, when the effect of NAC is compared to the baseline (BL) and surgery (SX). The table presents the estimates, standard errors (S.E.), t-values (t val.), degrees of freedom (d.f.), and *p*-values.

Source of variation	**Est.**	**S.E.**	***t* val.**	**d.f.**	***p*-value**
			Firmicutes		
BL	-0.036	0.034	-1.068	68.856	0.289
post-SX	-0.157	0.036	-4.407	70.517	**<0.0001**
			Bacteroidetes		
BL	0.013	0.031	0.431	68.509	0.668

Source of variation	Est.	S.E.	*t* val.	d.f.	*p*-value
post-SX	0.098	0.033	2.999	69.745	**0.004**
		Proteobacteria			
BL	0.022	0.015	1.466	99.000	0.146
post-SX	0.072	0.015	4.644	99.000	**<0.0001**
		Actinobacteria			
BL	-0.001	0.007	-0.193	64.098	0.848
post-SX	-0.023	0.007	-3.382	64.894	**0.001**

At the genus level, NAC treatment resulted in a significant decrease in the *Christensenellaceae R-7* group ($p = 0.041$) compared to BL samples. In contrast, radical surgery led to an increase in *Prevotella 9* ($p = 0.022$), *Streptococcus* ($p = 0.010$), and *Escherichia-Shigella* ($p = 0.001$). Radical surgery also caused a decrease in *Lactobacillus* ($p = 0.008$), *Collinsella* ($p = 0.005$), *Faecalibacterium* ($p = 0.030$), and the *Ruminococcus torques* group ($p = 0.006$) (**Fig. 3.8**, **Table 3.5**).

Table 3.5. Linear mixed-effects model results for the relative abundance of the most common genera when the effect of NAC is compared to the baseline (BL) and radical surgery (SX). The table presents the estimates, standard errors (S.E.), t-values (t val.), degrees of freedom (d.f.), and p-values.

Source of variation	Est.	S.E.	*t* val.	d.f.	*p*-value
		Bacteroides			
BL	0.010	0.016	0.593	64.741	0.555
post-SX	0.009	0.017	0.534	65.513	0.595
		Prevotella 9			
BL	-0.008	0.019	-0.414	67.248	0.680
post-SX	0.047	0.020	2.337	68.025	**0.022**
		Lactobacillus			
BL	-0.020	0.019	-1.040	61.598	0.302
post-SX	-0.055	0.020	-2.736	63.081	**0.008**
		Streptococcus			
BL	-0.013	0.018	-0.691	66.891	0.492
post-SX	0.051	0.019	2.642	68.131	**0.010**
		Holdemanella			
BL	-0.005	0.010	-0.441	67.572	0.661
post-SX	-0.014	0.011	-1.264	68.576	0.211
		Blautia			
BL	0.000	0.005	0.079	62.209	0.937
post-SX	0.003	0.005	0.555	62.490	0.581

Source of variation	Est.	S.E.	*t* val.	d.f.	*p*-value
Escherichia-Shigella					
BL	0.010	0.011	0.935	99.000	0.352
post-SX	0.037	0.011	3.386	99.000	**0.001**
Collinsella					
BL	-0.001	0.006	-0.196	64.197	0.845
post-SX	-0.017	0.006	-2.917	65.065	**0.005**
Faecalibacterium					
BL	0.010	0.005	1.948	65.900	0.056
post-SX	-0.012	0.005	-2.214	66.492	**0.030**
Roseburia					
BL	-0.007	0.006	-1.141	70.964	0.258
post-SX	0.004	0.006	0.592	72.703	0.555
Eubacterium hallii					
BL	0.000	0.004	0.033	67.796	0.974
post-SX	-0.001	0.004	-0.396	68.851	0.693
Christensenellaceae R-7 group					
BL	0.010	0.005	2.089	65.425	**0.041**
post-SX	-0.002	0.005	-0.457	65.691	0.649
Ruminococcus torques group					
BL	-0.001	0.004	-0.177	61.410	0.860
post-SX	-0.012	0.004	-2.864	62.994	**0.006**
Ruminococcaceae UCG-002 group					
BL	0.004	0.003	1.130	64.525	0.263
post-SX	-0.002	0.004	-0.621	65.713	0.537
Agathobacter					
BL	-0.005	0.007	-0.691	61.987	0.492
post-SX	-0.008	0.007	-1.180	64.035	0.242

LEfSe corroborated these findings, showing that after surgery, patients exhibited an enriched microbiome with an increased abundance of *Escherichia-Shigella*, *Streptococcus equinus*, uncultured *Streptococcus* bacterium, and Enterobacteriaceae species (**Fig. 3.9**). Additionally, ANCOM validated these results by demonstrating that post-surgery patients had higher levels of *Escherichia-Shigella* and lower levels of *Faecalibacterium* and the *Ruminococcus torques* group genera.

Fig. 3.9. The primary microbiome differences between post-surgery (post-SX) and post-neoadjuvant chemotherapy (post-NAC) treatment in patients with advanced gastric cancer.

This part of the study indicated significant changes in the gut microbiome during GC treatment, driven primarily by radical surgery rather than NAC. NAC alone did not impact the gut microbiome composition at the phylum level. In contrast, radical surgery led to an increased abundance of Bacteroidetes and Proteobacteria phylum and a decreased abundance of Firmicutes and Actinobacteria phylum. Furthermore, NAC did not affect alpha or beta diversity, whereas radical surgery impacted both. The microbiome composition after radical surgery was enriched with oralization-associated bacteria, as LEfSe analysis showed an increased abundance of

Escherichia-Shigella, Streptococcus equinus, and uncultured bacterium *Streptococcus* species, and species from Enterobacteriaceae family.

3.3. Development of *In Vitro* Model of Cancer Treatment Side Effects

Based on the results from clinical studies, it was observed that surgical treatment can significantly impact the gut microbiome composition and possible side effects. One of the most interesting observations was the increase of oralization-associated bacteria. This effect could be observed in different cancer treatment strategies, such as long-term usage of PPI and surgery. It was decided to try to develop *in vitro* model of this cancer-treatment side effect, and to test various probiotic products in order to decrease the oralization and possibly increase the quality of life of GI cancer patients.

3.3.1. Optimization of Anaerobic Microbiome Collection Procedure

The first step of an *in vitro* oralization model development was to optimize stool sampling conditions to preserve native microbiome composition from the collected stool samples effectively. An anaerobic microbiome kit GutAlive® was used for the stool collection procedure. Stool samples were stored in four containers for four different timepoints: <1 hour, 2, 24, and 48 hours after the sampling. The inoculum was prepared under anaerobic conditions and cultured in the DASbox® mini bioreactor system for 120 hours. This cultivation was conducted employing a continuous operation mode with a retention time of 28.3 h [293] under anaerobic conditions. The analysis did not reveal differences in process parameters based on the stool storage time in the GutAlive® stool collection containers.

The alpha diversity, measured through Richness, Shannon, Inverse Simpson, Evenness, and Phylogenetic Diversity decreased during the culture time (all $p \leq 0.002$). Importantly, these changes were independent of the stool storage time in the microbiome collection container (all $p > 0.050$; **Fig.3.10**, **Table 3.6**).

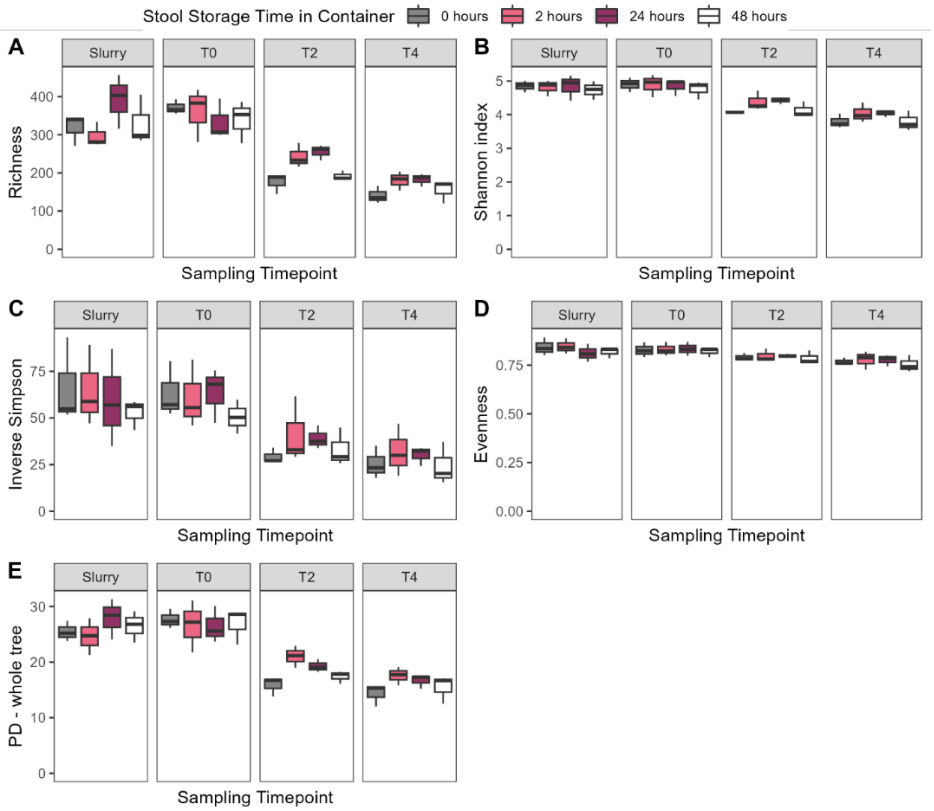

Fig. 3.10. Changes in the microbiome composition of the samples stored in the GutAlive® microbiome collection kit containers for different times (0-48 h) and cultured in the DASbox® mini bioreactor system for 96 hours. Slurry – inoculum, T0 – sampling at 0 hours after inoculation, T2 – sampling at 48 hours after inoculation, T4 – sampling at 96 hours after inoculation. Alpha-diversity parameters: (**A**) Richness, (**B**) Shannon index, (**C**) Inverse Simpson index, (**D**) Evenness, (**E**) Phylogenetic Diversity (PD).

Table 3.6. Linear mixed-effects model results for alpha-diversity parameters. The table presents the estimates, standard errors (S.E.), t-values (t val.), degrees of freedom (d.f.), and p-values for five alpha diversity indices: Richness, Shannon, Inverse Simpson, Evenness, and Phylogenetic Diversity (PD).

Source of variation	**Est.**	**S.E.**	***t* val.**	**d.f.**	***p*-value**
		Richness index			
Stool Storage Time	-0.591	0.605	-0.978	32.000	0.336
Culture Time	-2.069	0.262	-7.896	32.000	**<0.0001**

Source of variation	Est.	S.E.	*t* val.	d.f.	*p*-value
Stool Storage Time * Culture Time	0.007	0.010	0.692	32.000	0.494
Shannon index					
Stool Storage Time	-0.002	0.003	-0.721	32.000	0.476
Culture Time	-0.010	0.001	-6.881	32.000	**<0.0001**
Stool Storage Time * Culture Time	0.000	0.000	0.192	32.000	0.849
Inverse Simpson index					
Stool Storage Time	-0.178	0.162	-1.101	32.000	0.279
Culture Time	-0.358	0.070	-5.105	32.000	**<0.0001**
Stool Storage Time * Culture Time	0.002	0.003	0.579	32.000	0.566
Evenness index					
Stool Storage Time	-0.000	0.000	-0.432	32.000	0.669
Culture Time	-0.001	0.000	-3.457	32.000	**0.002**
Stool Storage Time * Culture Time	-0.000	0.000	-0.233	32.000	0.817
PD – whole tree					
Stool Storage Time	-0.011	0.040	-0.282	30.000	0.780
Culture Time	-0.114	0.017	-6.591	30.000	**<0.0001**
Stool Storage Time * Culture Time	0.000	0.001	0.053	30.000	0.958

The beta diversity analysis, coupled with principal coordinate analysis (PCoA), revealed a significant decline in beta diversity similarity metrics (the unique fraction metrics (*unifrac*), weighted unique (*wunifrac*) fraction matrix, Bray-Curtis dissimilarity (*bray*), and phylogenetic diversity (*PD – whole tree*)). This decline was determined to be dependent on the culture time (all $p = 0.001$), but interestingly, it showed no significant associations with the length of stool preservation in the GutAlive® stool collection container (all $p = 1.000$; **Fig. 3.11**, **Table 3.7**).

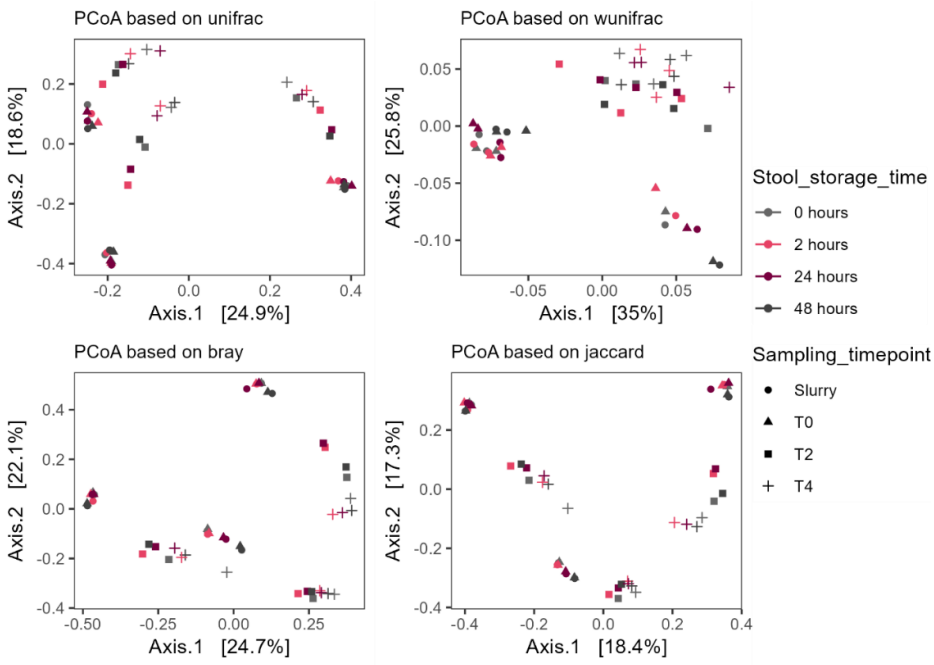

Fig. 3.11. Changes in the microbiome composition (beta diversity) of the samples stored in the GutAlive® microbiome collection kit containers for different times (0-48 h) and cultured in the DASbox® mini bioreactor system for 96 hours. Distances based on unique fraction metric, weighted unique fraction metric, Bray-Curtis, and Jaccard dissimilarity were plotted via PCoA.

Table 3.7. Results of PERMANOVA analysis. This table presents the PERMANOVA analysis results, including the proportion of explained variation (R^2), statistical significance (*p*-values), and the F value for each factor. The F value represents the ratio of between-group variation to within-group variation and assesses the significance of the factor's effect.

Source of variation	Df	Sum of sq.	R^2	F	*p*-value
PCoA analysis based on unifrac					
Stool Storage Time	3	0.3297	0.02784	0.4084	0.843
Culture Time	3	2.2551	0.19045	2.7937	**0.001**
Stool Storage Time* Culture Time	9	0.6460	0.05456	0.2668	1.000
PCoA analysis based on wunifrac					
Stool Storage Time	3	0.00625	0.01406	0.2276	0.983
Culture Time	3	0.13094	0.29469	4.7718	**0.001**
Stool Storage Time* Culture Time	9	0.01445	0.03253	0.1756	1.000
PCoA analysis based on bray					
Stool Storage Time	3	0.3546	0.02254	0.3373	0.846
Culture Time	3	3.6496	0.23198	3.4712	**0.001**
Stool Storage Time* Culture Time	9	0.5137	0.03265	0.1629	1.000
PCoA analysis based on jaccard					
Stool Storage Time	3	0.5840	0.03200	0.4695	0.847
Culture Time	3	3.3681	0.18455	2.7077	**0.001**
Stool Storage Time* Culture Time	9	1.0301	0.05644	0.2761	1.000

To distinguish the changes in the microbiome composition, the identified bacterial taxa were represented at several taxonomic levels. It was observed that microbiome composition remained relatively stable throughout cultivation time (**Fig. 3.12**).

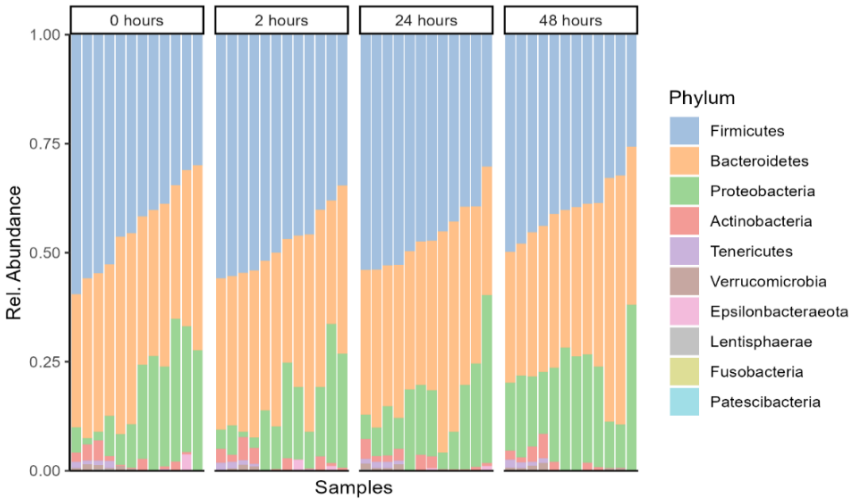

Fig. 3.12. Bacterial composition of the gut microbiome at the phylum level (top 10) in the groups of different stool storage times in GutAlive® anaerobic microbiome collection containers.

The collective data suggests that the bacterial composition in GutAlive® anaerobic microbiome collection containers remained stable at room temperature for up to 48 hours. Additionally, there was an indication that the decrease in alpha diversity parameters during the cultivation period may be associated with the chosen operation modes of the bioreactors.

3.3.2. Impact of Bioreactor Operation Modes

To evaluate the hypothesis that operational mode can significantly influence diversity, we examined the effects of various nutrient supplementation strategies on the stability of microbiome composition in the bioreactors throughout the culture period. We found out that process parameters were stable throughout the culture time. Only the semi-continuous operation mode had a characteristic decrease in pH during the medium exchange, while the continuous operation mode resulted in the most stable pH values.

Among the operation modes, semi-continuous medium exchange once daily led to a more stable microbiome composition than both semi-continuous medium exchanges twice daily and continuous operation mode, compared to batch operation mode. Alpha diversity analysis showed that culture time decreased Richness, Shannon, Inverse Simpson, and Phylogenetic Diversity indices (all $p < 0.050$). Interestingly, continuous operation mode throughout

the culture time resulted in a decrease in Shannon ($p < 0.001$), evenness ($p = 0.020$), and phylogenetic diversity ($p = 0.047$) indices. Similarly, a reduction in diversity was observed in semi-continuous operation mode (twice daily), as Shannon ($p = 0.001$) and evenness ($p = 0.030$) indices decreased throughout culture time (**Fig. 3.13**, **Table 3.8**). This finding is significant because while batch operation mode may offer stability, it is unsuitable for simulating daily substance or drug intake and has limited adaptability in clinical practice.

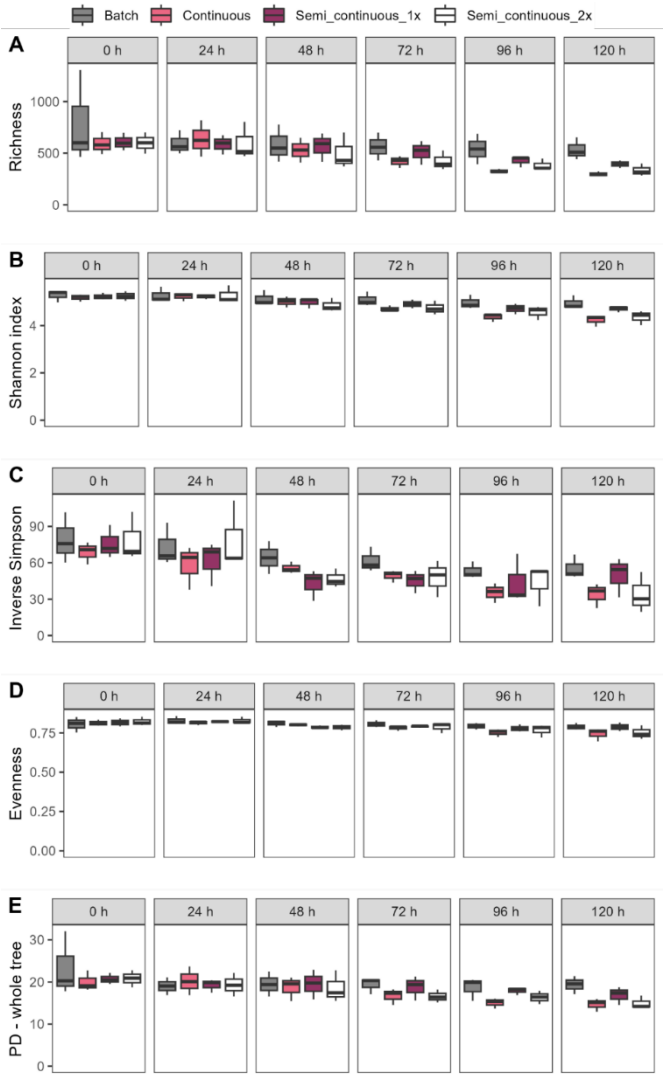

Fig. 3.13. Changes in the microbiome composition based on the operation modes (batch, continuous, and semi-continuous (once or twice daily)) throughout the culture time. Alpha-diversity parameters: (**A**) Richness, (**B**)

Shannon index, (**C**) Inverse Simpson index, (**D**) Evenness, (**E**) Phylogenetic Diversity (PD).

Table 3.8. Linear mixed-effects model results for alpha-diversity parameters. The table presents the estimates, standard errors (S.E.), t-values (t val.), degrees of freedom (d.f.), and *p*-values for alpha diversity indices: Richness, Shannon, Inverse Simpson, evenness, and phylogenetic diversity. Only bacterial pellet samples collected from the DASbox® were included in this analysis (3 stool samples and 3 slurry samples were excluded).

Source of variation	**Est.**	**S.E.**	***t* val.**	**d.f.**	***p*-value**
		Richness index			
Continuous	-64.143	53.749	-1.193	62.000	0.237
Semi_continuous_1x	-79.175	53.749	-1.473	62.000	0.146
Semi_continuous_2x	-92.603	53.749	-1.723	62.000	0.090
Culture Time	-1.801	0.523	-3.444	62.000	**0.001**
Culture Time * Continuous	-1.195	0.740	-1.615	62.000	0.111
Culture Time * Semi_continuous_1x	-0.148	0.740	-0.200	62.000	0.842
Culture Time * Semi_continuous_2x	-0.633	0.740	-0.855	62.000	0.396
		Shannon index			
Continuous	0.034	0.102	0.331	62.000	0.742
Semi_continuous_1x	-0.048	0.102	-0.475	62.000	0.636
Semi_continuous_2x	0.014	0.102	0.142	62.000	0.887
Culture Time	-0.003	0.001	-3.111	62.000	**0.003**
Culture Time * Continuous	-0.006	0.001	-4.364	62.000	**<0.0001**
Culture Time * Semi_continuous_1x	-0.002	0.001	-1.338	62.000	0.186
Culture Time * Semi_continuous_2x	-0.005	0.001	-3.503	62.000	**0.001**
		Inverse Simpson index			
Continuous	-8.879	8.354	-1.063	62.000	0.292
Semi_continuous_1x	-11.034	8.354	-1.321	62.000	0.191
Semi_continuous_2x	1.625	8.354	0.195	62.000	0.846
Culture Time	-0.211	0.081	-2.598	62.000	**0.012**
Culture Time * Continuous	-0.089	0.115	-0.778	62.000	0.439

Source of variation	Est.	S.E.	*t* val.	d.f.	*p*-value
Culture Time * Semi_continuous_1x	-0.003	0.115	-0.023	62.000	0.982
Culture Time * Semi_continuous_2x	-0.185	0.115	-1.608	62.000	0.113
Evenness index					
Continuous	0.006	0.014	0.398	62.000	0.692
Semi_continuous_1x	-0.004	0.014	-0.268	62.000	0.790
Semi_continuous_2x	0.010	0.014	0.712	62.000	0.479
Culture Time	-0.000	0.000	-1.638	62.000	0.106
Culture Time * Continuous	-0.000	0.000	-2.391	62.000	**0.020**
Culture Time * Semi_continuous_1x	-0.000	0.000	-0.432	62.000	0.667
Culture Time * Semi_continuous_2x	-0.000	0.000	-2.218	62.000	**0.030**
PD – whole tree					
Continuous	-0.729	0.973	-0.749	62.000	0.457
Semi_continuous_1x	-0.840	0.973	-0.863	62.000	0.392
Semi_continuous_2x	-1.141	0.973	-1.173	62.000	0.245
Culture Time	-0.026	0.009	-2.778	62.000	**0.007**
Culture Time * Continuous	-0.027	0.013	-2.028	62.000	**0.047**
Culture Time * Semi_continuous_1x	-0.005	0.013	-0.372	62.000	0.711
Culture Time * Semi_continuous_2x	-0.020	0.013	-1.470	62.000	0.147

Beta diversity analysis showed that operation mode and experimental time impacted the microbiome composition (all $p < 0.050$). Also, the operation mode significantly impacted the microbiome‘s composition throughout the culture time (all $p < 0.050$). Interestingly, beta diversity analysis revealed that the microbiomes from three donors exhibited distinct compositions. These donor-dependent differences in the microbiome composition remained consistent (**Fig. 3.14**, **Table 3.9**). This observation sheds further light on the stability of the reproducibility of the native microbiome composition within this novel *in vitro* system.

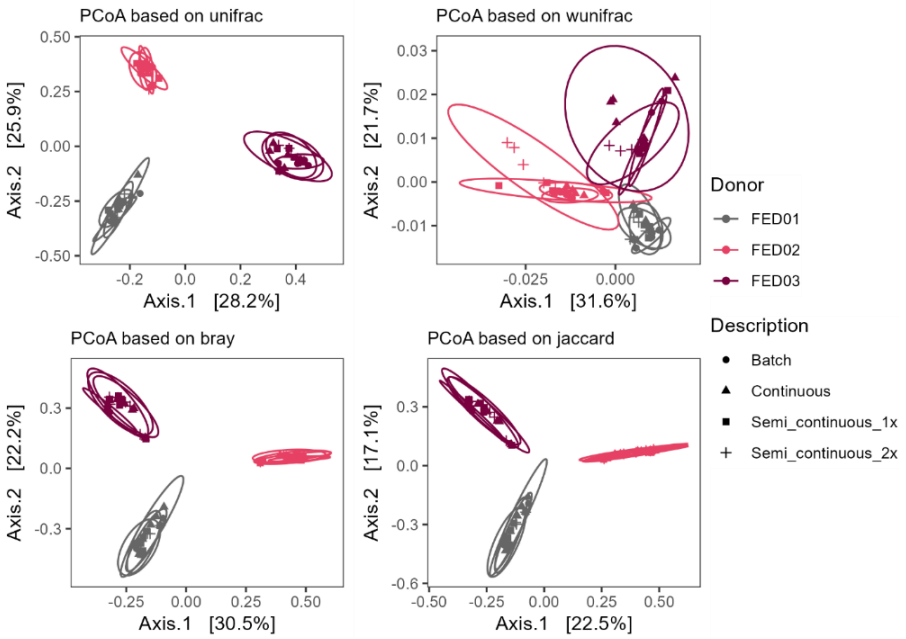

Fig. 3.14. Changes in the microbiome composition (beta diversity) of the stool samples from healthy donors (FED01-FED03) cultured in the DASbox® mini bioreactor system for up to 120 hours using different operation modes (batch, continuous, semi-continuous once daily, semi-continuous twice daily, with an 8-hour interval between nutrient supplementation). Distances based on unique fraction metric, weighted unique fraction metric, Bray-Curtis, and Jaccard dissimilarity were plotted via PCoA.

Table 3.9. PERMANOVA analysis results of microbiome composition changes throughout the treatment of experimental time, using different operation modes.

Source of variation	Df	Sum of sq.	R^2	F	*p*-value
PCoA analysis based on unifrac					
Timepoint	1	1.0604	0.05466	3.9784	**0.001**
Operation_Mode	3	0.7681	0.03959	0.9606	**0.001**
Timepoint* Operation_Mode	3	0.5140	0.02649	0.6428	**0.009**
PCoA analysis based on wunifrac					
Timepoint	1	0.002538	0.07863	6.1087	**0.001**
Operation_Mode	3	0.001883	0.05833	1.5105	**0.001**

Source of variation	Df	Sum of sq.	R^2	F	*p*-value
Timepoint* Operation_Mode	3	0.001265	0.03919	1.0150	**0.003**
PCoA analysis based on bray					
Timepoint	1	1.7435	0.07391	5.6250	**0.001**
Operation_Mode	3	1.2741	0.05401	1.3702	**0.001**
Timepoint* Operation_Mode	3	0.7338	0.03111	0.7891	**0.019**
PCoA analysis based on jaccard					
Timepoint	1	1.5969	0.05838	4.3942	**0.001**
Operation_Mode	3	1.5652	0.05722	1.4357	**0.001**
Timepoint* Operation_Mode	3	0.9349	0.03418	0.8575	**0.018**

More in-depth analysis of *16S rRNA* gene sequencing data showed that microbiome composition remained relatively stable in all operation modes with the mostly abundant phyla of Firmicutes, Bacteroidetes, and Proteobacteria, resembling stool and slurry microbiome compositions (**Fig. 3.15**).

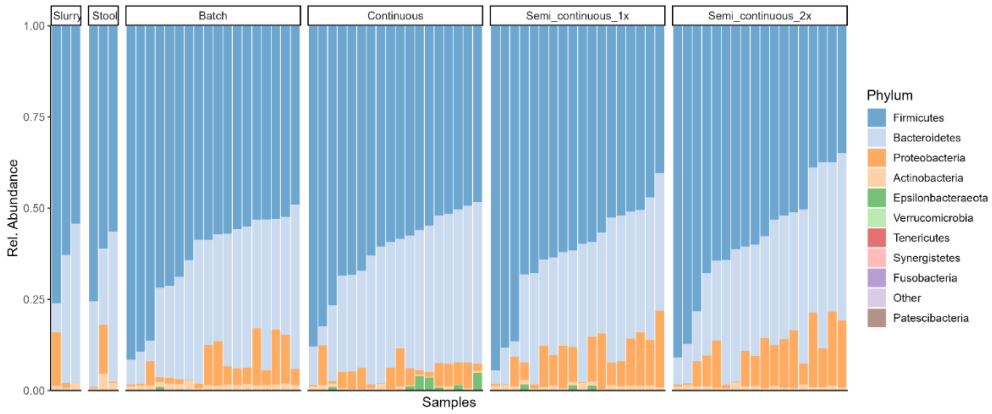

Fig. 3.15. Bacterial composition of the gut microbiome at the phylum level (top 10) in the groups of different operation modes. Stool and slurry (inoculum) samples are presented as references for the initial microbiome composition that was introduced into bioreactors.

3.3.3. *In Vitro* Modulation of Oralization Process

Next aim was to establish an *in vitro* model of gut microbiome oralization that could resemble the increase of oral bacteria abundance in the gut. For this, we tested four different oral bacteria presentation (spiking) strategies: (1) Spiking was done once, immediately after inoculation; (2) Once 48 hours after inoculation; (3) Every day, starting immediately after inoculation; (4) Every day, starting 48 hours after inoculation.

Upon observation, it was noted that the strategy of spiking every day, initiated immediately after inoculation, yielded the highest and sustained values throughout the entire experimental period (**Fig. 3.16**).

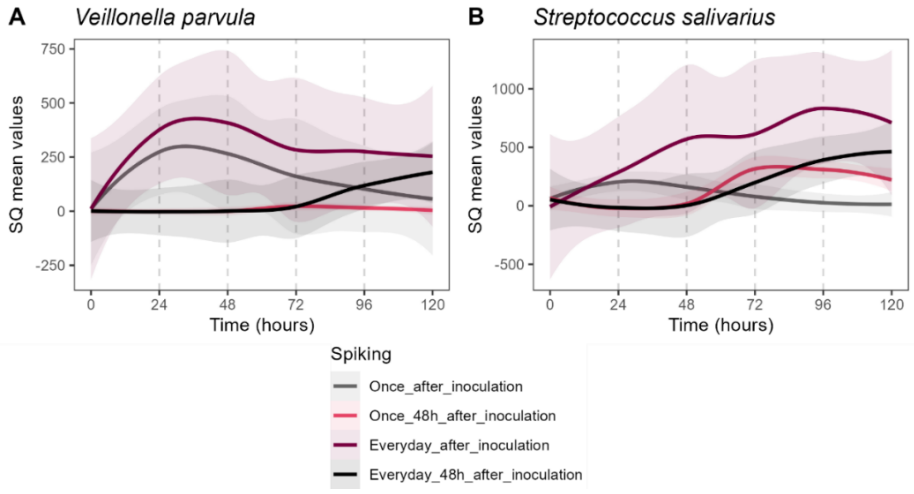

Fig. 3.16. Changes in *Veillonella parvula* and *Streptococcus salivarius* abundance in the DASbox® mini bioreactor system based on four spiking strategies. Results are presented as a mean starting quantity (SQ) values. Colours represent tested spiking strategies (and standard deviation), and dashed lines indicate semi-continuous medium exchange.

3.3.4. Testing of Probiotic Products to Prevent Oralization of the Gut

The abundances of the tested bacteria were significantly affected by the duration of the experiment. It was noted that the control groups (starch and placebo) showed the highest levels of oral bacteria. Additionally, the addition of prebiotics alone did not lead to the suppression of growth of oral bacteria. In contrast, both probiotic-containing products resulted in reduced growth of *V. parvula* throughout the experimental time, compared to placebo ($p < 0.050$). In the *S. salivarius* case, only the tendency was observed that tested

supplementation products that contained probiotics reduced the growth of bacteria when compared to placebo (both $p > 0.050$) (**Fig. 3.17**, **Table 3.10**).

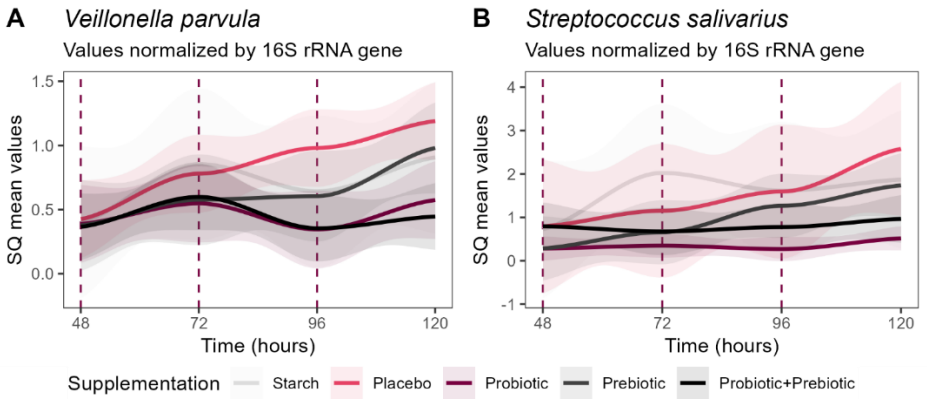

Fig. 3.17. Changes in *Veillonella parvula* and *Streptococcus salivarius* abundance before and after the supplementation with controls (placebo and corn starch), probiotic, and prebiotic products. Results are presented as a mean starting quantity (SQ) value, normalized by the *16S rRNA* gene; error bars represent standard deviation, dashed lines indicate semi-continuous medium exchange with supplementation.

Table 3.10. Linear mixed-effects model results for oral bacteria abundance. The table presents the estimates, standard errors (S.E.), t-values (t val.), degrees of freedom (d.f.), and *p*-values for supplementation products (starch, probiotic, prebiotic, and combination of probiotic and prebiotic), compared to placebo. Timepoints 0 and 24 hours are excluded, as supplementation started after 48 hours post-inoculation.

Source of variation	Est.	S.E.	t val.	d.f.	*p*-value
		Veillonella parvula			
Starch	0.137	0.462	0.298	110.000	0.767
Probiotic	0.605	0.365	1.657	110.000	0.100
Prebiotic	0.608	0.365	1.667	110.000	0.098
Probiotic+Prebiotic	1.050	0.365	2.877	110.000	**0.005**
Hours	0.008	0.003	3.185	110.000	**0.002**
Starch*Hours	-0.003	0.005	-0.559	110.000	0.578
Probiotic*Hours	-0.010	0.004	-2.438	110.000	**0.016**
Prebiotic*Hours	-0.005	0.004	-1.191	110.000	0.236
Probiotic+Prebiotic*Hours	-0.011	0.004	-2.618	110.000	**0.010**

Source of variation	Est.	S.E.	t val.	d.f.	*p*-value
Streptococcus salivarius					
Starch	1.043	1.349	0.774	110.000	0.441
Probiotic	0.375	1.066	0.352	110.000	0.726
Prebiotic	-0.558	1.066	-0.523	110.000	0.602
Probiotic+Prebiotic	0.870	1.066	0.816	110.000	0.416
Hours	0.021	0.008	2.808	110.000	**0.006**
Starch*Hours	-0.009	0.015	-0.583	110.000	0.561
Probiotic*Hours	-0.018	0.012	-1.498	110.000	0.137
Prebiotic*Hours	0.003	0.012	0.264	110.000	0.792
Probiotic+Prebiotic*Hours	-0.018	0.012	-1.473	110.000	0.144

This part of the study revealed that controls (corn starch and placebo) and prebiotics did not inhibit oral bacteria growth. Probiotic-containing supplementation products reduced the growth of *Veillonella parvula* (both $p < 0.050$) throughout the experimental time. They showed a tendency (both $p > 0.050$) to reduce the growth of *Streptococcus salivarius*, compared to placebo control.

4. DISCUSSION

In this doctoral dissertation, we aimed to examine how different GI cancer treatments affect gut microbiome composition and to develop a novel *in vitro* bioreactor model that accurately simulates the human gut microbiome. The ultimate objective of this work was to use this novel *in vitro* model to study GI cancer treatment side effects and to test various probiotic combinations that might mitigate the side effects of cancer treatments, thereby reducing the need for animal testing. The key objectives of this doctoral dissertation involved assessing how various types of preoperative MBP influence the gut microbiome and postoperative outcomes in patients with CRC. Additionally, it explored the effects of NAC and radical gastrectomy on the gut microbiome in patients with GC. The dissertation also included the development of a bioreactor-based *in vitro* gut microbiome model, which could be used to investigate the side effects of cancer treatments. This model was utilized to test probiotics designed to mitigate treatment-related side effects, such as the oralization of the gut microbiome.

In the literature analysis part we aimed to cover the main structural segments of the human GI tract and their physicochemical parameters, emphasizing the importance of their understanding for establishing an *in vitro* model of the gut microbiome. In the literature analysis, we highlighted variations of these parameters across different segments of the GI tract and the differences in microbiome composition in each segment. In this analysis, we also explored the development of GI cancers, including GC and CRC, their molecular mechanisms associated with the microbiome, and potential treatment strategies. Furthermore, we examined cancer treatment side effects modeling using bioreactor-based *in vitro* systems. A significant research gap was identified during the literature review analysis, noting that while *in vitro* models have been used to study GI cancer treatment side effects, they rarely include stool microbiome despite its crucial role in cancer development and treatment. Our recent review publication underscored this gap in more detail [270].

The main finding from our analysis of microbiome composition data from CRC patients was that OP and RE lead to similar and transient dysbiosis, with comparable outcomes after surgery. Additionally, we found distinct gut microbiome changes in patients who experienced postoperative infections, including an increased abundance of Pseudomonadales, Actinomycetales, Actinobacteria, Actinomycetaceae, *Actinomyces*, *Sutterella* uncultured, and *Enterococcus faecalis* bacterium on POD06.

Recently, there has been increasing interest in investigating the effects of MBP on gut microbiome composition, though current evidence presents conflicting findings. Several studies analyzing the microbiome following bowel cleansing with oral agents for colonoscopy have reported disruptions in microbial composition shortly after the procedure [294–298]. Interestingly, the study by Drago *et al.* found that oral agents trigger dysbiosis, characterized by a decrease in *Lactobacillaceae* probiotics, which lasts for at least a month. However, most other studies report that the gut microbiome tends to return to its baseline composition within a significantly shorter timeframe, usually around 14 days [295,297]. Our analysis reveals that MBP and colorectal resection significantly alter microbiome composition over 30 days. Although the microbiome shows potential for recovery during this time, it does not fully revert to its baseline composition by the 30-day mark.

Additionally, our study is the first to show that RE induces a dysbiotic state similar to that caused by oral agents. However, it is essential to acknowledge that in our research, MBP was combined with surgery, and changes in the gut microbiome may result not only from MBP but also from the surgical procedure itself [299, 300]. Surgical stress can lead to changes in the host that affect the intestinal microenvironment, ultimately resulting in dysbiosis [301]. It was observed that the composition and diversity of the gut microbiome in CRC patients one month after surgery were significantly different from both their pre-surgery microbiome and that of healthy individuals [299]. Dysbiosis observed in surgical patients may have significant clinical implications, as it could be linked to the development of postoperative complications, especially postoperative infections [302,303]. It is well-established that infections are the most common type of complication following CRC surgery [304,305]. This fact is supported by our doctoral dissertation work, which found that infections were common, affecting approximately one-third of the patients.

Patients with infections exhibited an increased abundance of Actinomycetaceae, *Actinomyces*, *Sutterela*, and *E. faecalis* in samples from POD06. Enterococci are opportunistic bacteria that can turn pathogenic when colonizing environments where they are generally absent. This group of bacteria is commonly found in patients who develop infections in hospital settings [306–308] and most infections among these patients are attributed to *E. faecalis*, which is one of over twenty different species within the *Enterococcus* genus [309,310]. The role of other bacteria, such as those from the *Actinomyces* and *Sutterella* genera, which have been observed to increase in abundance in patients with postoperative infections, remains poorly understood and needs further investigation.

Our study has notable limitations. Firstly, despite randomization, there were unexpected differences in baseline microbiome composition between the RE and oral OP groups. While a definitive explanation for this discrepancy remains unclear, variations in age among the study groups likely played a role. Previous research has shown that microbial stability and diversity often decline with age [311,312]. Secondly, our investigation into whether the microbes that showed enrichment in the gut microbiome on POD06 were present at the infection site was limited by the lack of samples from the infection site for sequencing. Additionally, culture reports were available for only a few patients with infections. Thirdly, as noted earlier, this study combined MBP with surgery. Therefore, the observed changes in the gut microbiome could be attributed to MBP, the surgical procedure, and the naturally changing diet during the postoperative period. Fourthly, recent guidelines recommend the use of oral antibiotics alongside MBP before left-side CRC surgery [313], a practice that was not implemented in our study. It is important to note that these guidelines were not available when this study was conducted. However, the potential impact of oral antibiotics on the gut microbiome might have influenced the effects observed from MBP.

Our primary results from the GC clinical study revealed that significant alterations in the gut microbiome during treatment are mainly attributed to radical surgery rather than NAC. NAC alone did not affect the gut microbiome composition at the phylum level. In contrast, radical surgery increased the abundance of Bacteroidetes and Proteobacteria phyla while decreasing the abundance of Firmicutes and Actinobacteria phyla. Furthermore, NAC did not affect alpha or beta diversity, whereas radical surgery significantly impacted both. Post-surgery, the microbiome exhibited an enrichment of bacteria associated with oralization. LEfSe analysis revealed an increased abundance of *Escherichia-Shigella*, *Streptococcus equinus*, and uncultured *Streptococcus* species, along with members of the Enterobacteriaceae family. ANCOM validated these findings by showing elevated levels of *Escherichia-Shigella* and reduced levels of the *Faecalibacterium* genus and the *Ruminococcus torques* group following radical surgery. Surprisingly, this study found no significant impact of NAC on gut microbiome composition. This contrasts with several prior studies showing systemic chemotherapy's effects on the gut microbiome in different types of cancer [314–317], including gastrointestinal cancers [318,319]. For example, a recent cross-sectional study by Li *et al.* found that the gut microbiome of patients with metastatic or locally advanced esophagogastric or CRC undergoing chemotherapy differed from that of healthy controls, exhibiting increased richness and compositional changes in cancer patients [319]. However, it is important to note that Li *et al.*'s study

was cross-sectional and did not include pre- and post-treatment comparisons, unlike our longitudinal study. In contrast, a longitudinal study by Kong *et al*. [320], which investigated gut microbiome changes during colorectal cancer treatment with radical surgery and adjuvant capecitabine plus oxaliplatin (CapeOx) chemotherapy, found that chemotherapy dramatically increased the Bacteroidetes to Firmicutes ratio. Specifically, Gram-negative Bacteroidetes became more abundant, while Firmicutes showed a trend towards decreased abundance. Additionally, chemotherapy reduced the presence of originally dominant pathogenic bacteria such as *Morganella*, *Pyramidobacter*, *Proteus*, and *Escherichia-Shigella*, but increased the abundance of conditionally pathogenic bacteria, including *Bilophila*, *Comamonas*, *Butyricimonas*, *Eggerthella*, and *Anaerostipes* [320]. Several methodological differences between Kong *et al*.'s [320] study and ours should be considered when interpreting these disparate findings. First, we assessed the effect of NAC on the microbiome before surgery, whereas Kong *et al*. [320] examined the impact of chemotherapy after colorectal resection. Second, we investigated the effects of FLOT (5-FU, leucovorin, oxaliplatin, docetaxel) chemotherapy in GC patients, while Kong *et al*. [320] focused on CapeOx in CRC patients. Most importantly, the timing of sample collection differed significantly. We collected samples approximately four weeks after NAC, just before surgery, whereas Kong *et al*. [320] collected samples after each cycle of chemotherapy. This suggests that chemotherapy-induced changes in the gut microbiome may be transient, with a four-week interval possibly allowing the microbiome to recover and reach a stable state. Another study by Chen *et al*. investigated the impact of surgery and chemotherapy on gut microbiome composition in GC patients [321]. Although the study was retrospective and cross-sectional and did not specify the types of chemotherapy or surgery, it found no significant differences in gut microbiome composition between patients who underwent chemotherapy and those who did not [321], which aligns with our present findings. In summary, our longitudinal study is the first to show that FLOT chemotherapy does not have a significant or lasting effect on the gut microbiome composition in gastric cancer patients four weeks after completing neoadjuvant treatment.

The most significant finding of our study is that, unlike NAC, radical surgery performed after NAC has a notable and long-lasting effect on gut microbiome composition. Dysbiosis induced by radical surgery is characterized by increased bacteria associated with oralization, such as *Streptococcus* and *Escherichia-Shigella* genera. The previous proof-of-concept study suggested that gastrectomy-related gut microbiome oralization is marked by an increased abundance of bacteria commonly found in the oral

cavity, including *Escherichia-Shigella, Enterococcus, Streptococcus, Veillonella, Oribacterium,* and *Mogibacterium* [322]. Early research on the effects of PPIs proposed that the loss of the gastric barrier leads to changes in both the gastric and distal gastrointestinal microbiome [323–326]. PPI intake alters the composition and increases the diversity of the gastric microbiome [326]. In the distal gastrointestinal tract, which is naturally rich in microbes, microbial diversity decreases after PPI intake [5,323–325]. Additionally, the fecal microbiome shows increased levels of predominantly oral bacteria, such as *Streptococcus, Veillonella, Rothia,* and *Oribacterium*, as well as potential pathogens like *Enterococcus, Escherichia-Shigella,* and *Haemophilus*, following PPI therapy. Concurrently, autochthonous and beneficial bacteria, including *Faecalibacterium, Ruminococcaceae*, and *Lachnospiraceae*, decrease significantly [5,323,324,327–329]. Furthermore, previous research has shown that the gut microbiome oralization is associated with gastrointestinal symptoms, including bloating, diarrhea, and abdominal discomfort, in survivors of GC [5]. This oralization process is mainly associated with intestinal inflammation and *Streptococcus* in the stool [5]. This doctoral dissertation compellingly confirmed that gastrectomy increases the abundance of *Streptococcus*, a bacterial taxon commonly found in the oral cavity and frequently associated with PPI-induced dysbiosis [323,324,327–329]. The present study showed a radical surgery-induced increase of *Escherichia-Shigella* level (both at the genus and species level) and lower levels of *Faecalibacterium* and the *Ruminococcus* genera. *Escherichia* is commonly implicated in small intestinal bacterial overgrowth [330], which often occurs in patients after gastrectomy and is linked to intestinal and postprandial symptoms [331].

Another result of this doctoral dissertation is developing a novel bioreactor-based *in vitro* model of the human gut microbiome using the DASbox® mini bioreactor system. Drawing from insights in a recent publication [332], we selected GutAlive® anaerobic microbiome collection kits for this study. Aligned with our findings, these kits effectively maintained bacterial viability and stability over time, preserving the original composition and diversity of the microbiome. Our detailed data analysis shows that the bacterial composition in GutAlive® anaerobic microbiome collection containers remains stable for up to 48 hours at room temperature. Additionally, user-friendly design facilitates self-collection of stool samples, making them a valuable tool for potential clinical use.

After successfully optimizing the stool collection process, the focus shifted to developing a robust culture system. This involved creating an environment that mimicked conditions in the human GI tract and provided

essential nutrients for the microbiome. Ensuring microbiome stability throughout the culture period was critical, leading to modifications in the system to support a diverse microbial community. The study investigated how different operational modes and nutrient additions could influence microbiome stability and composition. This exploration was driven by earlier observations of declining diversity parameters over time, particularly under continuous operation mode. Consequently, the experiment tested four distinct operational modes: batch, continuous, and semi-continuous (with medium exchange once or twice daily). We found continuous nutrient supply reduces alpha diversity throughout the culture time, whereas the batch mode provided the most stable microbiome composition. However, since the batch mode is unsuitable for testing supplements, we selected the semi-continuous operation mode with a daily medium exchange for further experiments.

As previously mentioned, oralization can result from several factors, including surgical procedures like radical gastrectomy or PPIs. PPIs, commonly used to reduce stomach acid, include medications such as Omeprazole, Esomeprazole, Lansoprazole, Rabeprazole, Pantoprazole, Dexlansoprazole, and Zegerid [333], and they are commonly used among cancer patients. Despite their widespread use, the potential adverse effects of PPIs have not been extensively researched. One significant side effect is the oralization process of the gut microbiome, characterized by an imbalance in the gut microbiome caused by the influx of oral bacteria into the GI tract. In this study, we developed a model of the oralization process within the bioreactor system. Our goal was to maintain a stable and relatively high concentration of oral bacteria throughout the culture period, as a decline in their concentration could lead to inaccurate results. Consistent levels were crucial for accurately assessing the true impact of the supplements when introduced into the model. Interestingly, another group recently developed an *in vitro* model to simulate oral-to-gut microbial invasion, featuring an experimental timeline of 11 days and incorporating saliva injections on days 9 and 10 [285]. However, this model relies on saliva samples for the oral bacteria spiking procedure, which can challenge standardization and lead to variability between experiments. In contrast, our model provides a standardized and simplified approach to oralization that avoids the need for additional biological samples. Instead, it utilizes two recently developed oralization biomarkers [6], enhancing efficiency and ease of use. Conversely, the oralization model outlined by Mesmin *et al.*, utilizing the M-ARCOL, was employed to investigate the mucus-associated microbiome. This feature is unavailable in the DASbox®-based *in vitro* model we used, underscoring a current limitation.

Lastly, the newly developed *in vitro* oralization model, incorporating both oral bacteria and stool microbiome, was adapted to investigate probiotic products to alleviate the oralization side effect caused by cancer treatment. Our goal was to identify the most suitable probiotic product that could enhance cancer patients' quality of life and reduce the side effects of the treatment. The results demonstrated a significant reduction in *Veillonella parvula* growth and a clear trend in the reduction of *Streptococcus salivarius* growth. In this doctoral dissertation, a bioreactor-based *in vitro* system with stool inoculum was employed for the first time to simulate cancer treatment-induced oralization and assess probiotics for alleviating this cancer treatment side effect. As a pioneering effort, it sets the stage for future advancements to enhance throughput and expand the model to investigate other side effects of GI cancer treatment without the need for animal models.

CONCLUSIONS

1. Preoperative mechanical bowel preparation in colorectal cancer patients results in a similar dysbiotic state of the gut microbiome, regardless of whether the preparation involves a rectal enema or an oral agent. This suggests that both methods have comparable impacts on gut microbiome composition and potential postoperative complications.
2. In the gastric cancer cohort, it was observed that neoadjuvant chemotherapy does not significantly impact the gut microbiome. However, the subsequent radical gastrectomy induces substantial dysbiosis, including the oralization of the gut microbiome, highlighting the profound effects of the radical surgery on microbiome composition.
3. A novel bioreactor-based *in vitro* model of the human gut microbiome was successfully developed and systematically optimized using the DASbox® mini bioreactor system with human stool samples. This model shows significant promise for investigating disease-specific microbiomes, including testing the impact of cancer treatments on the microbiome, and offers valuable insights for both fundamental research and clinical applications.
4. The newly developed *in vitro* model of the human gut microbiome was adapted to study probiotic products aimed at mitigating the oralization side effects of cancer treatment. The findings indicate that these products effectively reduce the proliferation of oral bacteria within the gut microbiome, even without introducing saliva from patients experiencing oralization, suggesting their potential for alleviating such side effects in clinical settings.

RECOMMENDATIONS

For colorectal cancer patients, both preoperative rectal enema and oral mechanical bowel preparations cause comparable disruptions to the gut microbiome, suggesting similar impacts on postoperative outcomes. Strategies for postoperative microbiome restoration may, therefore, be beneficial.

For gastric cancer patients, neoadjuvant chemotherapy has minimal effects on the microbiome's composition, while radical gastrectomy results in significant dysbiosis, including the oralization of the gut microbiome. Probiotic interventions following radical gastrectomy may help mitigate these changes.

ACKNOWLEDGMENTS

Finding the right words to express my gratitude is difficult, as many remarkable individuals have shaped this journey. From fellow scientists and students to medical professionals and cancer patients, each has left a lasting imprint on my heart.

First and foremost, I would like to extend my deepest gratitude to my supervisor, Prof. Dr. Sonata Jarmalaitė from the Institute of Biosciences, Life Sciences Center, Vilnius University, Lithuania, who has believed in me since my first year as a bachelor's student. Your trust and support laid the foundation for my scientific path and have shaped me into the researcher I am today.

I am profoundly grateful to Dr. Angela Horvath and Prof. Dr. Vanessa Stadlbauer-Köllner from the Division for Gastroenterology and Hepatology at the Department of Internal Medicine, Medical University of Graz, Austria. Thank you for welcoming me into your team and guiding me through scientific and personal challenges. You made me feel seen and heard; I will forever be grateful for that.

I want to express my sincere gratitude to Dr. Augustinas Baušys from the National Cancer Institute in Vilnius, Lithuania, for the opportunity to work with his patients' samples and data, as well as for his positive attitude, and to all the personnel who contributed to the collection of these samples.

To my incredible colleagues at the Division for Gastroenterology and Hepatology, Department of Internal Medicine, Medical University of Graz: thank you for enriching this journey with joy, friendships, and warmth. You, indeed, are the best colleagues anyone could hope for.

To my parents, Vilija and Arvydas, sister Viktorija, and my dear Šarūnas, I am deeply grateful for your unconditional love and support throughout this journey.

Although many incredible people have contributed to this work, I want to dedicate it to cancer patients, their families, and caregivers. Not a day has gone by without thinking of you. Every challenge I have overcome has been inspired by the strength and courage you demonstrate in life's hardest battle. You have been, and will always be, my constant source of *purpose*.

REFERENCES

1. Arnold, M.; Abnet, C.C.; Neale, R.E.; Vignat, J.; Giovannucci, E.L.; McGlynn, K.A.; Bray, F. Global Burden of 5 Major Types of Gastrointestinal Cancer. *Gastroenterology* **2020**, *159*, 335-349.e15, doi:10.1053/j.gastro.2020.02.068.
2. Sánchez-Alcoholado, L.; Ramos-Molina, B.; Otero, A.; Laborda-Illanes, A.; Ordóñez, R.; Medina, J.A.; Gómez-Millán, J.; Queipo-Ortuño, M.I. The Role of the Gut Microbiome in Colorectal Cancer Development and Therapy Response. *Cancers* **2020**, *12*, 1406, doi:10.3390/cancers12061406.
3. Mukherjee, P.; Roy, S.; Ghosh, D.; Nandi, S.K. Role of Animal Models in Biomedical Research: A Review. *Lab. Anim. Res.* **2022**, *38*, 18, doi:10.1186/s42826-022-00128-1.
4. Jansma, J.; El Aidy, S. Understanding the Host-Microbe Interactions Using Metabolic Modeling. *Microbiome* **2021**, *9*, 16, doi:10.1186/s40168-020-00955-1.
5. Horvath, A.; Bausys, A.; Sabaliauskaite, R.; Stratilatovas, E.; Jarmalaite, S.; Schuetz, B.; Stiegler, P.; Bausys, R.; Stadlbauer, V.; Strupas, K. Distal Gastrectomy with Billroth II Reconstruction Is Associated with Oralization of Gut Microbiome and Intestinal Inflammation: A Proof-of-Concept Study. *Ann. Surg. Oncol.* **2021**, *28*, 1198–1208, doi:10.1245/s10434-020-08678-1.
6. Horvath, A.; Rainer, F.; Bashir, M.; Leber, B.; Schmerboeck, B.; Klymiuk, I.; Groselj-Strele, A.; Durdevic, M.; Freedberg, D.E.; Abrams, J.A.; et al. Biomarkers for Oralization during Long-Term Proton Pump Inhibitor Therapy Predict Survival in Cirrhosis. *Sci. Rep.* **2019**, *9*, 12000, doi:10.1038/s41598-019-48352-5.
7. Eaton, S.E.; Kaczmarek, J.; Mahmood, D.; McDiarmid, A.M.; Norarfan, A.N.; Scott, E.G.; Then, C.K.; Tsui, H.Y.; Kiltie, A.E. Exploiting Dietary Fibre and the Gut Microbiota in Pelvic Radiotherapy Patients. *Br. J. Cancer* **2022**, *127*, 2087–2098, doi:10.1038/s41416-022-01980-7.
8. Possenti, L.; Mecchi, L.; Rossoni, A.; Sangalli, V.; Bersini, S.; Cicchetti, A.; Costantino, M.L.; Candrian, C.; Arrigoni, C.; Rancati, T.; et al. Radiobiological Studies of Microvascular Damage through In Vitro Models: A Methodological Perspective. *Cancers* **2021**, *13*, 1182, doi:10.3390/cancers13051182.
9. Treuting, P.M.; Arends, M.J.; Dintzis, S.M. Upper Gastrointestinal Tract. In *Comparative Anatomy and Histology*; Elsevier, 2018; pp. 191–211 ISBN 978-0-12-802900-8.
10. Anatomy and Physiology of the Gastrointestinal Tract. In *Intestinal Failure and Rehabilitation*; Matarese, L.E., Steiger, E., Seidner, D.L., Eds.; CRC Press, 2004 ISBN 978-0-429-21103-4.

11. Li, S.; Peppelenbosch, M.P.; Smits, R. Bacterial Biofilms as a Potential Contributor to Mucinous Colorectal Cancer Formation. *Biochim. Biophys. Acta BBA - Rev. Cancer* **2019**, *1872*, 74–79, doi:10.1016/j.bbcan.2019.05.009.
12. Delbaere, K.; Roegiers, I.; Bron, A.; Durif, C.; Van de Wiele, T.; Blanquet-Diot, S.; Marinelli, L. The Small Intestine : Dining Table of Host–Microbiota Meetings. *FEMS Microbiol. Rev.* **2023**, *47*, doi:10.1093/femsre/fuad022.
13. Tacchino, R.M. Bowel Length: Measurement, Predictors, and Impact on Bariatric and Metabolic Surgery. *Surg. Obes. Relat. Dis. Off. J. Am. Soc. Bariatr. Surg.* **2015**, *11*, 328–334, doi:10.1016/j.soard.2014.09.016.
14. Gustafsson, J.K.; Johansson, M.E.V. The Role of Goblet Cells and Mucus in Intestinal Homeostasis. *Nat. Rev. Gastroenterol. Hepatol.* **2022**, *19*, 785–803, doi:10.1038/s41575-022-00675-x.
15. Antfolk, M.; Jensen, K.B. A Bioengineering Perspective on Modelling the Intestinal Epithelial Physiology in Vitro. *Nat. Commun.* **2020**, *11*, 6244, doi:10.1038/s41467-020-20052-z.
16. Clevers, H. The Intestinal Crypt, a Prototype Stem Cell Compartment. *Cell* **2013**, *154*, 274–284, doi:10.1016/j.cell.2013.07.004.
17. Clevers, H.; Conder, R.K.; Li, V.S.W.; Lutolf, M.P.; Vallier, L.; Chan, S.; Grikscheit, T.C.; Jensen, K.B.; De Coppi, P. Tissue-Engineering the Intestine: The Trials before the Trials. *Cell Stem Cell* **2019**, *24*, 855–859, doi:10.1016/j.stem.2019.04.018.
18. Collins, J.T.; Nguyen, A.; Badireddy, M. Anatomy, Abdomen and Pelvis, Small Intestine. In *StatPearls*; StatPearls Publishing: Treasure Island (FL), 2022.
19. van der Flier, L.G.; Clevers, H. Stem Cells, Self-Renewal, and Differentiation in the Intestinal Epithelium. *Annu. Rev. Physiol.* **2009**, *71*, 241–260, doi:10.1146/annurev.physiol.010908.163145.
20. Peterson, L.W.; Artis, D. Intestinal Epithelial Cells: Regulators of Barrier Function and Immune Homeostasis. *Nat. Rev. Immunol.* **2014**, *14*, 141–153, doi:10.1038/nri3608.
21. Agarwal, T.; Onesto, V.; Lamboni, L.; Ansari, A.; Maiti, T.K.; Makvandi, P.; Vosough, M.; Yang, G. Engineering Biomimetic Intestinal Topological Features in 3D Tissue Models: Retrospects and Prospects. *Bio-Des. Manuf.* **2021**, *4*, 568–595, doi:10.1007/s42242-020-00120-5.
22. Barker, N. Adult Intestinal Stem Cells: Critical Drivers of Epithelial Homeostasis and Regeneration. *Nat. Rev. Mol. Cell Biol.* **2014**, *15*, 19–33, doi:10.1038/nrm3721.
23. Lueschow, S.R.; McElroy, S.J. The Paneth Cell: The Curator and Defender of the Immature Small Intestine. *Front. Immunol.* **2020**, *11*, 587, doi:10.3389/fimmu.2020.00587.

24. Gerbe, F.; Legraverend, C.; Jay, P. The Intestinal Epithelium Tuft Cells: Specification and Function. *Cell. Mol. Life Sci. CMLS* **2012**, *69*, 2907–2917, doi:10.1007/s00018-012-0984-7.
25. Gunawardene, A.R.; Corfe, B.M.; Staton, C.A. Classification and Functions of Enteroendocrine Cells of the Lower Gastrointestinal Tract. *Int. J. Exp. Pathol.* **2011**, *92*, 219–231, doi:10.1111/j.1365-2613.2011.00767.x.
26. Kulkarni, D.H.; Gustafsson, J.K.; Knoop, K.A.; McDonald, K.G.; Bidani, S.S.; Davis, J.E.; Floyd, A.N.; Hogan, S.P.; Hsieh, C.-S.; Newberry, R.D. Goblet Cell Associated Antigen Passages Support the Induction and Maintenance of Oral Tolerance. *Mucosal Immunol.* **2020**, *13*, 271–282, doi:10.1038/s41385-019-0240-7.
27. Hendel, S.K.; Kellermann, L.; Hausmann, A.; Bindslev, N.; Jensen, K.B.; Nielsen, O.H. Tuft Cells and Their Role in Intestinal Diseases. *Front. Immunol.* **2022**, *13*, 822867, doi:10.3389/fimmu.2022.822867.
28. Nevo, S.; Kadouri, N.; Abramson, J. Tuft Cells: From the Mucosa to the Thymus. *Immunol. Lett.* **2019**, *210*, 1–9, doi:10.1016/j.imlet.2019.02.003.
29. Min, S.; Kim, S.; Cho, S.-W. Gastrointestinal Tract Modeling Using Organoids Engineered with Cellular and Microbiota Niches. *Exp. Mol. Med.* **2020**, *52*, 227–237, doi:10.1038/s12276-020-0386-0.
30. Treuting, P.M.; Arends, M.J.; Dintzis, S.M. Lower Gastrointestinal Tract. In *Comparative Anatomy and Histology*; Elsevier, 2018; pp. 213–228 ISBN 978-0-12-802900-8.
31. Bouges, E.; Segers, C.; Leys, N.; Lebeer, S.; Zhang, J.; Mastroleo, F. Human Intestinal Organoids and Microphysiological Systems for Modeling Radiotoxicity and Assessing Radioprotective Agents. *Cancers* **2023**, *15*, 5859, doi:10.3390/cancers15245859.
32. Cummings, J.H.; Macfarlane, G.T. Role of Intestinal Bacteria in Nutrient Metabolism. *Clin. Nutr.* **1997**, *16*, 3–11, doi:10.1016/S0261-5614(97)80252-X.
33. Baothman, O.A.; Zamzami, M.A.; Taher, I.; Abubaker, J.; Abu-Farha, M. The Role of Gut Microbiota in the Development of Obesity and Diabetes. *Lipids Health Dis.* **2016**, *15*, 108, doi:10.1186/s12944-016-0278-4.
34. Nicholson, J.K.; Holmes, E.; Kinross, J.; Burcelin, R.; Gibson, G.; Jia, W.; Pettersson, S. Host-Gut Microbiota Metabolic Interactions. *Science* **2012**, *336*, 1262–1267, doi:10.1126/science.1223813.
35. Yamamura, R.; Nakamura, K.; Kitada, N.; Aizawa, T.; Shimizu, Y.; Nakamura, K.; Ayabe, T.; Kimura, T.; Tamakoshi, A. Associations of Gut Microbiota, Dietary Intake, and Serum Short-Chain Fatty Acids with Fecal Short-Chain Fatty Acids. *Biosci. Microbiota Food Health* **2020**, *39*, 11–17, doi:10.12938/bmfh.19-010.
36. Nigam, Y.; Knight, J.; Williams, N. Gastrointestinal Tract 5: The Anatomy and Functions of the Large Intestine | Nursing Times

Available online: https://www.nursingtimes.net/clinical-archive/gastroenterology/gastrointestinal-tract-5-anatomy-functions-large-intestine-23-09-2019/ (accessed on 11 July 2024).
37. Aulton, M.E.; Taylor, K. *Aulton's Pharmaceutics: The Design and Manufacture of Medicines*; Elsevier Health Sciences, 2013; ISBN 978-0-7020-4290-4.
38. Yamamura, R.; Inoue, K.Y.; Nishino, K.; Yamasaki, S. Intestinal and Fecal PH in Human Health. *Front. Microbiomes* **2023**, *2*, doi:10.3389/frmbi.2023.1192316.
39. Crawford, N.; Brooke, B.N. The PH and Buffering Power of Human Bile. *Lancet Lond. Engl.* **1955**, *268*, 1096–1097, doi:10.1016/s0140-6736(55)90590-0.
40. Conlon, M.A.; Bird, A.R. The Impact of Diet and Lifestyle on Gut Microbiota and Human Health. *Nutrients* **2015**, *7*, 17–44, doi:10.3390/nu7010017.
41. Scholz-Ahrens, K.E.; Schrezenmeir, J. Inulin and Oligofructose and Mineral Metabolism: The Evidence from Animal Trials. *J. Nutr.* **2007**, *137*, 2513S-2523S, doi:10.1093/jn/137.11.2513S.
42. Arturo Tozzi; Minella, R. Dynamics and Metabolic Effects of Intestinal Gases in Healthy Humans. *Biochimie* **2024**, *221*, 81–90, doi:10.1016/j.biochi.2024.02.001.
43. Levitt, M.D. Volume and Composition of Human Intestinal Gas Determined by Means of an Intestinal Washout Technic. *N. Engl. J. Med.* **1971**, *284*, 1394–1398, doi:10.1056/NEJM197106242842502.
44. Roccarina, D.; Lauritano, E.C.; Gabrielli, M.; Franceschi, F.; Ojetti, V.; Gasbarrini, A. The Role of Methane in Intestinal Diseases. *Off. J. Am. Coll. Gastroenterol. ACG* **2010**, *105*, 1250, doi:10.1038/ajg.2009.744.
45. Naito, Y.; Uchiyama, K.; Takagi, T. Redox-Related Gaseous Mediators in the Gastrointestinal Tract. *J. Clin. Biochem. Nutr.* **2018**, *63*, 1–4, doi:10.3164/jcbn.18-56.
46. Modesto, A.; Cameron, N.-R.; Varghese, C.; Peters, N.; Stokes, B.; Phillips, A.; Bissett, I.; O'Grady, G. Meta-Analysis of the Composition of Human Intestinal Gases. *Dig. Dis. Sci.* **2022**, *67*, 3842–3859, doi:10.1007/s10620-021-07254-1.
47. Ritz, P.; Cloarec, D.; Beylot, M.; Champ, M.; Charbonnel, B.; Normand, S.; Krempf, M. Effects of Colonic Fermentation on Respiratory Gas Exchanges Following a Glucose Load in Man. *Metabolism.* **1993**, *42*, 347–352, doi:10.1016/0026-0495(93)90085-3.
48. Louis, P.; Duncan, S.; Sheridan, P.; Walker, A.; Flint, H.J. Microbial Lactate Utilisation and the Stability of the Gut Microbiome. *Gut Microbiome* **2022**, *3*, e3, doi:10.1017/gmb.2022.3.
49. Schiller, C.; Fröhlich, C.-P.; Giessmann, T.; Siegmund, W.; Mönnikes, H.; Hosten, N.; Weitschies, W. Intestinal Fluid Volumes and Transit of Dosage Forms as Assessed by Magnetic Resonance Imaging. *Aliment.*

Pharmacol. Ther. **2005**, *22*, 971–979, doi:10.1111/j.1365-2036.2005.02683.x.
50. Camilleri, M.; Zinsmeister, A.R.; Greydanus, M.P.; Brown, M.L.; Proano, M. Towards a Less Costly but Accurate Test of Gastric Emptying and Small Bowel Transit. *Dig. Dis. Sci.* **1991**, *36*, 609–615, doi:10.1007/BF01297027.
51. Degen, L.P.; Phillips, S.F. Variability of Gastrointestinal Transit in Healthy Women and Men. *Gut* **1996**, *39*, 299–305, doi:10.1136/gut.39.2.299.
52. Graff, J.; Brinch, K.; Madsen, J.L. Gastrointestinal Mean Transit Times in Young and Middle-Aged Healthy Subjects. *Clin. Physiol. Oxf. Engl.* **2001**, *21*, 253–259, doi:10.1046/j.1365-2281.2001.00308.x.
53. Nandhra, G.K.; Mark, E.B.; Di Tanna, G.L.; Haase, A.-M.; Poulsen, J.; Christodoulides, S.; Kung, V.; Klinge, M.W.; Knudsen, K.; Borghammer, P.; et al. Normative Values for Region-Specific Colonic and Gastrointestinal Transit Times in 111 Healthy Volunteers Using the 3D-Transit Electromagnet Tracking System: Influence of Age, Gender, and Body Mass Index. *Neurogastroenterol. Motil.* **2020**, *32*, e13734, doi:10.1111/nmo.13734.
54. Tominaga, K.; Sato, H.; Yokomichi, H.; Tsuchiya, A.; Yoshida, T.; Kawata, Y.; Mizusawa, T.; Yokoyama, J.; Terai, S. Variation in Small Bowel Transit Time on Capsule Endoscopy. *Ann. Transl. Med.* **2020**, *8*, 348, doi:10.21037/atm.2020.02.40.
55. Wang, Y.T.; Mohammed, S.D.; Farmer, A.D.; Wang, D.; Zarate, N.; Hobson, A.R.; Hellström, P.M.; Semler, J.R.; Kuo, B.; Rao, S.S.; et al. Regional Gastrointestinal Transit and PH Studied in 215 Healthy Volunteers Using the Wireless Motility Capsule: Influence of Age, Gender, Study Country and Testing Protocol. *Aliment. Pharmacol. Ther.* **2015**, *42*, 761–772, doi:10.1111/apt.13329.
56. Worsøe, J.; Fynne, L.; Gregersen, T.; Schlageter, V.; Christensen, L.A.; Dahlerup, J.F.; Rijkhoff, N.J.M.; Laurberg, S.; Krogh, K. Gastric Transit and Small Intestinal Transit Time and Motility Assessed by a Magnet Tracking System. *BMC Gastroenterol.* **2011**, *11*, 145, doi:10.1186/1471-230X-11-145.
57. Weitschies, W.; Kosch, O.; Mönnikes, H.; Trahms, L. Magnetic Marker Monitoring: An Application of Biomagnetic Measurement Instrumentation and Principles for the Determination of the Gastrointestinal Behavior of Magnetically Marked Solid Dosage Forms. *Adv. Drug Deliv. Rev.* **2005**, *57*, 1210–1222, doi:10.1016/j.addr.2005.01.025.
58. McConnell, E.L.; Fadda, H.M.; Basit, A.W. Gut Instincts: Explorations in Intestinal Physiology and Drug Delivery. *Int. J. Pharm.* **2008**, *364*, 213–226, doi:10.1016/j.ijpharm.2008.05.012.
59. John, V.A.; Shotton, P.A.; Moppert, J.; Theobald, W. Gastrointestinal Transit of Oros Drug Delivery Systems in Healthy Volunteers: A Short

Report. *Br. J. Clin. Pharmacol.* **1985**, *19 Suppl 2*, 203S-206S, doi:10.1111/j.1365-2125.1985.tb02763.x.
60. Rebersek, M. Gut Microbiome and Its Role in Colorectal Cancer. *BMC Cancer* **2021**, *21*, 1325, doi:10.1186/s12885-021-09054-2.
61. Holmes, E.; Li, J.V.; Marchesi, J.R.; Nicholson, J.K. Gut Microbiota Composition and Activity in Relation to Host Metabolic Phenotype and Disease Risk. *Cell Metab.* **2012**, *16*, 559–564, doi:10.1016/j.cmet.2012.10.007.
62. LeBlanc, J.G.; Milani, C.; de Giori, G.S.; Sesma, F.; van Sinderen, D.; Ventura, M. Bacteria as Vitamin Suppliers to Their Host: A Gut Microbiota Perspective. *Curr. Opin. Biotechnol.* **2013**, *24*, 160–168, doi:10.1016/j.copbio.2012.08.005.
63. Makki, K.; Deehan, E.C.; Walter, J.; Bäckhed, F. The Impact of Dietary Fiber on Gut Microbiota in Host Health and Disease. *Cell Host Microbe* **2018**, *23*, 705–715, doi:10.1016/j.chom.2018.05.012.
64. Wong, S.H.; Yu, J. Gut Microbiota in Colorectal Cancer: Mechanisms of Action and Clinical Applications. *Nat. Rev. Gastroenterol. Hepatol.* **2019**, *16*, 690–704, doi:10.1038/s41575-019-0209-8.
65. Dubinsky, V.; Dotan, I.; Gophna, U. Strains Colonizing Different Intestinal Sites within an Individual Are Derived from a Single Founder Population. *mBio* **2023**, *14*, e0345622, doi:10.1128/mbio.03456-22.
66. Gough, E.K.; Bourke, C.D.; Berejena, C.; Shonhai, A.; Bwakura-Dangarembizi, M.; Prendergast, A.J.; Manges, A.R. Strain-Level Analysis of Gut-Resident pro-Inflammatory Viridans Group Streptococci Suppressed by Long-Term Cotrimoxazole Prophylaxis among HIV-Positive Children in Zimbabwe. *Gut Microbes* **2020**, *11*, 1104–1115, doi:10.1080/19490976.2020.1717299.
67. Schmidt, T.S.; Hayward, M.R.; Coelho, L.P.; Li, S.S.; Costea, P.I.; Voigt, A.Y.; Wirbel, J.; Maistrenko, O.M.; Alves, R.J.; Bergsten, E.; et al. Extensive Transmission of Microbes along the Gastrointestinal Tract. *eLife* **2019**, *8*, e42693, doi:10.7554/eLife.42693.
68. Avelar Rodriguez, D.; Ryan, P.M.; Toro Monjaraz, E.M.; Ramirez Mayans, J.A.; Quigley, E.M. Small Intestinal Bacterial Overgrowth in Children: A State-Of-The-Art Review. *Front. Pediatr.* **2019**, *7*, 363, doi:10.3389/fped.2019.00363.
69. Burcham, Z.M.; Garneau, N.L.; Comstock, S.S.; Tucker, R.M.; Knight, R.; Metcalf, J.L.; Genetics of Taste Lab Citizen Scientists Patterns of Oral Microbiota Diversity in Adults and Children: A Crowdsourced Population Study. *Sci. Rep.* **2020**, *10*, 2133, doi:10.1038/s41598-020-59016-0.
70. Crnčević, N.; Hukić, M.; Deumić, S.; Selimagić, A.; Dozić, A.; Gavrankapetanović, I.; Klepo, D.; Avdić, M. Gastrointestinal Tract Microbiome Effect and Role in Disease Development. *Diseases* **2022**, *10*, 45, doi:10.3390/diseases10030045.

71. Duan, X.; Chen, P.; Xu, X.; Han, M.; Li, J. Role of Gastric Microorganisms Other than Helicobacter Pylori in the Development and Treatment of Gastric Diseases. *BioMed Res. Int.* **2022**, *2022*, 6263423, doi:10.1155/2022/6263423.
72. Guo, X.; Okpara, E.S.; Hu, W.; Yan, C.; Wang, Y.; Liang, Q.; Chiang, J.Y.L.; Han, S. Interactive Relationships between Intestinal Flora and Bile Acids. *Int. J. Mol. Sci.* **2022**, *23*, 8343, doi:10.3390/ijms23158343.
73. Ruan, W.; Engevik, M.A.; Spinler, J.K.; Versalovic, J. Healthy Human Gastrointestinal Microbiome: Composition and Function After a Decade of Exploration. *Dig. Dis. Sci.* **2020**, *65*, 695–705, doi:10.1007/s10620-020-06118-4.
74. Yersin, S.; Vonaesch, P. Small Intestinal Microbiota: From Taxonomic Composition to Metabolism. *Trends Microbiol.* **2024**, doi:10.1016/j.tim.2024.02.013.
75. Zou, Q.; Feng, L.; Cai, X.; Qian, Y.; Xu, L. Esophageal Microflora in Esophageal Diseases. *Front. Cell. Infect. Microbiol.* **2023**, *13*, 1145791, doi:10.3389/fcimb.2023.1145791.
76. Sender, R.; Fuchs, S.; Milo, R. Revised Estimates for the Number of Human and Bacteria Cells in the Body. *PLOS Biol.* **2016**, *14*, e1002533, doi:10.1371/journal.pbio.1002533.
77. Friedman, E.S.; Bittinger, K.; Esipova, T.V.; Hou, L.; Chau, L.; Jiang, J.; Mesaros, C.; Lund, P.J.; Liang, X.; FitzGerald, G.A.; et al. Microbes vs. Chemistry in the Origin of the Anaerobic Gut Lumen. *Proc. Natl. Acad. Sci.* **2018**, *115*, 4170–4175, doi:10.1073/pnas.1718635115.
78. Singhal, R.; Shah, Y.M. Oxygen Battle in the Gut: Hypoxia and Hypoxia-Inducible Factors in Metabolic and Inflammatory Responses in the Intestine. *J. Biol. Chem.* **2020**, *295*, 10493–10505, doi:10.1074/jbc.REV120.011188.
79. Adlerberth, I.; Wold, A.E. Establishment of the Gut Microbiota in Western Infants. *Acta Paediatr. Oslo Nor. 1992* **2009**, *98*, 229–238, doi:10.1111/j.1651-2227.2008.01060.x.
80. Orrhage, K.; Nord, C.E. Factors Controlling the Bacterial Colonization of the Intestine in Breastfed Infants. *Acta Paediatr. Oslo Nor. 1992 Suppl.* **1999**, *88*, 47–57, doi:10.1111/j.1651-2227.1999.tb01300.x.
81. Li, G.; Yang, M.; Zhou, K.; Zhang, L.; Tian, L.; Lv, S.; Jin, Y.; Qian, W.; Xiong, H.; Lin, R.; et al. Diversity of Duodenal and Rectal Microbiota in Biopsy Tissues and Luminal Contents in Healthy Volunteers. *J. Microbiol. Biotechnol.* **2015**, *25*, 1136–1145, doi:10.4014/jmb.1412.12047.
82. Shin, A.S.; Gao, X.; Bohm, M.; Lin, H.; Gupta, A.; Nelson, D.E.; Toh, E.; Teagarden, S.; Siwiec, R.; Dong, Q.; et al. Characterization of Proximal Small Intestinal Microbiota in Patients With Suspected Small Intestinal Bacterial Overgrowth: A Cross-Sectional Study. *Clin.*

Transl. Gastroenterol. **2019**, *10*, e00073, doi:10.14309/ctg.0000000000000073.
83. Kahouli, I.; Tomaro-Duchesneau, C.; Prakash, S. Probiotics in Colorectal Cancer (CRC) with Emphasis on Mechanisms of Action and Current Perspectives. *J. Med. Microbiol.* **2013**, *62*, 1107–1123, doi:10.1099/jmm.0.048975-0.
84. Hillman, E.T.; Lu, H.; Yao, T.; Nakatsu, C.H. Microbial Ecology along the Gastrointestinal Tract. *Microbes Environ.* **2017**, *32*, 300–313, doi:10.1264/jsme2.ME17017.
85. Albenberg, L.; Esipova, T.V.; Judge, C.P.; Bittinger, K.; Chen, J.; Laughlin, A.; Grunberg, S.; Baldassano, R.N.; Lewis, J.D.; Li, H.; et al. Correlation between Intraluminal Oxygen Gradient and Radial Partitioning of Intestinal Microbiota. *Gastroenterology* **2014**, *147*, 1055-1063.e8, doi:10.1053/j.gastro.2014.07.020.
86. Chattopadhyay, I.; Dhar, R.; Pethusamy, K.; Seethy, A.; Srivastava, T.; Sah, R.; Sharma, J.; Karmakar, S. Exploring the Role of Gut Microbiome in Colon Cancer. *Appl. Biochem. Biotechnol.* **2021**, *193*, 1780–1799, doi:10.1007/s12010-021-03498-9.
87. Van Raay, T.; Allen-Vercoe, E. Microbial Interactions and Interventions in Colorectal Cancer. *Microbiol. Spectr.* **2017**, *5*, doi:10.1128/microbiolspec.BAD-0004-2016.
88. Sung, H.; Ferlay, J.; Siegel, R.L.; Laversanne, M.; Soerjomataram, I.; Jemal, A.; Bray, F. Global Cancer Statistics 2020: GLOBOCAN Estimates of Incidence and Mortality Worldwide for 36 Cancers in 185 Countries. *CA. Cancer J. Clin.* **2021**, *71*, 209–249, doi:10.3322/caac.21660.
89. Grabsch, H.I.; Tan, P. Gastric Cancer Pathology and Underlying Molecular Mechanisms. *Dig. Surg.* **2013**, *30*, 150–158, doi:10.1159/000350876.
90. Lauren, P. The Two Histological Main Types of Gastric Carcinoma: Diffuse and So-Called Intestinal-Type Carcinoma. An Attempt at a Histo-Clinical Classification. *Acta Pathol. Microbiol. Scand.* **1965**, *64*, 31–49, doi:10.1111/apm.1965.64.1.31.
91. Nagtegaal, I.D.; Odze, R.D.; Klimstra, D.; Paradis, V.; Rugge, M.; Schirmacher, P.; Washington, K.M.; Carneiro, F.; Cree, I.A.; WHO Classification of Tumours Editorial Board The 2019 WHO Classification of Tumours of the Digestive System. *Histopathology* **2020**, *76*, 182–188, doi:10.1111/his.13975.
92. Li, Y.; Feng, A.; Zheng, S.; Chen, C.; Lyu, J. Recent Estimates and Predictions of 5-Year Survival in Patients with Gastric Cancer: A Model-Based Period Analysis. *Cancer Control J. Moffitt Cancer Cent.* **2022**, *29*, 10732748221099228, doi:10.1177/10732748221099227.
93. Bausys, A.; Luksta, M.; Anglickiene, G.; Maneikiene, V.V.; Kryzauskas, M.; Rybakovas, A.; Dulskas, A.; Kuliavas, J.; Stratilatovas, E.; Macijauskiene, L.; et al. Effect of Home-Based

Prehabilitation on Postoperative Complications after Surgery for Gastric Cancer: Randomized Clinical Trial. *Br. J. Surg.* **2023**, *110*, 1800–1807, doi:10.1093/bjs/znad312.
94. Karanicolas, P.J.; Graham, D.; Gönen, M.; Strong, V.E.; Brennan, M.F.; Coit, D.G. Quality of Life after Gastrectomy for Adenocarcinoma: A Prospective Cohort Study. *Ann. Surg.* **2013**, *257*, 1039–1046, doi:10.1097/SLA.0b013e31828c4a19.
95. Lee, S.S.; Chung, H.Y.; Kwon, O.K.; Yu, W. Long-Term Quality of Life After Distal Subtotal and Total Gastrectomy: Symptom- and Behavior-Oriented Consequences. *Ann. Surg.* **2016**, *263*, 738–744, doi:10.1097/SLA.0000000000001481.
96. Xi, Y.; Xu, P. Global Colorectal Cancer Burden in 2020 and Projections to 2040. *Transl. Oncol.* **2021**, *14*, 101174, doi:10.1016/j.tranon.2021.101174.
97. Mizutani, S.; Yamada, T.; Yachida, S. Significance of the Gut Microbiome in Multistep Colorectal Carcinogenesis. *Cancer Sci.* **2020**, *111*, 766–773, doi:10.1111/cas.14298.
98. Fearon, E.R.; Vogelstein, B. A Genetic Model for Colorectal Tumorigenesis. *Cell* **1990**, *61*, 759–767, doi:10.1016/0092-8674(90)90186-i.
99. Murphy, N.; Moreno, V.; Hughes, D.J.; Vodicka, L.; Vodicka, P.; Aglago, E.K.; Gunter, M.J.; Jenab, M. Lifestyle and Dietary Environmental Factors in Colorectal Cancer Susceptibility. *Mol. Aspects Med.* **2019**, *69*, 2–9, doi:10.1016/j.mam.2019.06.005.
100. Li, F.; Lai, M. Colorectal Cancer, One Entity or Three. *J. Zhejiang Univ. Sci. B* **2009**, *10*, 219–229, doi:10.1631/jzus.B0820273.
101. Lengauer, C.; Kinzler, K.W.; Vogelstein, B. Genetic Instabilities in Human Cancers. *Nature* **1998**, *396*, 643–649, doi:10.1038/25292.
102. Pino, M.S.; Chung, D.C. The Chromosomal Instability Pathway in Colon Cancer. *Gastroenterology* **2010**, *138*, 2059–2072, doi:10.1053/j.gastro.2009.12.065.
103. Markowitz, S.D.; Bertagnolli, M.M. Molecular Origins of Cancer: Molecular Basis of Colorectal Cancer. *N. Engl. J. Med.* **2009**, *361*, 2449–2460, doi:10.1056/NEJMra0804588.
104. Grabsch, H.I.; Askham, J.M.; Morrison, E.E.; Pomjanski, N.; Lickvers, K.; Parsons, W.J.; Boecking, A.; Gabbert, H.E.; Mueller, W. Expression of BUB1 Protein in Gastric Cancer Correlates with the Histological Subtype, but Not with DNA Ploidy or Microsatellite Instability. *J. Pathol.* **2004**, *202*, 208–214, doi:10.1002/path.1499.
105. Ottini, L.; Falchetti, M.; Lupi, R.; Rizzolo, P.; Agnese, V.; Colucci, G.; Bazan, V.; Russo, A. Patterns of Genomic Instability in Gastric Cancer: Clinical Implications and Perspectives. *Ann. Oncol. Off. J. Eur. Soc. Med. Oncol.* **2006**, *17 Suppl 7*, vii97-102, doi:10.1093/annonc/mdl960.

106. Al-Sohaily, S.; Biankin, A.; Leong, R.; Kohonen-Corish, M.; Warusavitarne, J. Molecular Pathways in Colorectal Cancer. *J. Gastroenterol. Hepatol.* **2012**, *27*, 1423–1431, doi:10.1111/j.1440-1746.2012.07200.x.
107. Powell, S.M.; Zilz, N.; Beazer-Barclay, Y.; Bryan, T.M.; Hamilton, S.R.; Thibodeau, S.N.; Vogelstein, B.; Kinzler, K.W. APC Mutations Occur Early during Colorectal Tumorigenesis. *Nature* **1992**, *359*, 235–237, doi:10.1038/359235a0.
108. Su, L.K.; Vogelstein, B.; Kinzler, K.W. Association of the APC Tumor Suppressor Protein with Catenins. *Science* **1993**, *262*, 1734–1737, doi:10.1126/science.8259519.
109. Bokoch, G.M.; Der, C.J. Emerging Concepts in the Ras Superfamily of GTP-Binding Proteins. *FASEB J. Off. Publ. Fed. Am. Soc. Exp. Biol.* **1993**, *7*, 750–759, doi:10.1096/fasebj.7.9.8330683.
110. Wang, J.-Y.; Wang, Y.-H.; Jao, S.-W.; Lu, C.-Y.; Kuo, C.-H.; Hu, H.-M.; Hsieh, J.-S.; Chong, I.-W.; Cheng, T.-L.; Lin, S.-R. Molecular Mechanisms Underlying the Tumorigenesis of Colorectal Adenomas: Correlation to Activated K-Ras Oncogene. *Oncol. Rep.* **2006**, *16*, 1245–1252.
111. Fukuyama, R.; Niculaita, R.; Ng, K.P.; Obusez, E.; Sanchez, J.; Kalady, M.; Aung, P.P.; Casey, G.; Sizemore, N. Mutated in Colorectal Cancer, a Putative Tumor Suppressor for Serrated Colorectal Cancer, Selectively Represses Beta-Catenin-Dependent Transcription. *Oncogene* **2008**, *27*, 6044–6055, doi:10.1038/onc.2008.204.
112. Kohonen-Corish, M.R.J.; Sigglekow, N.D.; Susanto, J.; Chapuis, P.H.; Bokey, E.L.; Dent, O.F.; Chan, C.; Lin, B.P.C.; Seng, T.J.; Laird, P.W.; et al. Promoter Methylation of the Mutated in Colorectal Cancer Gene Is a Frequent Early Event in Colorectal Cancer. *Oncogene* **2007**, *26*, 4435–4441, doi:10.1038/sj.onc.1210210.
113. Pangon, L.; Sigglekow, N.D.; Larance, M.; Al-Sohaily, S.; Mladenova, D.N.; Selinger, C.I.; Musgrove, E.A.; Kohonen-Corish, M.R.J. The "Mutated in Colorectal Cancer" Protein Is a Novel Target of the UV-Induced DNA Damage Checkpoint. *Genes Cancer* **2010**, *1*, 917–926, doi:10.1177/1947601910388937.
114. Mehlen, P.; Fearon, E.R. Role of the Dependence Receptor DCC in Colorectal Cancer Pathogenesis. *J. Clin. Oncol. Off. J. Am. Soc. Clin. Oncol.* **2004**, *22*, 3420–3428, doi:10.1200/JCO.2004.02.019.
115. Martín, M.; Simon-Assmann, P.; Kedinger, M.; Martin, M.; Mangeat, P.; Real, F.X.; Fabre, M. DCC Regulates Cell Adhesion in Human Colon Cancer Derived HT-29 Cells and Associates with Ezrin. *Eur. J. Cell Biol.* **2006**, *85*, 769–783, doi:10.1016/j.ejcb.2006.02.013.
116. Kirley, S.D.; D'Apuzzo, M.; Lauwers, G.Y.; Graeme-Cook, F.; Chung, D.C.; Zukerberg, L.R. The Cables Gene on Chromosome 18Q Regulates Colon Cancer Progression in Vivo. *Cancer Biol. Ther.* **2005**, *4*, 861–863, doi:10.4161/cbt.4.8.1894.

117. Jung, B.; Staudacher, J.J.; Beauchamp, D. Transforming Growth Factor β Superfamily Signaling in Development of Colorectal Cancer. *Gastroenterology* **2017**, *152*, 36–52, doi:10.1053/j.gastro.2016.10.015.
118. Ahmad, R.; Singh, J.K.; Wunnava, A.; Al-Obeed, O.; Abdulla, M.; Srivastava, S.K. Emerging Trends in Colorectal Cancer: Dysregulated Signaling Pathways (Review). *Int. J. Mol. Med.* **2021**, *47*, 14, doi:10.3892/ijmm.2021.4847.
119. Sigal, A.; Rotter, V. Oncogenic Mutations of the P53 Tumor Suppressor: The Demons of the Guardian of the Genome. *Cancer Res.* **2000**, *60*, 6788–6793.
120. Teodoro, J.G.; Evans, S.K.; Green, M.R. Inhibition of Tumor Angiogenesis by P53: A New Role for the Guardian of the Genome. *J. Mol. Med. Berl. Ger.* **2007**, *85*, 1175–1186, doi:10.1007/s00109-007-0221-2.
121. Levine, A.J. P53, the Cellular Gatekeeper for Growth and Division. *Cell* **1997**, *88*, 323–331, doi:10.1016/s0092-8674(00)81871-1.
122. Boland, C.R.; Goel, A. Microsatellite Instability in Colorectal Cancer. *Gastroenterology* **2010**, *138*, 2073-2087.e3, doi:10.1053/j.gastro.2009.12.064.
123. Oliveira, C.; Seruca, R.; Seixas, M.; Sobrinho-Simões, M. The Clinicopathological Features of Gastric Carcinomas with Microsatellite Instability May Be Mediated by Mutations of Different "Target Genes": A Study of the TGFbeta RII, IGFII R, and BAX Genes. *Am. J. Pathol.* **1998**, *153*, 1211–1219, doi:10.1016/s0002-9440(10)65665-9.
124. Hayden, J.D.; Martin, I.G.; Cawkwell, L.; Quirke, P. The Role of Microsatellite Instability in Gastric Carcinoma. *Gut* **1998**, *42*, 300–303, doi:10.1136/gut.42.2.300.
125. Wirtz, H.C.; Müller, W.; Noguchi, T.; Scheven, M.; Rüschoff, J.; Hommel, G.; Gabbert, H.E. Prognostic Value and Clinicopathological Profile of Microsatellite Instability in Gastric Cancer. *Clin. Cancer Res. Off. J. Am. Assoc. Cancer Res.* **1998**, *4*, 1749–1754.
126. Hayden, J.D.; Cawkwell, L.; Dixon, M.F.; Pardal, F.; Murgatroyd, H.; Gray, S.; Quirke, P.; Martin, I.G. A Comparison of Microsatellite Instability in Early Onset Gastric Carcinomas from Relatively Low and High Incidence European Populations. *Int. J. Cancer* **2000**, *85*, 189–191.
127. Vauhkonen, M.; Vauhkonen, H.; Sajantila, A.; Sipponen, P. Differences in Genomic Instability between Intestinal- and Diffuse-Type Gastric Cancer. *Gastric Cancer Off. J. Int. Gastric Cancer Assoc. Jpn. Gastric Cancer Assoc.* **2005**, *8*, 238–244, doi:10.1007/s10120-005-0346-3.
128. Fleisher, A.S.; Esteller, M.; Wang, S.; Tamura, G.; Suzuki, H.; Yin, J.; Zou, T.T.; Abraham, J.M.; Kong, D.; Smolinski, K.N.; et al.

Hypermethylation of the HMLH1 Gene Promoter in Human Gastric Cancers with Microsatellite Instability. *Cancer Res.* **1999**, *59*, 1090–1095.
129. Nojadeh, J.N.; Behrouz Sharif, S.; Sakhinia, E. Microsatellite Instability in Colorectal Cancer. *EXCLI J.* **2018**, *17*, 159–168, doi:10.17179/excli2017-948.
130. Vilar, E.; Gruber, S.B. Microsatellite Instability in Colorectal Cancer—the Stable Evidence. *Nat. Rev. Clin. Oncol.* **2010**, *7*, 153–162, doi:10.1038/nrclinonc.2009.237.
131. van Rijnsoever, M.; Grieu, F.; Elsaleh, H.; Joseph, D.; Iacopetta, B. Characterisation of Colorectal Cancers Showing Hypermethylation at Multiple CpG Islands. *Gut* **2002**, *51*, 797–802, doi:10.1136/gut.51.6.797.
132. Wong, J.J.L.; Hawkins, N.J.; Ward, R.L. Colorectal Cancer: A Model for Epigenetic Tumorigenesis. *Gut* **2007**, *56*, 140–148, doi:10.1136/gut.2005.088799.
133. Kang, G.H.; Lee, H.J.; Hwang, K.S.; Lee, S.; Kim, J.-H.; Kim, J.-S. Aberrant CpG Island Hypermethylation of Chronic Gastritis, in Relation to Aging, Gender, Intestinal Metaplasia, and Chronic Inflammation. *Am. J. Pathol.* **2003**, *163*, 1551–1556, doi:10.1016/S0002-9440(10)63511-0.
134. Oue, N.; Oshimo, Y.; Nakayama, H.; Ito, R.; Yoshida, K.; Matsusaki, K.; Yasui, W. DNA Methylation of Multiple Genes in Gastric Carcinoma: Association with Histological Type and CpG Island Methylator Phenotype. *Cancer Sci.* **2003**, *94*, 901–905, doi:10.1111/j.1349-7006.2003.tb01373.x.
135. Toyota, M.; Ahuja, N.; Suzuki, H.; Itoh, F.; Ohe-Toyota, M.; Imai, K.; Baylin, S.B.; Issa, J.P. Aberrant Methylation in Gastric Cancer Associated with the CpG Island Methylator Phenotype. *Cancer Res.* **1999**, *59*, 5438–5442.
136. Seely, K.D.; Morgan, A.D.; Hagenstein, L.D.; Florey, G.M.; Small, J.M. Bacterial Involvement in Progression and Metastasis of Colorectal Neoplasia. *Cancers* **2022**, *14*, 1019, doi:10.3390/cancers14041019.
137. Tilg, H.; Adolph, T.E.; Gerner, R.R.; Moschen, A.R. The Intestinal Microbiota in Colorectal Cancer. *Cancer Cell* **2018**, *33*, 954–964, doi:10.1016/j.ccell.2018.03.004.
138. Chen, W.; Liu, F.; Ling, Z.; Tong, X.; Xiang, C. Human Intestinal Lumen and Mucosa-Associated Microbiota in Patients with Colorectal Cancer. *PloS One* **2012**, *7*, e39743, doi:10.1371/journal.pone.0039743.
139. Saffarian, A.; Mulet, C.; Regnault, B.; Amiot, A.; Tran-Van-Nhieu, J.; Ravel, J.; Sobhani, I.; Sansonetti, P.J.; Pédron, T. Crypt- and Mucosa-Associated Core Microbiotas in Humans and Their Alteration in Colon Cancer Patients. *mBio* **2019**, *10*, e01315-19, doi:10.1128/mBio.01315-19.

140. Wang, T.; Cai, G.; Qiu, Y.; Fei, N.; Zhang, M.; Pang, X.; Jia, W.; Cai, S.; Zhao, L. Structural Segregation of Gut Microbiota between Colorectal Cancer Patients and Healthy Volunteers. *ISME J.* **2012**, *6*, 320–329, doi:10.1038/ismej.2011.109.
141. Feng, Q.; Liang, S.; Jia, H.; Stadlmayr, A.; Tang, L.; Lan, Z.; Zhang, D.; Xia, H.; Xu, X.; Jie, Z.; et al. Gut Microbiome Development along the Colorectal Adenoma-Carcinoma Sequence. *Nat. Commun.* **2015**, *6*, 6528, doi:10.1038/ncomms7528.
142. Gao, Z.; Guo, B.; Gao, R.; Zhu, Q.; Wu, W.; Qin, H. Probiotics Modify Human Intestinal Mucosa-Associated Microbiota in Patients with Colorectal Cancer. *Mol. Med. Rep.* **2015**, *12*, 6119–6127, doi:10.3892/mmr.2015.4124.
143. Shen, X.J.; Rawls, J.F.; Randall, T.; Burcal, L.; Mpande, C.N.; Jenkins, N.; Jovov, B.; Abdo, Z.; Sandler, R.S.; Keku, T.O. Molecular Characterization of Mucosal Adherent Bacteria and Associations with Colorectal Adenomas. *Gut Microbes* **2010**, *1*, 138–147, doi:10.4161/gmic.1.3.12360.
144. Viljoen, K.S.; Dakshinamurthy, A.; Goldberg, P.; Blackburn, J.M. Quantitative Profiling of Colorectal Cancer-Associated Bacteria Reveals Associations between Fusobacterium Spp., Enterotoxigenic Bacteroides Fragilis (ETBF) and Clinicopathological Features of Colorectal Cancer. *PloS One* **2015**, *10*, e0119462, doi:10.1371/journal.pone.0119462.
145. Castellarin, M.; Warren, R.L.; Freeman, J.D.; Dreolini, L.; Krzywinski, M.; Strauss, J.; Barnes, R.; Watson, P.; Allen-Vercoe, E.; Moore, R.A.; et al. Fusobacterium Nucleatum Infection Is Prevalent in Human Colorectal Carcinoma. *Genome Res.* **2012**, *22*, 299–306, doi:10.1101/gr.126516.111.
146. Kostic, A.D.; Gevers, D.; Pedamallu, C.S.; Michaud, M.; Duke, F.; Earl, A.M.; Ojesina, A.I.; Jung, J.; Bass, A.J.; Tabernero, J.; et al. Genomic Analysis Identifies Association of Fusobacterium with Colorectal Carcinoma. *Genome Res.* **2012**, *22*, 292–298, doi:10.1101/gr.126573.111.
147. Wong, C.C.; Yu, J. Gut Microbiota in Colorectal Cancer Development and Therapy. *Nat. Rev. Clin. Oncol.* **2023**, *20*, 429–452, doi:10.1038/s41571-023-00766-x.
148. Rubinstein, M.R.; Baik, J.E.; Lagana, S.M.; Han, R.P.; Raab, W.J.; Sahoo, D.; Dalerba, P.; Wang, T.C.; Han, Y.W. Fusobacterium Nucleatum Promotes Colorectal Cancer by Inducing Wnt/β-Catenin Modulator Annexin A1. *EMBO Rep.* **2019**, *20*, e47638, doi:10.15252/embr.201847638.
149. Rubinstein, M.R.; Wang, X.; Liu, W.; Hao, Y.; Cai, G.; Han, Y.W. Fusobacterium Nucleatum Promotes Colorectal Carcinogenesis by Modulating E-Cadherin/β-Catenin Signaling via Its FadA Adhesin.

Cell Host Microbe **2013**, *14*, 195–206, doi:10.1016/j.chom.2013.07.012.
150. Fardini, Y.; Wang, X.; Témoin, S.; Nithianantham, S.; Lee, D.; Shoham, M.; Han, Y.W. Fusobacterium Nucleatum Adhesin FadA Binds Vascular Endothelial Cadherin and Alters Endothelial Integrity. *Mol. Microbiol.* **2011**, *82*, 1468–1480, doi:10.1111/j.1365-2958.2011.07905.x.
151. Abed, J.; Emgård, J.E.M.; Zamir, G.; Faroja, M.; Almogy, G.; Grenov, A.; Sol, A.; Naor, R.; Pikarsky, E.; Atlan, K.A.; et al. Fap2 Mediates Fusobacterium Nucleatum Colorectal Adenocarcinoma Enrichment by Binding to Tumor-Expressed Gal-GalNAc. *Cell Host Microbe* **2016**, *20*, 215–225, doi:10.1016/j.chom.2016.07.006.
152. Brennan, C.A.; Garrett, W.S. Fusobacterium Nucleatum - Symbiont, Opportunist and Oncobacterium. *Nat. Rev. Microbiol.* **2019**, *17*, 156–166, doi:10.1038/s41579-018-0129-6.
153. Mima, K.; Nishihara, R.; Qian, Z.R.; Cao, Y.; Sukawa, Y.; Nowak, J.A.; Yang, J.; Dou, R.; Masugi, Y.; Song, M.; et al. Fusobacterium Nucleatum in Colorectal Carcinoma Tissue and Patient Prognosis. *Gut* **2016**, *65*, 1973–1980, doi:10.1136/gutjnl-2015-310101.
154. Long, X.; Wong, C.C.; Tong, L.; Chu, E.S.H.; Ho Szeto, C.; Go, M.Y.Y.; Coker, O.O.; Chan, A.W.H.; Chan, F.K.L.; Sung, J.J.Y.; et al. Peptostreptococcus Anaerobius Promotes Colorectal Carcinogenesis and Modulates Tumour Immunity. *Nat. Microbiol.* **2019**, *4*, 2319–2330, doi:10.1038/s41564-019-0541-3.
155. Mu, W.; Jia, Y.; Chen, X.; Li, H.; Wang, Z.; Cheng, B. Intracellular Porphyromonas Gingivalis Promotes the Proliferation of Colorectal Cancer Cells via the MAPK/ERK Signaling Pathway. *Front. Cell. Infect. Microbiol.* **2020**, *10*, 584798, doi:10.3389/fcimb.2020.584798.
156. Abais, J.M.; Xia, M.; Zhang, Y.; Boini, K.M.; Li, P.-L. Redox Regulation of NLRP3 Inflammasomes: ROS as Trigger or Effector? *Antioxid. Redox Signal.* **2015**, *22*, 1111–1129, doi:10.1089/ars.2014.5994.
157. Xing, J.; Fang, Y.; Zhang, W.; Zhang, H.; Tang, D.; Wang, D. Bacterial Driver-Passenger Model in Biofilms: A New Mechanism in the Development of Colorectal Cancer. *Clin. Transl. Oncol. Off. Publ. Fed. Span. Oncol. Soc. Natl. Cancer Inst. Mex.* **2022**, *24*, 784–795, doi:10.1007/s12094-021-02738-y.
158. Cancer Genome Atlas Network Comprehensive Molecular Characterization of Human Colon and Rectal Cancer. *Nature* **2012**, *487*, 330–337, doi:10.1038/nature11252.
159. Zou, S.; Fang, L.; Lee, M.-H. Dysbiosis of Gut Microbiota in Promoting the Development of Colorectal Cancer. *Gastroenterol. Rep.* **2018**, *6*, 1–12, doi:10.1093/gastro/gox031.
160. Buc, E.; Dubois, D.; Sauvanet, P.; Raisch, J.; Delmas, J.; Darfeuille-Michaud, A.; Pezet, D.; Bonnet, R. High Prevalence of Mucosa-

Associated E. Coli Producing Cyclomodulin and Genotoxin in Colon Cancer. *PloS One* **2013**, *8*, e56964, doi:10.1371/journal.pone.0056964.
161. Allen-Vercoe, E.; Jobin, C. Fusobacterium and Enterobacteriaceae: Important Players for CRC? *Immunol. Lett.* **2014**, *162*, 54–61, doi:10.1016/j.imlet.2014.05.014.
162. Wilson, M.R.; Jiang, Y.; Villalta, P.W.; Stornetta, A.; Boudreau, P.D.; Carrá, A.; Brennan, C.A.; Chun, E.; Ngo, L.; Samson, L.D.; et al. The Human Gut Bacterial Genotoxin Colibactin Alkylates DNA. *Science* **2019**, *363*, eaar7785, doi:10.1126/science.aar7785.
163. Xue, M.; Kim, C.S.; Healy, A.R.; Wernke, K.M.; Wang, Z.; Frischling, M.C.; Shine, E.E.; Wang, W.; Herzon, S.B.; Crawford, J.M. Structure Elucidation of Colibactin and Its DNA Cross-Links. *Science* **2019**, *365*, eaax2685, doi:10.1126/science.aax2685.
164. Johnson, W.M.; Lior, H. A New Heat-Labile Cytolethal Distending Toxin (CLDT) Produced by Escherichia Coli Isolates from Clinical Material. *Microb. Pathog.* **1988**, *4*, 103–113, doi:10.1016/0882-4010(88)90052-6.
165. He, Z.; Gharaibeh, R.Z.; Newsome, R.C.; Pope, J.L.; Dougherty, M.W.; Tomkovich, S.; Pons, B.; Mirey, G.; Vignard, J.; Hendrixson, D.R.; et al. Campylobacter Jejuni Promotes Colorectal Tumorigenesis through the Action of Cytolethal Distending Toxin. *Gut* **2019**, *68*, 289–300, doi:10.1136/gutjnl-2018-317200.
166. Cao, Y.; Oh, J.; Xue, M.; Huh, W.J.; Wang, J.; Gonzalez-Hernandez, J.A.; Rice, T.A.; Martin, A.L.; Song, D.; Crawford, J.M.; et al. Commensal Microbiota from Patients with Inflammatory Bowel Disease Produce Genotoxic Metabolites. *Science* **2022**, *378*, eabm3233, doi:10.1126/science.abm3233.
167. Goodwin, A.C.; Destefano Shields, C.E.; Wu, S.; Huso, D.L.; Wu, X.; Murray-Stewart, T.R.; Hacker-Prietz, A.; Rabizadeh, S.; Woster, P.M.; Sears, C.L.; et al. Polyamine Catabolism Contributes to Enterotoxigenic Bacteroides Fragilis-Induced Colon Tumorigenesis. *Proc. Natl. Acad. Sci. U. S. A.* **2011**, *108*, 15354–15359, doi:10.1073/pnas.1010203108.
168. Wu, S.; Rhee, K.-J.; Zhang, M.; Franco, A.; Sears, C.L. Bacteroides Fragilis Toxin Stimulates Intestinal Epithelial Cell Shedding and Gamma-Secretase-Dependent E-Cadherin Cleavage. *J. Cell Sci.* **2007**, *120*, 1944–1952, doi:10.1242/jcs.03455.
169. Wang, X.; Huycke, M.M. Extracellular Superoxide Production by Enterococcus Faecalis Promotes Chromosomal Instability in Mammalian Cells. *Gastroenterology* **2007**, *132*, 551–561, doi:10.1053/j.gastro.2006.11.040.
170. McCool, K.W.; Miyamoto, S. DNA Damage-Dependent NF-KB Activation: NEMO Turns Nuclear Signaling inside Out. *Immunol. Rev.* **2012**, *246*, 311–326, doi:10.1111/j.1600-065X.2012.01101.x.

171. Global Cancer Update Programme Available online: https://www.wcrf.org/research-policy/global-cancer-update-programme/ (accessed on 7 January 2025).
172. Zhou, Z.; Kleis, L.; Depetris-Chauvin, A.; Jaskulski, S.; Damerell, V.; Michels, K.B.; Gigic, B.; Nöthlings, U.; Panagiotou, G. Beneficial Microbiome and Diet Interplay in Early-Onset Colorectal Cancer. *EMBO Mol. Med.* **2024**, doi:10.1038/s44321-024-00177-0.
173. Tong, Y.; Gao, H.; Qi, Q.; Liu, X.; Li, J.; Gao, J.; Li, P.; Wang, Y.; Du, L.; Wang, C. High Fat Diet, Gut Microbiome and Gastrointestinal Cancer. *Theranostics* **2021**, *11*, 5889–5910, doi:10.7150/thno.56157.
174. Kaźmierczak-Siedlecka, K.; Daca, A.; Roviello, G.; Catalano, M.; Połom, K. Interdisciplinary Insights into the Link between Gut Microbiome and Gastric Carcinogenesis—What Is Currently Known? *Gastric Cancer* **2022**, *25*, 1–10, doi:10.1007/s10120-021-01260-y.
175. Wu, X.; Chen, L.; Cheng, J.; Qian, J.; Fang, Z.; Wu, J. Effect of Dietary Salt Intake on Risk of Gastric Cancer: A Systematic Review and Meta-Analysis of Case-Control Studies. *Nutrients* **2022**, *14*, 4260, doi:10.3390/nu14204260.
176. Peleteiro, B.; Lopes, C.; Figueiredo, C.; Lunet, N. Salt Intake and Gastric Cancer Risk According to Helicobacter Pylori Infection, Smoking, Tumour Site and Histological Type. *Br. J. Cancer* **2011**, *104*, 198–207, doi:10.1038/sj.bjc.6605993.
177. Kolodziejczyk, A.A.; Zheng, D.; Elinav, E. Diet-Microbiota Interactions and Personalized Nutrition. *Nat. Rev. Microbiol.* **2019**, *17*, 742–753, doi:10.1038/s41579-019-0256-8.
178. Horvath, A.; Zukauskaite, K.; Hazia, O.; Balazs, I.; Stadlbauer, V. Human Gut Microbiome: Therapeutic Opportunities for Metabolic Syndrome-Hype or Hope? *Endocrinol. Diabetes Metab.* **2024**, *7*, e436, doi:10.1002/edm2.436.
179. Yang, J.; Yu, J. The Association of Diet, Gut Microbiota and Colorectal Cancer: What We Eat May Imply What We Get. *Protein Cell* **2018**, *9*, 474–487, doi:10.1007/s13238-018-0543-6.
180. Liu, W.; Zhang, X.; Xu, H.; Li, S.; Lau, H.C.-H.; Chen, Q.; Zhang, B.; Zhao, L.; Chen, H.; Sung, J.J.-Y.; et al. Microbial Community Heterogeneity Within Colorectal Neoplasia and Its Correlation With Colorectal Carcinogenesis. *Gastroenterology* **2021**, *160*, 2395–2408, doi:10.1053/j.gastro.2021.02.020.
181. Xia, X.; Wu, W.K.K.; Wong, S.H.; Liu, D.; Kwong, T.N.Y.; Nakatsu, G.; Yan, P.S.; Chuang, Y.-M.; Chan, M.W.-Y.; Coker, O.O.; et al. Bacteria Pathogens Drive Host Colonic Epithelial Cell Promoter Hypermethylation of Tumor Suppressor Genes in Colorectal Cancer. *Microbiome* **2020**, *8*, 108, doi:10.1186/s40168-020-00847-4.
182. Yuan, C.; Burns, M.B.; Subramanian, S.; Blekhman, R. Interaction between Host MicroRNAs and the Gut Microbiota in Colorectal

Cancer. *mSystems* **2018**, *3*, e00205-17, doi:10.1128/mSystems.00205-17.
183. Liu, S.; da Cunha, A.P.; Rezende, R.M.; Cialic, R.; Wei, Z.; Bry, L.; Comstock, L.E.; Gandhi, R.; Weiner, H.L. The Host Shapes the Gut Microbiota via Fecal MicroRNA. *Cell Host Microbe* **2016**, *19*, 32–43, doi:10.1016/j.chom.2015.12.005.
184. Tomkovich, S.; Gharaibeh, R.Z.; Dejea, C.M.; Pope, J.L.; Jiang, J.; Winglee, K.; Gauthier, J.; Newsome, R.C.; Yang, Y.; Fodor, A.A.; et al. Human Colon Mucosal Biofilms and Murine Host Communicate via Altered MRNA and MicroRNA Expression during Cancer. *mSystems* **2020**, *5*, e00451-19, doi:10.1128/mSystems.00451-19.
185. Sicard, J.-F.; Le Bihan, G.; Vogeleer, P.; Jacques, M.; Harel, J. Interactions of Intestinal Bacteria with Components of the Intestinal Mucus. *Front. Cell. Infect. Microbiol.* **2017**, *7*, 387, doi:10.3389/fcimb.2017.00387.
186. Mirzaei, R.; Sadeghi, J.; Talebi, M.; Irajian, G. Prevalence of AtlE, Ica, MecA, and MupA Genes in Staphylococcus Epidermidis Isolates. *Infect. Dis. Clin. Pract.* **2017**, *25*, 37, doi:10.1097/IPC.0000000000000437.
187. Matsuo, K.; Ota, H.; Akamatsu, T.; Sugiyama, A.; Katsuyama, T. Histochemistry of the Surface Mucous Gel Layer of the Human Colon. *Gut* **1997**, *40*, 782–789, doi:10.1136/gut.40.6.782.
188. Dejea, C.M.; Wick, E.C.; Hechenbleikner, E.M.; White, J.R.; Mark Welch, J.L.; Rossetti, B.J.; Peterson, S.N.; Snesrud, E.C.; Borisy, G.G.; Lazarev, M.; et al. Microbiota Organization Is a Distinct Feature of Proximal Colorectal Cancers. *Proc. Natl. Acad. Sci. U. S. A.* **2014**, *111*, 18321–18326, doi:10.1073/pnas.1406199111.
189. Drewes, J.L.; White, J.R.; Dejea, C.M.; Fathi, P.; Iyadorai, T.; Vadivelu, J.; Roslani, A.C.; Wick, E.C.; Mongodin, E.F.; Loke, M.F.; et al. High-Resolution Bacterial 16S RRNA Gene Profile Meta-Analysis and Biofilm Status Reveal Common Colorectal Cancer Consortia. *NPJ Biofilms Microbiomes* **2017**, *3*, 34, doi:10.1038/s41522-017-0040-3.
190. Raskov, H.; Kragh, K.N.; Bjarnsholt, T.; Alamili, M.; Gögenur, I. Bacterial Biofilm Formation inside Colonic Crypts May Accelerate Colorectal Carcinogenesis. *Clin. Transl. Med.* **2018**, *7*, 30, doi:10.1186/s40169-018-0209-2.
191. Belcheva, A.; Irrazabal, T.; Robertson, S.J.; Streutker, C.; Maughan, H.; Rubino, S.; Moriyama, E.H.; Copeland, J.K.; Surendra, A.; Kumar, S.; et al. Gut Microbial Metabolism Drives Transformation of MSH2-Deficient Colon Epithelial Cells. *Cell* **2014**, *158*, 288–299, doi:10.1016/j.cell.2014.04.051.
192. den Besten, G.; Lange, K.; Havinga, R.; van Dijk, T.H.; Gerding, A.; van Eunen, K.; Müller, M.; Groen, A.K.; Hooiveld, G.J.; Bakker, B.M.; et al. Gut-Derived Short-Chain Fatty Acids Are Vividly Assimilated

into Host Carbohydrates and Lipids. *Am. J. Physiol. Gastrointest. Liver Physiol.* **2013**, *305*, G900-910, doi:10.1152/ajpgi.00265.2013.
193. Marsh, A.M.; Buicko Lopez, J.L. Gastric Resection for Malignancy. In *StatPearls*; StatPearls Publishing: Treasure Island (FL), 2024.
194. Díaz De Liaño, A.; Oteiza Martínez, F.; Ciga, M.A.; Aizcorbe, M.; Cobo, F.; Trujillo, R. Impact of Surgical Procedure for Gastric Cancer on Quality of Life. *Br. J. Surg.* **2003**, *90*, 91–94, doi:10.1002/bjs.4011.
195. Eom, B.W.; Lee, H.-J.; Yoo, M.-W.; Cho, J.J.; Kim, W.H.; Yang, H.-K.; Lee, K.U. Synchronous and Metachronous Cancers in Patients with Gastric Cancer. *J. Surg. Oncol.* **2008**, *98*, 106–110, doi:10.1002/jso.21027.
196. Ikeda, Y.; Saku, M.; Kawanaka, H.; Nonaka, M.; Yoshida, K. Features of Second Primary Cancer in Patients with Gastric Cancer. *Oncology* **2003**, *65*, 113–117, doi:10.1159/000072335.
197. Erawijantari, P.P.; Mizutani, S.; Shiroma, H.; Shiba, S.; Nakajima, T.; Sakamoto, T.; Saito, Y.; Fukuda, S.; Yachida, S.; Yamada, T. Influence of Gastrectomy for Gastric Cancer Treatment on Faecal Microbiome and Metabolome Profiles. *Gut* **2020**, *69*, 1404–1415, doi:10.1136/gutjnl-2019-319188.
198. Kuipers, E.J.; Grady, W.M.; Lieberman, D.; Seufferlein, T.; Sung, J.J.; Boelens, P.G.; van de Velde, C.J.H.; Watanabe, T. Colorectal Cancer. *Nat. Rev. Dis. Primer* **2015**, *1*, 15065, doi:10.1038/nrdp.2015.65.
199. Hoshino, N.; Hasegawa, S.; Hida, K.; Kawada, K.; Ganeko, R.; Sugihara, K.; Sakai, Y. Nomogram for Predicting Recurrence in Stage II Colorectal Cancer. *Acta Oncol. Stockh. Swed.* **2016**, *55*, 1414–1417, doi:10.1080/0284186X.2016.1223881.
200. Newland, R.C.; Chan, C.; Chapuis, P.H.; Keshava, A.; Rickard, M.J.F.X.; Young, C.J.; Dent, O.F. Competing Risks Analysis of the Effect of Local Residual Tumour on Recurrence and Cancer-Specific Death after Resection of Colorectal Cancer: Implications for Staging. *Pathology (Phila.)* **2018**, *50*, 600–606, doi:10.1016/j.pathol.2018.07.003.
201. Guyton, K.; Alverdy, J.C. The Gut Microbiota and Gastrointestinal Surgery. *Nat. Rev. Gastroenterol. Hepatol.* **2017**, *14*, 43–54, doi:10.1038/nrgastro.2016.139.
202. Ralls, M.W.; Miyasaka, E.; Teitelbaum, D.H. Intestinal Microbial Diversity and Perioperative Complications. *JPEN J. Parenter. Enteral Nutr.* **2014**, *38*, 392–399, doi:10.1177/0148607113486482.
203. Ohigashi, S.; Sudo, K.; Kobayashi, D.; Takahashi, T.; Nomoto, K.; Onodera, H. Significant Changes in the Intestinal Environment after Surgery in Patients with Colorectal Cancer. *J. Gastrointest. Surg. Off. J. Soc. Surg. Aliment. Tract* **2013**, *17*, 1657–1664, doi:10.1007/s11605-013-2270-x.
204. Deng, X.; Li, Z.; Li, G.; Li, B.; Jin, X.; Lyu, G. Comparison of Microbiota in Patients Treated by Surgery or Chemotherapy by 16S

RRNA Sequencing Reveals Potential Biomarkers for Colorectal Cancer Therapy. *Front. Microbiol.* **2018**, *9*, 1607, doi:10.3389/fmicb.2018.01607.
205. Scarborough, J.E.; Schumacher, J.; Kent, K.C.; Heise, C.P.; Greenberg, C.C. Associations of Specific Postoperative Complications With Outcomes After Elective Colon Resection: A Procedure-Targeted Approach Toward Surgical Quality Improvement. *JAMA Surg.* **2017**, *152*, e164681, doi:10.1001/jamasurg.2016.4681.
206. Martínez-Montoro, J.I.; Martínez-Sánchez, M.A.; Balaguer-Román, A.; Gil-Martínez, J.; Mesa-López, M.J.; Egea-Valenzuela, J.; Ruiz-Alcaraz, A.J.; Queipo-Ortuño, M.I.; Ferrer, M.; Fernández-García, J.C.; et al. Dietary Modulation of Gut Microbiota in Patients with Colorectal Cancer Undergoing Surgery: A Review. *Int. J. Surg.* **2022**, *104*, 106751, doi:10.1016/j.ijsu.2022.106751.
207. García-Alfonso, P.; Muñoz Martín, A.J.; Ortega Morán, L.; Soto Alsar, J.; Torres Pérez-Solero, G.; Blanco Codesido, M.; Calvo Ferrandiz, P.A.; Grasso Cicala, S. Oral Drugs in the Treatment of Metastatic Colorectal Cancer. *Ther. Adv. Med. Oncol.* **2021**, *13*, 17588359211009000, doi:10.1177/17588359211009001.
208. Mocan, L. Surgical Management of Gastric Cancer: A Systematic Review. *J. Clin. Med.* **2021**, *10*, 2557, doi:10.3390/jcm10122557.
209. Song, Z.; Wu, Y.; Yang, J.; Yang, D.; Fang, X. Progress in the Treatment of Advanced Gastric Cancer. *Tumor Biol.* **2017**, *39*, 1010428317714626, doi:10.1177/1010428317714626.
210. Ichinohe, T.; Pang, I.K.; Kumamoto, Y.; Peaper, D.R.; Ho, J.H.; Murray, T.S.; Iwasaki, A. Microbiota Regulates Immune Defense against Respiratory Tract Influenza A Virus Infection. *Proc. Natl. Acad. Sci. U. S. A.* **2011**, *108*, 5354–5359, doi:10.1073/pnas.1019378108.
211. McAleer, J.P.; Kolls, J.K. Maintaining Poise: Commensal Microbiota Calibrate Interferon Responses. *Immunity* **2012**, *37*, 10–12, doi:10.1016/j.immuni.2012.07.001.
212. Iida, N.; Dzutsev, A.; Stewart, C.A.; Smith, L.; Bouladoux, N.; Weingarten, R.A.; Molina, D.A.; Salcedo, R.; Back, T.; Cramer, S.; et al. Commensal Bacteria Control Cancer Response to Therapy by Modulating the Tumor Microenvironment. *Science* **2013**, *342*, 967–970, doi:10.1126/science.1240527.
213. Liu, Y.; Lau, H.C.-H.; Cheng, W.Y.; Yu, J. Gut Microbiome in Colorectal Cancer: Clinical Diagnosis and Treatment. *Genomics Proteomics Bioinformatics* **2023**, *21*, 84–96, doi:10.1016/j.gpb.2022.07.002.
214. Yang, J.; Liu, K.; Qu, J.; Wang, X. The Changes Induced by Cyclophosphamide in Intestinal Barrier and Microflora in Mice. *Eur. J. Pharmacol.* **2013**, *714*, 120–124, doi:10.1016/j.ejphar.2013.06.006.

215. Fei, Z.; Lijuan, Y.; Xi, Y.; Wei, W.; Jing, Z.; Miao, D.; Shuwen, H. Gut Microbiome Associated with Chemotherapy-Induced Diarrhea from the CapeOX Regimen as Adjuvant Chemotherapy in Resected Stage III Colorectal Cancer. *Gut Pathog.* **2019**, *11*, 18, doi:10.1186/s13099-019-0299-4.
216. Allison, R.R.; Patel, R.M.; McLawhorn, R.A. Radiation Oncology: Physics Advances That Minimize Morbidity. *Future Oncol. Lond. Engl.* **2014**, *10*, 2329–2344, doi:10.2217/fon.14.176.
217. Barton, M.B.; Jacob, S.; Shafiq, J.; Wong, K.; Thompson, S.R.; Hanna, T.P.; Delaney, G.P. Estimating the Demand for Radiotherapy from the Evidence: A Review of Changes from 2003 to 2012. *Radiother. Oncol. J. Eur. Soc. Ther. Radiol. Oncol.* **2014**, *112*, 140–144, doi:10.1016/j.radonc.2014.03.024.
218. Verma, V.; Lin, S.H.; Simone, C.B.; Mehta, M.P. Clinical Outcomes and Toxicities of Proton Radiotherapy for Gastrointestinal Neoplasms: A Systematic Review. *J. Gastrointest. Oncol.* **2016**, *7*, 644–664, doi:10.21037/jgo.2016.05.06.
219. Bae, S.H.; Kim, D.W.; Kim, M.-S.; Shin, M.-H.; Park, H.C.; Lim, D.H. Radiotherapy for Gastric Mucosa-Associated Lymphoid Tissue Lymphoma: Dosimetric Comparison and Risk Assessment of Solid Secondary Cancer. *Radiat. Oncol. J.* **2017**, *35*, 78–89, doi:10.3857/roj.2016.01942.
220. Nam, Y.-D.; Kim, H.J.; Seo, J.-G.; Kang, S.W.; Bae, J.-W. Impact of Pelvic Radiotherapy on Gut Microbiota of Gynecological Cancer Patients Revealed by Massive Pyrosequencing. *PloS One* **2013**, *8*, e82659, doi:10.1371/journal.pone.0082659.
221. Villa, A.; Sonis, S.T. Mucositis: Pathobiology and Management. *Curr. Opin. Oncol.* **2015**, *27*, 159–164, doi:10.1097/CCO.0000000000000180.
222. Ferreira, M.R.; Muls, A.; Dearnaley, D.P.; Andreyev, H.J.N. Microbiota and Radiation-Induced Bowel Toxicity: Lessons from Inflammatory Bowel Disease for the Radiation Oncologist. *Lancet Oncol.* **2014**, *15*, e139-147, doi:10.1016/S1470-2045(13)70504-7.
223. Gremy, O.; Benderitter, M.; Linard, C. Acute and Persisting Th2-like Immune Response after Fractionated Colorectal Gamma-Irradiation. *World J. Gastroenterol.* **2008**, *14*, 7075–7085, doi:10.3748/wjg.14.7075.
224. Kalita, B.; Ranjan, R.; Gupta, M.L. Combination Treatment of Podophyllotoxin and Rutin Promotes Mouse Lgr5+ ve Intestinal Stem Cells Survival against Lethal Radiation Injury through Wnt Signaling. *Apoptosis Int. J. Program. Cell Death* **2019**, *24*, 326–340, doi:10.1007/s10495-019-01519-x.
225. Phillips, F.; Muls, A.C.G.; Lalji, A.; Andreyev, H.J.N. Are Bile Acid Malabsorption and Bile Acid Diarrhoea Important Causes of Loose Stool Complicating Cancer Therapy? *Colorectal Dis.* **2015**, *17*, 730–734, doi:10.1111/codi.12932.

226. Wang, Z.; Wang, Q.; Wang, X.; Zhu, L.; Chen, J.; Zhang, B.; Chen, Y.; Yuan, Z. Gut Microbial Dysbiosis Is Associated with Development and Progression of Radiation Enteritis during Pelvic Radiotherapy. *J. Cell. Mol. Med.* **2019**, *23*, 3747–3756, doi:10.1111/jcmm.14289.
227. Zhang, S.; Wang, Q.; Zhou, C.; Chen, K.; Chang, H.; Xiao, W.; Gao, Y. Colorectal Cancer, Radiotherapy and Gut Microbiota. *Chin. J. Cancer Res. Chung-Kuo Yen Cheng Yen Chiu* **2019**, *31*, 212–222, doi:10.21147/j.issn.1000-9604.2019.01.16.
228. Liu, J.; Liu, C.; Yue, J. Radiotherapy and the Gut Microbiome: Facts and Fiction. *Radiat. Oncol.* **2021**, *16*, 9, doi:10.1186/s13014-020-01735-9.
229. Touchefeu, Y.; Montassier, E.; Nieman, K.; Gastinne, T.; Potel, G.; Bruley des Varannes, S.; Le Vacon, F.; de La Cochetière, M.F. Systematic Review: The Role of the Gut Microbiota in Chemotherapy- or Radiation-Induced Gastrointestinal Mucositis - Current Evidence and Potential Clinical Applications. *Aliment. Pharmacol. Ther.* **2014**, *40*, 409–421, doi:10.1111/apt.12878.
230. Manichanh, C.; Varela, E.; Martinez, C.; Antolin, M.; Llopis, M.; Doré, J.; Giralt, J.; Guarner, F.; Malagelada, J.-R. The Gut Microbiota Predispose to the Pathophysiology of Acute Postradiotherapy Diarrhea. *Am. J. Gastroenterol.* **2008**, *103*, 1754–1761, doi:10.1111/j.1572-0241.2008.01868.x.
231. Kuwahara, Y.; Oikawa, T.; Ochiai, Y.; Roudkenar, M.H.; Fukumoto, M.; Shimura, T.; Ohtake, Y.; Ohkubo, Y.; Mori, S.; Uchiyama, Y.; et al. Enhancement of Autophagy Is a Potential Modality for Tumors Refractory to Radiotherapy. *Cell Death Dis.* **2011**, *2*, e177, doi:10.1038/cddis.2011.56.
232. Yu, T.; Guo, F.; Yu, Y.; Sun, T.; Ma, D.; Han, J.; Qian, Y.; Kryczek, I.; Sun, D.; Nagarsheth, N.; et al. Fusobacterium Nucleatum Promotes Chemoresistance to Colorectal Cancer by Modulating Autophagy. *Cell* **2017**, *170*, 548-563.e16, doi:10.1016/j.cell.2017.07.008.
233. Yi, Y.; Lu, W.; Shen, L.; Wu, Y.; Zhang, Z. The Gut Microbiota as a Booster for Radiotherapy: Novel Insights into Radio-Protection and Radiation Injury. *Exp. Hematol. Oncol.* **2023**, *12*, 48, doi:10.1186/s40164-023-00410-5.
234. Huh, D.; Hamilton, G.A.; Ingber, D.E. From 3D Cell Culture to Organs-on-Chips. *Trends Cell Biol.* **2011**, *21*, 745–754, doi:10.1016/j.tcb.2011.09.005.
235. Creff, J.; Malaquin, L.; Besson, A. In Vitro Models of Intestinal Epithelium: Toward Bioengineered Systems. *J. Tissue Eng.* **2021**, *12*, 2041731420985202, doi:10.1177/2041731420985202.
236. Snyder, J.; Wang, C.-M.; Zhang, A.Q.; Li, Y.; Luchan, J.; Hosic, S.; Koppes, R.; Carrier, R.L.; Koppes, A. Materials and Microenvironments for Engineering the Intestinal Epithelium. *Ann.*

Biomed. Eng. **2020**, *48*, 1916–1940, doi:10.1007/s10439-020-02470-8.

237. Thorne, C.A.; Chen, I.W.; Sanman, L.E.; Cobb, M.H.; Wu, L.F.; Altschuler, S.J. Enteroid Monolayers Reveal an Autonomous WNT and BMP Circuit Controlling Intestinal Epithelial Growth and Organization. *Dev. Cell* **2018**, *44*, 624-633.e4, doi:10.1016/j.devcel.2018.01.024.
238. Hirt, C.; Papadimitropoulos, A.; Muraro, M.G.; Mele, V.; Panopoulos, E.; Cremonesi, E.; Ivanek, R.; Schultz-Thater, E.; Droeser, R.A.; Mengus, C.; et al. Bioreactor-Engineered Cancer Tissue-like Structures Mimic Phenotypes, Gene Expression Profiles and Drug Resistance Patterns Observed "in Vivo." *Biomaterials* **2015**, *62*, 138–146, doi:10.1016/j.biomaterials.2015.05.037.
239. Jensen, C.; Teng, Y. Is It Time to Start Transitioning From 2D to 3D Cell Culture? *Front. Mol. Biosci.* **2020**, *7*.
240. VanDussen, K.L.; Marinshaw, J.M.; Shaikh, N.; Miyoshi, H.; Moon, C.; Tarr, P.I.; Ciorba, M.A.; Stappenbeck, T.S. Development of an Enhanced Human Gastrointestinal Epithelial Culture System to Facilitate Patient-Based Assays. *Gut* **2015**, *64*, 911–920, doi:10.1136/gutjnl-2013-306651.
241. Fogh, J.; Fogh, J.M.; Orfeo, T. One Hundred and Twenty-Seven Cultured Human Tumor Cell Lines Producing Tumors in Nude Mice. *J. Natl. Cancer Inst.* **1977**, *59*, 221–226, doi:10.1093/jnci/59.1.221.
242. Ferrari, G.; Cusella-De Angelis, G.; Coletta, M.; Paolucci, E.; Stornaiuolo, A.; Cossu, G.; Mavilio, F. Muscle Regeneration by Bone Marrow-Derived Myogenic Progenitors. *Science* **1998**, *279*, 1528–1530, doi:10.1126/science.279.5356.1528.
243. Pittenger, M.F.; Mackay, A.M.; Beck, S.C.; Jaiswal, R.K.; Douglas, R.; Mosca, J.D.; Moorman, M.A.; Simonetti, D.W.; Craig, S.; Marshak, D.R. Multilineage Potential of Adult Human Mesenchymal Stem Cells. *Science* **1999**, *284*, 143–147, doi:10.1126/science.284.5411.143.
244. Choi, R.S.; Vacanti, J.P. Preliminary Studies of Tissue-Engineered Intestine Using Isolated Epithelial Organoid Units on Tubular Synthetic Biodegradable Scaffolds. *Transplant. Proc.* **1997**, *29*, 848–851, doi:10.1016/s0041-1345(96)00164-9.
245. Gu, W.; Hong, X.; Le Bras, A.; Nowak, W.N.; Issa Bhaloo, S.; Deng, J.; Xie, Y.; Hu, Y.; Ruan, X.Z.; Xu, Q. Smooth Muscle Cells Differentiated from Mesenchymal Stem Cells Are Regulated by MicroRNAs and Suitable for Vascular Tissue Grafts. *J. Biol. Chem.* **2018**, *293*, 8089–8102, doi:10.1074/jbc.RA118.001739.
246. Dalerba, P.; Dylla, S.J.; Park, I.-K.; Liu, R.; Wang, X.; Cho, R.W.; Hoey, T.; Gurney, A.; Huang, E.H.; Simeone, D.M.; et al. Phenotypic Characterization of Human Colorectal Cancer Stem Cells. *Proc. Natl.*

Acad. Sci. U. S. A. **2007**, *104*, 10158–10163, doi:10.1073/pnas.0703478104.
247. McKay, D.M.; Philpott, D.J.; Perdue, M.H. Review Article: In Vitro Models in Inflammatory Bowel Disease Research--a Critical Review. *Aliment. Pharmacol. Ther.* **1997**, *11 Suppl 3*, 70–80, doi:10.1111/j.1365-2036.1997.tb00811.x.
248. Pereira, C.; Costa, J.; Sarmento, B.; Araújo, F. 3.3 - Cell-Based in Vitro Models for Intestinal Permeability Studies. In *Concepts and Models for Drug Permeability Studies*; Sarmento, B., Ed.; Woodhead Publishing, 2016; pp. 57–81 ISBN 978-0-08-100094-6.
249. Costa, J.; Ahluwalia, A. Advances and Current Challenges in Intestinal in Vitro Model Engineering: A Digest. *Front. Bioeng. Biotechnol.* **2019**, *7*.
250. Sato, T.; Vries, R.G.; Snippert, H.J.; van de Wetering, M.; Barker, N.; Stange, D.E.; van Es, J.H.; Abo, A.; Kujala, P.; Peters, P.J.; et al. Single Lgr5 Stem Cells Build Crypt-Villus Structures in Vitro without a Mesenchymal Niche. *Nature* **2009**, *459*, 262–265, doi:10.1038/nature07935.
251. Ootani, A.; Li, X.; Sangiorgi, E.; Ho, Q.T.; Ueno, H.; Toda, S.; Sugihara, H.; Fujimoto, K.; Weissman, I.L.; Capecchi, M.R.; et al. Sustained in Vitro Intestinal Epithelial Culture within a Wnt-Dependent Stem Cell Niche. *Nat. Med.* **2009**, *15*, 701–706, doi:10.1038/nm.1951.
252. Preksha, G.; Yesheswini, R.; Srikanth, C.V. Cell Culture Techniques in Gastrointestinal Research: Methods, Possibilities and Challenges. *Indian J. Pathol. Microbiol.* **2021**, *64*, S52–S57, doi:10.4103/IJPM.IJPM_933_20.
253. Bartfeld, S.; Bayram, T.; van de Wetering, M.; Huch, M.; Begthel, H.; Kujala, P.; Vries, R.; Peters, P.J.; Clevers, H. In Vitro Expansion of Human Gastric Epithelial Stem Cells and Their Responses to Bacterial Infection. *Gastroenterology* **2015**, *148*, 126-136.e6, doi:10.1053/j.gastro.2014.09.042.
254. Schlaermann, P.; Toelle, B.; Berger, H.; Schmidt, S.C.; Glanemann, M.; Ordemann, J.; Bartfeld, S.; Mollenkopf, H.J.; Meyer, T.F. A Novel Human Gastric Primary Cell Culture System for Modelling Helicobacter Pylori Infection in Vitro. *Gut* **2016**, *65*, 202–213, doi:10.1136/gutjnl-2014-307949.
255. Wilson, S.S.; Tocchi, A.; Holly, M.K.; Parks, W.C.; Smith, J.G. A Small Intestinal Organoid Model of Non-Invasive Enteric Pathogen–Epithelial Cell Interactions. *Mucosal Immunol.* **2015**, *8*, 352–361, doi:10.1038/mi.2014.72.
256. Perrone, F.; Zilbauer, M. Biobanking of Human Gut Organoids for Translational Research. *Exp. Mol. Med.* **2021**, *53*, 1451–1458, doi:10.1038/s12276-021-00606-x.

257. Zhou, Z.; Cong, L.; Cong, X. Patient-Derived Organoids in Precision Medicine: Drug Screening, Organoid-on-a-Chip and Living Organoid Biobank. *Front. Oncol.* **2021**, *11*.
258. Leonard, F.; Collnot, E.-M.; Lehr, C.-M. A Three-Dimensional Coculture of Enterocytes, Monocytes and Dendritic Cells to Model Inflamed Intestinal Mucosa in Vitro. *Mol. Pharm.* **2010**, *7*, 2103–2119, doi:10.1021/mp1000795.
259. Zakhem, E.; Raghavan, S.; Suhar, R.A.; Bitar, K.N. Bioengineering and Regeneration of Gastrointestinal Tissue: Where Are We Now and What Comes Next? *Expert Opin. Biol. Ther.* **2019**, *19*, 527–537, doi:10.1080/14712598.2019.1595579.
260. Dynamic Tissue Engineering Scaffolds with Stimuli-Responsive Macroporosity Formation - PubMed Available online: https://pubmed.ncbi.nlm.nih.gov/23489920/ (accessed on 19 June 2024).
261. Li, Y.; Kilian, K.A. Bridging the Gap: From 2D Cell Culture to 3D Microengineered Extracellular Matrices. *Adv. Healthc. Mater.* **2015**, *4*, 2780–2796, doi:10.1002/adhm.201500427.
262. Ağagündüz, D.; Cocozza, E.; Cemali, Ö.; Bayazıt, A.D.; Nanì, M.F.; Cerqua, I.; Morgillo, F.; Saygılı, S.K.; Berni Canani, R.; Amero, P.; et al. Understanding the Role of the Gut Microbiome in Gastrointestinal Cancer: A Review. *Front. Pharmacol.* **2023**, *14*, 1130562, doi:10.3389/fphar.2023.1130562.
263. Wroblewski, L.E.; Peek, R.M.; Coburn, L.A. The Role of the Microbiome in GI Cancer. *Gastroenterol. Clin. North Am.* **2016**, *45*, 543–556, doi:10.1016/j.gtc.2016.04.010.
264. Nienow, A.W. Stirring and Stirred-Tank Reactors. *Chem. Ing. Tech.* **2014**, *86*, 2063–2074, doi:10.1002/cite.201400087.
265. Comprehensive Biotechnology Available online: http://www.sciencedirect.com:5070/referencework/9780080885049/comprehensive-biotechnology (accessed on 27 May 2024).
266. Wu, W.-K.; Chen, C.-C.; Panyod, S.; Chen, R.-A.; Wu, M.-S.; Sheen, L.-Y.; Chang, S.-C. Optimization of Fecal Sample Processing for Microbiome Study — The Journey from Bathroom to Bench. *J. Formos. Med. Assoc.* **2019**, *118*, 545–555, doi:10.1016/j.jfma.2018.02.005.
267. Sardelli, L.; Perottoni, P.; Tunesi, M.; Boeri, L.; Fusco, F.; Petrini, P.; Albani, D.; Giordano, C. *Biotechnology and Bioengineering*. 2021, pp. 2886–2905.
268. Cui, J.; Zheng, X.; Hou, W.; Zhuang, Y.; Pi, X.; Yang, J. The Study of a Remote-Controlled Gastrointestinal Drug Delivery and Sampling System. *Telemed. J. E-Health Off. J. Am. Telemed. Assoc.* **2008**, *14*, 715–719, doi:10.1089/tmj.2007.0118.
269. El Houari, A.; Ecale, F.; Mercier, A.; Crapart, S.; Laparre, J.; Soulard, B.; Ramnath, M.; Berjeaud, J.-M.; Rodier, M.-H.; Crépin, A.

Development of an in Vitro Model of Human Gut Microbiota for Screening the Reciprocal Interactions With Antibiotics, Drugs, and Xenobiotics. *Front. Microbiol.* **2022**, *13*.
270. Žukauskaitė, K.; Li, M.; Horvath, A.; Jarmalaitė, S.; Stadlbauer, V. Cellular and Microbial In Vitro Modelling of Gastrointestinal Cancer. *Cancers 16*, doi:https://doi.org/10.3390/cancers16173113.
271. Benam, K.H.; Dauth, S.; Hassell, B.; Herland, A.; Jain, A.; Jang, K.-J.; Karalis, K.; Kim, H.J.; MacQueen, L.; Mahmoodian, R.; et al. Engineered in Vitro Disease Models. *Annu. Rev. Pathol.* **2015**, *10*, 195–262, doi:10.1146/annurev-pathol-012414-040418.
272. Manfredonia, C.; Muraro, M.G.; Hirt, C.; Mele, V.; Governa, V.; Papadimitropoulos, A.; Däster, S.; Soysal, S.D.; Droeser, R.A.; Mechera, R.; et al. Maintenance of Primary Human Colorectal Cancer Microenvironment Using a Perfusion Bioreactor-Based 3D Culture System. *Adv. Biosyst.* **2019**, *3*, e1800300, doi:10.1002/adbi.201800300.
273. La Rocca, A.; De Gregorio, V.; Lagreca, E.; Vecchione, R.; Netti, P.A.; Imparato, G. Colorectal Cancer Bioengineered Microtissues as a Model to Replicate Tumor-ECM Crosstalk and Assess Drug Delivery Systems In Vitro. *Int. J. Mol. Sci.* **2023**, *24*, 5678, doi:10.3390/ijms24065678.
274. Chen, Z.-Y.; Jiang, N.; Guo, S.; Li, B.-B.; Yang, J.-Q.; Chai, S.-B.; Yan, H.-F.; Sun, P.-M.; Zhang, T.; Sun, H.-W.; et al. Effect of Simulated Microgravity on Metabolism of HGC-27 Gastric Cancer Cells. *Oncol. Lett.* **2020**, *19*, 3439–3450, doi:10.3892/ol.2020.11451.
275. Rembiałkowska, N.; Baczyńska, D.; Dubińska-Magiera, M.; Choromańska, A.; Bieżuńska-Kusiak, K.; Gajewska-Naryniecka, A.; Novickij, V.; Saczko, J.; Przystupski, D.; Kulbacka, J. RCCS Bioreactor-Based Modeled Microgravity Affects Gastric Cancer Cells and Improves the Chemotherapeutic Effect. *Membranes* **2022**, *12*, 448, doi:10.3390/membranes12050448.
276. Ichim, T.E.; Kesari, S.; Shafer, K. Protection from Chemotherapy- and Antibiotic-Mediated Dysbiosis of the Gut Microbiota by a Probiotic with Digestive Enzymes Supplement. *Oncotarget* **2018**, *9*, 30919–30935, doi:10.18632/oncotarget.25778.
277. Verdier, C.; Denis, S.; Gasc, C.; Boucinha, L.; Uriot, O.; Delmas, D.; Dore, J.; Le Camus, C.; Schwintner, C.; Blanquet-Diot, S. An Oral FMT Capsule as Efficient as an Enema for Microbiota Reconstruction Following Disruption by Antibiotics, as Assessed in an In Vitro Human Gut Model. *Microorganisms* **2021**, *9*, 358, doi:10.3390/microorganisms9020358.
278. Holma, R.; Korpela, R.; Sairanen, U.; Blom, M.; Rautio, M.; Poussa, T.; Saxelin, M.; Osterlund, P. Colonic Methane Production Modifies Gastrointestinal Toxicity Associated with Adjuvant 5-Fluorouracil

Chemotherapy for Colorectal Cancer. *J. Clin. Gastroenterol.* **2013**, *47*, 45–51, doi:10.1097/MCG.0b013e3182680201.
279. Blaustein, R.A.; Seed, P.C.; Hartmann, E.M. Biotransformation of Doxorubicin Promotes Resilience in Simplified Intestinal Microbial Communities. *mSphere* **2021**, *6*, e0006821, doi:10.1128/mSphere.00068-21.
280. Xin, J.-Y.; Wang, J.; Ding, Q.-Q.; Chen, W.; Xu, X.-K.; Wei, X.-T.; Lv, Y.-H.; Wei, Y.-P.; Feng, Y.; Zu, X.-P. Potential Role of Gut Microbiota and Its Metabolites in Radiation-Induced Intestinal Damage. *Ecotoxicol. Environ. Saf.* **2022**, *248*, 114341, doi:10.1016/j.ecoenv.2022.114341.
281. Roeder, F.; Meldolesi, E.; Gerum, S.; Valentini, V.; Rödel, C. Recent Advances in (Chemo-)Radiation Therapy for Rectal Cancer: A Comprehensive Review. *Radiat. Oncol. Lond. Engl.* **2020**, *15*, 262, doi:10.1186/s13014-020-01695-0.
282. Hauer-Jensen, M.; Denham, J.W.; Andreyev, H.J.N. Radiation Enteropathy – Pathogenesis, Treatment, and Prevention. *Nat. Rev. Gastroenterol. Hepatol.* **2014**, *11*, 470–479, doi:10.1038/nrgastro.2014.46.
283. Tsuda, A.; Suda, W.; Morita, H.; Takanashi, K.; Takagi, A.; Koga, Y.; Hattori, M. Influence of Proton-Pump Inhibitors on the Luminal Microbiota in the Gastrointestinal Tract. *Clin. Transl. Gastroenterol.* **2015**, *6*, e89, doi:10.1038/ctg.2015.20.
284. Engstrand, L.; Graham, D.Y. Microbiome and Gastric Cancer. *Dig. Dis. Sci.* **2020**, *65*, 865–873, doi:10.1007/s10620-020-06101-z.
285. Etienne-Mesmin, L.; Meslier, V.; Uriot, O.; Fournier, E.; Deschamps, C.; Denis, S.; David, A.; Jegou, S.; Morabito, C.; Quinquis, B.; et al. In Vitro Modelling of Oral Microbial Invasion in the Human Colon. *Microbiol. Spectr.* **2023**, *11*, e0434422, doi:10.1128/spectrum.04344-22.
286. Caporaso, J.G.; Kuczynski, J.; Stombaugh, J.; Bittinger, K.; Bushman, F.D.; Costello, E.K.; Fierer, N.; Peña, A.G.; Goodrich, J.K.; Gordon, J.I.; et al. QIIME Allows Analysis of High-Throughput Community Sequencing Data. *Nat. Methods* **2010**, *7*, 335–336, doi:10.1038/nmeth.f.303.
287. Callahan, B.J.; McMurdie, P.J.; Rosen, M.J.; Han, A.W.; Johnson, A.J.A.; Holmes, S.P. DADA2: High-Resolution Sample Inference from Illumina Amplicon Data. *Nat. Methods* **2016**, *13*, 581–583, doi:10.1038/nmeth.3869.
288. Bolyen, E.; Rideout, J.R.; Dillon, M.R.; Bokulich, N.A.; Abnet, C.C.; Al-Ghalith, G.A.; Alexander, H.; Alm, E.J.; Arumugam, M.; Asnicar, F.; et al. Reproducible, Interactive, Scalable and Extensible Microbiome Data Science Using QIIME 2. *Nat. Biotechnol.* **2019**, *37*, 852–857, doi:10.1038/s41587-019-0209-9.

289. GitHub - Jbisanz/Qiime2R: Import Qiime2 Artifacts to R Available online: https://github.com/jbisanz/qiime2R (accessed on 14 June 2024).
290. Cao, Y.; Dong, Q.; Wang, D.; Zhang, P.; Liu, Y.; Niu, C. MicrobiomeMarker: An R/Bioconductor Package for Microbiome Marker Identification and Visualization. *Bioinforma. Oxf. Engl.* **2022**, *38*, 4027–4029, doi:10.1093/bioinformatics/btac438.
291. Bates, D.; Mächler, M.; Bolker, B.; Walker, S. Fitting Linear Mixed-Effects Models Using Lme4. *J. Stat. Softw.* **2015**, *67*, 1–48, doi:10.18637/jss.v067.i01.
292. Yu, G. Convert Plot to "grob" or "Ggplot" Object 2021.
293. Haindl, R.; Engel, J.; Kulozik, U. Establishment of an In Vitro System of the Human Intestinal Microbiota: Effect of Cultivation Conditions and Influence of Three Donor Stool Samples. *Microorganisms* **2021**, *9*, 1049, doi:10.3390/microorganisms9051049.
294. Mai, V.; Greenwald, B.; Glenn Morris, J.; Raufman, J.-P.; Stine, O.C. Effect of Bowel Preparation and Colonoscopy on Post-Procedure Intestinal Microbiota Composition. *Gut* **2006**, *55*, 1822–1823, doi:10.1136/gut.2006.108266.
295. Nagata, N.; Tohya, M.; Fukuda, S.; Suda, W.; Nishijima, S.; Takeuchi, F.; Ohsugi, M.; Tsujimoto, T.; Nakamura, T.; Shimomura, A.; et al. Effects of Bowel Preparation on the Human Gut Microbiome and Metabolome. *Sci. Rep.* **2019**, *9*, 4042, doi:10.1038/s41598-019-40182-9.
296. Powles, S.T.R.; Gallagher, K.I.; Chong, L.W.L.; Alexander, J.L.; Mullish, B.H.; Hicks, L.C.; McDonald, J.A.K.; Marchesi, J.R.; Williams, H.R.T.; Orchard, T.R. Effects of Bowel Preparation on Intestinal Bacterial Associated Urine and Faecal Metabolites and the Associated Faecal Microbiome. *BMC Gastroenterol.* **2022**, *22*, 240, doi:10.1186/s12876-022-02301-1.
297. Jalanka, J.; Salonen, A.; Salojärvi, J.; Ritari, J.; Immonen, O.; Marciani, L.; Gowland, P.; Hoad, C.; Garsed, K.; Lam, C.; et al. Effects of Bowel Cleansing on the Intestinal Microbiota. *Gut* **2015**, *64*, 1562–1568, doi:10.1136/gutjnl-2014-307240.
298. Drago, L.; Toscano, M.; De Grandi, R.; Casini, V.; Pace, F. Persisting Changes of Intestinal Microbiota after Bowel Lavage and Colonoscopy: *Eur. J. Gastroenterol. Hepatol.* **2016**, *28*, 532–537, doi:10.1097/MEG.0000000000000581.
299. Cong, J.; Zhu, H.; Liu, D.; Li, T.; Zhang, C.; Zhu, J.; Lv, H.; Liu, K.; Hao, C.; Tian, Z.; et al. A Pilot Study: Changes of Gut Microbiota in Post-Surgery Colorectal Cancer Patients. *Front. Microbiol.* **2018**, *9*.
300. Jin, Y.; Liu, Y.; Zhao, L.; Zhao, F.; Feng, J.; Li, S.; Chen, H.; Sun, J.; Zhu, B.; Geng, R.; et al. Gut Microbiota in Patients after Surgical Treatment for Colorectal Cancer. *Environ. Microbiol.* **2019**, *21*, 772–783, doi:10.1111/1462-2920.14498.

301. Shimizu, K.; Ogura, H.; Goto, M.; Asahara, T.; Nomoto, K.; Morotomi, M.; Yoshiya, K.; Matsushima, A.; Sumi, Y.; Kuwagata, Y.; et al. Altered Gut Flora and Environment in Patients with Severe SIRS. *J. Trauma* **2006**, *60*, 126–133, doi:10.1097/01.ta.0000197374.99755.fe.
302. Hyoju, S.; Machutta, K.; Krezalek, M.A.; Alverdy, J.C. What Is the Role of the Gut in Wound Infections? *Adv. Surg.* **2023**, *57*, 31–46, doi:10.1016/j.yasu.2023.05.002.
303. Lederer, A.-K.; Chikhladze, S.; Kohnert, E.; Huber, R.; Müller, A. Current Insights: The Impact of Gut Microbiota on Postoperative Complications in Visceral Surgery-A Narrative Review. *Diagn. Basel Switz.* **2021**, *11*, 2099, doi:10.3390/diagnostics11112099.
304. Pak, H.; Maghsoudi, L.H.; Soltanian, A.; Gholami, F. Surgical Complications in Colorectal Cancer Patients. *Ann. Med. Surg.* **2020**, *55*, 13–18, doi:10.1016/j.amsu.2020.04.024.
305. Rovera, F.; Dionigi, G.; Boni, L.; Piscopo, C.; Masciocchi, P.; Alberio, M.G.; Carcano, G.; Diurni, M.; Dionigi, R. Infectious Complications in Colorectal Surgery. *Surg. Oncol.* **2007**, *16*, 121–124, doi:10.1016/j.suronc.2007.10.029.
306. Fisher, K.; Phillips, C. The Ecology, Epidemiology and Virulence of Enterococcus. *Microbiol. Read. Engl.* **2009**, *155*, 1749–1757, doi:10.1099/mic.0.026385-0.
307. Suetens, C.; Latour, K.; Kärki, T.; Ricchizzi, E.; Kinross, P.; Moro, M.L.; Jans, B.; Hopkins, S.; Hansen, S.; Lyytikäinen, O.; et al. Prevalence of Healthcare-Associated Infections, Estimated Incidence and Composite Antimicrobial Resistance Index in Acute Care Hospitals and Long-Term Care Facilities: Results from Two European Point Prevalence Surveys, 2016 to 2017. *Euro Surveill. Bull. Eur. Sur Mal. Transm. Eur. Commun. Dis. Bull.* **2018**, *23*, 1800516, doi:10.2807/1560-7917.ES.2018.23.46.1800516.
308. Weiner, L.M.; Webb, A.K.; Limbago, B.; Dudeck, M.A.; Patel, J.; Kallen, A.J.; Edwards, J.R.; Sievert, D.M. Antimicrobial-Resistant Pathogens Associated With Healthcare-Associated Infections: Summary of Data Reported to the National Healthcare Safety Network at the Centers for Disease Control and Prevention, 2011-2014. *Infect. Control Hosp. Epidemiol.* **2016**, *37*, 1288–1301, doi:10.1017/ice.2016.174.
309. Olawale, K.O.; Fadiora, S.O.; Taiwo, S.S. Prevalence of Hospital-Acquired Enterococci Infections in Two Primary-Care Hospitals in Osogbo, Southwestern Nigeria. *Afr. J. Infect. Dis.* **2011**, *5*, 40–46.
310. Selleck, E.M.; Van Tyne, D.; Gilmore, M.S. Pathogenicity of Enterococci. *Microbiol. Spectr.* **2019**, *7*, 10.1128/microbiolspec.GPP3-0053–2018, doi:10.1128/microbiolspec.GPP3-0053-2018.

311. Conway, J.; A Duggal, N. Ageing of the Gut Microbiome: Potential Influences on Immune Senescence and Inflammageing. *Ageing Res. Rev.* **2021**, *68*, 101323, doi:10.1016/j.arr.2021.101323.
312. Walrath, T.; Dyamenahalli, K.U.; Hulsebus, H.J.; McCullough, R.L.; Idrovo, J.-P.; Boe, D.M.; McMahan, R.H.; Kovacs, E.J. Age-Related Changes in Intestinal Immunity and the Microbiome. *J. Leukoc. Biol.* **2021**, *109*, 1045–1061, doi:10.1002/JLB.3RI0620-405RR.
313. Antoniou, S.A.; Huo, B.; Tzanis, A.A.; Koutsiouroumpa, O.; Mavridis, D.; Balla, A.; Dore, S.; Kaiser, A.M.; Koraki, E.; Massey, L.; et al. EAES, SAGES, and ESCP Rapid Guideline: Bowel Preparation for Minimally Invasive Colorectal Resection. *Surg. Endosc.* **2023**, *37*, 9001–9012, doi:10.1007/s00464-023-10477-0.
314. Montassier, E.; Gastinne, T.; Vangay, P.; Al-Ghalith, G.A.; Bruley des Varannes, S.; Massart, S.; Moreau, P.; Potel, G.; de La Cochetière, M.F.; Batard, E.; et al. Chemotherapy-Driven Dysbiosis in the Intestinal Microbiome. *Aliment. Pharmacol. Ther.* **2015**, *42*, 515–528, doi:10.1111/apt.13302.
315. Zwielehner, J.; Lassl, C.; Hippe, B.; Pointner, A.; Switzeny, O.J.; Remely, M.; Kitzweger, E.; Ruckser, R.; Haslberger, A.G. Changes in Human Fecal Microbiota Due to Chemotherapy Analyzed by TaqMan-PCR, 454 Sequencing and PCR-DGGE Fingerprinting. *PloS One* **2011**, *6*, e28654, doi:10.1371/journal.pone.0028654.
316. Dörffel, Y.; Swidsinski, A.; Loening-Baucke, V.; Wiedenmann, B.; Pavel, M. Common Biostructure of the Colonic Microbiota in Neuroendocrine Tumors and Crohn's Disease and the Effect of Therapy. *Inflamm. Bowel Dis.* **2012**, *18*, 1663–1671, doi:10.1002/ibd.21923.
317. Galloway-Peña, J.R.; Smith, D.P.; Sahasrabhojane, P.; Ajami, N.J.; Wadsworth, W.D.; Daver, N.G.; Chemaly, R.F.; Marsh, L.; Ghantoji, S.S.; Pemmaraju, N.; et al. The Role of the Gastrointestinal Microbiome in Infectious Complications during Induction Chemotherapy for Acute Myeloid Leukemia. *Cancer* **2016**, *122*, 2186–2196, doi:10.1002/cncr.30039.
318. Kong, C.; Gao, R.; Yan, X.; Huang, L.; He, J.; Li, H.; You, J.; Qin, H. Alterations in Intestinal Microbiota of Colorectal Cancer Patients Receiving Radical Surgery Combined with Adjuvant CapeOx Therapy. *Sci. China Life Sci.* **2019**, *62*, 1178–1193, doi:10.1007/s11427-018-9456-x.
319. Li, N.; Bai, C.; Zhao, L.; Sun, Z.; Ge, Y.; Li, X. The Relationship Between Gut Microbiome Features and Chemotherapy Response in Gastrointestinal Cancer. *Front. Oncol.* **2021**, *11*, doi:10.3389/fonc.2021.781697.
320. Kong, C.; Gao, R.; Yan, X.; Huang, L.; He, J.; Li, H.; You, J.; Qin, H. Alterations in Intestinal Microbiota of Colorectal Cancer Patients Receiving Radical Surgery Combined with Adjuvant CapeOx

Therapy. *Sci. China Life Sci.* **2019**, *62*, 1178–1193, doi:10.1007/s11427-018-9456-x.
321. Chen, C.; Shen, J.; Du, Y.; Shi, X.; Niu, Y.; Jin, G.; Liu, Y.; Shi, Y.; Lyu, J.; Lin, L. Characteristics of Gut Microbiota in Patients with Gastric Cancer by Surgery, Chemotherapy and Lymph Node Metastasis. *Clin. Transl. Oncol. Off. Publ. Fed. Span. Oncol. Soc. Natl. Cancer Inst. Mex.* **2022**, *24*, 2181–2190, doi:10.1007/s12094-022-02875-y.
322. Horvath, A.; Bausys, A.; Sabaliauskaite, R.; Stratilatovas, E.; Jarmalaite, S.; Schuetz, B.; Stiegler, P.; Bausys, R.; Stadlbauer, V.; Strupas, K. Distal Gastrectomy with Billroth II Reconstruction Is Associated with Oralization of Gut Microbiome and Intestinal Inflammation: A Proof-of-Concept Study. *Ann. Surg. Oncol.* **2020**, doi:10.1245/s10434-020-08678-1.
323. Imhann, F.; Bonder, M.J.; Vich Vila, A.; Fu, J.; Mujagic, Z.; Vork, L.; Tigchelaar, E.F.; Jankipersadsing, S.A.; Cenit, M.C.; Harmsen, H.J.M.; et al. Proton Pump Inhibitors Affect the Gut Microbiome. *Gut* **2016**, *65*, 740–748, doi:10.1136/gutjnl-2015-310376.
324. Jackson, M.A.; Goodrich, J.K.; Maxan, M.-E.; Freedberg, D.E.; Abrams, J.A.; Poole, A.C.; Sutter, J.L.; Welter, D.; Ley, R.E.; Bell, J.T.; et al. Proton Pump Inhibitors Alter the Composition of the Gut Microbiota. *Gut* **2016**, *65*, 749–756, doi:10.1136/gutjnl-2015-310861.
325. Seto, C.T.; Jeraldo, P.; Orenstein, R.; Chia, N.; DiBaise, J.K. Prolonged Use of a Proton Pump Inhibitor Reduces Microbial Diversity: Implications for Clostridium Difficile Susceptibility. *Microbiome* **2014**, *2*, 42, doi:10.1186/2049-2618-2-42.
326. Tseng, C.-H.; Lin, J.-T.; Ho, H.J.; Lai, Z.-L.; Wang, C.-B.; Tang, S.-L.; Wu, C.-Y. Gastric Microbiota and Predicted Gene Functions Are Altered after Subtotal Gastrectomy in Patients with Gastric Cancer. *Sci. Rep.* **2016**, *6*, doi:10.1038/srep20701.
327. Tsuda, A.; Suda, W.; Morita, H.; Takanashi, K.; Takagi, A.; Koga, Y.; Hattori, M. Influence of Proton-Pump Inhibitors on the Luminal Microbiota in the Gastrointestinal Tract. *Clin. Transl. Gastroenterol.* **2015**, *6*, e89, doi:10.1038/ctg.2015.20.
328. Bajaj, J.S.; Cox, I.J.; Betrapally, N.S.; Heuman, D.M.; Schubert, M.L.; Ratneswaran, M.; Hylemon, P.B.; White, M.B.; Daita, K.; Noble, N.A.; et al. Systems Biology Analysis of Omeprazole Therapy in Cirrhosis Demonstrates Significant Shifts in Gut Microbiota Composition and Function. *Am. J. Physiol. Gastrointest. Liver Physiol.* **2014**, *307*, G951-957, doi:10.1152/ajpgi.00268.2014.
329. Clooney, A.G.; Bernstein, C.N.; Leslie, W.D.; Vagianos, K.; Sargent, M.; Laserna-Mendieta, E.J.; Claesson, M.J.; Targownik, L.E. A Comparison of the Gut Microbiome between Long-Term Users and Non-Users of Proton Pump Inhibitors. *Aliment. Pharmacol. Ther.* **2016**, *43*, 974–984, doi:10.1111/apt.13568.

330. Sachdev, A.H.; Pimentel, M. Gastrointestinal Bacterial Overgrowth: Pathogenesis and Clinical Significance. *Ther. Adv. Chronic Dis.* **2013**, *4*, 223–231, doi:10.1177/2040622313496126.
331. Paik, C.N.; Choi, M.-G.; Lim, C.H.; Park, J.M.; Chung, W.C.; Lee, K.-M.; Jun, K.-H.; Song, K.Y.; Jeon, H.M.; Chin, H.-M.; et al. The Role of Small Intestinal Bacterial Overgrowth in Postgastrectomy Patients. *Neurogastroenterol. Motil. Off. J. Eur. Gastrointest. Motil. Soc.* **2011**, *23*, e191-196, doi:10.1111/j.1365-2982.2011.01686.x.
332. Montero, I.; Barrientos, D.; Hidalgo-Cantabrana, C.; Martínez-Álvarez, N. GutAlive® Enables DNA-Based Microbiome Analysis without Disrupting the Original Composition and Diversity. *Front. Microbiol.* **2023**, *14*.
333. Proton Pump Inhibitors: MedlinePlus Medical Encyclopedia Available online: https://medlineplus.gov/ency/patientinstructions/000381.htm (accessed on 29 January 2024).

SUPPLEMENTARY MATERIALS

Supplementary Material 1 Technical details of setup of the *in vitro* human gut microbiome model, based on the DASbox® mini bioreactor system.

Devices	Company	Cat. Number
Base of the System		
DASbox® Mini Bioreactor System MP8-pHpO	Eppendorf	-
Process Computer for Small-Scale Systems	Eppendorf	76DGPCS
Uninterruptible Power Supply	Eppendorf	76DGUPSU1
DASbox® Vessel (with 2 Rushton-type impellers)	Eppendorf	76SR0250ODLS
DASbox® Feed Line Set	Eppendorf	76DXFL05C11
DASbox® Overhead Drive	Eppendorf	78525185
DASbox® Autoclavable Carrier	Eppendorf	76DXBKT4
Sensors to Monitor Bioprocessess		
OxyFerm FDA 120 (DO sensor)	Hamilton	237450
VisiFerm DO ECS 120 (DO sensor)	Hamilton	243666-211
Dencytee 120 (OD sensor)	Hamilton	243750
EasyFerm Plus, PHI K8 120 (pH sensor)	Hamilton	238633-1513
Platinum RTD Temperature Sensor	Eppendorf	78103304
Level Sensor	Eppendorf	78103145
Connecting Parts for the Sensors		
DO Sensor Cable	Eppendorf	78522042
Cell Density Combox	Hamilton	243810
Dencytee Pre-Amp	Hamilton	243755
Cables for Dencytee sensors	Hamilton	-
pH Sensor Cable	Eppendorf	78522020
Level Sensor Cable	Eppendorf	78522031
Additional Exchangable Parts		
Sampling Port Systems	Eppendorf	78510145
Gassing Port Systems	Eppendorf	78532034
Medium Exchange Systems	Eppendorf	78532036
Tubing Clamp	Eppendorf	78200119
Rushton-Type Impeller	Eppendorf	78107304

Supplementary Material 2 List of all materials used in this study.

Reagents	Company	Cat. Number
Bryant and Burkey medium suitable for microbiology, NutriSelect® Plus	Merck	91903
Peptone from caseine, tryptic digest	SIGMA-ALDRICH	70172
Yeast Extract, for use in microbial growth medium	SIGMA-ALDRICH	Y1625
Meat extract	SIGMA-ALDRICH	70164
Sodium acetate	ROTH	X891.1
L-cysteine hydrochloride	SIGMA-ALDRICH	C1276
Resazurin sodium salt	SIGMA-ALDRICH	R7017
Potassium carbonate, 1 kg ≥98 %	ROTH	7956.1
Hydrochloric acid (2 N)	ROTH	T134.1
Tryptic soy broth	SIGMA-ALDRICH	T8907
L(+)-Lactic acid calcium salt pentahydrate	ROTH	4071.1
TWEEN® 80, Viscous liquid	SIGMA-ALDRICH	P1754
D-(+)-Glucose ≥99.5%	SIGMA-ALDRICH	G8270
Putrescin, ≥99 %	ROTH	8379.1
Sodium thioglycolate	SIGMA	T0632
Ethanol absolut	Merck	1.00983.5000
Sodium sulfate	ROTH	8560.1
QUANTOM™ Total Cell Staining Kit	Logos Biosystems	Q13501
Tris	ROTH	5429.1
EDTA	ROTH	8043.1
Triton® X-100	ROTH	3051.3
Lysozym	ROTH	8259.3
DNeasy Blood & Tissue Kit	QIAGEN	69506
GoTaq® qPCR Master Mix	Promega GmbH	A6002
Target Specific PCR Primers	Eurofins Genomics	-
Nuclease-Free Water	Promega	P119E
ALPHAGAZ™ 1 N_2	Air Liquide	-
Gas mixture: CO_2 N45 H N30	Air Liquide	-

Reagents	Company	Cat. Number
Rest N50		

Supplementary Material 3 List of the materials and devices used in this study.

Materials and Devices	Company	Cat. Number
GutAlive® Anaerobic microbiome collection kit	MicroViable Therapeutics	-
Thermo Heraeus Multifuge 3 L-R Refrigerated Centrifuge	Thermo Heraeus Kendro	2962
Thermo Scientific™ Fresco™ 17 Microcentrifuge	Fisher Scientific	75002402
QUANTOM Tx™ Microbial Cell Counter	Logos Biosystems	Q10001
QUANTOM™ Centrifuge	Logos Biosystems	Q10002
QUANTOM™ M50 Cell Counting Slides	Logos Biosystems	Q12001
RH basic 2 Magnetic Stirrer/Hotplate	IKA	0003339000
RCT standard Magnetic Stirrer/Hotplate	IKA	0003622000
MS 3 Basic Vortex Mixer	IKA	0003617000
New Brunswick™ Excella® E24/E24R Shaker	Eppendorf	Discontinued
Grant Bio PCV-2400 Combined Centrifuge and Vortex Mixer	Grant Instruments	11441028
Whitley A85 anaerobic workstation	Don Whitley Scientific	-
Disposable cuvettes	BRAND GmbH	7590
Aluminum crimp caps, 20 mm	Ochs Glasgeratebau	102050
Manual decapper for 20 mm aluminum crimp caps	LLG LABWARE	9.003 369
Manual crimper, height adjustable, for 20 mm aluminum crimp caps	LLG LABWARE	9.003 475
15 mL Conical Polypropylene Centrifuge Tube with Dome Seal Screw Cap	Corning	352097
50 mL Polypropylene Centrifuge Tube with Flat Screw Cap	Corning	352098
SmartBoats™ weighing boats	LevGo	20202
Nalgene® Syringe Filter with SFCA Cellulose Acetate Membrane,	Thermo Scientific	190-2520

Materials and Devices	Company	Cat. Number
Sterile, Diameter: 25mm, Pore Size: 0.2µm		
Nalgene® Syringe Filter, Sterile SFCA membrane, Diameter: 25mm, Pore Size: 0.2µm	Thermo Scientific	723-2520
VACUETTE® Luer Adapter 20G sterile	Manufacturer: Nipro Medical Industries Ltd.; Imported by: Greiner bio-one	450070
Sterican Disposable Injection Needle 0.6x30mm 23G	Braun	4657640
Luer-Lok™ 50-mL syringe	BD	300865
2-part disposable syringes 20 mL	CHIRANA	CH020L
Injekt® Solo Syringe (Luer) 10 ml	Braun	4606108V
2-part disposable syringes 5 mL	CHIRANA	CH002L
Luer-Lok™ 1-mL syringe	BD	309628
CFX96 Touch Real-Time PCR Detection System	BIO-RAD	1855196
Hard-Shell PCR Plates 96-well, thin-wall	BIO-RAD	HSP9655
Microseal® 'B' PCR Plate Sealing Film, adhesive, optical	BIO-RAD	MSB1001
Glass pellets	Assistent	41401001
1.5 mL SC Micro Tube PCR-PT	SARSTEDT	8082711
NanoDrop™ 2000/2000c Spectrophotometer	Fisher Scientific	ND2000
PARAFILM® Sealing film	CARL-ROTH	CNP8.1

Supplementary Material 4 The composition of Bryant and Burkey medium used for anaerobic fermentation.

Reagent	Company	Cat. Number	Concentration (g/L)
Peptone from caseine, tryptic digest	SIGMA-ALDRICH	70172	15
Yeast Extract, for use in microbial growth medium	SIGMA-ALDRICH	Y1625	5
Meat extract	SIGMA-ALDRICH	70164	7.5
Sodium acetate	ROTH	X891.1	5
L-cysteine hydrochloride	SIGMA-ALDRICH	C1276	0.5

Reagent	Company	Cat. Number	Concentration (g/L)
Resazurin (0.07 g in 70 mL distilled water)	SIGMA-ALDRICH		800 μL
Distilled water			To 1 L

Supplementary Material 5 The composition of oral bacteria fermentation medium of *Veillonella parvula* and *Streptococcus salivarius*.

Reagent	Company	Cat. Number	Concentration (g/L)
Veillonella parvula			
Peptone from caseine, tryptic digest	SIGMA-ALDRICH	70172	5
Yeast Extract, for use in microbial growth medium	SIGMA-ALDRICH	Y1625	3
L(+)-Lactic acid calcium salt pentahydrate	ROTH	4071.1	7.5
Sodium thioglycolate	SIGMA	T0632	0.75
TWEEN® 80, Viscous liquid	SIGMA-ALDRICH	P1754	1
D-(+)-Glucose ≥99.5%	SIGMA-ALDRICH	G8270	1
Putrescin, ≥99 %	ROTH	8379.1	0.003
Resazurin sodium salt	SIGMA-ALDRICH	R7017	0.001
Distilled water			To 1 L
Potassium carbonate, 1 kg ≥98 %	ROTH	7956.1	
***Streptococcus salivarius* (M92 medium)**			
Tryptic soy broth	SIGMA-ALDRICH	T8907	30
Yeast Extract, for use in microbial growth medium	SIGMA-ALDRICH	Y1625	3
Distilled water			To 1 L
Hydrochloric acid (2 N)	ROTH	T134.1	

Supplementary Material 6 The composition of lysis buffer used for DNA extraction.

Reagent	Company	Cat. Number	Concentration
Hydrochloric acid (2 N)	ROTH	T134.1	20 mM Tris·Cl, pH = 8.0
TRIS	ROTH	5429.1	

Reagent	Company	Cat. Number	Concentration
EDTA	ROTH	8043.1	2 mM
Triton® X-100	ROTH	3051.3	1.2%
Lysozym	ROTH	8259.3	20 mg/mL
Nuclease-Free Water	Promega	P119E	

LIST OF PUBLICATIONS

Articles directly related to the topic of a doctoral dissertation, published in journals with a citation index factor (IF) in the Clarivate Analytics Web of Science Platform:

1. **Žukauskaitė, K.**, Horvath, A., Gricius, Ž., Kvietkauskas, M., Baušys, B., Dulskas, A., Kuliavas, J., Baušys, R., Letautienė, S. R., Vaicekauskaitė, I., Sabaliauskaitė, R., Baušys, A., Stadlbauer, V., & Jarmalaitė, S. (2024). Impact of mechanical bowel preparation on the gut microbiome of patients undergoing left-sided colorectal cancer surgery: randomized clinical trial. *The British Journal of Surgery*, *111*(9), znae213. *https://doi.org/10.1093/bjs/znae213*

   I have performed the 16S rRNA gene sequencing data analysis, wrote the initial version of the manuscript, created visualizations, revised and corrected manuscript drafts, and submitted the publication.

2. **Žukauskaitė K,** Baušys B, Horvath A, Sabaliauskaitė R, Mlynska A, Jarmalaitė S, Stadlbauer V, Baušys R, Baušys A. (2024). Gut Microbiome Changes After Neoadjuvant Chemotherapy and Surgery in Patients with Gastric Cancer. *Cancers*. 2024; 16(23):4074. *https://doi.org/10.3390/cancers16234074*

   I have performed the 16S rRNA gene sequencing data analysis, wrote the initial version of the manuscript, created visualizations, revised and corrected manuscript drafts, and submitted the publication.

3. **Žukauskaitė, K.**, Li, M., Horvath, A., Jarmalaitė, S., & Stadlbauer, V. (2024). Cellular and Microbial In Vitro Modelling of Gastrointestinal Cancer. *Cancers*, 16(17), 3113. *https://doi.org/10.3390/cancers16173113*

   I have performed the literature analysis, wrote the initial version of the manuscript, created visualizations, revised and corrected manuscript drafts, and submitted the publication.

Other publications not directly related to the topic of a doctoral dissertation but published during the period of doctoral studies in journals with a citation index factor (IF) in the Clarivate Analytics Web of Science platform:

1. Pacher-Deutsch, C., Schweighofer, N., Hanemaaijer, M., Marut, W., **Žukauskaitė, K.**, Horvath, A., & Stadlbauer, V. (2024). The Microplastic-Crisis: Role of Bacteria in Fighting Microplastic-Effects in the Digestive System. *Environmental Pollution*, *366*, 125437. *https://doi.org/10.1016/j.envpol.2024.125437*

2. Horvath, A., Haller, R., Feldbacher, N., Habisch, H., **Žukauskaitė, K.**, Madl, T., & Stadlbauer, V. (2024). Probiotic Therapy of Gastrointestinal Symptoms During COVID-19 Infection: A Randomized, Double-Blind, Placebo-Controlled, Remote Study. *Nutrients*, *16*(22), 3970. *https://doi.org/10.3390/nu16223970*

3. Horvath, A., Habisch, H., Prietl, B., Pfeifer, V., Balazs, I., Kovacs, G., Foris, V., John, N., Kleinschek, D., Feldbacher, N., Grønbæk, H., Møller, H. J., **Žukauskaitė, K.**, Madl, T., & Stadlbauer, V. (2024). Alteration of the Gut–Lung Axis After Severe COVID-19 Infection and Modulation Through Probiotics: A Randomized, Controlled Pilot Study. *Nutrients*, *16*(11), 3840. *https://doi.org/10.3390/nu16223840*

4. Horvath, A., **Zukauskaite, K.**, Hazia, O., Balazs, I., & Stadlbauer, V. (2024). Human gut microbiome: Therapeutic opportunities for metabolic syndrome-Hype or hope?. *Endocrinology, diabetes & metabolism*, 7(1), e436. *https://doi.org/10.1002/edm2.436*

5. Matulevičius, A., **Žukauskaitė, K.**, Gineikaitė, R., Dasevičius, D., Trakymas, M., Naruševičiūtė, I., Ušinskienė, J., Ulys, A., Jankevičius, F., & Jarmalaitė, S. (2023). Combination of DNA methylation biomarkers with multiparametric magnetic resonance and ultrasound imaging fusion biopsy to detect the local spread of prostate cancer. The *Prostate*, 83(16), 1572–1583. *https://doi.org/10.1002/pros.24615*
6. Snipaitiene, K., Zablockiene, B., Sabaliauskaite, R., **Zukauskaite, K.**, Matulyte, E., Smalinskaite, T., Paulauskas, M., Zablockis, R., Lopeta,

M., Gagilas, J., Puriene, A., Jancoriene, L., & Jarmalaite, S. (2023). SARS-CoV-2 RT-qPCR Ct values in saliva and nasopharyngeal swab samples for disease severity prediction. *Journal of oral microbiology*, 15(1), 2213106.
https://doi.org/10.1080/20002297.2023.2213106

7. Žalimas, A., Kubiliūtė, R., **Žukauskaitė, K.**, Sabaliauskaitė, R., Trakymas, M., Letautienė, S., Kaubrienė, E. M., Ušinskienė, J., Ulys, A., & Jarmalaitė, S. (2022). Urine Molecular Biomarkers for Detection and Follow-Up of Small Renal Masses. *International journal of molecular sciences*, *23*(24), 16110.
https://doi.org/10.3390/ijms232416110

8. Matulevičius, A., Bakavičius, A., Ulys, A., Trakymas, M., Ušinskienė, J., Naruševičiūtė, I., Sabaliauskaitė, R., **Žukauskaitė, K.**, Jarmalaitė, S., & Jankevičius, F. (2022). Multiparametric MRI fusion-guided prostate biopsy for detection of clinically significant prostate cancer eliminates the systemic prostate biopsy. *Applied Sciences*, *12*(19), 10151.
https://doi.org/10.3390/app121910151

9. Klimaitė, R., Kazokaitė, M., Kondrotienė, A., Daukšienė, D., Sabaliauskaitė, R., **Žukauskaitė, K.**, Žilaitienė, B., Jarmalaitė, S., & Daukša, A. (2022). The Role of *TSHR*, *PTEN* and *RASSF1A* Promoters' Methylation Status for Non-Invasive Detection of Papillary Thyroid Carcinoma. *Journal of clinical medicine*, *11*(16), 4917.
https://doi.org/10.3390/jcm11164917

10. Kubiliūtė, R., **Žukauskaitė, K.**, Žalimas, A., Ulys, A., Sabaliauskaitė, R., Bakavičius, A., Želvys, A., Jankevičius, F., & Jarmalaitė, S. (2022). Clinical significance of novel DNA methylation biomarkers for renal clear cell carcinoma. *Journal of cancer research and clinical oncology*, *148*(2), 361–375.
https://doi.org/10.1007/s00432-021-03837-7

LIST OF INTERNATIONAL CONGRESSES

Poster presentations directly related to the topic of the doctoral dissertation:

1. **Kristina Žukauskaitė**, Christian Pacher, Selina Kofler, Irina Balazs, Angela Horvath, Vanessa Stadlbauer. Optimizing conditions for *in vitro* modeling of the human gut microbiome to study intestinal health and disease. United European Gastroenterology (UEG) Week 2023. Copenhagen, Denmark. 2023.10.14-17. *The presentation was rewarded with the best abstract presentation prize.* *https://doi.org/10.1002/ueg2.12460*

2. Angela Horvath, **Kristina Žukauskaitė**, Christian Pacher, Selina Kofler, Irina Balazs, Vanessa Stadlbauer. Optimizing conditions for *in vitro* modeling of the human gut microbiome to study intestinal health and disease. World of Microbiome. Sofia, Bulgaria. 2023.10.25-28.

3. **Kristina Žukauskaitė**, Christian Pacher, Selina Kofler, Irina Balazs, Angela Horvath, Vanessa Stadlbauer. Development of an in vitro microbiome model of the human gut utilizing the DASbox® mini bioreactor system. Berchtesgaden Microbiome Science Days 2023. Berchtesgaden, Germany. 2023.09.07-09.

4. **Kristina Žukauskaitė**, Christian Pacher, Selina Kofler, Irina Balazs, Angela Horvath, Vanessa Stadlbauer. Establishment of an in vitro microbiome model of the human gut microbiome using the DASbox® mini bioreactor system. Österreichischen Gesellschaft für Gastroenterologie und Hepatologie (ÖGGH) congress 2023. Graz, Austria. 2023.06.14-17.
   https://doi.org/10.1055/s-0043-1769043

5. **Kristina Žukauskaitė**, Angela Horvath, Žilvinas Gricius, Audrius Dulskas, Rimantas Baušys, Rasa Sabaliauskaitė, Sonata Jarmalaitė, Vanessa Stadlbauer, Augustinas Baušys. Preoperative Mechanical Bowel Preparation Impact on the Intestinal Microbiome in Patients Undergoing Left-Sided Colorectal Cancer Surgery. Doctoral Day 2023. Medical University of Graz, Graz, Austria. 2023.02.09.

6. **Kristina Žukauskaitė**, Angela Horvath, Žilvinas Gricius, Audrius Dulskas, Rimantas Baušys, Rasa Sabaliauskaitė, Sonata Jarmalaitė, Vanessa Stadlbauer, Augustinas Baušys. Bowel preparation impact on the intestinal microbiome in patients undergoing left-sided colorectal cancer surgery: results from a pilot randomized control trial comparing oral preparation vs enema. Österreichischen Gesellschaft für

Gastroenterologie und Hepatologie (ÖGGH) congress 2022. Vienna, Austria. 2022.09.07-09.
https://doi.org/10.1055/s-0042-1755736

Other presentations not directly related to the topic of the doctoral dissertation but presented during the period of doctoral studies:

1. Christian Pacher-Deutsch, Natascha Schweighofer, Mark Hanemaaijer, Wioleta Marut, **Kristina Žukauskaitė**, Angela Horvath, Vanessa Stadlbauer. The Microplastic-Crisis: Role of Bacteria in Fighting Microplastic-Effects in the Digestive System - A Comprehensive Literature Review. microONE summit 2024. Graz, Austria. 2024.11.29.

2. Christian Pacher-Deutsch, **Kristina Žukauskaitė**, Cigdem Erdogan, Maximilian Nepel, Lukas Kogler, Hansjörg Habisch, Serena Ducoli, Stefania Federici, Tobias Madl, Verena Pichler, Angela Horvath, Vanessa Stadlbauer. The Influence of true-to-life Microplastic Particles on the Human Gut Microbiome – A Series of Bioreactor Experiments. microONE summit 2024. Graz, Austria. 2024.11.29.

3. Christian Pacher, Angela Horvath, Irina Balazs, **Kristina Zukauskaite**, Nicole Feldbacher, Rosa Haller, Olha Hazia, Vanessa Stadlbauer. Impact of microplastics on the human gut – A series of bioreactor experiments. microONE summit 2023.Vienna, Austria. 2023.12.01.

4. Raimonda Kubiliute, **Kristina Zukauskaite**, Algirdas Zalimas, Rasa Sabaliauskaite, Albertas Ulys, Sonata Jarmalaite. Novel urinary methylated DNA biomarkers for kidney cancer detection and prognosis. ESMO „Molecular analysis for precision oncology“. Amsterdam, The Netherlands, 2022.10.14-16.
https://doi.org/10.1016/j.annonc.2020.08.2184

5. Algirdas Zalimas, Raimonda Kubiliute, Mantas Trakymas, Simona Letautiene, **Kristina Zukauskaite**, Albertas Ulys, Sonata Jarmalaite. Urinary biomarkers for prognosis of histologically confirmed small renal tumors. ESMO „Molecular analysis for precision oncology“. Amsterdam, The Netherlands, 2022.10.14-16. *https://doi.org/10.1016/j.annonc.2022.09.069*

6. Augustinas Matulevičius, **Kristina Žukauskaitė**, Aistė Gerulaitytė, Mantas Trakymas, Albertas Ulys, Rasa Sabaliauskaitė, Sonata Jarmalaitė. Analysis of DNA methylation biomarkers in mpMRI/US guided targeted prostate biopsies. 7th Baltic Meeting in conjunction with the EAU. Vilnius, Lithuania. 2022.05.27-28. *https://doi.org/10.1016/S2666-1683(22)00641-3*
7. Mintautė Kazokaitė, **Kristina Žukauskaitė**, Raimonda Klimaitė, Aistė Kondrotienė, Dalia Daukšienė, Birute Žilaitienė, Rasa Sabaliauskaitė, Albertas Daukša. TSHR promoter methylation level changes as a prognostic blood-based biomarker in follicular thyroid carcinoma. European Congress of Endocrinology 2022. Milan, Italy. 2022.05.21-22. *https://doi.org/10.1530/endoabs.81.EP1024*
8. Augustė Vipartaitė, **Kristina Žukauskaitė**, Rasa Sabaliauskaitė, Sonata Jarmalaitė. Identification of Liquid Biopsy-Based Biomarkers for Clear Cell Renal Cell Carcinoma Diagnosis. The COINS 2022. Vilnius, Lithuania. 2022.03.03.

FINANCIAL SUPPORT

Clinical studies were funded by the Research Council of Lithuania (LMTLT), agreement Nos S-PD-24-87 and S-MIP-22-30. *In vitro* model establishment was funded by MicroONE, a COMET Modul under the lead of CBmed GmbH (Austria), which is supported by the federal ministries BMK and BMDW, the provinces of Styria and Vienna, and managed by the Austrian Research Promotion Agency (FFG) within the COMET—Competence Centers for Excellent Technologies—program. The research was supported by Vilnius University in Vilnius, Lithuania, which also provided a scholarship.

TRAINEESHIPS

- 2022-2023 Mobility program of ERASMUS+: Division for Gastroenterology and Hepatology, Department of Internal Medicine, Medical University of Graz, Graz, Austria;
- 2023-2024 Extended stay at the Division for Gastroenterology and Hepatology, Department of Internal Medicine, Medical University of Graz, Graz, Austria, with permission from the Vilnius University, Vilnius, Lithuania.

SANTRAUKA

Gastroenterologinis (GE) vėžys, įskaitant storosios žarnos ir skrandžio vėžius, yra reikšmingas mirtingumo veiksnys visame pasaulyje ir kelia didelį iššūkį visuomenės sveikatai [1]. Kritiškai svarbus, tačiau vis dar mažai ištirtas GE vėžio aspektas yra jo sąsaja su žarnyno mikrobiomu. Žinoma, kad žarnyno mikrobiomas keičiasi ne tik vystantis ar progresuojant GE vėžiui, bet ir gydymo metu [2]. Vis dėlto, sudėtingi vėžio, jo gydymo ir žarnyno mikrobiomo sąveikos aspektai vis dar lieka menkai ištyrinėti.

Vėžio tyrimuose dažnai naudojami gyvūnų modeliai, tačiau svarbūs išlieka bioetiniai apribojimai ir biologiniai skirtumai nuo žmonių [3]. Tradiciniai *in vitro* modeliai – alternatyva *in vivo* modeliams – vis dar nėra pakankamai kompleksiški, kad galėtų tiksliai atkartoti dinamiškas sąveikas tarp šeimininko ląstelių ir žarnyno mikrobiomo [4]. Siekiant užpildyti šią spragą, buvo sukurti bioreaktoriais pagrįsti *in vitro* modeliai, leidžiantys detaliau tirti šias sąveikas nenaudojant gyvūnų modelių. Nepaisant jų potencialo, šie modeliai (ypač tie, kurie naudoja išmatų mikrobiomą) vis dar nėra plačiai naudojami tiriant vėžio gydymo šalutinius poveikius.

Šiuo disertaciniu darbu siekta sumažinti gyvūnų modelių naudojimą, sukuriant lengvai naudojamą bioreaktoriais paremtą *in vitro* modelį, kuris panaudoja žmogaus žarnyno mikrobiomą. Šis metodą pasirinktas tam, kad tiksliau atspindėtume žmogaus žarnyno aplinką ir sukurtume patikimesnę platformą, skirtą tyrinėti GE vėžio, jo gydymo bei šalutinių poveikių sąveikas su žarnyno mikrobiomu. Nors dauguma tyrimų yra sutelkti į naujų ir efektyvesnių vėžio vaistų kūrimą, šiame darbe dėmesys skiriamas esamų gydymo metodų šalutinių poveikių mažinimui, siekiant pagerinti vėžiu sergančių pacientų, kuriems taikomas dabartinis gydymas, gyvenimo kokybę. Todėl šio tyrimo metu pritaikėme naujai sukurtą *in vitro* modelį, siekdami įvertinti probiotikų turinčius produktus, kurie galėtų potencialiai sumažinti vėžio gydymo sukeltus šalutinius poveikius.

Tikslas ir uždaviniai

Šiame darbe pirmiausia buvo siekiama ištirti įvairių GE vėžio gydymo metodų poveikį žarnyno mikrobiomo sudėčiai, o antra – sukurti naują bioreaktoriais pagrįstą *in vitro* modelį, skirtą žmogaus žarnyno mikrobiomo modeliavimui. Galutinis tikslas buvo pasitelkti šią *in vitro* sistemą naujos probiotinių produktų kombinacijos testavimui, kuri galėtų potencialiai sumažinti vėžio gydymo šalutinius poveikius ir taip sumažinti tyrimų priklausomybę nuo gyvūnų modelių.

Norint pasiekti šį tikslą, buvo iškelti šie uždaviniai:

1. Nustatyti priešoperacinio mechaninio žarnyno paruošimo su oraliniais preparatais ir tiesiosios žarnos klizmos poveikį žarnyno mikrobiomo sudėčiai bei pooperacinėms komplikacijoms storosios žarnos vėžiu sergantiems pacientams;
2. Nustatyti neoadjuvacinės chemoterapijos ir radikalios operacijos poveikį žarnyno mikrobiomui skrandžio vėžiu sergantiems pacientams;
3. Sukurti naują bioreaktorių pagrįstą *in vitro* žmogaus žarnyno modelį, kurį būtų galima naudoti gastroenterologinio vėžio gydymo šalutinių poveikių modeliavimo tikslais;
4. Pritaikyti naujai sukurtą *in vitro* modelį probiotinių produktų testavimui, siekiant sumažinti gastroenterologinio vėžio gydymo šalutinius poveikius, tokius kaip žarnyno mikrobiomo oralizacija.

Mokslinis naujumas ir praktinė tyrimo reikšmė

Šis tyrimas išsiskiria keliais svarbiais aspektais. Pirmiausia, jis įtraukia du perspektyvius klinikinius tyrimus, kurie nagrinėja GE vėžiu sergančius pacientus, turinčius dvi skirtingas vėžio formas – skrandžio ir storosios žarnos vėžį. Iš šių pacientų surinkti išmatų mėginiai buvo naudojami išsamiam žarnyno mikrobiomo sudėties tyrimui.

Storosios žarnos vėžio pacientų tyrimas suteikė vertingų įžvalgų apie priešoperacinio mechaninio žarnyno paruošimo metodus. Pirmą kartą buvo nustatyta, kad tiesiosios žarnos klizmos poveikis žarnyno mikrobiomo sudėčiai yra panašus į oralinių preparatų poveikį. Šie rezultatai rodo, kad abu metodai gali būti efektyviai naudojami mechaniniam žarnyno paruošimui prieš kairiosios storosios žarnos vėžio operacijas.

Skrandžio vėžio pacientų tyrimas atskleidė, kad neoadjuvatinė chemoterapija prieš radikalią gastrektomiją neturėjo reikšmingo poveikio žarnyno mikrobiomo sudėčiai. Tačiau radikali gastrektomija, kuri sekė po adjuvantinės chemoterapijos, sukėlė reikšmingus žarnyno mikrobiomo pokyčius, įskaitant žarnyno mikrobiomo oralizaciją.

Kitas tyrimo etapas apėmė naujo bioreaktoriumi pagrįsto *in vitro* modelio kūrimą, skirtą ištirti GE vėžio gydymo šalutinius poveikius, įskaitant žarnyno mikrobiomo oralizaciją, ir jų poveikį žarnyno mikrobiomui. Ši sritis yra mažai ištirta, kadangi iki šiol nebuvo daug tyrimų, kurie įtrauktų išmatų mikrobiomą studijuojant vėžio gydymo šalutinius poveikius.

Oralizacija – ilgalaikio protonų siurblio inhibitorių vartojimo žinomas šalutinis poveikis ir taip pat identifikuotas kaip radikalios gastrektomijos gydymo šalutinis poveikis skrandžio vėžio pacientams – buvo modeliuota naudojant naujai sukurtą bioreaktoriais pagrįstą *in vitro* modelį, kuris naudojo išmatų mėginius. Šis modelis pasirodė esantis efektyvus tiriant žarnyno mikrobiomo oralizaciją ir buvo toliau pritaikytas probiotikų produktų, galinčių sumažinti šį šalutinį poveikį, įvertinimui. *In vitro* modelis parodė, kad ištirta probiotikų sudėtis gali sumažinti burnos bakterijų augimą žarnyno mikrobiomo kontekste, siūlydama jų potencialą naudoti vėžiu sergantiems pacientams, siekiant sumažinti šį vėžio gydymo šalutinį poveikį.

Ginamieji teiginiai

1. Abu mechaninio žarnyno paruošimo metodai – naudojant oralinius preparatus ir tiesiosios žarnos klizmas – sukelia panašius disbiozės pokyčius storosios žarnos vėžiu sergantiems pacientams. Be to, pacientai, kurie patiria pooperacines infekcijas, turi išskirtinę žarnyno mikrobiomo sudėtį šeštąją pooperacinę dieną.
2. Skrandžio vėžio radikalus gydymas, apimantis neoadjuvatinę chemoterapiją ir radikalią chirurgiją, turi ilgalaikių pasekmių žarnyno mikrobiomui, kurios pasireiškia žarnyno mikrobiomo oralizacija. Šie ilgalaikiai pokyčiai daugiausia priskiriami radikalios gastrektomijos, o ne neoadjuvatinės chemoterapijos poveikiui.
3. Eksperimentinės sąlygos žmogaus žarnyno mikrobiomo *in vitro* modeliui buvo sistemingai optimizuotos naudojant DASbox® mini bioreaktorių sistemą ir žmogaus išmatų mėginius. Šis naujas *in vitro* žarnyno mikrobiomo modelis gali būti pritaikytas tirti GE vėžio gydymo šalutinius poveikius.
4. Testuota probiotikų sudėtis parodė reikšmingą burnos bakterijų augimo sumažėjimą bioreaktorių pagrindu sukurtame *in vitro* modelyje, kas rodo jos potencialą kaip vertingą papildą vėžiu sergantiems pacientams, kuriems taikomas gydymas. Tai palaiko probiotikų naudojimą klinikinėje praktikoje siekiant pagerinti pacientų rezultatus tiek gydymo metu, tiek po jo.

TIRIAMOSIOS GRUPĖS IR METODAI

Šis darbas įtraukia du perspektyvius klinikinius tyrimus, kurie apima skrandžio (SV) ir kolorektalinio (KV) vėžio pacientus, taip pat *in vitro* tyrimą, kuriame naudoti sveikų savanorių mikrobiomai.

Mokslinio tyrimo dizainas ir etika

Klinikiniai tyrimai buvo atlikti Nacionaliniame vėžio institute, Vilniuje, Lietuvoje, po to, kai protokolai buvo patvirtinti Vilniaus regioninės biomedicinos tyrimų etikos komiteto (Nr. 2019/6-1133-631 ir 2020/1-1185-675) ir įregistruoti klinikinių tyrimų registre *clinicaltrials.gov* (NCT04013841 ir NCT04223401). *In vitro* modeliavimo tyrimas buvo atliktas Graco Medicinos universitete, Grace, Austrijoje, po to, kai vietinis etikos komitetas patvirtino tyrimą (protokolo Nr. 34-323 ex 21/22 1126/2022). Visi tyrimo etapai buvo vykdomi laikantis 2013 metų Helsinkio deklaracijos etikos standartų. Visi tyrimo dalyviai buvo bent 18 metų amžiaus ir prieš dalyvavimą pateikė rašytinį informuotą sutikimą.

Tyrimo dalyviai

Klinikiniai tyrimai apėmė GE vėžio pacientus, kurie buvo 18 metų ar vyresni ir atitiko šiuos kriterijus: (i) histologiškai patvirtintas arba kliniškai įtariamas kairiosios storosios žarnos vėžys, (ii) SV pacientai, numatyti radikaliai chirurgijai po neoadjuvacinės chemoterapijos (NAC), kaip nustatyta multidisciplininių komandų posėdžiuose. *In vitro* modeliavimo tyrimuose buvo įtraukti tik sveiki savanoriai.

KV tiriamosios grupės pašalinimo kriterijai: (a) Operacija su prevencine ileostomija, (b) Alergija oraliniams preparatams (OP), (c) Reikalinga multivisceralinė rezekcija, (d) Skubioji operacija, (e) Uždegiminės žarnos ligos anamnezė, (f) Ankstesnės gastroenterologinės operacijos, (g) Klinikiniai žarnyno obstrukcijos požymiai, kurie būtų kontraindikacija OP, (h) Nėštumas.

SV tiriamosios grupės pašalinimo kriterijai: (a) Operacija dėl skrandžio vėžio atkryčio, (b) Paciento būklė, neleidžianti atidėti operacijos bent 4 savaitėms, (c) Dalyvavimas neįmanomas dėl paciento fizinės arba psichinės būklės, (d) Chemoterapija arba radioterapija per 12 mėnesių prieš įtraukimą į tyrimą, (e) Antibiotikų, probiotikų, prebiotikų arba sinbiotikų vartojimas per 1 mėnesį prieš įtraukimą į tyrimą, (f) Didelių GE trakto rezekcijų anamnezė, (g) Ne skrandžio piktybiniai navikai tyrimo metu.

In vitro modelio kūrimo tiriamosios grupės pašalinimo kriterijai: antibiotikų, probiotikų, prebiotikų arba sinbiotikų vartojimas bent 1 mėnesis prieš įtraukimą į tyrimą.

Nuo 2021 m. balandžio 4 d. iki 2021 m. lapkričio 30 d. 40 storosios žarnos vėžiu sergančių pacientų buvo atsitiktinai paskirstyti į dvi grupes: paruošimas oraliniais preparatais (OP; n = 20) ir tiesiosios žarnos klizma (TŽK; n = 20). Po paskirstymo 2 (10%) pacientai OP grupėje buvo pašalinti dėl to, kad nepateikė išmatų mėginių tiek šeštąją pooperacinę dieną (POD06), tiek trisdešimtąją pooperacinę dieną (POD30). Priešoperacinis mechaninis žarnyno paruošimas (MŽP) buvo atliktas taip: OP grupei priklausantys pacientai gavo 4 litrus oralinio preparato „Macrogol 4000“ (73,69 g viename litre; Fortrans; Ipsen Pharma, Paryžius, Prancūzija), kuris buvo pradėtas vartoti dieną prieš operaciją. TŽK grupei priklausantys pacientai gavo 2 litrus 0,9% NaCl tirpalo per irrigatorių (Plasti-med, Istanbulas, Turkija) operacijos išvakarėse. Visiems KV pacientams prieš operaciją buvo taikoma antibiotikų profilaktika: viena dozė cefazolino 2 g ir metronidazolo 500 mg buvo skiriama intraveniniu būdu 30-60 minučių prieš pjūvį. Visiems pacientams operacijos atliktos pagal Nacionaliniame vėžio institute, Vilniuje, Lietuvoje patvirtintus protokolus.

Nuo 2021 m. balandžio 13 d. iki 2022 m. rugsėjo 22 d. į tyrimą buvo įtraukti 38 SV sergantys pacientai, kuriems buvo diagnozuotos tolimosios metastazės su teigiama peritonine citologija, tačiau nebuvo kitų tolimų metastazių. Įtraukus į tyrimą, visi pacientai gavo NAC, po kurios sekė radikali operacija.

Nuo 2022 m. balandžio 20 d. iki 2024 m. liepos 22 d. į *in vitro* tyrimą, skirtą vėžio gydymo šalutinių poveikių modeliavimui, buvo įtraukti 9 sveiki donorai. Donorams nebuvo atliktos jokios intervencijos, jie pateikė šviežius išmatų mėginius. Anaerobinio mikrobiomo surinkimo optimizavimo ir oralizacijos modelio kūrimo etape buvo įtrauktos trys sveikos moterys, amžius nuo 25 iki 30 metų (vidutinis amžius 27,7 ± 5 metų). Operacijos režimų optimizavimo etape dalyvavo dvi sveikos moterys ir vienas sveikas vyras, amžius nuo 26 iki 31 metų (vidutinis amžius 28,7 ± 5 metų). *In vitro* oralizacijos modeliavime dalyvavo šeši sveiki savanoriai: trys vyrai (vidutinis amžius 28,0 metų; amžiaus intervalas 26-29) ir trys moterys (vidutinis amžius 29,7 metų; amžiaus intervalas 27-32).

Šviežių išmatų mėginių rinkimas

Švieži išmatų mėginiai buvo surinkti iš KV pacientų pradiniame etape 1 dieną prieš žarnyno paruošimą, POD06 ir POD30. Iš SV pacientų švieži

išmatų mėginiai buvo surinkti pradiniame etape, prieš operaciją, per savaitę po neoadjuvantinės chemoterapijos (post-NAC) ir 12 mėnesių po gydymo pradžios, užtikrinant, kad nuo operacijos būtų praėję ne mažiau kaip 6 mėnesiai (post-SX). Išmatų mėginiai buvo nedelsiant užšaldomi -80 °C temperatūroje iki DNR išskyrimo. Švieži išmatų mėginiai *in vitro* modeliavimui buvo surinkti iš tyrimo dalyvių naudojant anaerobinius mikrobiomo surinkimo konteinerius GutAlive® (MicroViable Therapeutics, Ispanija) pagal gamintojo nurodymus ir laikomi kambario temperatūroje iki dviejų dienų.

16S rRNA geno sekoskaita

Po to, kai visi klinikinių tyrimų mėginiai buvo surinkti, užšaldyti išmatų mėginiai iš Nacionalinio vėžio instituto, Vilniuje, Lietuvoje, buvo siunčiami sausame lede į Graco medicinos universitetą, Grace, Austrijoje. DNR iš užšaldytų išmatų mėginių ir bakterijų plokštelių (angl. *pellets*) buvo išskirta naudojant MagNA Pure LC DNA Isolation Kit III (Bacteria, Fungi) (Roche, Mannheim, Vokietija) arba SphaeraMag® Genomic DNA Fecal Purification Kit (Procomcure Biotech, Austrija) pagal gamintojo nurodymus. Mėginiai buvo ruošimai atskirai, siekiant sumažinti kryžminės taršos riziką. Bibliotekos paruošimas ir *16S rRNA* geno sekoskaita buvo atliekama naudojant Illumina protokolą. Hypervariabilūs regionai V1–V2 buvo padauginti (naudoti pradmenys: 27F-AGAGTTTGATCCTGGCTCAG; R357-CTGCTGCCTYCCGTA) ir nuskaityti naudojant Illumina MiSeq arba Illumina NextSeq2000 prietaisus pagal gamintojo rekomendacijas.

Sekoskaitos duomenų apdorojimas

Sekoskaitos duomenys buvo apdoroti naudojant BaseSpace Sequence Hub su BaseSpace DRAGEN Analysis (v1.3.0) arba BCL Convert (v2.4.0) programomis bei toliau naudojant QIIME 2 įrankius vietiniame Galaxy serveryje (*https://galaxy.medunigraz.at/*) [286], o sekoskaitos duomenų kokybė buvo patikrinta naudojant FastQC ir MultiQC įrankius. Atsižvelgiant į kokybės ataskaitas, siekiant užtikrinti sekoskaitos duomenų vientisumą, buvo trumpinamos tiek priekinės, tiek galinės sekos. Duomenų charakteristikos pateikiamos **Table 2.1**. Triukšmo mažinimas buvo atliktas naudojant DADA2, pasiekiamą per QIIME2 įrankį [287,288]. Taksonomija buvo priskirta pagal Silva 132 duomenų bazę. Filogenetiniai medžiai buvo sukurti naudojant MAFFT. Jei filogenetinis medis buvo kuriamas, gauti duomenys buvo importuoti į R pagrįstą CBmed mikrobiomo analizės

platformą naudojant *qza_to_phyloseq()* funkciją iš qiime2R paketo [289]. Duomenys buvo filtruojami naudojant neigiamas sekoskaitos kontroles ir iš tolimesnės analizės pašalinant *Cyanobacteria*.

Sekoskaitos duomenų analizė

Alfa įvairovės analizė buvo kiekybiškai įvertinta pagal turtingumo (angl. *Richness*), Shannon, atvirkštinio Simpson indekso (angl. *Inverse Simpson*), tolygumo (angl. *Evenness*) bei filogenetinės įvairovės (angl. *Phylogenetic Diversity*) rodiklius. Beta įvairovė buvo tiriama naudojant principinių koordinačių analizę, remiantis *unique fraction metric* (*unifrac*), *weighted unifrac* (*wunifrac*), Bray-Curtis ir Jaccard dissimilarumo matricomis, o rezultatai buvo vertinami naudojant *Permutational Multivariate Analysis of Variance* (PERMANOVA), naudojant R (R Core Team, 2023, versija 4.3.0) programą per RStudio sąsają. PERMANOVA rezultatai buvo patvirtinti atlikus *redundancy* analizę (RDA), kuri buvo atlikta naudojant *vegan* paketą. Vėliau buvo atlikta linijinės diskriminantinės analizės efekto dydžio analizė, siekiant nustatyti požymius, kurie rodo skirtumus tarp lyginamų grupių, ir nustatyti jų efekto dydžius, naudojant *microbiomeMarker* paketą [290]. Vėliau buvo kuriamas linijinis modelis, siekiant nustatyti gautų rezultatų statistinę reikšmę, naudojant *lme4* paketą [291]. Gauti rezultatai grafikšai iliustruoti naudojant *ggplotify* paketą [292].

In vitro modelio kurimas

Sukurtas *in vitro* modelis paremtas komerciškai prieinamo DASbox® mini bioreaktoriaus sistema (Eppendorf, Vokietija), kurią sudaro keturi stikliniai indai, aprūpinti optiniais ir elektrocheminiais jutikliais (**Fig. 2.1**). Jutikliai naudojami stebėti pagrindinius bioprocesų rodiklius, įskaitant temperatūrą (Eppendorf, Vokietija), optinį ląstelių tankį esant 600 nm bangos ilgiui, pH ir ištirpusio deguonies matavimui (visi Hamilton, Jungtinės Amerikos Valstijos) (**Table 2.2**). Šios sistemos procesų rodikliai buvo automatiškai stebimi ir valdomi realiu laiku naudojant specializuotą DASware® control 5 programinę įrangą (Eppendorf, Vokietija). Techniniai duomenys ir sistemos specifikacijos pateikiamos **Supplementary Material 1**. Visos medžiagos, įrenginiai ir reagentai naudoti šiame tyrime pateikiami **Supplementary Material 2-3**.

Anaerobiškai laikyti išmatų mėginiai buvo atidaryti Whitley A85 anaerobinėje darbo stotyje (Don Whitley Scientific, Jungtinė Karalystė). Išmatų mėginiai buvo maišomi su *Bryant ir Burkey* anaerobine mitybine terpe

(NutriSelect® Plus, Merck, Vokietija, arba paruošti iš atskirų komponentų pagal **Supplementary Material 4**). Anaerobinės mitybinės terpės būklė buvo nustatoma kolorimetriškai, kaip parodyta **Fig. 2.2**.

Remiantis bioreaktoriuje esančiu tūriu, buvo paruošta 10% arba 20% inokuliantas. Stikliniai buteliai arba mėgintuvėliai (50 mL polipropileno centrifugavimo mėgintuvėliai su plokščiu užsukamu kamščiu, Corning, Meksika) buvo uždaryti ir centrifuguoti 180 *x g* greičiu 10 minučių 4°C temperatūroje, kad nusėstų netirpios išmatų dalelės. Stikliniai buteliai su inokuliatu buvo atidaryti anaerobinėje darbo stotyje, supernatantas buvo filtruojamas nuo nuosėdų naudojant 0,2 µM filtrą ir perkeliamas į sterilius stiklinius inokuliacijos mėgintuvėlius. Stikliniai mėgintuvėliai su inokuliatu buvo uždaryti, o išorėje nuo anaerobinės darbo stoties buvo pripildyti azotu naudojant švirkštų filtrus (Nalgene® Syringe Filter with SFCA Cellulose Acetate Membrane or Nalgene® Syringe Filter, Sterile SFCA membrane, abu Thermo Scientific, Kinija), kad būtų sukuriamas aukštesnis slėgis mėgintuvėlyje (**Fig. 2.3**). Šie slėgio skirtumai tarp bioreaktoriaus ir inokuliacijos mėgintuvėlio leido atlikti inokuliacijos procedūrą anaerobiškai, prijungiant mėgintuvėlį su inokuliatu prie bioreaktoriaus maistinių medžiagų pateikimo prievado naudojant sterilią adatą (VACUETTE® Luer Adapter 20G sterile, Nipro Medical Industries Ltd., Japonija).

Šviežia *Bryant ir Burkey* mitybinė terpė buvo pateikiama kasdien, pradėjus 24 valandoms po inokuliacijos. Tyrimo metu išbandytos keturios skirtingos maistinių medžiagų pateikimo strategijos (toliau – operaciniai režimai): (1) *batch* operacinis režimas, kai per kultivavimo laiką mitybinė terpė nebuvo pridedama ar pašalinama; (2) nuolatinis operacinis režimas su nuolatiniu mitybinių medžiagų srautu (~3 mL/valandą) kartu su atliekų pašalinimu; (3) pusiau nuolatinis operacinis režimas su 50% terpės keitimu kasdien; (4) pusiau nuolatinis operacinis režimas su 25% terpės keitimu du kartus per dieną, su 8 valandų intervalu tarp keitimų. Pusiau nuolatinio terpės keitimo procedūra iliustruota **Fig. 2.4**.

Oralizacijos modelis buvo sukurtas bioreaktorius papildant burnos ertmės bakterijomis *Veillonella parvula* ir *Streptococcus salivarius*. Šie oralizacijos biožymenys buvo parinkti remiantis ankstesniu tyrimu [6]. Burnos ertmės bakterijos buvo iš anksto kultivuotos per naktį *S. salivarius* atveju ir 48 valandas *V. parvula* atveju. Burnos ertmės bakterijų mitybinių terpių sudėtis pateikta **Supplementary Material 5**. Bakterijų koncentracija bioreaktoriuose buvo nustatyta naudojant QUANTOM™ Total Cell Staining Kit ir QUANTOM Tx™ Microbial Cell Counter (Logos Biosystems, Pietų Korėja), vadovaujantis gamintojo rekomendacijomis. Bakterijų papildymo procedūra buvo integruota su pusiau nuolatiniu terpės keitimu, vykstančiu

kartą per dieną. Remiantis klinikiniais duomenimis, *V. parvula* papildymo koncentracija buvo 0,2%, o *S. salivarius* – 0,6% visos apskaičiuotos bakterijų koncentracijos bioreaktoriuose. Buvo pasirinkti keturi skirtingi papildymo strategijos variantai: (1) papildymas burnos ertmės bakterijomis vieną kartą po inokuliacijos; (2) papildymas burnos ertmės bakterijomis vieną kartą po 48 valandų nuo inokuliacijos žarnyno bakterijomis; (3) papildymas burnos ertmės bakterijomis kiekvieną dieną, pradedant po inokuliacijos žarnyno bakterijomis; (4) papildymas burnos ertmės bakterijomis kiekvieną dieną, pradedant po 48 valandų nuo inokuliacijos burnos ertmės bakterijomis. Mėginiai iš DASbox® mini bioreaktorių sistemos buvo renkami kas 24 valandas per 120 valandų kultivavimo laikotarpį ir iš jų paruošiamos bakterijų plokštelės.

Žarnyno mikrobiomo oralizacijos sumažinimui buvo tirti penki skirtingi produktai: (i) Placebas, (ii) Kukurūzų krakmolas, (iii) Probiotikai, (iv) Prebiotikai ir (v) Probiotikų ir prebiotikų mišinys. Kiekvienas produktas buvo pasveriamas anaerobinėje aplinkoje ir 2 gramai produkto sumaišyti su šviežia anaerobine maistinių medžiagų terpe. Šis etapas buvo atliktas anaerobinėje darbo stotyje, siekiant išvengti deguonies. Paruošti stikliniai buteliai su ištirpintu produktu buvo papildomai pripildyti anaerobiniu dujų mišiniu, kad būtų užtikrintos anaerobinės sąlygos. Šis etapas buvo atliktas remiantis „keturių akių“ principu, kai nepriklausomas darbuotojas stebi terpės paruošimo ir pakeitimo procedūrą. Ištirti probiotikai turėjo šių bakterijų mišinį: *Lactobacillus plantarum, Bifidobacterium animalis, Lactobacillus acidophilus, Lactobacillus casei, Lactobacillus rhamnosus, Pediococcus acidilactici*. Tiriamieji prebiotikai buvo fruktooligosacharidai.

Siekiant išlaikyti kokybės kontrolę, bendradarbiaujant su nepriklausomu tyrėju, buvo tikrinamas placebo sterilumas ir probiotinių bakterijų gyvybingumas. Nepriklausomas tyrėjas steriliais medvilniniais tamponais paskirstė tiriamuosius produktus ant sterilios *Bryant ir Burkey* agaro terpės Petri lėkštelėse. Be to, darbo aplinkoje papildomai buvo palikta atvira Petri lėkštelė, kad būtų patvirtintas aplinkos sterilumas, kurioje buvo tiriami produktai, o švarus medvilninis tamponas buvo naudojamas tamponų sterilumui patikrinti. Visos Petri lėkštelės buvo anaerobiškai inkubuojamos 48 valandas 37°C temperatūroje. Tiriamųjų produktų tinkamumas buvo patvirtintas, kai placebo ir prebiotiko produktai nerodė bakterijų augimo, o probiotikų turintys produktai parodė bakterijų augimą. Kiekvienas abejotinas mėginys buvo papildomai analizuojamas naudojant *Matrix-assisted laser desorption/ionization* (MALDI-TOF) metodą, atliktą nepriklausomų tyrėjų.

DNR išskyrimas kiekybinės polimerazės grandininės reakcijos (kPGR) tyrimams buvo atliekama sumaišius bakterijų plokštelę su 180 µL TRIS-HCl

lizės buferiu (**Supplementary Material 6**) ir perkeliant į mėgintuvėlį (1,5 mL SC Micro Tube PCR-PT, SARSTEDT, Vokietija), kuriame buvo stikliniai rutuliukai (Assistent, Vokietija). Mėginiai buvo apdoroti MagNa Lyser (Roche Company, Penzberg, Vokietija) prietaisu, centrifuguojant 45 sekundes 6500 *x g* greičiu, taip mechaniškai ir chemiškai pažeidžiant bakterijų sienelę. DNR iš bakterijų plokštelės buvo išskirta naudojant DNeasy Blood & Tissue Kit (QIAGEN, Valencia, CA, JAV), laikantis gamintojo instrukcijų. DNR grynumas ir koncentracija buvo matuojami NanoDrop™ 2000/2000c spektrofotometru (Fisher Scientific, JAV). Galutinė DNR koncentracija, naudojama kPGR buvo 2,5 ng/µL.

KPGR buvo naudojamas siekiant nustatyti burnos ertmės bakterijų kiekį DASbox® mini bioreaktorių sistemoje (Eppendorf, Vokietija). KPGR tyrimas buvo atliekamas naudojant Bio-Rad CFX instrumentą ir Bio-Rad CFX Maestro programinę įrangą (v1.1) iš Bio-Rad, JAV. Pradmenų sekos, naudojamos burnos ertmės bakterijų nustatymui bei duomenų normalizavimui, PGR reakcijos mišinių sudėtis ir temperatūros režimai pateikti **Table 2.3-2.5**. Visi mėginiai buvo tiriami dublikatuose, siekiant užtikrinti rezultatų patikimumą.

Klinikinių rodiklių statistinė analizė buvo atlikta naudojant IBM SPSS Statistics (IBM Corp., Čikaga, IL, JAV, versija 29.0.1.0). Duomenų normalumo nustatymui buvo naudojamas Shapiro-Wilk testas. Kategoriniai kintamieji buvo lyginami naudojant Chi-kvadrato testą arba *Fisher* tikslumo testą, tuo tarpu tolydieji kintamieji buvo vertinami naudojant *Mann-Whitney U* testą. *Spearman* rangų koreliacijos koeficientas buvo naudojamas nagrinėti kintamųjų tarpusavio ryšius. KPGR rezultatų statistinei analizei buvo naudojamas linijinis modelis, taikant *lme4* paketą [291]. Statistinė reikšmė buvo laikoma reikšminga, kai *p* reikšmė buvo mažesnė nei 0,05.

REZULTATAI

Priešoperacinio gydymo ir operacijos įtaka žarnyno mikrobiomui

Iš pradžių buvo įvertintas priešoperacinių intervencijų poveikis žarnyno mikrobiomo sudėčiai ir pooperaciniams rezultatams gydant vėžį. Pacientai, kuriems buvo planuojama kairiosios pusės KV operacija, buvo paruošti vienu iš dviejų priešoperacinio žarnyno paruošimo būdų – TŽK arba OP, o po to jiems buvo atlikta operacija. Išmatų mėginiai buvo surinkti prieš gydymą, POD06 ir POD30, siekiant nustatyti, ar žarnyno paruošimas daro ilgalaikį poveikį žarnyno mikrobiomui.

Alfa įvairovė viso tyrimo metu reikšmingai nesiskyrė tarp OP ir TŽK grupių. Ji šiek tiek sumažėjo OP grupėje POD06 ir POD30 pooperacinę dieną, tačiau TŽK grupėje tokio sumažėjimo nebuvo pastebėta. Labiausiai pastebimi pokyčiai buvo tolygumo ir atvirkštinio Simpson indekso rodikliuose (**Fig. 3.1**, **Table 3.1**). Pradinė beta įvairovė tarp tiriamųjų grupių buvo panaši (p = 0,226). Rezultatų analizė parodė, kad beta įvairovė POD06 tarp tiriamųjų grupių nesiskyrė (p = 0,198). Panašiai, jokie skirtumai nebuvo pastebėti ir POD30 (p = 0,310). (**Fig. 3.2A**).

Nepaisant skirtumų nebuvimo tarp tiriamųjų grupių, abu mechaninio žarnyno paruošimo (OP arba TŽK) metodai, po kurių sekė storosios žarnos rezekcija, sukėlė reikšmingus žarnyno mikrobiomo sudėties pokyčius POD06, palyginti su pradine žarnyno mikrobiomo sudėtimi (p = 0,001). Šie skirtumai išliko reikšmingi ir praėjus 30 dienų po operacijos, palyginti su pradine žarnyno mikrobiomo sudėtimi (p = 0,001). (**Fig. 3.2B**). POD06 ir POD30 palyginimas taip pat parodė reikšmingus skirtumus (p = 0,002). Pastebima, kad mechaninio žarnyno paruošimo sukeltos mikrobiomo sudėties pokyčiai pradeda atsistatyti laikui bėgant. Vis dėlto, šiam atsistatymo procesui galimai reikia daugiau nei 30 dienų po intervencijos.

LEfSe analizė kartu su linijinio modelio analize atskleidė reikšmingus mikrobiomo pokyčius tyrimo laikotarpiu abiejose grupėse. TŽK atveju po rezekcijos, pastebėtas padidėjęs *Actinomyces, Enterococcus, Parabacteroides* ir *Ruminococcus* 2 genčių gausumas trumpuoju laikotarpiu (POD06 palyginus su pradiniu lygiu) po intervencijos. Tačiau dauguma šių pokyčių grįžo į pradinį lygį iki POD30, išskyrus *Ruminococcus* 2 gentį, kurios gausumas POD30 dar labiau padidėjo (**Fig. 3.3**).

OP grupėje intervencija lėmė laikiną *Dialister* genties gausumo sumažėjimą, kuris buvo pastebėtas POD06 ir grįžo į pradinį lygį iki POD30. Tiek POD06, tiek POD30 buvo nustatyti ilgalaikiai pokyčiai: sumažėjo *Porphyromonas* ir padidėjo *Citrobacter* genčių gausumas. Be to, ilgalaikis OP poveikis, matuojamas POD30, parodė padidėjusį *Eubacterium coprostanoligenes, Eubacterium hallii* grupės, and *Collinsella* genčių gausumą (**Fig. 3.4**).

Buvo atlikta ir žarnyno mikrobiomo pokyčių bei pooperacinių infekcijų sąsajos analizė. Pacientams, kurie patyrė pooperacines infekcijas (nepriklausomai nuo MŽP metodo), POD06 buvo nustatytas didesnis Pseudomonadales, Actinomycetales būrių, Actinobacteria klasės, Actinomycetaceae šeimos, *Actinomyces* genties, nekultivuotos *Sutterella* ir *Enterococcus faecalis* rūšies gausumas, palyginti su pacientais, kuriems pooperacinės infekcijos neišsivystė (**Fig. 3.5**).

Neoadjuvantinės chemoterapijos ir gastrektomijos poveikis žarnyno mikrobiomui

Toliau siekėme nustatyti, kaip NAC, po kurios seka chirurginis gydymas, gali paveikti žarnyno mikrobiomo sudėtį. Ši tyrimo dalis buvo skirta atskleisti žarnyno mikrobiomo pokyčius SV gydymo metu ir išryškinti NAC bei radikalios chirurgijos specifinius poveikius.

Įdomu tai, kad tyrimo rezultatai parodė, jog NAC neturėjo reikšmingos įtakos alfa įvairovės rodikliams, tuo tarpu chirurginis gydymas turėjo reikšmingą poveikį gausumui, Shannon indeksui ir filogenetinei įvairovei (visi $p<0.001$ **Fig. 3.6**, **Table 3.2**). Beta įvairovės analizė parodė reikšmingus skirtumus tarp pooperacinių ir post-NAC laikotarpių (visi $p = 0,001$) (**Fig. 3.7**, **Table 3.3**). *Redundancy* analizė patvirtino, kad radikali operacija turėjo reikšmingą poveikį žarnyno mikrobiomo pokyčiams ($p = 0,014$). Tai parodė, kad žarnyno mikrobiomo sudėtis reikšmingai keitėsi SV gydymo metu (**Fig. 3.8A**).

Tipo lygmenyje, NAC gydymas nepakeitė mikrobiomo sudėties. Priešingai, radikali operacija lėmė padidėjusią Bacteroidetes ($p = 0,004$) ir Proteobacteria ($p < 0,0001$) tipų gausą bei sumažėjusią Firmicutes ($p < 0,0001$) ir Actinobacteria ($p = 0,001$) tipams priklausančių bakterijų gausą, palyginti su NAC (**Table 3.4**). Genties lygmenyje NAC gydymas lėmė reikšmingą *Christensenellaceae R-7* grupės sumažėjimą ($p = 0,041$) palyginti su pirminiais mėginiais. Priešingai, radikali operacija sukėlė *Prevotella 9* ($p = 0,022$), *Streptococcus* ($p = 0,010$) ir *Escherichia-Shigella* ($p = 0,001$) gausos padidėjimą. Radikali operacija taip pat sukėlė *Lactobacillus* ($p = 0,008$), *Collinsella* ($p = 0,005$), *Faecalibacterium* ($p = 0,030$) ir *Ruminococcus torques* grupės ($p = 0,006$) sumažėjimą (**Fig. 3.8B**, **Table 3.5**).

LEfSe analizė patvirtino šiuos rezultatus, parodant, kad po operacijos pacientų mikrobiomas buvo praturtintas, padidėjusiomis *Escherichia-Shigella, Streptococcus equinus,* nekultivuotis *Streptococcus,* and *Enterobacteriaceae* rūšimis (**Fig. 3.9**). Be to, ANCOM analizė patvirtino šiuos rezultatus, parodant, kad po operacijos pacientams buvo padidėjęs *Escherichia-Shigella* lygis (tiek genties, tiek rūšies lygmenyje) ir sumažėjęs *Faecalibacterium* ir *Ruminococcus torques* grupės gentims priklausančių bakterijų lygiai.

Šios tyrimo dalies rezultatai rodo reikšmingus žarnyno mikrobiomo pokyčius gydant SV, kuriuos pirmiausia lėmė radikali chirurgija, o ne NAC. Radikali chirurgija padidino Bacteroidetes ir Proteobacteria bei sumažino Firmicutes ir Actinobacteria tipų gausumą. Be to, NAC neturėjo poveikio alfa ar beta įvairovei, tuo tarpu radikali chirurgija paveikė abi. Po radikalios

chirurgijos mikrobiomas buvo praturtintas burnos bakterijomis, nes LEfSe analizė parodė padidėjusią *Escherichia-Shigella, Streptococcus equinus* ir nekultivuotų *Streptococcus* rūšių, taip pat *Enterobacteriaceae* šeimai priklausančių rūšių gausą.

In vitro modelio sukūrimas vėžio gydymo šalutinių poveikių modeliavimui

Remiantis klinikinių tyrimų rezultatais, pastebėta, kad chirurginis gydymas gali turėti reikšmingą poveikį žarnyno mikrobiomo sudėčiai ir galimiems šalutiniams poveikiams. Vienas iš įdomiausių pastebėjimų šiame tyrime buvo burnos bakterijų, susijusių su oralizacija, padidėjimas. Šis poveikis galėjo būti stebimas įvairiose vėžio gydymo strategijose, pavyzdžiui, naudojant protonų siurblio inhibitorius ar chirurginį gydymą. Šio tyrimo metu buvo nuspręsta sukurti *in vitro* modelį, imituojantį šį vėžio gydymo šalutinį poveikį, ir išbandyti įvairius probiotikų produktus, siekiant sumažinti oralizacijos reiškinį ir potencialiai pagerinti GE vėžiu sergančių pacientų gyvenimo kokybę.

Pirmasis žingsnis kuriant *in vitro* oralizacijos modelį buvo optimizuoti išmatų surinkimo sąlygas, kad būtų efektyviai išsaugota natyvi mikrobiomo sudėtis iš surinktų mėginių. Išmatų surinkimui buvo naudojamas anaerobinis mikrobiomo rinkinys GutAlive®. Išmatų mėginiai buvo laikomi keturiuose konteineriuose, atsižvelgiant į keturis skirtingus laikotarpius: mažiau nei 1 valandą, 2 valandas, 24 valandas ir 48 valandas po surinkimo. Inokuliatas buvo paruoštas anaerobinėmis sąlygomis ir žarnyno bakterijos buvo kultivuotos DASbox® mini bioreaktorių sistemoje 120 valandų. Ši kultivacija buvo atliekama naudojant nuolatinį veikimo režimą (išlaikymo laikas 28,3 valandos [290]) anaerobinėmis sąlygomis.

Nustatyta, kad alfa įvairovė sumažėjo kultivavimo metu (visi $p \leq 0{,}002$). Svarbu pažymėti, kad šie pokyčiai buvo nepriklausomi nuo išmatų laikymo laiko surinkimo konteineryje (visi $p > 0.050$; **Fig.3.10**, **Table 3.6**). Beta įvairovės analizė parodė reikšmingą rodiklių sumažėjimą. Šis sumažėjimas buvo nustatytas kaip priklausomas nuo kultivavimo laiko (visi $p = 0{,}001$), tačiau, įdomu, kad jis neparodė reikšmingų ryšių su išmatų laikymo trukme GutAlive® išmatų surinkimo konteineryje (visi $p = 1.000$; **Fig. 3.11**, **Table 3.7**). Buvo pastebėta, kad mikrobiomo sudėtis išliko santykinai stabili per visą kultivavimo laiką (**Fig. 3.12**).

Surinkti duomenys rodo, kad žarnyno mikrobiomo sudėtis GutAlive® anaerobiniuose mikrobiomo surinkimo konteineriuose išliko stabili kambario temperatūroje iki 48 valandų. Be to, buvo iškelta hipotezė, kad alfa įvairovės

sumažėjimas kultivavimo laikotarpiu gali būti susijęs su pasirinktais maistinių medžiagų pateikimo režimais.

Operacinio režimo poveikis žarnyno mikrobiomo sudėčiai

Norint įvertinti, kaip skirtingi operaciniai režimai veikia žarnyno mikrobiomo sudėtį bioreaktoriuose, buvo atlikti tyrimai, kurių metu analizuota, kaip įvairios maistinių medžiagų papildymo strategijos veikia mikrobiomo stabilumą kultivavimo proceso metu.

Tyrimai parodė, kad tarp skirtingų operacinių režimų, pusiau nuolatinis maistinių medžiagų keitimas vieną kartą per dieną užtikrino stabilesnę mikrobiomo sudėtį nei pusiau nuolatinis maistinių medžiagų keitimas du kartus per dieną arba nuolatinis veikimo režimas, palyginti su *batch* režimu. Alfa įvairovės analizė parodė, kad kultivavimo laikui didėjant, alfa įvairovė mažėjo (visi $p < 0{,}050$). Įdomu, kad nuolatinis veikimo režimas per visą kultivavimo laiką lėmė Shannon ($p < 0{,}001$), tolygumo ($p = 0{,}020$) ir filogenetinės įvairovės ($p = 0{,}047$) rodiklių sumažėjimą. Panašūs alfa įvairovės sumažėjimai buvo pastebėti ir pusiau nuolatinio veikimo režimo (du kartus per dieną) atveju, kur Shannon ($p = 0{,}001$) ir tolygumo ($p = 0{,}030$) rodikliai sumažėjo kultivavimo proceso metu (**Fig. 3.13**, **Table 3.8**). Šis atradimas yra reikšmingas, nes nors *batch* veikimo režimas gali užtikrinti stabilumą, jis nėra tinkamas kasdieniam medžiagų ar vaistų vartojimui imituoti ir turi ribotą pritaikomumą klinikinėje praktikoje. Beta įvairovės analizė parodė, kad tiek veikimo režimas, tiek kultivavimo laikas turėjo reikšmingą įtaką mikrobiomo sudėčiai (visi $p < 0{,}050$). Įdomu, kad beta įvairovės analizė atskleidė, jog mikrobiomai iš trijų sveikų donorų turėjo skirtingą sudėtį. Šie donorui priklausantys skirtumai mikrobiomo sudėtyje išliko nuoseklūs (**Fig. 3.14**, **Table 3.9**). Šis stebėjimas papildomai pabrėžia natūralios mikrobiomo sudėties stabilumą šiame naujame *in vitro* žarnyno mikrobiomo modelyje.

Išsamesnė *16S rRNA* geno sekoskaitos duomenų analizė parodė, kad mikrobiomo sudėtis visose mitybinių medžiagų pateikimo režimuose išliko santykinai stabili, su daugiausia gausiai atstovaujančiais tipais Firmicutes, Bacteroidetes ir Proteobacteria (**Fig. 3.15**).

Oralizacijos proceso modeliavimas *in vitro*

Tolimesnis tikslas buvo sukurti *in vitro* modelį, imituojantį žarnyno mikrobiomo oralizaciją, kuris galėtų atspindėti burnos bakterijų gausėjimą žarnyne, sukeltą vėžio gydymo. Tam buvo išbandytos keturios skirtingos

burnos bakterijų įterpimo strategijos. Atlikus stebėjimus buvo pastebėta, kad strategija, kai burnos bakterijos buvo įterpiamos kiekvieną dieną, pradedant iškart po žarnyno bakterijų inokuliacijos, suteikė pastovias vertes per visą eksperimentinį laikotarpį (**Fig. 3.16**).

Probiotikų produktų testavimas, siekiant išvengti žarnyno oralizacijos

Probiotikų produktų testavimas, siekiant išvengti žarnyno oralizacijos, parodė, kad bakterijų gausa buvo reikšmingai paveikta eksperimentinės trukmės. Kontrolinėse grupėse, kurios gavo krakmolą arba placebą, buvo pastebėta didžiausia burnos ertmės bakterijų koncentracija. Be to, prebiotikų papildai vieni patys nesukėlė burnos ertmės bakterijų augimo slopinimo. Priešingai, produktai, kuriuose buvo probiotikų, sumažino *V. parvula* augimą viso eksperimento metu, palyginti su placebo grupe ($p < 0,050$). Tuo tarpu *S. salivarius* atveju buvo pastebėta tik tendencija, kad probiotikus turintys produktai sumažino bakterijų augimą, tačiau skirtumai su placebo grupe nebuvo statistiškai reikšmingi ($p > 0,050$). (**Fig. 3.17**, **Table 3.10**).

Ši tyrimo dalis parodė, kad kontrolinės grupės (kukurūzų krakmolas ir placebo) bei prebiotikai nesugebėjo slopinti burnos ertmės bakterijų augimo. Tuo tarpu produktai, turintys probiotikų, viso eksperimento metu sumažino *V. parvula* augimą ($p < 0,050$) ir parodė tendenciją ($p > 0,050$) mažinti *S. salivarius* augimą, palyginti su placebo kontrole.

APTARIMAS

Šioje daktaro disertacijoje buvo siekiama ištirti, kaip skirtingi virškinimo trakto vėžio gydymo metodai veikia žarnyno mikrobiomo sudėtį ir sukurti novatorišką *in vitro* bioreaktoriaus modelį, imituojantį žmogaus žarnyno mikrobiomą. Galutinis šio darbo tikslas buvo panaudoti šį *in vitro* modelį tiriant GE vėžio gydymo šalutinius poveikius ir išbandyti įvairias probiotikų kombinacijas, galinčias sumažinti vėžio gydymo šalutinius. Pagrindinės šio tyrimo užduotys buvo įvertinti, kaip skirtingi priešoperacinio žarnyno paruošimo metodai veikia žarnyno mikrobiomą ir pooperacinius rezultatus KV pacientams, tirti NAC ir radikalios gastrektomijos poveikį žarnyno mikrobiomui SV pacientams, sukurti bioreaktoriaus pagrindu veikiantį *in vitro* žarnyno mikrobiomo modelį, kuris galėtų būti naudojamas studijuojant vėžio gydymo šalutinius poveikius, ir panaudoti šį modelį tirti probiotikams, skirtiems sumažinti vėžio gydymo šalutinius poveikius, tokius kaip žarnyno mikrobiomo oralizacija.

Literatūros analizės dalyje buvo aptariami pagrindiniai žmogaus virškinimo trakto segmentai ir jų fizikiniai bei cheminiai parametrai, pabrėžiant šių parametrų svarbą kuriant *in vitro* žarnyno mikrobiomo modelį. Analizėje buvo atkreiptas dėmesys į rodiklių kintamumą skirtinguose virškinimo trakto segmentuose ir mikrobiomo sudėties skirtumus kiekviename segmente. Taip pat buvo aptartas GE vėžio, įskaitant skrandžio ir storosios žarnos vėžį, vystymasis, jų molekuliniai mechanizmai, susiję su mikrobiomu, ir galimos gydymo strategijos. Be to, buvo nagrinėjamas vėžio gydymo šalutinių poveikių modeliavimas naudojant bioreaktoriais pagrįstas *in vitro* sistemas. Literatūros apžvalgoje buvo nustatyta reikšminga tyrimų spraga: nors *in vitro* modeliai dažnai naudojami tiriant GE vėžio gydymo šalutinius poveikius, į šiuos tyrimus vis dar retai įtraukiamas išmatų mikrobiomas. Mūsų neseniai paskelbtas apžvalginis straipsnis išsamiau atskleidžia šią spragą [270].

Pagrindinis klinikinio tyrimo, kuriame dalyvavo KV pacientai, atradimas buvo tas, kad OP ir TŽK sukelia panašią ir laikiną disbiozę, turinčią panašias pasekmes po operacijos. Be to, tyrimas išryškino skirtingus žarnyno mikrobiomo pokyčius pacientams, patyrusiems pooperacinių infekcijų. Pastaruoju metu vis daugiau dėmesio skiriama MŽP poveikio žarnyno mikrobiomo sudėčiai tyrimams, tačiau esami įrodymai dažnai yra prieštaringi. Keli tyrimai, analizavę mikrobiomą po MŽP naudojant oralinius preparatus kolonoskopijai, pranešė apie mikrobiomo sudėties pokyčius netrukus po procedūros [294–298]. Įdomu, kad Drago ir kt. tyrimas nustatė, jog OP sukelia disbiozę, kuriai būdinga *Lactobacillaceae* probiotinių bakterijų kiekio sumažėjimas ir ši disbiozė trunka mažiausiai mėnesį. Tačiau kiti tyrimai rodo, kad žarnyno mikrobiomo sudėtis paprastai grįžta į pradinę sudėtį per žymiai trumpesnį laiką, paprastai apie 14 dienų [295,297]. Mūsų tyrimas atskleidžia, kad MŽP ir storosios žarnos rezekcija reikšmingai pakeičia mikrobiomo sudėtį per 30 dienų. Nors mikrobiomas rodo potencialą atsistatyti per šį laikotarpį, visgi jo sudėtis visiškai negrįžta į pradinę sudėtį iki 30 dienų pabaigos.

Be to, šis tyrimas pirmą kartą parodo, kad TŽK sukelia disbiozę, panašią į tą, kurią sukelia OP. Tačiau svarbu pripažinti, kad mūsų tyrime mechaninis žarnyno paruošimas buvo derinamas su chirurgine procedūra, todėl mikrobiomo pokyčiai gali kilti ne tik dėl MŽP, bet ir dėl pačios chirurginės operacijos [299,300]. Chirurginis stresas gali sukelti pokyčius organizme, kurie paveikia žarnyno mikroaplinką ir galiausiai lemia disbiozę [301]. Buvo pastebėta, kad KV pacientų žarnyno mikrobiomo sudėtis ir įvairovė mėnesis po operacijos buvo reikšmingai skirtinga tiek nuo jų mikrobiomo prieš operaciją, tiek nuo sveikų asmenų mikrobiomo [299].

Disbiozė, stebima operuotuose pacientuose gali turėti reikšmingų klinikinių pasekmių, nes ji gali būti susijusi su pooperacinių komplikacijų, ypač pooperacinių infekcijų, vystymusi [302,303]. Pacientams, patyrusiems infekcijas, buvo pastebėtas padidėjęs *E. faecalis* rūšies gausumas POD06 mėginiuose. Enterokokai yra oportunistinės bakterijos, kurios gali tapti patogeninės, kolonizuodamos aplinkas, kuriose paprastai jų nėra. Ši bakterijų grupė dažnai randama pacientuose, kurie susiduria su infekcijomis ligoninėse [306–308]. Kita bakterijų, pavyzdžiui, *Actinomyces* ir *Sutterella* genčių atstovų, kurių gausa padidėjo pacientams, patyrusiems pooperacines infekcijas, tačiau jų vaidmuo lieka mažai ištirtas ir reikalauja tolesnių tyrimų.

Ši tyrimo dalis turi reikšmingų trūkumų. Pirmiausia, nors buvo atliktas atsitiktinis pacientų skirstymas į grupes, pastebėti netikėti skirtumai pradinėje mikrobiomo sudėtyje tarp TŽK ir OP grupių. Nors aiški šios nesutapimo priežastis nėra nustatyta, tikėtina, kad amžiaus skirtumai tarp tyrimo grupių vaidino svarbų vaidmenį. Anksčiau atlikti tyrimai rodo, kad mikrobiomo stabilumas ir įvairovė dažnai mažėja su amžiumi [311,312]. Antra, mūsų tyrimas buvo ribotas dėl to, kad trūko infekcijos vietos mėginių sekoskaitos rezultatų. Be to, klinikiniai pasėlio tyrimai buvo atlikti tik keletui pacientų, kurie patyrė pooperacines infekcijas. Trečia, kaip minėta anksčiau, šiame tyrime buvo derinamas MŽP su operacija. Todėl pastebėti mikrobiomo pokyčiai gali būti priskirti ne tik MŽP, bet ir chirurginiam procedūrų poveikiui bei natūraliai besikeičiančiai dietai pooperaciniu laikotarpiu. Ketvirta, naujausios gairės rekomenduoja naudoti geriamuosius antibiotikus kartu su MŽP prieš kairiosios pusės KV operaciją [313] ir ši strategija klinikinio tyrimo metu nebuvo pritaikyta. Svarbu pažymėti, kad šios gairės nebuvo prieinamos, kai buvo vykdomas šis tyrimas. Tačiau galimas geriamųjų antibiotikų poveikis žarnyno mikrobiomui galėjo turėti įtakos mechaninio žarnyno paruošimo stebėtiems poveikiams. Nors tai yra mūsų tyrimo apribojimas, jis taip pat pabrėžia galimą stipriąją tyrimo pusę, kadangi galėjome sutelkti dėmesį specifiniams MŽP poveikiams žarnyno mikrobiomui.

Pagrindiniai rezultatai iš SV klinikinio tyrimo parodė, kad reikšmingi žarnyno mikrobiomo pokyčiai gydymo metu daugiausia priskiriami radikaliam chirurginiam gydymui, o ne NAC. Priešingai, radikali chirurgija lėmė padidėjusią Bacteroidetes ir Proteobacteria tipų gausą, tuo tarpu Firmicutes ir Actinobacteria tipų gausa sumažėjo. Be to, NAC nepaveikė alfa arba beta įvairovės, tuo tarpu radikali chirurgija reikšmingai paveikė abi. Po operacijos mikrobiomas parodė bakterijų, susijusių su oralizacija, gausėjimą. LEfSe analizė atskleidė padidėjusią *Escherichia-Shigella*, *Streptococcus equinus* ir neapibrėžtų *Streptococcus* rūšių gausą, kartu su *Enterobacteriaceae*

šeimos nariais. ANCOM patvirtino šiuos duomenis, parodant padidėjusias *Escherichia-Shigella* (ir genties, ir rūšies lygyje) ir sumažėjusias Faecalibacterium genties ir Ruminococcus torques grupės lygmenis po radikalios operacijos. Nustebino, kad šis tyrimas nerado reikšmingo NAC poveikio žarnyno mikrobiomui. Tai prieštarauja keliems ankstesniems tyrimams, kurie parodė sisteminės chemoterapijos poveikį žarnyno mikrobiomui skirtingų rūšių vėžiui [314–317], įskaitant GE vėžį [318,319]. Pavyzdžiui, neseniai atliktas Li ir kt. tyrimas nustatė, kad pacientų, sergančių metastazavusiu ar lokaliai pažengusiu stemplės, skrandžio ar kolorektaliniu vėžiu ir gaunančių chemoterapiją, žarnyno mikrobiomas skyrėsi nuo sveikų kontrolinių grupių, tyrime parodant padidėjusią įvairovę ir kompozicinius pokyčius vėžiu sergantiems pacientams [319]. Tačiau svarbu pažymėti, kad šis tyrimas nesiejo duomenų prieš ir po gydymo, priešingai nei mūsų ilgalaikis tyrimas. Tuo tarpu ilgalaikis Kong ir kt. tyrimas [320], kuris tyrė žarnyno mikrobiomo pokyčius gydant KV radikaliu chirurginiu gydymu ir kapecitabino bei oksaliplatino (CapeOx) chemoterapija, parodė, kad chemoterapija dramatiškai padidino Bacteroidetes ir Firmicutes tipų santykį. Be to, chemoterapija sumažino pirmiausia dominavusių patogeninių bakterijų, tokių kaip *Morganella*, *Pyramidobacter*, *Proteus* ir *Escherichia-Shigella*, buvimą, tačiau padidino sąlyginai patogeninių bakterijų, tokių kaip *Bilophila*, *Comamonas*, *Butyricimonas*, *Eggerthella* ir *Anaerostipes*, gausumą [320]. Keli metodologiniai skirtumai tarp Kong ir kt. bei mūsų tyrimo turėtų būti apsvarstyti interpretuojant šiuos skirtumus. Pirma, mes įvertinome NAC poveikį mikrobiomui prieš operaciją, tuo tarpu Kong ir kt. tyrimas nagrinėjo chemoterapijos poveikį po storosios žarnos rezekcijos. Antra, mes tyrėme FLOT (5-fluorouracilas, leucovinas, oksaliplatinas, doksatekselis) chemoterapijos poveikį SV pacientams, o Kong ir kt. tyrimas sutelkė dėmesį į CapeOx chemoterapiją KV pacientams. Svarbiausia, mėginių surinkimo laikai labai skyrėsi. Mes surinkome mėginius maždaug po keturių savaičių nuo NAC, prieš pat operaciją, o Kong ir kt. mėginius rinko po kiekvieno chemoterapijos ciklo. Tai rodo, kad chemoterapijos sukelti pokyčiai žarnyno mikrobiome gali būti laikini, ir keturių savaičių intervalas galėjo leisti mikrobiomui pasiekti stabilų būvį. Kitas tyrimas, atliktas Chen ir kt., nagrinėjo chirurgijos ir chemoterapijos poveikį žarnyno mikrobiomo sudėčiai SV sergantiems pacientams [321]. Nors tyrimas buvo retrospektyvus ir krossekcinis bei nenurodė chemoterapijos ar chirurgijos tipų, jis nerado reikšmingų skirtumų žarnyno mikrobiomo sudėtyje tarp pacientų, kurie gavo chemoterapiją, ir tų, kurie jos negavo [321], tai atitinka mūsų gautus rezultatus. Apibendrinant, šis tyrimas yra pirmasis, kuris parodė, kad FLOT NAC neturi reikšmingo ar ilgalaikio poveikio žarnyno mikrobiomo sudėčiai

SV pacientams keturios savaitės po gydymo pabaigos. Pagrindinis šios dalies atradimas yra tas, kad, skirtingai nei NAC, radikali chirurgija, atlikta po NAC, turi reikšmingą ir ilgalaikį poveikį žarnyno mikrobiomo sudėčiai. Disbiozė, kurią sukelia radikali chirurgija, pasižymi padidėjusia bakterijų, susijusių su oralizacija, tokių kaip *Streptococcus* ir *Escherichia-Shigella* gausa. Ankstesni tyrimai parodo, kad gastrektomija susijusi su žarnyno mikrobiomo oralizacija, įskaitant *Escherichia-Shigella*, *Enterococcus*, *Streptococcus*, *Veillonella*, *Oribacterium* ir *Mogibacterium*. [322]. Ankstyvieji tyrimai apie protonų siurblio inhibitorių poveikį siūlė, kad skrandžio barjero praradimas sukelia mikrobiomo sudėties pokyčius tiek skrandyje, tiek distaliniame virškinimo trakte [323–326]. Protonų siurblio inhibitorių vartojimas keičia skrandžio mikrobiomo sudėtį ir didina jo įvairovę [326]. Tolimesniame virškinimo trakte, kuris natūraliai yra gausus mikroorganizmų, mikrobinė įvairovė sumažėja po protonų siurblio inhibitorių vartojimo [5,323–325]. Be to, išmatų mikrobiomas po protonų siurblio inhibitorių vartojimo rodo padidėjusį burnos ertmės bakterijų kiekį, tokių kaip *Streptococcus*, *Veillonella*, *Rothia* ir *Oribacterium*, taip pat potencialių patogenų, tokių kaip *Enterococcus*, *Escherichia-Shigella* ir *Haemophilus*. Tuo pačiu metu naudingos bakterijos, įskaitant *Faecalibacterium*, *Ruminococcaceae* ir *Lachnospiraceae*, reikšmingai sumažėja. [5,323,324,327–329]. Be to, ankstesni tyrimai parodė, kad žarnyno mikrobiomo oralizacija yra susijusi su virškinimo trakto simptomais, tokiais kaip pilvo pūtimas, viduriavimas ir pilvo diskomfortas, skrandyje išgyvenusiems pacientams [5]. Šis oralizacijos procesas dažniausiai susijęs su žarnyno uždegimu ir *Streptococcus* bakterijų padidėjimu išmatose [5]. Šiame tyrime patvirtinta, kad radikali gastrektomija didina *Streptococcus*, bakterijų taksono, dažnai randamo burnos ertmėje ir dažnai susijusio su protonų siurblio inhibitorių sukelta disbioze, gausą [323,324,327–329]. Šis tyrimas parodė, kad radikali operacija padidina *Escherichia-Shigella* lygį (tiek genčių, tiek rūšių lygmenyje) ir sumažina *Faecalibacterium* bei *Ruminococcus* genčių lygį.

Šiame tyrime taip pat buvo pristatytas naujas bioreaktoriaus pagrindu sukurtas *in vitro* žmogaus žarnyno mikrobiomo modelis, naudojant DASbox® mini bioreaktoriaus sistemą. Atsižvelgiant į naujausias įžvalgas, pateiktas neseniai paskelbtame straipsnyje [332], mes pasirinkome GutAlive® anaerobinius mikrobiomo rinkimo rinkinius šiam tyrimui. Remiantis mūsų rezultatais, šie rinkiniai efektyviai išsaugojo bakterijų gyvybingumą ir stabilumą laikui bėgant, išlaikydami pradinę mikrobiomo sudėtį ir įvairovę. Išsami duomenų analizė parodė, kad bakterijų sudėtis GutAlive® anaerobiniuose mikrobiomo rinkimo konteineriuose išlieka stabili iki 48 valandų kambario temperatūroje. Be to, patogus dizainas palengvina išmatų

mėginių savarankišką rinkimą, todėl šie rinkiniai gali būti lengvai pritaikomi klinikinėje praktikoje.

Po sėkmingo išmatų rinkimo proceso optimizavimo, dėmesys buvo sutelktas į stabilios kultūros sistemos kūrimą. Tyrimas nagrinėjo, kaip skirtingi operaciniai režimai gali paveikti mikrobiomo stabilumą ir sudėtį. Tai buvo paskatinta ankstesnių pastebėjimų apie mažėjančią alfa įvairovę kultivacijos metu, ypač nuolatinio maistinių medžiagų pateikimo režimo sąlygomis. Todėl eksperimentas išbandė keturis skirtingus maistinių medžiagų pateikimo režimus: *batch*, nuolatinį ir pusiau nuolatinį (su maistinių medžiagų papildymu kartą arba du kartus per dieną). Buvo nustatyta, kad nuolatinis maistinių medžiagų tiekimas mažina alfa įvairovę viso kultivavimo laikotarpio metu, tuo tarpu *batch* režimas užtikrino stabiliausią mikrobiomo sudėtį. Tačiau kadangi *batch* režimas netinka vaistų ar kitų medžiagų kasdieninio vartojimo testavimui, tolesniems eksperimentams buvo pasirinktas pusiau nuolatinis eksploatacijos režimas su kasdieniu maistinių medžiagų keitimu. Kaip jau buvo minėta, oralizacija gali būti susijusi su įvairiais veiksniais, įskaitant chirurgines procedūras, tokias kaip radikali gastrektomija, arba protonų siurblio inhibitorių vartojimu. Protonų siurblio inhibitoriai, kurie dažnai naudojami skrandžio rūgšties sumažinimui, apima tokius vaistus kaip omeprazol, esomeprazol, lansoprazol, rabeprazol, pantoprazol, dekslansoprazolas ir zegerid [333], kurie yra dažnai vartojami vėžiu sergančių pacientų. Nors šie vaistai plačiai naudojami, jų galimi neigiami poveikiai nėra išsamiai ištirti. Vienas reikšmingas šalutinis poveikis yra oralizacijos procesas, kuris pasižymi žarnyno mikrobiomos disbalansu, sukeltu dėl burnos ertmės bakterijų patekimo į virškinimo traktą. Šiame tyrime sukūrėme oralizacijos proceso modelį bioreaktorių sistemoje, siekdami bioreaktoriuose išlaikyti stabilią ir santykinai aukštą burnos ertmės bakterijų koncentraciją viso kultivavimo laikotarpio metu. Jei bakterijų koncentracija sumažėtų, rezultatai galėtų būti netikslūs, todėl nuoseklūs lygiai buvo svarbūs tiksliai įvertinti papildų poveikį modelyje. Įdomu, kad kita grupė neseniai sukūrė *in vitro* modelį, simuliuojantį burnos ertmės bakterijų invaziją į žarnyną, kurio eksperimentinis laikotarpis truko 11 dienų ir apėmė seilių injekcijas 9 ir 10 dienomis [285]. Tačiau šiame modelyje naudojami seilių mėginiai burnos ertmės bakterijų papildymo procedūrai, kas gali kelti standartizavimo iššūkių ir kintamumą tarp eksperimentų. Priešingai, mūsų modelis siūlo standartizuotą ir supaprastintą požiūrį į oralizacijos modeliavimą, išvengiant papildomų biologinių mėginių poreikio. Vietoje to, jis naudoja du neseniai identifikuotus oralizacijos biožymenis [6]. Kita vertus, šis modelis taip pat turi trūkumų. Mesmin ir kt. aprašytas oralizacijos modelis, naudojantis M-ARCOL sistemą, buvo taikomas gleivių mikrobiomui tirti. Ši

funkcija kol kas dar nėra prieinama mūsų DASbox®-pagrįstame *in vitro* modelyje, kas pabrėžia dabartinį dalinį sistemos apribojimą.

Galiausiai, naujai sukurtas *in vitro* oralizacijos modelis, integruojantis tiek burnos ertmės bakterijas, tiek išmatų mikrobiomą, buvo pritaikytas probiotinių produktų tyrimui, siekiant sumažinti oralizacijos šalutinį poveikį, sukeltą vėžio gydymo. Mūsų tikslas buvo nustatyti tinkamiausią probiotinį produktą, kuris galėtų pagerinti vėžio pacientų gyvenimo kokybę ir sumažinti gydymo šalutinius poveikius. Tiriamieji probiotiniai produktai parodė reikšmingą *Veillonella parvula* augimo sumažėjimą ir aiškią tendenciją mažinti *Streptococcus salivarius* augimą. Tai pirmasis tyrimas, naudojantis bioreaktoriaus pagrindu sukurtą *in vitro* sistemą su išmatų inokuliatu, kuri imituotų vėžio gydymo sukeltą oralizaciją ir įvertintų probiotikus, skirtus šio šalutinio poveikio mažinimui. Kaip novatoriškas darbas, jis sudaro pagrindą būsimoms pažangoms, siekiant padidinti perdirbimo našumą ir išplėsti modelį, kad būtų ištirti kiti GE vėžio gydymo šalutiniai poveikiai.

IŠVADOS

1. Priešoperacinis mechaninis žarnyno paruošimas storosios žarnos vėžio pacientams sukelia panašią disbiozės būklę žarnyno mikrobiome, nepriklausomai nuo to, ar paruošimas atliekamas naudojant tiesiosios žarnos klizmą, ar geriamuosius preparatus. Tai rodo, kad abu metodai turi panašų poveikį žarnyno mikrobiomo sudėčiai ir galimoms pooperacinėms komplikacijoms.
2. Skirtingai nuo neoadjuvantinės chemoterapijos, kuri neparodė reikšmingo poveikio žarnyno mikrobiomo pokyčiams, radikali gastrektomija sukelia reikšmingą disbiozę, įskaitant žarnyno mikrobiomo oralizaciją, tai parodo reikšmingą radikalios chirurgijos poveikį mikrobiomo sudėčiai.
3. Šio tyrimo metu sėkmingai sukurtas ir sistemingai optimizuotas naujas bioreaktoriaus pagrindu veikiantis *in vitro* modelis, naudojant DASbox® mini bioreaktorių sistemą su žmogaus išmatomis, kaip inokuliatu. Šis modelis rodo aukštą potencialą tirti ligoms specifinius mikrobiomo pokyčius, įskaitant vėžio gydymo poveikio mikrobiomui tyrimus, ir teikia vertingų įžvalgų tiek moksliniuose tyrimuose, tiek klinikinėse taikymo srityse.
4. Šis naujas žmogaus žarnyno mikrobiomo *in vitro* modelis pritaikytas tyrinėti probiotikus turinčius produktus, skirtus mažinti vėžio gydymo sukeltą žarnyno oralizacijos šalutinį poveikį. Tyrimo rezultatai rodo, kad šie produktai veiksmingai mažina burnos ertmės bakterijų proliferaciją

žarnyno mikrobiome, ir toks modeliavimas gali būti atliekamas net ir be paciento seilių, kuriems pasireiškia oralizacija, įtraukimo. Tai rodo šios sistemos potencialą ir pritaikomumą vėžio gydymo šalutiniams poveikiams tirti bei juos pritaikyti klinikinėje praktikoje.

REKOMENDACIJOS

Kolorektaliniu vėžiu sergantiems pacientams ir tiesiosios žarnos klizma, ir geriamieji mechaniniai žarnyno paruošimo preparatai sukelia panašius žarnyno mikrobiomo pokyčius, o tai rodo panašų poveikį ir pooperaciniams rezultatams.

Skrandžio vėžiu sergantiems pacientams neoadjuvantinė chemoterapija turi minimalų poveikį mikrobiomo sudėčiai, o radikali gastrektomija sukelia reikšmingą disbiozę, įskaitant žarnyno mikrobiomo oralizaciją. Probiotinės intervencijos po radikalios gastrektomijos gali padėti sušvelninti šiuos pokyčius.

CURRICULUM VITAE

Education

PhD Biology (2021 – 2025) – Institute of Biosciences, Life Sciences Centre, Vilnius University, Vilnius, Lithuania
Academic Supervisor: Prof. Sonata Jarmalaitė, PhD
Academic Consultant: Angela Horvath, PhD, Medical University of Graz, Graz, Austria

MSc Molecular Biology (2019 – 2021) – *Magna Cum Laude*; Institute of Biosciences, Life Sciences Centre, Vilnius University, Vilnius, Lithuania
Academic Supervisor: Prof. Sonata Jarmalaitė, PhD

BSc Genetics (2015 – 2019); Institute of Biosciences, Life Sciences Centre, Vilnius University, Vilnius, Lithuania
Academic Supervisor: Prof. Sonata Jarmalaitė, PhD

Work and teaching experience

Guest Researcher / Scientific Staff Member (2023.03.06 – present) – Division for Gastroenterology and Hepatology, Department of Internal Medicine, Medical University of Graz, Graz, Austria

Trainee (2022.03.01 – 2023.02.28) – Division for Gastroenterology and Hepatology, Department of Internal Medicine, Medical University of Graz, Graz, Austria. Program: ERASMUS+

Junior Researcher (2021 – 2022) – National Cancer Institute, Laboratory of Genetic Diagnostic; Vilnius, Lithuania

Teaching Assistant (Oncogenetics) (2021 – 2022) – Institute of Biosciences, Life Sciences Centre, Vilnius University

COVID-19 Researcher (2020 – 2022) – National Cancer Institute, Laboratory of Genetic Diagnostic; Vilnius, Lithuania

Biologist (2020 – 2021) – National Cancer Institute, Laboratory of Genetic Diagnostic; Vilnius, Lithuania

Trainee (2016 – 2019) – Life Sciences Centre, Human Genome Research Group, Vilnius, Lithuania

NOTES

NOTES

Vilniaus universiteto leidykla
Saulėtekio al. 9, III rūmai, LT-10222 Vilnius
El. p. info@leidykla.vu.lt, www.leidykla.vu.lt
bookshop.vu.lt, journals.vu.lt
Tiražas 20 egz.